[redacted]

CENTRAL RESEARCH LIBRARY
DOCUMENT COLLECTION

MARTIN MARIETTA ENERGY SYSTEMS LIBRARIES
3 4456 0360940 5

INV. 63

ORNL-1280
Progress
74 A

LABORATORY RECORDS
1954

INV. 63

INV. 55

HOMOGENEOUS REACTOR PROJECT

QUARTERLY PROGRESS REPORT

FOR PERIOD ENDING MARCH 15, 1952

CENTRAL RESEARCH LIBRARY
DOCUMENT COLLECTION

LIBRARY LOAN COPY

DO NOT TRANSFER TO ANOTHER PERSON

If you wish someone else to see this document, send in name with document and the library will arrange a loan.

OAK RIDGE NATIONAL LABORATORY
OPERATED BY
CARBIDE AND CARBON CHEMICALS COMPANY
A DIVISION OF UNION CARBIDE AND CARBON CORPORATION
UCC
POST OFFICE BOX P
OAK RIDGE, TENNESSEE

[redacted]

[redacted]

ORNL-1280

CLASSIFICATION CHANGED TO: DECLASSIFIED

BY AUTHORITY OF: TID-1148

BY: R. Morrison 7/25/57

This document consists of 248 pages.

Copy 74 of 187 copies. Series A.

Contract No. W-7405-eng-26

HOMOGENEOUS REACTOR PROJECT

QUARTERLY PROGRESS REPORT

for Period Ending March 15, 1952

J. A. Swartout, Acting Project Director

C. H. Secoy, Project Chemist

T. A. Welton, Project Physicist

C. E. Winters, Project Engineer

Compiled by W. E. Thompson

DATE ISSUED

JUN 25 1952

OAK RIDGE NATIONAL LABORATORY

operated by

CARBIDE AND CARBON CHEMICALS COMPANY

A Division of Union Carbide and Carbon Corporation

Post Office Box P

Oak Ridge, Tennessee

[redacted]

MARTIN MARIETTA ENERGY SYSTEMS LIBRARIES

3 4456 0360940 5

[redacted]

[redacted]

ORNL-1280
Progress

INTERNAL DISTRIBUTION

1. G. T. Felbeck (C&CCC)
2-3. Chemistry Library
4. Physics Library
5. Health Physics Library
6. Metallurgy Library
7-8. Reactor Experimental Engineering Division Library
9-10. Training School Library
11-20. Central Files
21. R. E. Aven
22. S. E. Beall
23. E. P. Blizard
24. E. G. Bohlmann
25. G. E. Boyd
26. W. M. Breazeale
27. R. C. Briant
28. R. B. Briggs
29. F. R. Bruce
30. J. H. Buck
31. A. D. Callihan
32. D. W. Cardwell
33. C. E. Center
34. G. H. Clewett
35. D. D. Cowen
36. J. L. English
37. W. R. Gall
38. J. P. Gill
39. C. B. Graham
40. J. H. Gross
41. C. S. Harrill
42. C. G. Heisig
43. A. Hollaender
44. A. S. Householder
45. W. B. Humes (K-25)
46. C. P. Keim
47. M. T. Kelley
48. E. M. King
49. A. S. Kitzes
50. J. A. Lane
51. C. E. Larson
52. L. B. Emlet (Y-12)
53. S. C. Lind
54. R. S. Livingston
55. R. N. Lyon
56. W. L. Marshall
57. H. F. McDuffie
58. J. R. McWherter
59. E. C. Miller
60. K. Z. Morgan
61. E. J. Murphy
62. P. M. Reyling
63. H. C. Savage
64. C. H. Secoy
65. C. L. Segaser
66. E. D. Shipley
67. A. H. Snell
68. F. L. Steahly
69. C. D. Susano
70. J. A. Swartout
71. E. H. Taylor
72. W. E. Thompson
73. S. Visner
74. A. M. Weinberg
75. T. A. Welton
76. C. E. Winters
77. F. C. Vondy Lage
78. F. C. Zapp
79. P. C. Zmola
80-83. Central Files (O.P.)

[redacted]

[redacted]

[redacted]

EXTERNAL DISTRIBUTION

[redacted]-94. Argonne National Laboratory
[redacted]5. Armed Forces Special Weapons Project (Sandia)
96-[redacted] Atomic Energy Commission, Washington
10[redacted] Battelle Memorial Institute
105-107. Brookhaven National Laboratory
108. Bureau of Ships
109-114. Carbide and Carbon Chemicals Company (Y-12 Area)
115. Chicago Patent Group
116. Chief of Naval Research
117-121. duPont Company
122-124. General Electric Company (ANPP)
125-128. General Electric Company, Richland
129. Hanford Operations Office
130-136. Idaho Operations Office
137. Iowa State College
138-141. Knolls Atomic Power Laboratory
142-144. Los Alamos
145. Massachusetts Institute of Technology (Kaufmann)
146-148. Mound Laboratory
149. National Advisory Committee for Aeronautics
150-151. New York Operations Office
152-153. North American Aviation, Inc.
154. Nuclear Development Associates (NDA)
155. Patent Branch, Washington
156. Savannah River Operations Office (Augusta)
157. Savannah River Operations Office (Wilmington)
158-159. University of California Radiation Laboratory
160. Vitro Corporation of America
161-164. Westinghouse Electric Corporation
165-172. Wright Air Development Center
173-187. Technical Information Service, Oak Ridge

[redacted]

[redacted]

[redacted]

Reports previously issued in this series are as follows:

ORNL-527	Date Issued, December 28, 1949
ORNL-630	Period Ending February 28, 1950
ORNL-730	Feasibility Report - Date Issued, July 6, 1950
ORNL-826	Period Ending August 31, 1950
ORNL-925	Period Ending November 30, 1950
ORNL-990	Period Ending February 28, 1951
ORNL-1057	Period Ending May 15, 1951
ORNL-1121	Period Ending August 15, 1951
ORNL-1221	Period Ending November 15, 1951

[redacted]

[redacted]

[redacted]

SUMMARY

PART I

HOMOGENEOUS REACTOR EXPERIMENT

Status of the HRE

Following the completion of construction of the HRE on November 15, 1951, engineering tests were made on all major components of the fuel, reflector, and gas-handling systems. During the period of testing, various difficulties were encountered and overcome. The major difficulties are explained in some detail in this report.

The experimental physics program for obtaining nuclear information in the HRE has been established. The experiments to be performed fall in the following general categories: low-power, low-temperature experiments; low-power, high-temperature experiments; high-power, high-temperature experiments; miscellaneous experiments.

Calculations have been made of the anticipated poisoning in the HRE owing to Xe^{135} under a variety of possible operating conditions. In no case does it appear that xenon poisoning is a major problem.

Engineering Studies of Components

The HRE mockup has been used in making a thorough study of pulsafeeder pump performance. Some difficulty has been experienced with failure of the pump diaphragms, and the reasons for these failures have been investigated.

HRE Design

The major item in the HRE design that had not been completed at the beginning of this quarter was the high-pressure fuel-sampling device. A design that is believed to be satisfactory has been developed, and some attention has been given to the design of improved components to serve as alternates to those now installed in the HRE.

Corrosion

Scouting Studies. A possible mechanism for the corrosion of type-347 stainless steel in uranyl sulfate solutions has been investigated further, and additional support for the proposed mechanism has been obtained. The effect of various substances added to the uranyl sulfate solution has been studied, and some of the results suggest that the hydrolytic

[redacted]

[redacted]

[redacted]

properties of ferric and chromic ions greatly affect the rate of corrosion.

Dynamic Corrosion Studies. The dynamic corrosion and solution stability test program for homogeneous reactor solutions is being carried out in 100-gpm circulating test loops. To date only solutions of uranyl sulfate of various concentrations and with various additives have been tested. The test loops are described in detail, and the results of the tests are reported. It appears that the amount of oxygen required for solution stability may be independent of the uranium concentration. The effect of copper and fission products on corrosion, while significant, does not seem so severe as other effects such as turbulence or erosion-promoted attack.

Static Corrosion Studies. Results of static tests on the effect of oxygen concentration in uranyl sulfate containing 40 g of uranium per liter on the corrosion of type-347 stainless steel at 250°C are described. Oxygen partial pressures ranging from 75 to 650 psia were investigated, and little difference between corrosion rates with varying oxygen concentrations was observed.

Radiation Stability

The superiority of chromate pretreated surfaces over unpretreated surfaces both with and without copper added to the solution has been confirmed for type-347 stainless steel systems containing uranyl sulfate fuel solutions. Fundamental studies of gas production have shown that the decrease in *G* value as the concentration of uranium is increased is apparently a specific property of uranium, rather than being associated with the total mass of solute. Further studies on the homogeneous recombination of hydrogen and oxygen catalyzed by copper ions in solution have been conducted, and pressure-temperature-time data have been obtained for which a mathematical relationship has been developed.

Controls and Instrumentation

The program of testing and observing the operation of the process instruments installed in the HRE has been completed and a number of adjustments, most of them minor, have been made. Changes made as a result of the experimental testing program are described.

Chemical Concentration Determination. Emphasis has been placed on improving and testing a Densitrol unit intended for operation in solutions at room temperature. It has been found necessary to use stainless steel or titanium floats, since Pyrex floats were shattered by sudden gas surges through the Densitrol tank. A low-temperature Densitrol unit that will automatically record solution densities between 1.033 and 1.053 g/cc,

[redacted]

[redacted]

[redacted]

corresponding to solutions containing approximately 20 and 43 g of uranium per liter, has been installed in the Y-12 mockup of the HRE for evaluation.

PART II

BOILING REACTOR AND SLURRY STUDIES

Slurry and Boiling Reactor Research

Slurry Studies. Engineering studies of slurry systems have been hampered by a lack of uniformity of the UO_3 available for testing. However, in the tests to date no evidence of caking or excessive abrasion in circulating systems has been disclosed at temperatures up to 150°C. Measurements have been made on viscosity, density, sedimentation rates, and crystal growth of slurries.

Boiling Reactor Studies. Equipment has been designed and is being assembled for a laboratory experiment to determine the maximum power density attainable in a boiling liquid at high pressures. Calculations have been made on the density variation in a hypothetical boiling reactor. These indicate that the mean density of the boiling solution is strongly dependent on hydrodynamic losses in the system and also the possibility that steam separation rates rather than density decreases may be the limiting factor in reaching higher specific powers. Equipment has been set up to measure the average bulk density of a boiling liquid (at atmospheric pressure) as a function of specific power.

Preliminary results of an experiment to study the effect of fission fragments as nuclei for bubble formation in superheated liquids indicate that nucleation by fission fragments is not so effective as was postulated.

Kinetic calculations relating to the stability of boiling reactors indicate that although boiling reactors appear stable, further work is needed to determine the conditions that assure stability.

Even though the studies described are necessary to establish the relationships that determine the characteristics of a boiling reactor, it is clear that a complete definition of these relationships can be obtained with assurance only by studying an actual boiling reactor. Therefore, plans are being made for setting up a temporary, outdoor, chain-reacting unit in which the characteristics of boiling reactors can be studied.

Slurry Fuel Studies

Uranium Trioxide Chemistry. Emphasis on slurry fuel development has centered on the chemistry of uranium trioxide, including investigation of its allotropic modifications, solubilities and stabilities of the various forms, and methods for preparing them. Studies conducted with slurries of the rod and platelet modifications of

[redacted]

[redacted]

[redacted]

uranium trioxide showed that slurries of the rods were slightly more easily dispersed than those of platelets, after being heated at 250°C and standing at room temperature for prolonged periods. However, slurries of neither material exhibited appreciable caking and both are considered to be potentially valuable as slurry fuels.

Magnesium uranate, a compound that permits preparation of high pH slurries, was rejected since slurries of this material caked badly and were not easily redispersible after heating at 250°C.

Investigations of the chemistry of the allotropic forms of uranium trioxide continued and inpile irradiation experiments were started. Studies were also initiated on valence-state stability under atmospheres of hydrogen and oxygen and crystal growth in uranium trioxide slurries; a boiler to investigate the foaming problem encountered in boiling slurries was constructed and tested. A literature survey on the oxides of uranium was published. Work performed during this quarter has continued to substantiate the belief that uranium trioxide slurries are very attractive fuels for nuclear reactors.

PART III

GENERAL HOMOGENEOUS REACTOR STUDIES

ISHR Design

The uncertainties of aqueous homogeneous reactor systems and the lack of experience make the most logical next step in homogeneous reactor development, following the successful operation of the HRE, the design and construction of a pilot plant in which the nuclear, chemical, engineering, and economic feasibilities can be demonstrated at a cost that is small in comparison with that of production reactors. The conclusion resulting from a general study of the characteristics of plutonium-producing reactors is that designing, constructing, and operating the intermediate-scale homogeneous reactor with a core 6 ft in diameter and a power of 48 megawatts will provide the experience and information necessary for reasonable extrapolation from the HRE to a full-scale production reactor. Work in progress on the predesign of the ISHR is devoted to the development of a general conceptual design for the reactor to meet the following requirements:

1. The response to change in reactivity must be similar so that once the control characteristics of the ISHR are demonstrated, extrapolation to the production machines can be made with assurance.

2. Mechanical components must be designed so that representative experience will be obtained in design, operation, and maintenance of equipment.

3. The hydrodynamics of flow in the core must be similar to those of the production reactor.

[redacted]

[redacted]

[redacted]

4. The chemistry of fuel solutions and reactor materials and the process for plutonium extraction must be such that extrapolation to the production processes will be possible.

Engineering Studies of Components

Preliminary investigation of suitable turbines and generators for large-scale homogeneous reactors indicates high probability that a standard turbine with minor alternations can be used with a 200-psig saturated steam supply. One of the first experimental tests of larger scale reactor components will make use of the 4000-gpm centrifugal pump now available for installation in a test loop. A 20,000-gpm pump is being designed by the Allis Chalmers Mfg. Co. under subcontract. A similar contract is being negotiated with the Worthington Pump & Machinery Corp. for the design and development of a 20,000-gpm pump of a different type. As a result of preliminary discussions with manufacturers, a tentative heat exchanger design that appears both feasible and practical has been developed. Further discussions with manufacturers on design and cost considerations are in process.

Through the use of small-scale models, various geometries and flow patterns in spherical core vessels have been studied. Major emphasis has been placed on the investigation of rotating and straight-through flow and use of baffles and vanes for directing the flow.

Fundamental Radiation Chemistry Studies

Published data for gas production in the Los Alamos Water Boiler have been checked and found to agree well with studies of uranyl nitrate made at ORNL.

Studies of the rate of peroxide decomposition in uranyl sulfate solutions are in progress and are yielding data that will be of interest in connection with the estimation of steady-state concentrations of peroxide under reactor conditions. In HRE fuel solution at 780°C, peroxide is decomposed in a first-order reaction with a half life of around 23 minutes.

Studies of the homogeneous recombination of hydrogen and oxygen in solutions have continued with emphasis on improvement of experimental techniques, the role of diffusion of hydrogen through the liquid under non-equilibrium conditions, the effect of agitation in removing diffusion-induced complications, and the confirmation of previous evidence for the order of the reaction with respect to hydrogen and to copper.

Pressure-temperature-time data taken throughout the course of short-term (one week) exposures of HRE fuel containing copper sulfate to the high flux of the LITR have been analyzed by means of the differential equation, $dP/dt = K_1 - K_2P$, which represents the difference between production of gas at a constant rate (K_1) and its consumption at a rate (K_2) dependent

[redacted]

[redacted]

[redacted]

on pressure (of hydrogen) and a fixed concentration of some catalyst. Experimental points taken during a run at different temperatures and plotted as dP/dt vs. P are expected to fall on a series of straight lines, one for each temperature. Results of these analyses are encouraging in that during the course of an experiment they supply information that indicates whether any change is taking place and, if so, whether this is the result of a change in intercept (K_1, gas production) or a change in slope (K_2, gas recombination). As data from additional experiments become available, it should be possible to establish the limits of accuracy with which these values can be determined.

Solution Chemistry

Further investigation of the solubility of plutonium in uranyl sulfate and uranyl fluoride solutions has yielded data which indicate that in both cases plutonium precipitates, probably as a result of a first-order hydrolysis reaction. Solubility data for fission-product mixtures in uranyl sulfate solutions have been obtained experimentally. Several fission products have been studied individually for solubility in uranyl sulfate solutions.

Phase studies of uranyl sulfate solutions have shown that when the solvent is D_2O, the two-liquid-phase region occurs at a temperature about 10 deg lower than that observed when the solvent is water. It also appears that the purity of the uranyl sulfate salt has a large effect upon the temperature at which two-liquid phases appear. Conductivity studies show that uranyl sulfate behaves as a weak electrolyte at temperatures up to 90°C and that uranyl fluoride has similar characteristics but with a considerably lower equivalent conductance.

Apparatus has been constructed, tested, and modified to enable accurate measurements of vapor pressure over uranyl sulfate solutions up to 150°C. Equations for correlating density, weight per cent, and molarity of uranyl sulfate-water solutions at 25°C and between 100 and 300°C are reported.

Static Corrosion Tests of Alternate Systems

The corrosion resistance of the hot-rolled commercial-grade titanium metal was affected little by varying the oxygen concentration in uranyl sulfate containing 40 g of uranium per liter at 250°C. Corrosion rates after 2016 hr were 0.05 mpy. Increasing the uranium concentration to 100, 200, and 300 g/l in uranyl sulfate at a constant oxygen partial pressure of 150 psia similarly had little effect on the corrosion behavior of titanium. Corrosion rates in these tests averaged 0.03 mpy after 2016 hr at 250°C.

Bureau of Mines zirconium containing 5.37% tin exhibited excellent

[redacted]

[redacted]

[redacted]

corrosion resistance in uranyl sulfate solution containing 530 to 540 g of uranium per liter and no excess oxygen at 250°C. The corrosion rate on the specimen was <0.01 mpy after 1344 hours.

The status of the uranyl fluoride-oxygen solution corrosion of type-347 stainless steel at 250°C is discussed. Exploratory test results on type-347 stainless steel, Inconel, Stellite 98M2, and tantalum are included.

Fundamental Corrosion Studies

A series of experiments is being performed in an attempt to develop a high-temperature reference electrode that might be useful in studying passive films on stainless steel. Three electrodes, lead amalgam-lead sulfate, platinum-lead amalgam-lead sulfate, and silver-silver sulfate, have been tested in uranyl sulfate solutions at various temperatures. Of these electrodes only the silver-silver sulfate showed promise of being an acceptable reference electrode for use in uranyl sulfate solutions, and further work with it is being carried out.

Metallurgy

The major effort of the metallurgy group has been the correlation and evaluation of existing data relating to the following general fields of interest:

1. metallurgical factors affecting corrosion,
2. development of specifications and procedures for procurement, acceptance, and fabrication of materials and components,
3. materials development including the evaluation of their properties,
4. application of nondestructive testing methods to homogeneous reactor problems,
5. radiation damage studies.

An additional problem has been the development of alternate safety plates for the HRE to replace those which had given trouble earlier. Suitable plates were fabricated by using copper powder mixed with boron carbide, which was pressed and rolled with stainless steel cladding at 1000°C. A set of the plates was supplied for use in the HRE.

Chemical Processing

The development of homogeneous reactor chemical processing has been based on a plutonium-producing reactor using a uranyl sulfate-heavy water solution as fuel. The general approach has been to study application of tributyl phosphate solvent extraction to this separation problem and to use the process as a yardstick for evaluating attractive alternate methods of separation. The work has progressed to the point at which a reliable chemical flow sheet has been obtained;

[redacted]

[redacted]

however, the flow sheet does not necessarily represent the optimum method of chemical processing. For instance, the inherent advantage of starting with uranium in solution is lost because of the necessity of heavy water recovery, and the long cooling period for neptunium decay necessitates large storage facilities and large inventories of valuable materials.

[redacted]

[redacted]

[redacted]

TABLE OF CONTENTS

	PAGE
PART I HRE	
STATUS OF THE HRE	3
Component Testing of HRE Equipment	4
Let-down system	4
Fuel off-gas recombiners	6
Reflector dump tests	6
Core dump tests	6
Turbine-generator unit	8
Review of Operational Difficulties Encountered	9
Leaks in fuel and D_2O systems	9
Air operated valves	9
Failure of pulsafeeder pumping heads	10
Control rods	10
Sealed-rotor circulating pumps	10
Cold traps	10
Electric steam generators	10
Leak detector systems	11
Experimental Physics Program	11
Xenon-135 Poisoning in the HRE	13
ENGINEERING STUDIES OF COMPONENTS	15
Operation of the HRE Mockup and Pulsafeeder Pumps	15
Dirt problem	15
Study of ruptured diaphragms	15
Investigation of the hydraulic system	17
HRE DESIGN	21
High-Pressure Fuel-Sampling Device	21
Alternate Piston Type of Feed Pump	25
Alternate Safety and Regulating Plate Design	25

[redacted]

[redacted]

[redacted]

	PAGE
Alternate Tube Bundle Assembly for the Main Heat Exchanger	27
CORROSION	31
Scouting Studies: Corrosion of Stainless Steel by Uranyl Sulfate Solutions	31
Correlation between the consumption of oxygen and the production of nickel ions	32
Change in corrosion rate with time	33
Investigation of inhibitors	34
Nitric acid pretreatment of stainless steel vs. no pretreatment	35
Discussion and future work	39
Dynamic Corrosion Studies	40
Test facilities	40
Loop operation	48
Status of the loops	51
Fuel system test results	51
Corrosion	54
Future work	62
Static Corrosion Studies	62
Uranyl sulfate corrosion studies	62
Reflector corrosion studies	68
RADIATION STABILITY	69
Long-Term Exposures in the X-10 Graphite Pile	69
Short-Term Exposures in the LITR	69
Long-Term Exposures in the LITR	71
CONTROLS AND INSTRUMENTATION	73
Chemical Concentration Determination	74

[redacted]

[redacted]

[redacted]

PAGE

PART II BOILING REACTOR AND SLURRY STUDIES

SLURRY AND BOILING REACTOR RESEARCH 83

Slurry Studies 83

Loops 83
Pumps 83

Physical Properties of Slurries 84

Viscosity measurements of $UO_3 \cdot H_2O$-H_2O slurries 84
Density 85
Sedimentation rates 85
Crystal growth 85
Criticality experiments 86

Boiling Reactor Studies 86

Power density experiment 86
Expected density of boiling solutions 86
Volume boiling of aqueous solutions 89
Survey of experience of boiler manufacturers 89
Studies on the promotion of boiling by fission in superheated uranium solutions 89
Boiling reactor kinetics 90
Small-scale boiling reactor experiment 94

SLURRY FUEL STUDIES 101

Uranium Trioxide Chemistry 101

Uranium trioxide allotropy 101
Valence state studies 102
Copper sulfate catalysis of hydrogen and oxygen recombination 104
Deuterates of uranium trioxide 104
NO_2 and HNO_3 vapor oxidation of U_3O_8 105
Preparation of uranium trioxide by oxidation of U_3O_8 105

Radiation Chemistry 105

Particle Size Growth in UO_3 Slurries 106

Studies of Normal Uranyl Phosphate Slurries 108

[redacted]

[redacted]

[redacted]

	PAGE
Preparation of UO_3 by Spray Calcination	109
Slurry Equipment Studies	109

PART III GENERAL HOMOGENEOUS REACTOR STUDIES

ISHR DESIGN	113
Basis for Selection of Reactor Size	115
Control	115
Hydrodynamics	119
Mechanical Components	120
Chemical Considerations	121
Basis for Favoring Spherical Core	121
Heat Production in the Reactor Shell	121
Sources of heat	122
Total heat production	124
Shielding Studies	124
Reactor shield	124
Induced radioactivity in equipment	126
Gamma-ray leakage through pipes	126
Hydrogen-Oxygen Explosions	126
Explosions in the core vessel	128
Explosions in other parts of the system	131
Safety precautions for the recombiner system	131
ENGINEERING STUDIES OF COMPONENTS	135
Steam Turbines and Generators	135
Test Loop for 4000-gpm Pump	136

[redacted]

[redacted]

[redacted]

PAGE

Main Pumps and Valves 137

Main Heat Exchanger 139

Isolation Valves 140

Miscellaneous Additional Valves 141

HRE Recombiners 141

Small Canned-Rotor Pump 141

ISHR Fuel Feed Pumps 142

Bearings for 100-gpm Pump 142

Reactor Core Development and Gas Separators 143

Rotating types cores – small models 144
Straight-through cores 149
Eight-foot sphere 151
Gas separators 151

FUNDAMENTAL RADIATION CHEMISTRY STUDIES 155

Gas Production from Uranium Solutions and Slurries 155

Uranyl sulfate 155
Uranyl nitrate 156
Uranyl fluoride 157
Uranium oxide slurries 157

Peroxide Studies in Uranyl Sulfate Solutions 158

Homogeneous Recombination of Hydrogen and Oxygen in Aqueous Systems 161

Gas Kinetics of Inpile Radiation Studies 163

SOLUTION CHEMISTRY 173

Plutonium Solubilities in Uranyl Salt Solutions 173

Stability of plutonium sulfate in uranyl sulfate solutions 173
Stability of plutonium ion in uranyl fluoride solutions 173
Effects of radiation on the valence state of plutonium 175

[redacted]

[redacted]

[redacted]

	PAGE
Calculated Fission-Product Buildups and Experimental Solubilities of Fission-Product Mixtures in Uranyl Sulfate Solutions	175
Fission-Product Solubilities in Uranyl Sulfate Solutions	177
Cesium sulfate	177
Cadmium sulfate	177
Silver sulfate	179
Interpretation of data	180
Two-Liquid-Phase Transition Temperatures for the Deuterium Oxide-Uranyl Sulfate and Uranyl Fluoride Systems	180
Conductivity of Uranyl Sulfate and Uranyl Fluoride Solutions	183
Vapor Pressures of Aqueous Uranyl Sulfate Solutions	186
Density-Weight Per Cent-Molarity Conversion Equations for Uranyl Sulfate-Water Solutions at 25.0°C and Between 100 and 300°C	188
Equations applicable at 25°C	188
Equations applicable between 100 and 300°C	189
STATIC CORROSION TESTS OF ALTERNATE SYSTEMS	193
Corrosion Studies with Concentrated Uranyl Sulfate	193
Corrosion of titanium	193
Corrosion of zirconium	194
Corrosion Studies with Uranyl Fluoride	196
Effect of oxygen and uranium content on corrosion of type-347 stainless steel at 250°C	196
Corrosion of tantalum in uranyl fluoride containing 40 and 300 g of uranium per liter at 250°C	196
Corrosion tests at 100°C in uranyl fluoride solutions	197
Analysis of precipitates removed from uranyl fluoride solutions	198
FUNDAMENTAL CORROSION STUDIES	199
An Attempt to Develop a High-Temperature Reference Electrode	199

[redacted]

[redacted]

[redacted]

	PAGE
METALLURGY	203
Metallurgical Factors in Corrosion	203
Specifications and Fabrication Procedures	205
Alternate and Supplementary Materials	205
HRE Safety Plates	207
Nondestructive Testing	208
Radiation Damage Studies	208
CHEMICAL PROCESSING	209
Plutonium Chemistry	209
Behavior of plutonium(VI) in uranyl sulfate solution	209
Effect of oxygen pressure on plutonium solubility	210
Effect of type-347 stainless steel and copper sulfate on plutonium solubility	211
Adsorption of plutonium on stainless steel	213
Filtration of PuO_2	213
Dissolution of PuO_2	213
Heavy Water Recovery	213
Solvent Extraction	214
Extraction of plutonium from solutions containing the sulfate ion and uranium	214
Application of TBP extraction after short cooling periods	221
Flowsheets	224

[redacted]

[redacted]

Part I

HOMOGENEOUS REACTOR EXPERIMENT

HRP QUARTERLY PROGRESS REPORT

STATUS OF THE HRE

S. E. Beall, Section Chief
J. S. Culver
J. J. Hairston
J. W. Hill, Jr.
T. H. Mauney
C. G. Lawson
V. Paré
J. A. Ransohoff
L. H. Thacker
T. H. Thomas
S. Visner
P. M. Wood

The HRE has been operated with water and unenriched uranyl sulfate in the fuel system and ordinary water in the reflector system since November 15 for the purpose of performing engineering tests on all major components of the system.

Chronologically, the period from November 21 to November 27 was spent in hydrostatic pressure and leak testing of both the fuel and reflector systems. The reactor core and its immediate connections were isolated from the system and tested separately. Strain gages mounted at a number of critical points were used to indicate stresses in the 3/16-in.-thick stainless steel sphere during the pressure application. A maximum hoop stress of 29,000 psi was measured at 1200-psi hydrostatic pressure.

After installation of the reactor core, the high-pressure systems were tested at 1800 psi, the maximum pressure that could be contained without leakage past the air-operated valves, and the low-pressure systems at 450 psi. Following the hydrostatic tests, the system was prepared for the addition of unenriched uranyl sulfate solution by cleaning and treating the high- and low-pressure fuel systems according to the following procedure:

1. washed 3 hr with 3% trisodium phosphate at 150 °C,
2. treated with 5% nitric acid for 4 hr at 70 to 90 °C,
3. washed with distilled water,
4. step 1 repeated – four washes required,
5. flushed with distilled water,
6. retreated with nitric acid,
7. rinsed with distilled water until pH was above 4.0,
8. charged with distilled water and circulated for 2 hr at 250 °C, 1000 psi,
9. operated with distilled water containing 500 ppm oxygen for 4 days,
10. drained, refilled with distilled water, and system brought to temperature and pressure with 500 ppm oxygen.

A number of faults that needed correction became obvious at this point. The control plates had to be replaced because gas that leaked into the sandwich type of plate while it was under pressure expanded after removal of the reflector pressure and caused the walls of the plates to bulge. The reflector dump valve leaked excessively and was replaced.

Piping changes were necessary in the fuel concentration system to prevent unscheduled concentration changes. The pulsafeeder pumping systems were modified to improve their performance, and the main fuel-circulating pump had to be replaced because of the faulty electrical windings. Changes were made to improve the operation of the air-operated valves and a number of instruments. The turbine-generator unit was operated during this period on the house steam system and performed satisfactorily after minor modifications were made.

After the necessary corrections and repairs in the fuel and reflector systems were made, the first quantity of unenriched uranyl sulfate was added and the operating conditions (1000 psi and 250°C) were attained on January 5, 1952. After 24 hr the gasketed joint (designed to be seal welded) at the main heat exchanger flange began to leak so much that another shutdown was required; during shutdown the heat exchanger was removed, inspected, and seal welded.

Another leak test was made, and the system was operated with water at full temperature and pressure without interruption, except for various engineering tests, for two weeks. Then, two severe leaks that appeared in the entrance and exit welds at the head of the main heat exchanger necessitated minor redesign and replacement of the head.

Soon after the repair was completed, failure of the diaphragms occurred in both the intermediate and remote pumping heads of the pulsafeeder pumps. Dissection of the heads showed the cause of failure to be small metal chips that had penetrated the thin metal diaphragms. After replacement of the pulsafeeder heads on February 22, the entire fuel system was helium leak tested and recleaned with trisodium phosphate and nitric acid solutions.

On February 27, the second charge of unenriched uranyl sulfate was admitted to the system, and the system was operated, except for minor interruptions, at 1000 psi and 250°C during the following 17 days.

At present it is believed that this last successful operating period is sufficient evidence that the reactor is ready for the critical experiments outlined in the following. Plans are being completed for the performance of these experiments early in the next quarter.

COMPONENT TESTING OF HRE EQUIPMENT

The various pieces of equipment comprising the HRE have been tested in the normal course of operating the reactor as a complete assembly. The adequacy of most of the components has been fully demonstrated, although a few parts appear to be on the borderline of design requirements. In measuring the performance characteristics of the equipment, the high-pressure fuel system was operated at 1000 psig and 250°C with a fuel circulation rate of 100 to 120 gpm and simulated decomposition-gas ($H_2 + O_2$) flow rates as high as 20 scfm. The high-pressure reflector system was run at 175 to 200°C and 400 to 1000 psig helium pressure with simulated decomposition gas rates as high as 0.4 scfm. The parts considered to be satisfactory are listed here, along with performance data collected on a few of the most important parts.

Let-Down System. The maximum quantity of decomposition gases that can be bled from the reactor core without upsetting the balance of reactivity is controlled by the heat exchanger and valve that are known as the let-down system. The gas-handling capacity of this system was

measured by feeding both helium and mixtures of hydrogen and oxygen into the reactor core. Results are given in Table 1 and Fig. 1.

The wide spread of the plotted points in Fig. 1 is attributed to the difficulty of judging the exact control position of the air-operated let-down valve at a given gas and liquid flow. Furthermore, the liquid flow rates listed may be slightly in error because of suspected leakage through the dump valve that parallels the let-down valve.

A series of pressure drop measurements was taken by using temporary pressure gages at each end of the let-down heat exchanger directly upstream of the let-down valve. The results of these measurements (Table 2) support the evidence (Table 1) that the gas-handling capacity increases as the liquid flow is decreased. With a liquid flow of only 1 gpm, the system can easily handle the 15 cfm of gas expected at a 1-megawatt power level.

The limit to the gas-handling capacity may be the operating temperature of the let-down system, since corrosion and erosion by the liquid-gas mixture are expected to increase with temperature. Table 3 was compiled to indicate the temperatures to be expected at several gas and liquid flows. Although the temperatures of the stream out of the hot side are approximately 20°C higher than recommended, it is thought that removal of the insulation from the heat exchanger will be a satisfactory means of lowering the temperature to approximately 100°C for the maximum operating state.

TABLE 1

Approximate Maximum Gas Flows Handled and Controlled by the HRE Let-Down System

PULSAFEEDER LIQUID OUTPUT (gpm)	GAS	CORE PRESSURE (psig)	APPROXIMATE GAS FLOW (cfm, STP)
1.6	Helium	940	<12
1.5	Helium	1000	~13
1.36	Helium	1000	12.8 to 14.7
1.27	Helium	980	9.4 to 13
1.14	Helium	1000	16 to 18
0.35	Helium	1000	~30 to 32
1.3	$2H_2 + O_2$	1000	9.2 to 12.5
1.2	$2H_2 + O_2$	1000	15
1.2	$2H_2 + O_2$	1000	13.5
1.12	$2H_2 + O_2$	1000	12 to 16
0.9	$2H_2 + O_2$	1000	15.8 to 18
0.8	$2H_2 + O_2$	1000	18.5 to 21
1.5	Helium	800	4.2 to 6.0
1.26	Helium	830	6.9
1.5	Oxygen	425	2.46
1.6	Helium	230	0.8

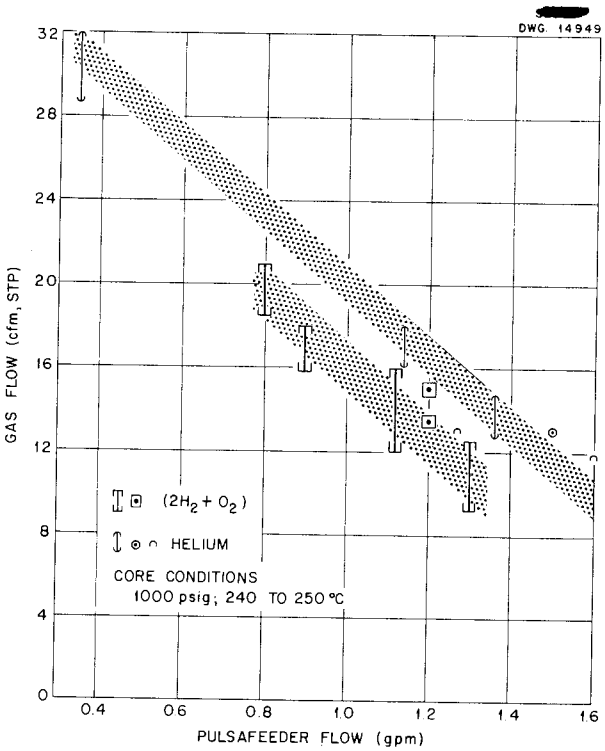

Fig. 1. Approximate Maximum Flows of Gas that can be Handled and Controlled by the HRE Let-down System vs. Liquid Flow from the Pulsafeeder Pump.

Fuel Off-Gas Recombiners. The decomposition-gas mixture of hydrogen and oxygen from the let-down system must be recombined to water, which is returned to the reactor core. Recombination is effected by a burner and a catalytic bed of platinized alumina. Satisfactory operation of the recombiner system has been demonstrated at flow rates of from 0.02 to 20 cfm of combustible gas.

It is conceivable that the flame at the recombiner nozzle could be propagated to the dump tanks, thence through the let-down system, and on into the core. In normal operation the mixture of gas is kept diluted below the explosive limit with steam from the dump tank evaporator. In an effort to determine whether a flashback might travel to the core, the diluting steam was purposely turned off. Immediately, a series of flashbacks occurred from the recombiner to the dump tanks, and finally the flame began to burn in the dump tanks. However, it did not travel up the let-down system to the core. While the soup evaporator was being operated to generate dilution steam as in the normal case, flashbacks were always quenched in the off-gas condenser. The catalytic recombiner handled flows from 0.02 to 0.3 cfm of uncombined gases from the burner without difficulty.

Reflector Dump Tests. One means of shutting down the reactor is rapid lowering of the reflector. This method will be used to back up the safety plates, which drop in a fraction of a second. Several tests have shown that the reflector can be completely dumped from a height of about 28 in. in approximately 12 seconds. It is likely that the reactor would be stopped by the decreasing reflector level alone after less than 4 seconds.

All the 175°C water from the reflector is discharged to the reflector dump tanks. The resulting maximum pressure and temperature in the dump system were measured at <350 psi and 128°C, approximately as predicted.

Core Dump Test. In the event that neither the safety plates nor the reflector is sufficient to stop a rise in reactor power level, the fuel solution could be discharged also. Tests show that in approximately 30 sec sufficient fuel can be dumped to make the reactor subcritical. Ten minutes are required to drain the entire 75 liters of fuel solution from the high-pressure system.

TABLE 2

Pressure Drops in the Let-Down System for Various Gas and Liquid Flows

CORE PRESSURE (psig)	PULSAFEEDER LIQUID FLOW (gpm)	HELIUM FLOW (cfm, STP)	PRESSURE DROP		
			CORE TO HEAT EXCHANGER	ACROSS HEAT EXCHANGER	ACROSS VALVE
1000	0.35	0	0	5 to 25	975 to 995
1010	0.35	6	80	275	655
1010	0.375	21	30	25 to 225	755 to 955
1010	0.375	29 to 31	70	85 to 385	555 to 855
1000	1.14	0	25	100	875
1000	1.14	0	95	0	905
1000	1.13	0	20	105	875
1010	1.14	5	70	235 to 335	605 to 705
1010	1.14	10	80	275 to 525	405 to 655
1000	1.14	13	40 to 60	405 to 635	305 to 555
1000	1.14	18	80	695	225
1000	1.14	20	70	705	225
1000	1.53	0	40	125	835
1000	1.53	5	70	245	685
1000	1.53	10	50 to 80	245 to 465	455 to 705
1000	1.53	13	70	605	325
1000	1.53	13.5	80	725	195

TABLE 3

Let-Down Heat Exchanger Temperatures

PULSAFEEDER FLOW (gpm)	GAS FLOW (cfm, STP)	TEMPERATURES (°C)			
		FROM CORE (Hot Side)		TO CORE (Cold Side)	
		TEMP. IN (Line 104)	TEMP. OUT (Line 105)	TEMP. OUT (Line 111)	TEMP. IN (Line 227)
0.8	19.5 ($2H_2 + O_2$)	242	151		
1.05	16 ($2H_2 + O_2$)	243	122	237	52
1.2	9 ($2H_2 + O_2$)	246	112	242	62
0.35	0	238	51	218	38
0.375	21.4 (He)	243	206	241	51
1.14	0	249	75	214	56
1.14	10 (He)	248	107	237	57
1.14	13 (He)	248	123	237	59
1.53	0	247	83	211	59
1.53	10 (He)	248	112	232	61
1.53	13 (He)	246	122	231	62

Turbine-Generator Unit. The turbine-generator unit attached to the Homogeneous Reactor has been operated by a group from the MIT Practice School. Steam flow requirements were determined at several steam-chest pressures, from 65 to 215 psia, and various power outputs, from 0 to 75 kw. Steam at a rate of 650 lb/hr was required at zero load, and 2000 lb/hr was necessary at 75 kw. However, the effect of steam pressure variations could not be accurately measured under the conditions of operation.

TABLE 4

Steam Flow Rate as a Function of Steam-Chest Pressure

STEAM CHEST PRESSURE (psia)	STEAM FLOW RATE (lb/hr)
10	900
50	724
100	665
150	640
200	634

In another test the minimum steam flow at the no-load rated speed of the turbine was measured as a function of steam-chest pressure. The results of this test are listed in Table 4.

The no-load excitation characteristics of the generator were determined by varying the field current and measuring the voltage output. Armature current was also measured at various field currents and a series of *V* curves was obtained for several loads. In all the tests the turbine-generator unit performed well, and it is considered adequate for its purpose.

Other components that have performed satisfactorily are:

1. fuel concentration system,
2. oxygen addition system,
3. fuel off-gas condensers,
4. pressurizer system,
5. fuel and D_2O evaporator,
6. D_2O condensers,
7. D_2O and fuel heat exchangers,
8. D_2O high- and low-pressure catalytic recombiners,
9. emergency cooling system for dump tanks,
10. D_2O liquid level indicators,
11. off-gas charcoal beds.

REVIEW OF OPERATIONAL DIFFICULTIES ENCOUNTERED

In operating an assembly with such a variety of components, it is inevitable that some will not function as expected. The major troubles experienced in three months of start-up testing are discussed in the following.

Leaks in Fuel and D_2O Systems. Approximately 27 leaks have been discovered in the fuel and reflector systems during nearly four months of operation. Leaks occurred in fabricated sections, flanges, and temporary experimental connections. The leaks in fabricated sections and flanges are obviously more serious than in the temporary connections, which will not be present when the system is operated as a reactor. More than 30% of the leaks observed have been in temporary connections.

Six of the leaks detected were in fabricated portions of the system. Two of these leaks, one in the fuel system and one in the reflector system, were in valve bellows (already mentioned). Two leaks appeared simultaneously in cracked welds at the head of the main fuel heat exchanger; both welds were made by the manufacturer. One weld of a nozzle type of joint on the pumping head of the pulsafeeder pump failed. This weld was made by ORNL forces. Failure was attributed to vibration fatigue as a result of repeated excessive shock by improper seating of the check valves in the line. One other extremely small leak appeared in a machined fitting on the let-down heat exchanger. Although this was not a weld leak, it was repaired by welding.

Eleven ring-joint flange leaks have been found. Seven of these leaks were the result of improper tightening after reconnection; they were corrected by subsequent tightening. In four cases the oval-ring gaskets were removed and found to be scored. Although it is likely that these leaks could have been stopped by further tightening, the practice of replacing gaskets at leaking flanges has been adopted.

Two joints with flat gaskets, intended to be seal welded later, have leaked. One of these was on the main fuel heat exchanger and the other on the rear flange of the main circulating pump. Both seal welds will be made before power operation is attempted.

Air-Operated Valves. Considerable difficulty has been experienced in securely fastening the various parts of the bellows type of operating mechanism on the air-driven valves. The components of the operating mechanism were made of cast aluminum. Piping vibrations caused by the

pulsafeeder pumps loosened the fastening screws in the aluminum and made it necessary to install steel inserts and lock washers.

Several valves leaked past their seats under operating conditions. In two cases sufficient force could not be applied to the valve stem to prevent the stem from being lifted off its seat by high-pressure surges from the pulsafeeder pumps. These valves have been removed and one is to be replaced by a similar valve with a smaller seating area. Leakage through three other valves has been attributed to foreign matter on the seats, but the reason for leakage has not been definitely established.

The helium bleed valve from the reflector gas space and the fuel-gas let-down valve have permitted leakage into the shield because of failure of the bellows that is used instead of a packing gland as a seal between the stem and body of the valve.

As a result of these difficulties, the fuel dump and pressurizer bleed valves are being provided with flanges so that they can be replaced remotely.

Failure of Pulsafeeder Pumping Heads. After approximately 300 hr and 10^6 strokes, both the isolation and pumping heads of the fuel pulsafeeder pump were determined to have ruptured diaphragms. Subsequent removal of the 0.020-in.-thick stainless steel diaphragms showed the reason for failure to be metal chips that had punched through the thin metal despite extreme precautions that had been taken to keep all foreign matter out of the system. These failures were similar to one that occurred in the HRE mockup pump. Both heads were replaced by new units. Procedures adopted to prevent reoccurrence of this type of failure are described in Part III of this report.

Control Rods. The drive mechanisms on the safety, shim, and control rods have not been satisfactory. A series of difficulties, mostly electrical, has kept one or more of the rods out of service since testing began. Revisions have been made to limit switches, electromagnets, electrical wiring, and the position-indicating mechanism. Acceptable performance is yet to be demonstrated.

Sealed-Rotor Circulating Pumps. Replacement of both the reflector and fuel-circulating pumps (Westinghouse Models 30A and 100A, respectively) has been necessary because of failure of the stator windings. The cause of failure has not been determined. A second fuel-circulating pump had a cracked Stellite front bearing after 700 to 900 hr of operation and is being replaced.

Cold Traps. The refrigerated traps that prevent loss of water vapor from the fuel and reflector systems have been troublesome because of premature plugging and air leakage into the refrigeration lines. Although this system was not considered inoperable, several modifications such as replacement of float valves by expansion valves and adding steam tracing to the inlet gas lines to prevent freezing have been made.

Electric Steam Generators. The high-pressure steam (800 to 1200 psi) needed to heat the pressurizer section of the fuel system and to maintain the fuel temperature at 250°C (without neutrons) is supplied from two generators of 10- and 40-kw capacity. The calrod heaters in the 10-kw boiler failed because of low water level and had to be replaced. The output of the 40-kw boiler had to be augmented by the addition of about 20 kw of strip heaters in order to maintain the incompletely insulated fuel system at 250°C.

Leak Detector Systems. Each flange in the fuel pipe lines is provided with a leak detector line filled with water and maintained at a pressure greater than the fuel pressure. Leaks are detected by observing whether the pressure on the detector line decreases, which indicates leakage of water through the flange and into the fuel system or into the shield. Each detector line is connected through a small Hoke valve into a header so that the various lines can be isolated. The packing glands of the Hoke valves leaked after repeated operation and they are being replaced by diaphragm-sealed Kerotest valves.

Pressure on the detector system has been maintained, rather unsatisfactorily, by a Sprague air piston pump. It is likely that this means of pressurization will be replaced by helium pressure over a water reservoir if performance of the pump cannot be improved. Otherwise, the leak detector system is satisfactory and has been successfully employed in the location of leaking flanges.

EXPERIMENTAL PHYSICS PROGRAM

S. Visner V. K. Paré
P. M. Wood

An experimental program that was prepared for the HRE has been described in detail in a memorandum.[1] Essentially, the program was intended to extend the proposals made earlier[2] to cover additional experiments and, furthermore, to correlate the experiments more directly with the instrumentation and anticipated performance of the reactor. The twofold objectives of the program are to obtain experimental data that will be of direct operational value but cannot be predicted too reliably from theory and to check other theoretical predictions in order to increase the confidence in theory when designing large reactors.

The general plan of the nuclear experimental program will be to perform the earlier experiments under the simplest possible conditions consistent with the belief that experimental safety is increased with operating simplicity. Thus, the initial experiments will be performed at room temperature, near atmospheric pressure, with no flow of fuel in the reactor, and without use of the concentration or off-gas systems. It is planned to isolate the reactor core and its associated heat removal loop from the low-pressure system.

The first experiment will be the determination of the critical concentration of the full-reflected reactor at room temperature. This will be followed by measurements of control rod, safety plate, and reflector level effectiveness, and the temperature coefficient of reactivity between 20 and 100°C. As a safety measure in these experiments, the safety plate can be thrust into position and the reflector dumped.

The considerable uncertainty in the calculated critical concentration of the bare reactor at room temperature requires that this quantity be determined experimentally by measuring the critical concentration at successively lower reflector levels. The introduction of a stream of gas through the bottom of the reactor will be relied upon as a safety feature in addition to dumping the remaining reflector. (The lowest reflector

[1] S. Visner, *Experimental Physics Program for the HRE*, ORNL CF-51-11-149, Nov. 28, 1951.

[2] J. M. Stein, C. H. Secoy, and L. R. Quarles, "Experimental Program for the HRE," *Homogeneous Reactor Experiment Quarterly Progress Report for Period Ending February 28, 1951*, ORNL-990, p. 118.

level planned is 3 in. above the bottom of the core.) The safety plates located in the reflector region will not be effective at low reflector levels.

After the simpler experiment has been made, criticality will be investigated under conditions of circulating fuel, elevated temperatures and pressure, and gas generation. Studies of reactor dynamics are also planned in which the reactivity of the reactor will be changed and the time response observed. Finally, a group of experiments that are presently considered of secondary importance will be taken up as time permits. The experiments are summarized in the following in the order in which they will probably be performed.

Low-Power, Low-Temperature Experiment

1. Criticality of the fully reflected reactor at room temperature.
2. Calibration of reactivity control devices at room temperature – control plates, shim and safety plates, reflector level.
3. Temperature coefficient of reactivity below 100°C.
4. Period as a function of excess reactivity at room temperature.
5. Criticality of the bare reactor at room temperature.
6. Flux normalization for calibration of instruments.

Low-Power, High-Temperature Experiment

1. Temperature coefficient of reactivity above 100°C.
2. Calibration of reactivity control devices near operating temperature.
3. Pressure coefficient of reactivity.
4. Period as a function of excess reactivity near operating temperature.

High-Power, High-Temperature Experiment

1. Rate of gas production in the fuel system.
2. Rate of gas production in the reflector.
3. Effect of gas production on reactivity.
4. Control of the reactor by fuel concentration.
5. Determination of power level: measurement of heat output and build-up of fission products.
6. Heat generated after shutdown.

Miscellaneous Experiments

1. Lifetime of prompt neutrons.
2. Response of the reactor to rapid changes in reactivity in order to obtain information on gas delay time, transient power levels, and control of the reactor by change in power demand.
3. Kinetic experiments relating to possible hydraulic instabilities.
4. Minimum stable operating pressure.
5. Gas rate and composition of fission products.
6. Temperature distribution in the shield.

7. Effectiveness of the shield for neutron and gamma radiation.

8. Other fuel and reflector systems.

XENON-135 POISONING IN THE HRE

S. Visner V. K. Paré

Calculations were made of the anticipated Xe^{135} poisoning in the reactor under a variety of possible operating conditions. At 1 megawatt the equilibrium poisoning, with no removal of xenon, is 2.5%, where the poisoning is defined as the ratio of thermal-neutron absorptions in the poison to absorptions in the fuel. The decrease in reactivity in the reactor is roughly equal to the poisoning. A maximum poisoning of 2.9% would be reached 5 hr after shutdown. However, with the xenon swept out of the reactor by the decomposition gases, the poisoning becomes very small, 0.01%. Xenon is also effectively removed by the boiling in the fuel concentrator. In fact, when no gas is evolved from the core (as with the addition of copper as a homogeneous recombination catalyst to eliminate bubbles) the poisoning would be only 0.1%. In either case the maximum poisoning after shutdown would be 1.3% with the evaporator turned off after shutdown and 0.09% with the evaporator continuing to function after shutdown.

It should be pointed out that in the absence of inert gas flow from the system to the charcoal beds no stripping of xenon would occur, because the xenon that is carried out by the steam and decomposition gas (H_2 and O_2) would only return into solution in the condensers and be swept back to the dump tanks and thence to the core. If in normal operation, addition of a flow of 0.04 cfm of O_2 to the reactor will be sufficient to remove practically all the xenon from the off-gas system to the charcoal absorbers.

The results of the poisoning calculations are presented in Table 5 for operating power densities of 20 and 60 kw per liter, even though a power density of 60 kw per liter is probably not possible or desirable in the HRE. It was assumed that equilibrium is essentially attained in all cases between the xenon in solution and in the vapor state and that Henry's Law applies. Values of Henry's constants were postulated as follows:

$$3.2 \times 10^5 \text{ psi at } 100°C,$$

$$0.7 \times 10^5 \text{ psi at } 250°C.$$

It is significant to note that the introduction of copper into the reactor to the extent of eliminating gas decomposition should not materially affect the xenon poisoning in the reactor provided the evaporator is kept running.

TABLE 5

Xenon Poisoning Data

EQUILIBRIUM OPERATING CONDITIONS			EQUILIBRIUM POISONING RATIO*		POISONING RATIO AT 250°C AFTER SHUTDOWN			
					Evaporator on**		Evaporator off	
Decomposition Gas Flow (scfm)	Evaporator Steam Flow (lb/hr)	Power Density (kw/liter)	In Core at 250°C	In Dump Tanks at 100°C	Maximum	Time to Reach Max. (hr)	Maximum	Time to Reach Max. (hr)
0	0	20	0.025	0.022	0.025	0	0.029	5
0	0	60	0.037	0.033	0.038	0	0.063	8
0	55	20	0.0010	1.4×10^{-7}	0.0010	0	0.015	11
0	55	60	0.0028	4.2×10^{-7}	0.0028	0.16	0.046	11
15	0	20	0.00011	0.00052	0.0010	1	0.015	11
45	0	60	0.00013	0.00096	0.0041	1	0.045	11
15	55	20	0.000074	2.1×10^{-7}	0.00010	1	0.015	11
45	55	60	0.00010	4.0×10^{-7}	0.0041	1	0.045	11

*With 0.04 cfm O_2 flow in the off-gas system. The equilibrium poisoning ratio is approximately numercially equal to a corresponding change in k_{eff}.

**In the event that the fuel from the core is not released to the dump tanks, it is assumed that circulation between core and dump tank is maintained after shutdown by means of the pulsafeeder pump.

ENGINEERING STUDIES OF COMPONENTS

C. B. Graham, Section Chief
J. S. Culver C. W. Keller
D. Toombs

OPERATION OF THE HRE MOCKUP AND PULSAFEEDER PUMP

The HRE mockup was operated with normal fuel for 500 hr under simulated reactor conditions. Oxygen was injected at various rates during the operation, and no serious troubles were encountered until a leak developed in the diaphragm of the 1-gpm pulsafeeder pump. Shortly thereafter the diaphragm of the intermediate head also developed a leak. These and later failures in the HRE precipitated a thorough study of the problem. The study has not been completed but considerable pertinent information has been gathered.

Dirt Problem. Construction of the heads is shown in Fig. 2, and the area where failure occurred is indicated. In all four heads that failed there was evidence of metal chips or hard foreign material that had piled up behind the diaphragm and caused severe bending stress and eventual failure. Two of the heads failed because a large particle had punched a hole through the 0.018-in.-thick stainless steel diaphragm. It is reasonable to assume that the particles were in the system when it was assembled.

The only apparent remedy is absolute cleanness in assembly of the system – although reduction of maximum pressures will improve conditions. The heads replaced in the HRE were thoroughly degreased and flushed. All pipes were plugged while the ends were being prepared for welding and all lines were flushed before welding. Barring spattered material from welding, the system should be as free from foreign material as is possible. In the original installation a sintered metal filter was provided in the fuel line immediately ahead of the pump. Suitable additional precautionary measures have been taken at other points where dirt could possibly enter the system. No further failures have occurred in subsequent operation of the reactor system.

Study of Ruptured Diaphragms. In addition to observing obvious points of severe stress in the diaphragms, microscopic studies were made of sections cut radially from the top half where there was no evidence of damage by foreign material. These studies showed fatigue failure in progress at the outer edge of the diaphragm. Although the cracks had not progressed completely through the diaphragm, they indicated incipient failure that must be eliminated.

A study of the contours of the flanges that back up the diaphragm (see note on Fig. 3) showed a discrepancy from the contours specified by Lapp Insulator Company in their design. The principal deviation was noted at the outer edge of the contoured surface where fatigue cracks in the diaphragm indicated that excessive stresses were present. The deviation from specifications carried over into the outer 1-in. rim, which was supposed to be perfectly flat but was found to have an appreciable amount of curvature. Calculations also indicate that excessive stress exists at this point because of imperfections in the machining of the face.

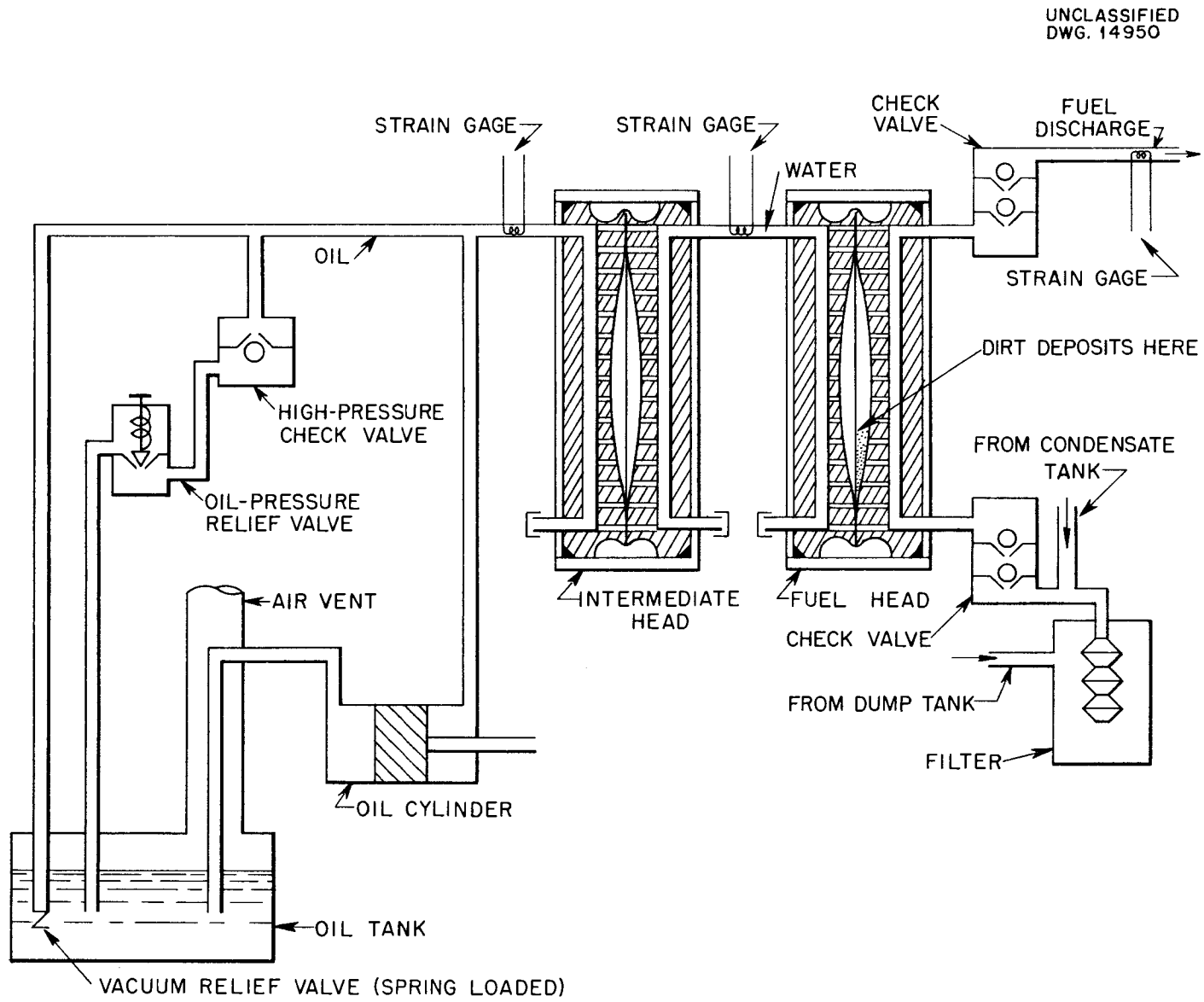

Fig. 2. Schematic Diagram of Fuel Pulsafeeder Pump.

UNCLASSIFIED
DWG. 14951

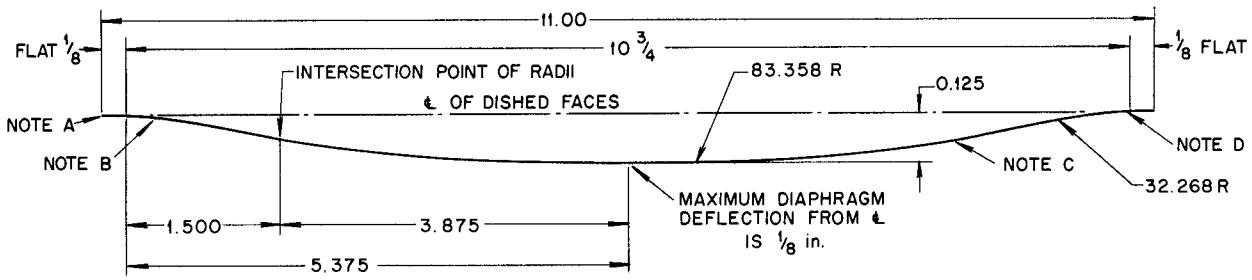

NOTE A. THERE IS A 1-in. EXTENSION OF THIS FLAT WHERE THE PRESSURE IS APPLIED TO THE DIAPHRAGM TO HOLD IT IN PLACE.

NOTE B. POINT WHERE LARGE DISCREPANCIES IN CONTOUR WERE FOUND TO OCCUR.

NOTE C. PROFILE VIEW OF THE CONTOURED FACE OF THE PULSAFEEDER HEAD. THE OPPOSITE FACE IS SYMMETRICAL.

NOTE D. THE OUTER EDGE OF THE MACHINED FACE IS THE POINT OF MAXIMUM STRESS IN THE DIAPHRAGM. MAXIMUM CALCULATED STRESS IS ABOUT 20,000 psi.

ALL DIMENSIONS IN INCHES.
NOT TO SCALE.

Fig. 3. Details of 11-in. Dish for Metal Diaphragm of Lapp Pulsafeeder.

Figure 3 shows a profile view of the contour for the machined faces on the heads, specified by Lapp, which limit the calculated maximum stress in the diaphragm to about 20,000 psi. The pulsafeeder head assembly consists of two machined flanges, with the diaphragm between them. A seal weld is made by fusing the outer edge of the flanges and the diaphragm together. A hoop is then placed around the assembly and a strength weld made on one side. After the hoop is heated to 500°F, the remaining strength weld is made. When the hoop cools, the shrinkage places a sufficient load on the flanges to keep the seal weld from being stressed during operation at high pressures.

Since the fatigue limit of stainless steel is in the order of 40,000 psi and the calculated maximum stress on the diaphragms is about 20,000 psi, the diaphragms should last indefinitely if the contours are properly machined and dirt is eliminated. Microscopic examination of used diaphragms show no signs of stress corrosion.

The shop has made and used a template to cut the contour. The new fuel head in the reactor has been successfully refinished by using the template, and all future assemblies will be machined similarly.

Investigation of the Hydraulic System. One of the four diaphragms that failed was punctured on the oil side of the intermediate head (see Fig. 2). Since this diaphragm normally does not touch the back head except on the suction stroke where the pressure is limited to 10-in. Hg, the damage must have occurred when the fuel check valves failed to close and allowed the system pressure (1000 psi) to be transmitted back to the intermediate diaphragm. When

this slip past the check valves occurs, pump operation becomes very noisy and high shock pressures are produced in various parts of the pulsafeeder system. To study this, strain gages were installed on the mockup, as indicated in Fig. 2, to measure pressure.

Early experiments with these devices were conducted with the original experimental (bolted) fuel head and check valves. Frequent and very severe slip-backs occurred in the system. Pressure recordings indicated high shock pressures, but before the instrumentation had been sufficiently developed to measure them, the diaphragm failed because of metal chips. The slip-backs are believed to have been caused by faulty valve operation. The valves had been designed with excessive clearance between the guides and the balls so that the balls could roll in the guides before seating. All subsequent valves have been built with reduced clearance in the guides. It should be noted that the Stellite balls and seats had chattered severely and damage was anticipated. However, no damage was observed when the valves were dismantled, which led to the conclusion that they are not likely to chip or crack. After examination of the bolted head, a rebuilt, welded head with low-clearance valves was installed in the mockup, and further improvements were made in the instrumentation. Relatively quiet operation of the pump resulted and more reliable pressure readings were obtained. A typical trace, representing normal quiet operation without oxygen in the O_2 absorber, is shown in Fig. 4*a*. Although the pressures indicated are considerably higher than the system pressure, they are not high enough to be alarming. The absolute value of these pressures has not been reliably established. A theoretical analysis to be published in the near future indicates that the instrument is probably reading high.

Although the traces cannot yet be explained in detail, their general shape is very logical. The complete cycle of one stroke is indicated from *a* to *a* by an electrical impulse that occurs at the 0- and 360-deg points of rotation of the crank. From *a* to *b* the oil and water in the hydraulic lines is compressed until at *b* it reaches 1000 psi. Fuel then flows into the system from *b* to *c*. The curvature of the line is a result of inertia forces, friction, and changing piston velocity. At *c* one of the diaphragms (in this case the fuel diaphragm) reaches the end of its stroke (bottoms), and the liquid stops flowing from the pump. From *c* to *d* the hydraulic fluid is further compressed, and from *d* to *e* the oil relief valve operates. At *e* the piston has reached the end of its travel, and decompression takes place from *e* to *f*. The suction stroke and oil intake occur from *f* to *a*.

During the stroke, particularly in the fuel-discharge pressure reading, a relatively high-frequency oscillation superimposed on a low-frequency damped oscillation starts at *c* when the discharge check valves close. The high-frequency oscillation coincides with the natural frequency of the 1/8-in. pipe that connects the valve to the oxygen absorber. The longer period oscillation coincides with the natural frequency of the let-down heat exchanger. Readings taken at the pressurizer connection indicate that no appreciable pressure change is transmitted to the core.

The addition of O_2 decreases the fuel-discharge pressure but has little effect on other pressures. Figure 4*b* shows operation of the pumps with oxygen and with the oil line shortened

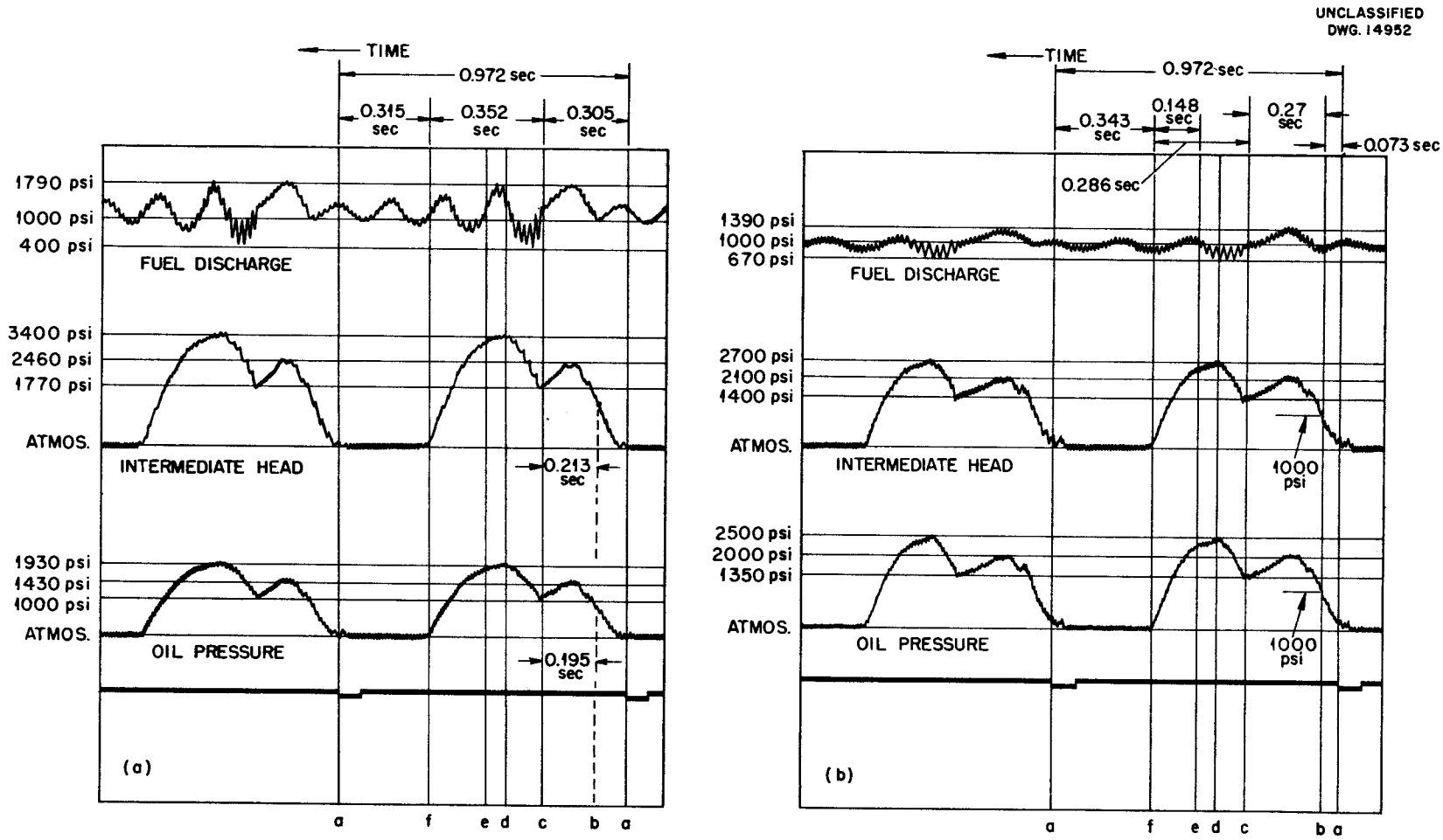

Fig. 4. System Pressure Traces Taken on HRE Mockup with a Hathaway Oscillograph. (*a*) Long oil line, no oxygen. (*b*) Short oil line, with oxygen.

from 22 to 8 feet. This arrangement has resulted in extremely quiet operation of the pump in the mockup plus increased output. With some difficulty, a similar change could be made in the reactor, if desired. It can be seen that a very small increase in pressure, 390 psi, occurs at the fuel discharge, as contrasted to the 780 psi shown in Fig. 4*a*.

All the curves (Fig. 4*a* and *b*) were taken with the pump operating at 58 rpm. When received, these pumps operated at 78 rpm. Based on the assumption that a great deal of the noisy operation was caused by check valve trouble and that this was related to pump speed, tests were run with the reactor fuel pump at various speeds. Since these tests indicated that operation became much quieter when the speed was reduced to approximately 60 rpm, the motors on the pumps on the reactor and the mockup were changed to reduce the speed accordingly.

Study will continue on the pulsafeeder problem until reliable operation is obtained with the pumps in the HRE.

HRE DESIGN

R. B. Briggs, Section Chief
C. L. Segaser F. C. Zapp

The major effort of the HRE design group during the past quarter was the preparation of working drawings for the proposed high-pressure fuel-sampling device. Other work of the group consisted of the following:

1. submission of an alternate design for an improved tube bundle assembly for the main heat exchanger to A. O. Smith Corporation for analysis and comments,

2. submission of two alternate proposals for improved safety and regulating plate designs,

3. completion by the Engineering Department of drawings for an alternate high-pressure feed pump as a possible substitute for the pulsafeeder type of pump,

4. preparation of a design manual for the HRE.

HIGH-PRESSURE FUEL-SAMPLING DEVICE

The requirements upon which the design of the high-pressure fuel-sampling device is based were originally proposed during a conference on analytical sampling and procedures for the HRE (held July 18, 1951), and they were formally presented in a memorandum to J. A. Swartout from C. H. Secoy, dated July 31, 1951. In brief, this memorandum outlined the samples required for analytical analysis of the fuel, as shown in Table 6.

Recognition of the extremely difficult conditions encountered in taking a representative sample from the high-pressure, high-temperature, and intensely radioactive fuel solution was made in specifying the following sampling procedure as the basis of design for the sampling device:

1. Isolate about 30 cc of the fuel.

2. Adjust pressure and temperature to a standard condition - preferably 1 atmosphere and room temperature. Vent gas from the sample and minimize loss of water vapor by cooling before gas is released.

3. Open isolation chamber by remote operation and remove about 0.5 ml of solution to a shielded container. Bring the sample out through a suitably designed opening in the pile shield and transport it to the analytical laboratory.

4. Weigh sample in the laboratory, dilute it to an appropriate volume, and take aliquots for the various analytical procedures.

TABLE 6

Samples Required for the Analyses of Fuel

ANALYSIS REQUIRED	SAMPLE REQUIRED (ml)
Total uranium	0.03
Tetravalent uranium	0.10
pH of the solution	0.05
Nickel	0.05
Suspended solids	
Fission products	

Several locations were proposed for obtaining the samples. The most satisfactory proposal involved connecting the sample lines to the inlet and exit lines on the heat exchanger in the high-pressure recirculating loop. The pressure differential across the exchanger is great enough to cause the solution to circulate through the sampler. Figures 5 through 8 show schematically the system as finally evolved.

Figure 5 is a schematic drawing of the high-pressure sampling apparatus. All operations involving extraction of the reactor fuel sample are performed remotely above a 12-in.-thick shielding plug. Seven extension valve handles, the manipulator assembly, the indexing shaft, the charging hole, and the viewing window extend through this plug. Clearance space around each shaft through the plug is maintained at less than 1/32 in. to minimize the radiation streaming through the openings.

The isolation chamber, isolation valves, indexing table, and periscope apparatus are housed within a stainless steel sheet metal, water-tight box suspended within the top shielding concrete and below the lead barrier so that in operation all components of the apparatus containing fuel may be flooded with water. With the water and lead combination it will be possible to reduce the radiation dosage to barely tolerable levels directly above the sampler. Lead and hydrogenous material are required to attenuate the gamma rays and neutrons emitted by the sample which escape from the core through the reduced thickness of shield at the sampler. It has been calculated that without the hydrogenous shield the neutron current at the top of the lead would be 4.5×10^6 neutrons/cm^2·sec.

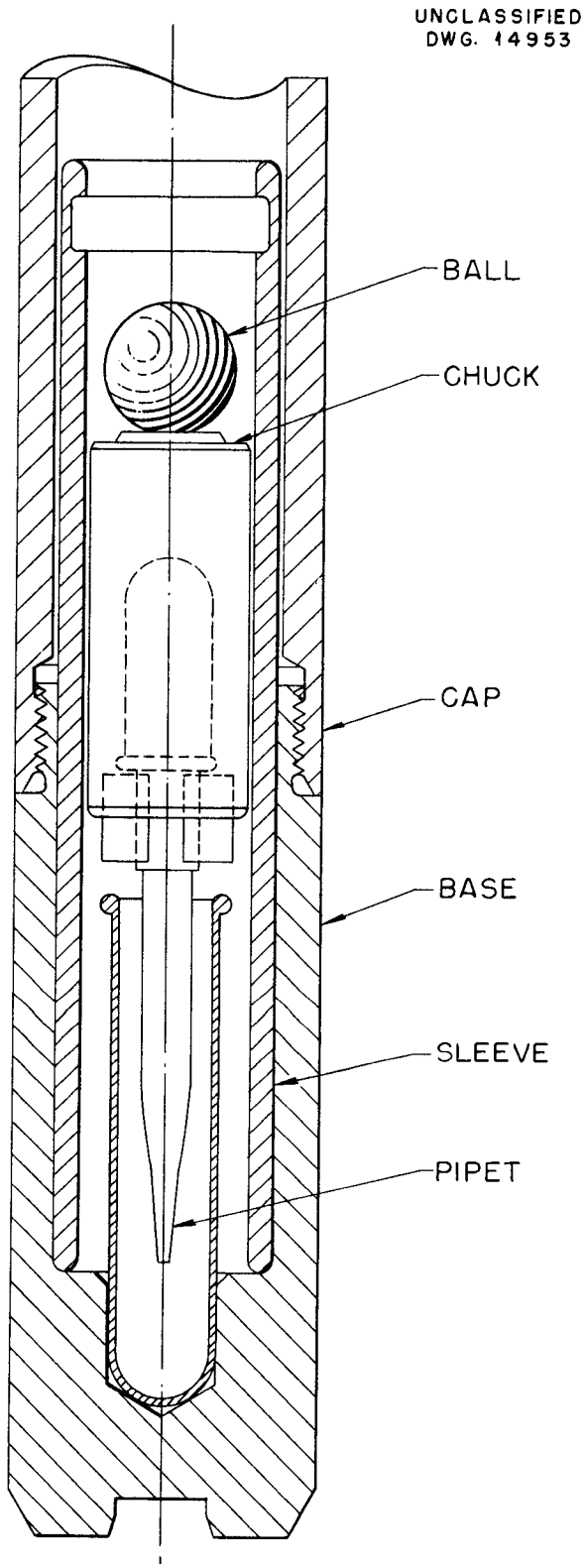

Fig. 5. Sample Carrier.

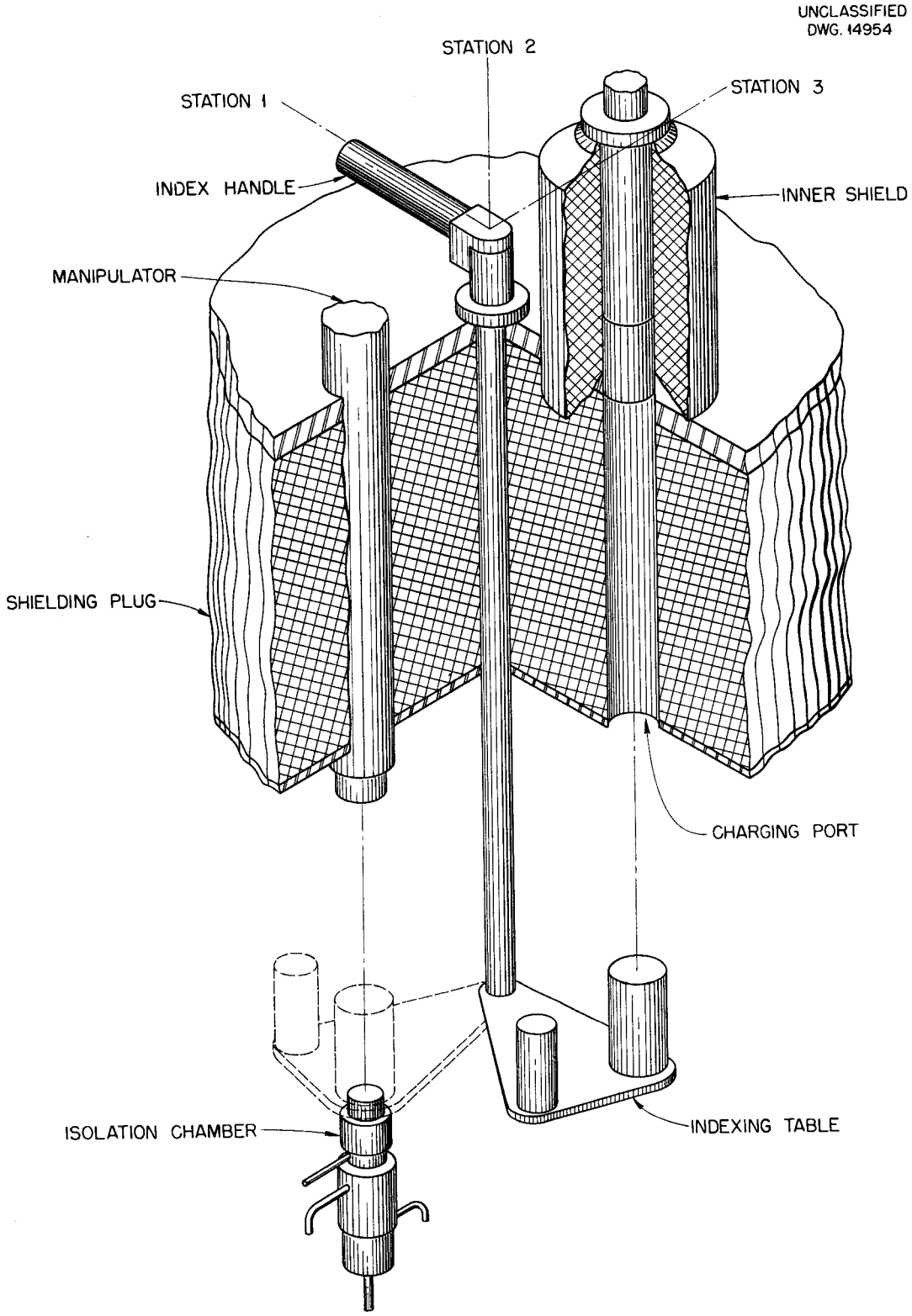

Fig. 6. Apparatus for Remotely Handling the Sampler.

The procedure for extracting a sample of the reactor solution may be divided into four major processes: (1) preparation of equipment, (2) handling procedure, (3) circulating procedure, and (4) transfer procedure. Each major process is referenced to one or more of Figs. 5 through 8, which show the particular portions of the apparatus required to perform each process.

Preparation of Equipment. Figure 5 shows a part of the sample carrier. To prepare the equipment for sampling, a new ball is placed in the carrier chuck with the pipet and the assembly is inserted in the carrier base. The sample carrier is then lowered through the hole in the inner carrier shield to the sampler housing chamber. This procedure must be followed for each sample.

Handling Procedure. Figures 6 and 7 show graphically the apparatus and controls required to handle the sampler by remote means from the top of the shield. The handling of the sampler is accomplished principally by means of the indexing table and manipulator. All stations on the manipulator and indexing handle controls are marked so that with the aid of a prepared chart the operator will know exactly the position of the internal components. As an additional check and operating aid, a viewing window and tilting mirror are provided.

Circulating Procedure. Figure 8 is a flow diagram of the sampling system showing the relationship of the required valves to the isolation chamber. It is important that these valves be operated in the proper

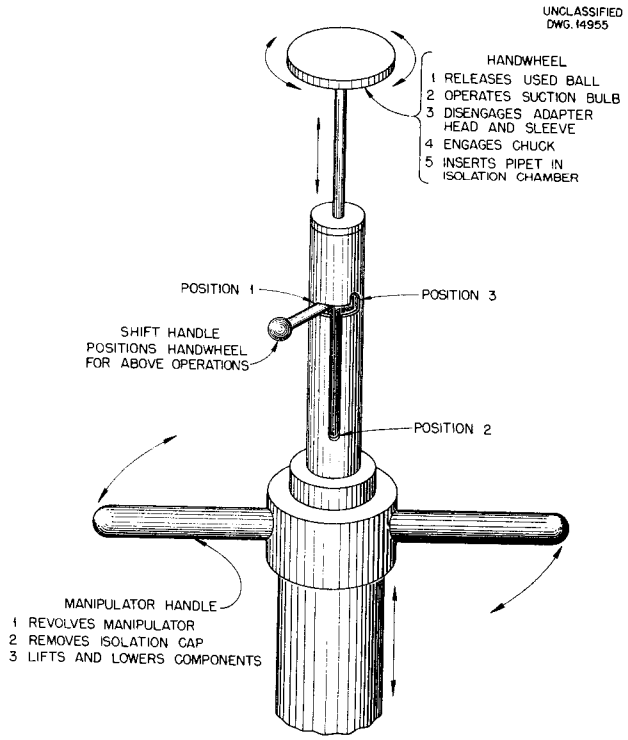

Fig. 7. Manipulator Controls for Remotely Handling the Sampler.

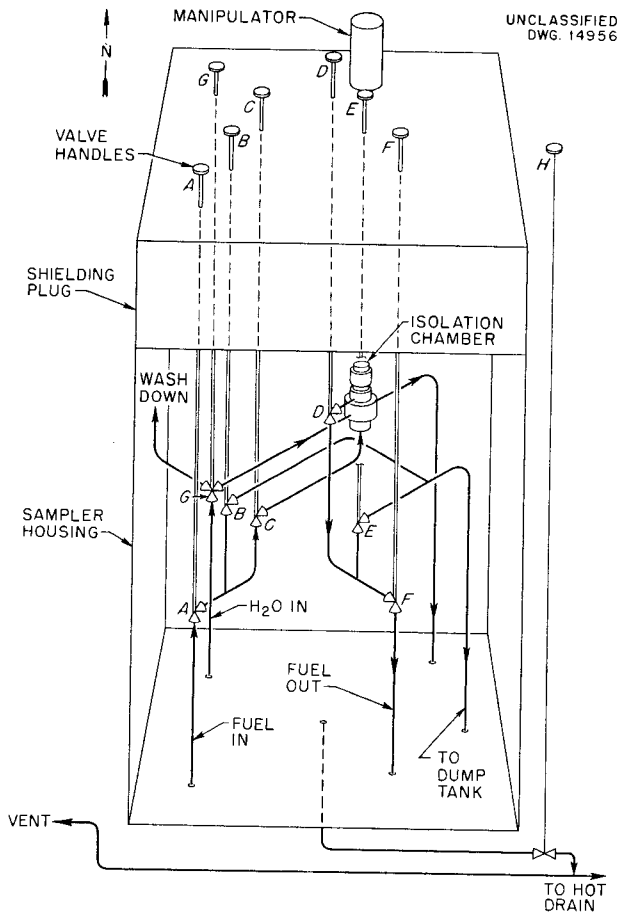

Fig. 8. Flow Diagram of Fuel Sampler Showing Relationship of the Valves to the Isolation Chamber.

sequence; therefore the operator's chart outlines in exact sequence the proper opening and closing of the valves for safely extracting a sample of solution.

Transfer Procedure. After all components are in their proper position within the sampler housing and the sample has been isolated and depressurized, the isolation chamber may be opened, the pipet inserted, and the sample taken. The sample carrier must then be removed from the sampler housing, transferred to the carrier shield, and transported to the chemical laboratory. The same equipment used in the handling procedure and preparation of equipment, Figs. 5 through 8, are used to effect the transfer but in roughly the reverse order.

ALTERNATE PISTON TYPE OF FEED PUMP

In the last HRE Quarterly Progress Report, the advantages of a simple piston type of feed pump as an alternate design for the existing pulsafeeder feed pumps were tabulated. The design of this pump (ORNL Dwg. D-10171) has been submitted by the Engineering Department for study. A complete set of working drawings for fabrication of an experimental model is ready for issuance to the shop pending final design approval.

Figure 9 shows the principal features of the proposed pump. The design, which is a modified version of a simple piston type of reciprocating pump, incorporates several innovations not available in commercial pumps of the same general type. The differences are evident in the drawing. Specifications for the pump are given in Table 7.

Since the cylinder is vertically mounted on a frame of the same dimensions as the existing pulsafeeder pump frame, the old assembly may be removed from the reactor shield and the alternate assembly inserted with a minimum of disturbance to the piping system. The pump piston is driven by a Tomkins-Johnson, Model HH-5, double-acting hydraulic cylinder mounted in a universal adjusting bracket.

From correspondence with manufacturers of Stellite items it was learned that hard facing of Stellite on stainless steel as a method of fabricating the piston and cylinder is feasible or that both items may be cast and machined entirely from Stellite. A purchase requisition has been issued to obtain one cast Stellite cylinder and piston combination for experimental use.

ALTERNATE SAFETY AND REGULATING PLATE DESIGN

Recent tests of the HRE revealed that very small pin hole leaks in the edge welds of the existing control plates allowed gas under pressure to diffuse into the plate sheathing. During a reflector dump the pressure on these plates is reduced rapidly. The gas trapped in the sheathing cannot escape at a commensurate rate, and the resulting pressure differential over the comparatively thin sheathing causes the plates to balloon and bind between the core tank and the pressure vessel.

Two alternate designs for rectifying the above condition have been submitted. One design incorporates a sheath for the boral absorber rolled from 16-gage or thinner stainless steel tubing of a selected diameter to form a plate of the required width and thickness. The absorber is

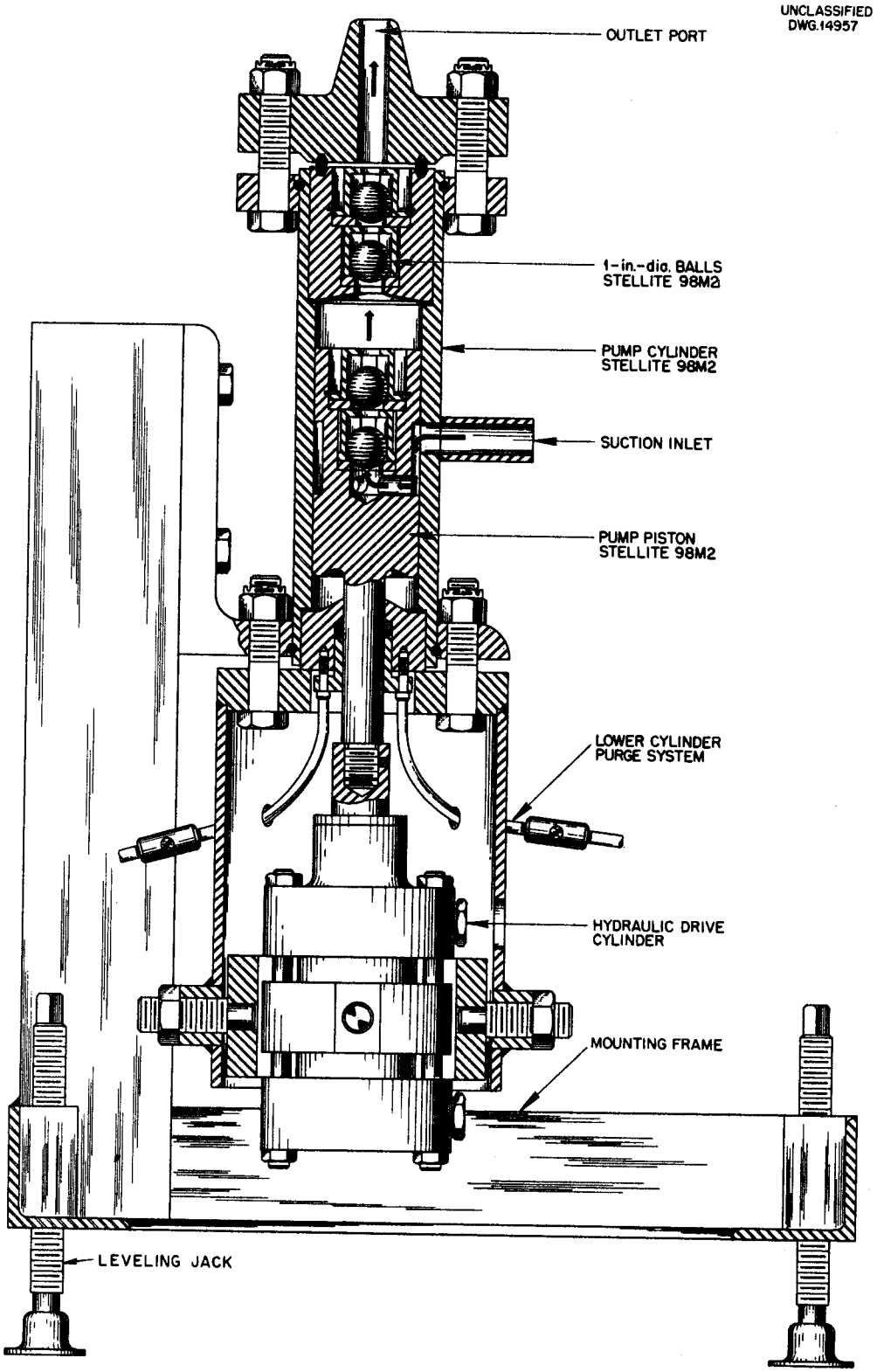

Fig. 9. Alternate Experimental High-Pressure Piston-Type Feed Pump.

TABLE 7

General Specifications for Pump and Drive Cylinder

	PUMP	DRIVE CYLINDER
Capacity	2 gpm	
Working pressure	1000 psi	1000 psi
Design pressure	2500 psi	1500 psi
Inside diameter of cylinder	2.5 in.	2.5 in.
Piston stroke length	1.125 in., normal 1.500 in., maximum	1/2-in. cushion both ends
Pump speed	60 strokes/min	60 strokes/min
Diameter of check valve balls	1 in.	
Diameter of check valve cage	1.06 in.	
Minimum cylinder volume	2.4 in.^{3}	
Maximum cylinder volume	9.8 in.^{3}	
Outlet pipe size	1/4 in., Sch. 80	
Inlet pipe size	3/4 in., Sch. 80	

inserted in the flattened tube, and only the ends are edge welded to form a hermetically sealed plate. The total amount of seal welding required is materially reduced and the design of the weld is simplified.

The second design, proposed by the Metallurgy Division, incorporates a boron carbide-copper compact clad with stainless steel. A metallurgical bond between the core and cladding provides a solid plate. Since this method of fabrication appears superior to the first, developmental work is proceeding on the sandwich type of construction.

ALTERNATE TUBE BUNDLE ASSEMBLY FOR THE MAIN HEAT EXCHANGER

The revised drawings of an alternate tube bundle assembly for the HRE main heat exchanger have been submitted to the engineers of the A. O. Smith Corporation for analysis and comments prior to fabrication. The alternate design, Fig. 10, was submitted at the request of the HRE experimental group to provide an improved type of tube bundle for replacing the existing bundle if it fails in service. Experience with the existing heat exchanger has shown that changes in design are desirable.

The tube ends should be flared into the tube sheet before welding to prevent weld metal from obstructing the entrance. A gradual transition from 1 1/2-in. inlet and exit pipes to the distribution headers should be provided to improve flow characteristics through the exchanger. In making the final seal weld around the existing distribution header it was found that the new weld coincided with parts of previous welds in the inlet and outlet pipes. As a result, circumferential cracks extending

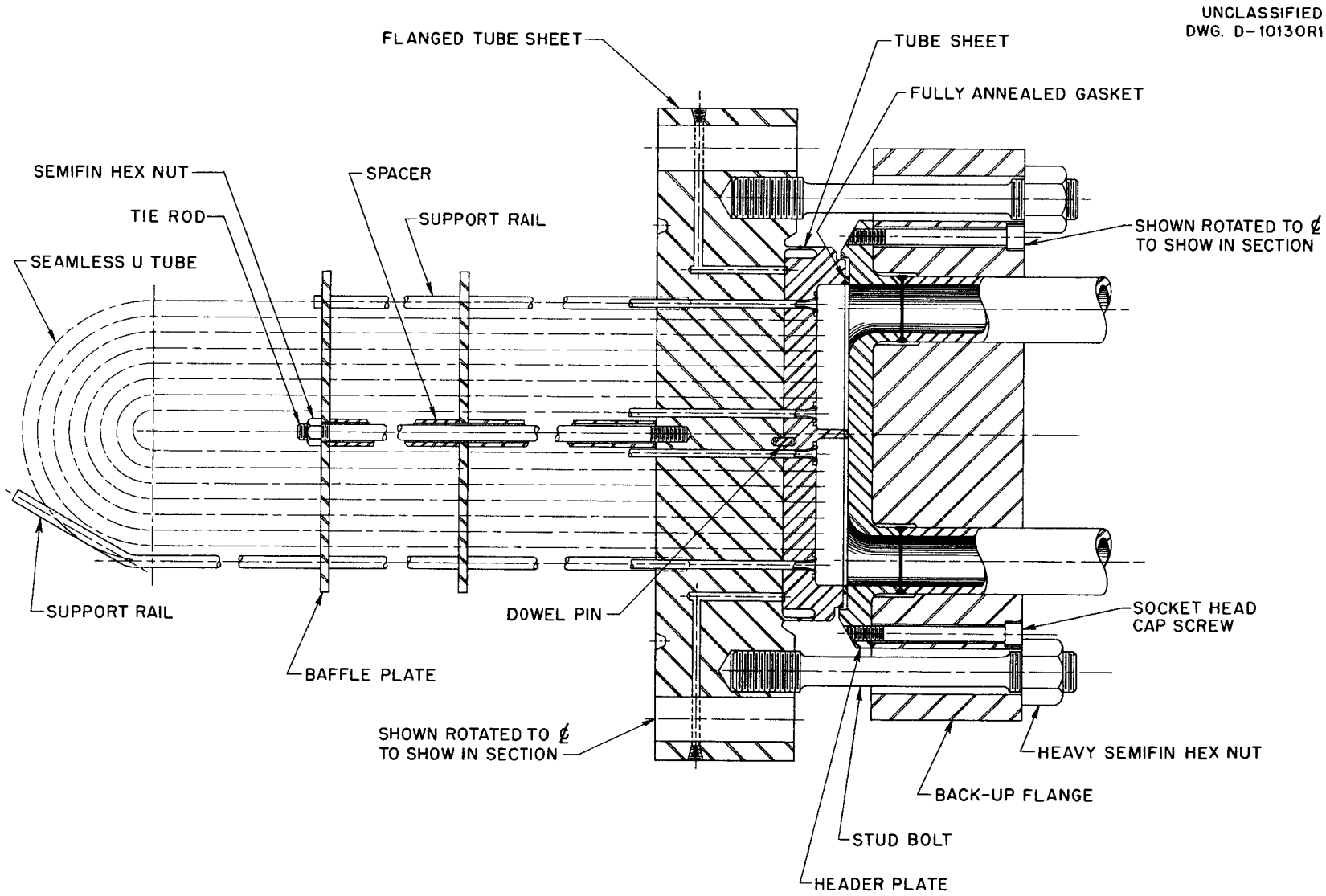

Fig. 10. Alternate Tube Bundle.

halfway around the inlet- and outlet-pipe welds developed and allowed fuel solution to leak from the exchanger. The new head is designed so that these welds are far enough apart to eliminate this problem. Also the thermal stresses are minimized in the new design, and an effort has been made to prevent undue distortion by heat during welding.

CORROSION

E. G. Bohlmann, Section Chief

SCOUTING STUDIES: CORROSION OF STAINLESS STEEL BY URANYL SULFATE SOLUTIONS

J. C. Griess D. J. Sasmor

A possible mechanism for the corrosion of type-347 stainless steel in dilute uranyl sulfate solutions was presented in the last quarterly report. Since that time additional support for the proposed mechanism has been obtained, and the effect of various substances added to the corrosive liquids has been studied. Some of the results obtained strongly suggest that the hydrolytic properties of ferric and chromic ions greatly affect the rate of corrosion.

Most of the experiments described in this report were performed in 120-ml, type-347 stainless steel reaction vessels. Clean surfaces were obtained before each set of experiments by removing any scale with emery paper. All bombs had been used and cleaned prior to these experiments and had received the same mechanical surface treatment. The walls of the bombs used to contain the corrosive solutions served as the corrosion specimens. The surface area of the steel exposed to the solutions was approximately 100 cm^2.

When it was desirable to determine the composition of the gas in a bomb, a valve was connected to the head of the bomb by means of stainless steel tubing. After the bomb cooled, the steel tubing was connected directly to the gas analysis equipment.

Some experiments were run in 12-mm-ID quartz tubes. The desired solutions and a corrosion specimen were placed in the tube and the tube was sealed. Since 12-mm-ID quartz tubes will not generally withstand pressures greater than 200 psi, it was necessary to pressurize the tubes externally in steel bombs. The corrosion specimens used in the tube experiments were cut from a single sheet of type-347 stainless steel 19 mils thick. A surface area of approximately 3 cm^2 was exposed to the solution.

In both types of experiments the walls of the bombs and the sheets were cleaned with trichloroethylene and then given an acetone rinse. The steel was not chemically etched before use. All experiments were run at 250°C under static conditions.

Most of the uranyl sulfate solutions used were from a single batch prepared by Cameron's group at Y-12. Table 8 shows analyses reported by the production group (first analysis) and those obtained by more precise methods recently developed (second analysis). The experiments that demonstrate

TABLE 8

Differences in Analyses of the Same Batch of Uranyl Sulfate Solution

DETERMINATION	FIRST ANALYSIS	SECOND ANALYSIS
U	0.3310 g/g	591.6 g/l
SO_4	0.1341 g/g	229.5 g/l
SO_4:U	1.004	0.961
NO_3	347 ppm	3250 ppm
C		250 ppm
Fe		6 ppm
Halides	$<$ 5 ppm	
pH (1:10 dilution)	2.21	
Density	1.7750	

decreasing corrosion rate with time were run with pure uranyl sulfate solutions that (according to the first analysis) contained no detectable carbon. Silica was introduced into the solutions as a colloidal dispersion of amorphous silica in water. This material is produced by Monsanto Chemical Company and sold under the trade name of "Syton." Molybdenum was added to the solutions as molybdic acid. This material contained approximately 10% ammonia and to date the effect of the ammonia has not been determined. Other solutions were prepared with standard reagent-grade chemicals and distilled water.

Correlation Between the Consumption of Oxygen and the Production of Nickel Ions. It was established previously that nickel ions in relatively low concentrations remain in uranyl sulfate solutions at 250°C. Both ferric and chromic ions are hydrolytically precipitated from uranyl sulfate solutions (40 g of uranium per liter); therefore it is difficult to determine whether the major alloying constituents of the steel dissolve in the ratio in which they are present. However, if the following equation represents the over-all reaction during the corrosion process, the nickel concentration of the solution should be proportional to the oxygen consumed.

$$(Ni, Fe, Cr) + 2\ O_2 + 2H^+ \longrightarrow$$

$$\tfrac{1}{2}Fe_2O_3 + \tfrac{1}{2}Cr_2O_3 + Ni^{+2} + H_2O\ . \quad (1)$$

If the nickel, iron, and chromium contents of the steel are known, it should be possible to determine from the nickel concentration in solution whether the oxygen consumed is equivalent to the steel oxidized.

Four freshly cleaned steel bombs were pretreated with 1% nitric acid for 24 hours. After rinsing the acid from the bombs, 60 ml of uranyl sulfate solution (40 g of uranium per liter) was added to two of the bombs. The other two bombs contained the same volume and concentration of uranium in uranyl sulfate solution in addition to 1 mg of molybdenum (as molybdic acid) per milliliter of solution. All bombs were closed at atmospheric pressure and heated for a given period of time. At the completion of heating, both the gas and the solution in each bomb were analyzed. Aliquots of the same solutions were then placed in the bombs and the procedure was repeated. In all, three separate runs were made with each bomb. Table 9 shows the comparison between the oxygen consumed, as determined from the gas analyses, and the calculated amount of oxygen theoretically consumed on the basis of the nickel analyses. To calculate the oxygen consumption it was assumed that the composition of the alloy was 10% nickel, 18% chromium, and 72% iron. Bombs numbered M1 and M3 contained the molybdenum.

It appears that molybdenum was of no value in reducing the corrosion rate, but it should be pointed out that the very low corrosion rates make it difficult to determine accurately any inhibitor effect with tests of such short duration. The individual comparisons between the measured and calculated oxygen consumptions are not good, but the total oxygen consumed is in good agreement with the total calculated from the nickel ion concentrations. Consideration of the manner in which the oxygen consumed was measured and the analytical accuracy with which such low nickel concentrations could be determined makes these discrepancies understandable. Since a part of the carbon in the uranyl sulfate solution was also oxidized at the high temperature, it was necessary to analyze the gas remaining in the bomb for both carbon

TABLE 9

Comparison Between Calculated and Measured Oxygen Consumption

BOMB NO.	RUN NO.	TIME (hr)	NICKEL (ppm)	CORROSION RATE (mpy)	O_2 CONSUMED (ml)	
					CALCULATED*	MEASURED
M1	1	66	7.5	0.30	1.73	1.04
	2	89	4.5	0.13	1.04	(-0.36)
	3	66	3	0.12	0.69	(-0.16)
2	1	66	7	0.28	1.61	2.12
	2	89	7	0.20	1.61	2.56
	3	66	5	0.20	1.15	1.30
M3	1	66	8	0.31	1.84	0.90
	2	89	9.5	0.28	2.18	2.74
	3	66	7	0.28	1.61	1.11
4	1	66	4	0.16	0.92	1.91
	2	89	5.5	0.16	1.27	3.03
	3	66	4	0.16	0.92	1.33
TOTAL			72		16.57	17.52

*Calculated on the basis of equation 1 by assuming that the alloy was composed of 10% nickel, 18% chronium, and 72% iron.

dioxide and oxygen and to make a correction for the oxygen used to convert the carbon to carbon dioxide. Part of the difference between the calculated and measured oxygen consumption may be the result of determining the measured oxygen consumption by two analyses. The data suggest that selective attack on the components of the alloy did not occur to any great extent when the corrosion rate was low.

Change in Corrosion Rate with Time. A number of experiments have indicated that the corrosion rate observed in a given bomb decreased with time, as can be seen from Fig. 11. Each curve on the graph represents a series of runs of various lengths of time in each of four bombs. All the bombs were pretreated with 1% nitric acid for 24 hr and then heated with uranyl sulfate (40 g of uranium per liter) for given periods. The solution used to obtain curve I contained 0.01 *M* KCl in addition

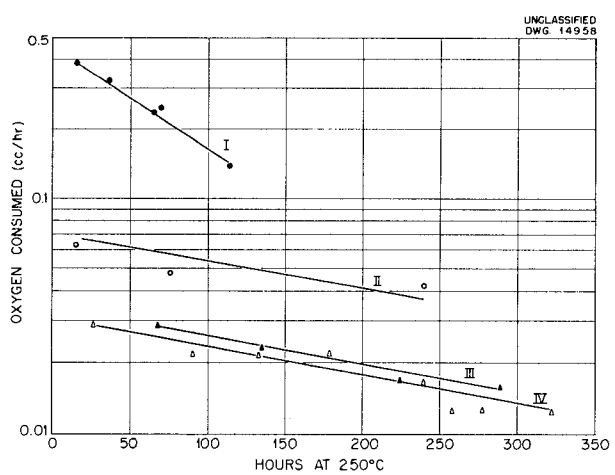

Fig. 11. Decrease of Corrosion Rate with Time.

to uranyl sulfate. Curves I and III were plotted from the data on the nickel in solution, and curves II and IV were plotted from the gas analysis data. As shown above, these two methods are equivalent, but the oxygen analyses were based on the difference between two comparatively large numbers and the nickel analyses depended on only one determination, which probably accounts for the better fit of the points on curves I and III than is obtained on curves II and IV.

Curve I demonstrates the high corrosion rate when chloride ions are present and also indicates that the corrosion rate decreases with time. Curves II, III, and IV have very nearly the same slope, but the rate of decrease is not so large as in curve I. Since each experiment was performed in an identical manner (except I), the displacement of curves II, III, and IV from each other gives an idea of the nonreproducibility of the corrosion rates. It should be noted that the decreasing rate indicated a decrease in the total corrosion but did not give information about localized attack. Pitting was severe in the run that contained chloride ions; with continued use the number of active pits decreased but the depths of those that remained active increased.

Investigation of Inhibitors. In a number of cases the addition of a small amount of a substance to the corrosive medium will materially reduce the corrosion rate. An inhibitor that can be used in reactor solutions must meet the requirements of stability at high temperatures in intense radiation fields, sufficient solubility, and a low neutron cross section. These three requirements eliminate many of the well-known inhibitors; studies are being made of the effectiveness of others.

To date, the only inhibitors that have been studied in uranyl sulfate solutions are silica and molybdic acid. It was thought that silica might be of value because it has been shown to retard the initial attack of chloride ions on stainless steel.[1] Robertson[2] has shown that at room temperature the corrosion of cold-rolled steel by distilled water was greatly retarded when molybdate ions were present in the solution. In fact, under the conditions of the study both molybdate and tungstate ions were as effective as dichromate ions.

In experiments of short duration the corrosion rate of pretreated type-347 stainless steel in uranyl sulfate solutions containing 40 g of uranium per liter was very low. In order to determine the effectiveness of a given inhibitor it was necessary to increase the corrosion rate by increasing the concentration of the uranyl sulfate solution. Solutions containing approximately 300 g of uranium per liter were arbitrarily chosen. A given amount of inhibitor was added to 60 ml of uranyl sulfate solution that was placed in a nitric acid pretreated bomb and heated for a given period. The gas phase contained only air; no excess oxygen was added. Table 10 gives typical data obtained both in the presence and absence of inhibitors. In all cases heating times of 16 hr were used.

There was little if any difference between the attack of solutions that contained silica and those that contained no inhibitors. In both cases

(1) J. C. Griess, "Electrochemical Corrosion Study," *Homogeneous Reactor Project Quarterly Progress Report for Period Ending May 15, 1951*, ORNL-1057, p. 65.

(2) W. D. Robertson, "Molybdate and Tungstate as Corrosion Inhibitors and the Mechanism of Inhibition," *J. Electrochem. Soc.* **98**, 94 (1951).

TABLE 10

Comparative Corrosion Damage in the Presence of Inhibitors

INHIBITOR	ANALYSES								
	URANIUM (g/l)		Ni (ppm)	Fe (ppm)	Cr (ppm)	pH		INHIBITORS (ppm)	
	INITIAL	FINAL				INITIAL	FINAL	INITIAL	FINAL
SiO_2	281	263	585	9	250	1.33	0.65	750	64
H_2MoO_4	272	272	18	6	17	1.40	1.60	3000	1000
	289	290	28	57	32	1.33	1.39	1500	350
None	281	246	737	4	395	1.33	0.61		

severe pitting resulted and it was concluded that silica, by itself, was of no particular value. Molybdic acid seemed to be quite effective at both concentrations. However, when longer heating periods were used both bombs developed large pits. Thus far molybdenum appears to be effective in lengthening the time before rapid corrosion begins but is of little value in retarding corrosion once it starts. Both silica and molybdate were removed from the solution during the corrosion process. Experiments in which molybdic acid was present in untreated steel vessels containing oxygen pressures are reported below.

Some experiments of a qualitative nature have been carried out in quartz tubes to determine the effectiveness of various inhibitors in reducing the corrosiveness of nitric acid to type-347 stainless steel. In these experiments 5 ml of 1% nitric acid containing the inhibitor was sealed in the quartz tube that contained the corrosion specimen. After the tubes were heated for 24 hr, the specimens were examined visually and the solutions analyzed for their nickel content. Table 11 gives the results obtained to date.

Molybdate even at very low concentrations appeared to be the most effective of the inhibitors studied. All specimens showed interference colors which indicated very thin films. However, close examination by Willmarth showed the films to be considerably thicker than indicated by interference colors. A more comprehensive study of these films is being made.

It does not necessarily follow that those substances that decrease the corrosiveness of nitric acid on steel are also effective in reducing the corrosive action of uranyl sulfate on steel, but with molybdate this appeared to be true. The ease and rapidity with which this method can be applied seems to justify its use in obtaining general information about the action of inhibitors.

Nitric Acid Pretreatment of Stainless Steel vs. No Pretreatment. Loop operations indicate that uranyl sulfate solutions can be contained satisfactorily in stainless steel systems that have not received pretreatment. The mere exposure of stainless steel to oxygenated uranyl sulfate at 250°C produces a protective coating with resulting low corrosion rates. A series of experiments was run to compare the differences in behavior between nitric acid pretreated and

TABLE 11

Effect of Inhibitors on the Attack of Type-347 Stainless Steel by 1% Nitric Acid

INHIBITOR	Ni (ppm)	APPEARANCE OF SPECIMEN
None	63	Nonlustrous, black
10 ppm of Mo (as H_2MoO_4)	23	Thin, lustrous; showed interference tints
25 ppm of Mo (as H_2MoO_4)	23	Thin, lustrous; showed interference tints
50 ppm of Mo (as H_2MoO_4)	28	Thin, lustrous; showed interference tints
100 ppm of Mo (as H_2MoO_4)	27	Thin, lustrous; showed interference tints
100 ppm of Mo and 150 ppm of SiO_2	19	Thin, lustrous; showed interference tints
150 ppm of SiO_2	48	Nonlustrous, black
370 ppm of W (as Na_2WO_4)	53	Dark, nonuniform
90 ppm of W (as Na_2WO_4)	52	Dark, nonuniform
1900 ppm of Cu (as $CuSO_4$)	27	Lustrous, showed interference tints
190 ppm of Cu (as $CuSO_4$)	45	Lustrous, brownish black
2000 ppm of $BiONO_3$	33	Lustrous, black

untreated stainless steels on exposure to uranyl sulfate solution. At the same time, the effect of molybdic acid in the system was investigated.

The following solutions were placed in each of four, freshly cleaned bombs. Bomb 5 contained 60 ml of uranyl sulfate solution (300 g of uranium per liter), 2 ml of 30% hydrogen peroxide, and enough solid molybdic acid to make the solution 0.03 *M* in molybdate ion. Bomb 6 contained the same materials as bomb 5, except that the molybdic acid was omitted. Bomb 7 contained 60 ml of 1% nitric acid and bomb 8 contained 60 ml of uranyl sulfate solution (300 g of uranium per liter), 2 ml of 30% hydrogen peroxide, and 160 ppm of molybdenum as molybdic acid. The thermal decomposition of the peroxide produced enough oxygen to give an oxygen partial pressure of approximately 90 psi at 250°C. The bombs were then sealed and heated for 24 hours. After cooling, the solutions in the bombs were analyzed for corrosion products. Then solutions of the same compositions and volumes as the solutions previously used in bombs 5, 6, and 8 were again added, and all the bombs were heated for a given period. In this and all subsequent runs, bomb 7 contained uranyl sulfate solution (300 g of uranium per liter) and 2 ml of 30% hydrogen peroxide. The above procedure was repeated several times; Table 12 summarizes the results.

The only difference between the experiments in bombs 6 and 7 was that bomb 7 received the standard 1% nitric acid pretreatment and bomb 6 received no pretreatment. Since there was no real difference in total corrosion products removed from the two bombs, it appeared that the exposure of stainless steel to an oxygenated uranyl sulfate solution accomplished essentially the same final result as the nitric acid pretreatment.

TABLE 12

Effect of Nitric Acid Pretreatment and Molybdic Acid Addition on the Corrosion of Type-347 Stainless Steel by 1.3 *M* UO_2SO_4 Solution with 90 psi Oxygen

BOMB NO.	RUN NO.	TIME (hr)	Ni (ppm)	Cr (ppm)	Fe (ppm)	INITIAL Mo (ppm)
5	1	24	67	53	16	3000
	2	47	30	34	22	3000
	3	89	16	22	18	3000
	4	64	8	13	19	3000
	5	138	17	20	13	3000
TOTAL		362	148	142	88	
6	1	24	180	10	8	0
	2	47	45	59	13	0
	3	89	15	15	13	0
	4	64	6	13	16	0
	5	138	11	15	12	0
TOTAL		362	257	112	63	
7	1*	24	165	<1	2	0
	2	88	77	85	20	0
	3	66	17	15	11	0
	4	160	15	22	23	0
TOTAL		338	274	122	56	
8	1	24	107	69	7	160
	2	88	9	12	16	160
	3	66	13	7	6	160
	4	160	13	7	6	160
TOTAL		338	142	95	35	

*Contained 1% nitric acid, no added oxygen. Hence Bomb 7 had a standard nitric acid pretreatment but the others had none.

Bombs 5 and 8 were treated in an identical fashion except that bomb 5 contained 0.03 *M* molybdic acid and bomb 8 contained 0.0017 *M* molybdic acid. There was no difference between the results obtained in bombs 5 and 8, but both bombs showed less corrosion than was apparent in either bombs 6 or 7. Table 12 shows the similarity between bombs 6 and 7 and 5 and 8. There was no pitting attack in any of the bombs and no evidence of localized attack even at the water line.

A series of experiments was performed to gain information about the effects of uranyl sulfate and oxygen concentrations on the corrosion rate of untreated stainless steel. For comparative purposes, the experiments were run both with and without molybdic acid, and one set of experiments was run with 0.1 *N* sulfuric acid. A 5-ml aliquot of the solution was placed in a quartz tube containing a corrosion specimen and sufficient hydrogen peroxide to give the necessary oxygen

pressure. The tubes were then sealed and heated for 24 hours. At the end of this time the solutions were analyzed for chromium, iron, and nickel. The molybdenum concentration was arbitrarily chosen as 100 ppm. Table 13 gives the results.

As indicated by the nickel analyses, the stainless steel exposed to 0.1 *N* sulfuric acid was severely, but uniformly, corroded, and both the specimen and the walls of the tube were coated with a heavy layer of mixed iron and chromium oxides. The appearance of the oxides of iron and chromium uniformly deposited on the walls of the tube indicated that since the pH of this solution did not allow for rapid hydrolysis, the iron and chromium ions diffused into the body of the solution. As the corrosion proceeded, the pH of the solution gradually increased with the resulting precipitation of the iron and chromium oxides. The relatively small amount of loosely adhering iron and chromium oxides that precipitated on the steel did not form a very protective coating, and the corrosion rate decreased only as the pH increased.

When the solution contained 40 g of uranium per liter, a uniform, rather thin coat of oxide was deposited on the stainless steel, and there were only very faint traces of red iron oxide deposited on the walls of the tube. The pH of these solutions was apparently high enough to cause complete, rapid hydrolysis very close to the surface of the steel, and the adherent precipitate of iron and chromium oxides formed minimized further attack on the steel. The low iron and chromium concentrations in the solutions and the near absence of precipitated oxides on the surface of the tubes indicated that the hydrolysis was rapid and very nearly complete.

TABLE 13

Effect of Oxygen Pressure on the Corrosion of Type-347 Stainless Steel by Uranyl Sulfate and Sulfuric Acid

SOLUTION AND ORIGINAL pH	OXYGEN PRESSURE (psi)	ANALYSES							
		NO INHIBITOR				WITH INHIBITOR			
		Ni (ppm)	Fe (ppm)	Cr (ppm)	FINAL pH	Ni (ppm)	Fe (ppm)	Cr (ppm)	FINAL pH
H_2SO_4	40	830	7	1	1.50	580	16	2	1.40
0.1 *N*	80	570	3	1	1.40	470	7	1	1.37
pH = 1.19	120	810	9	1	1.50	580	7	1	1.42
UO_2SO_4	40	40	<1	10	2.28	20	1	5	2.30
40 g of U per liter	80	32	1	10	2.16	17	1	5	2.22
pH = 2.40	120	36	<1	10	2.30	18	<1	6	2.03
UO_2SO_4	40	79	17	55	1.40	61	29	44	1.35
315 g of U per liter	80	80	16	55	1.37	65	17	45	1.28
pH = 1.40	120	54	7	57	1.42	45	5	33	1.31

At a concentration of 300 g of uranium per liter the extent of corrosion was somewhat greater. All specimens contained an oxide coating somewhat heavier than that obtained in the less concentrated solutions. The oxide appeared to be less compact than in the previous case, but there was no evidence of a precipitate on the walls of the tube. However, the solutions contained appreciable concentrations of iron and chromium, which indicated less complete hydrolysis than in the more dilute uranyl sulfate solutions.

The effect of the oxygen concentration was of interest. The nickel analyses obtained with 0.1 *N* sulfuric acid and dilute uranyl sulfate solutions indicate that there may be an optimum oxygen concentration. With the more concentrated uranyl sulfate solutions, the corrosion rate continued to decrease and no minimum was found up to the highest oxygen pressures studied. The same phenomenon was observed both in the presence and the absence of molybdic acid.

The presence of molybdate ions in solution decreased the corrosion rate in all cases, but its inhibitor characteristics were not outstanding. Only with the dilute uranyl sulfate solutions was there a pronounced difference in the appearance of the corrosion specimens. The specimens from the solutions containing the molybdate ions had lustrous, copper-colored films, whereas those from the other solutions were nonlustrous and very nearly black.

Discussion and Future Work. The corrosive action of a solution in a metal-solution system may be decreased by the addition of inhibitors. However, it does not necessarily follow that an inhibitor in one system will also inhibit corrosion in another system. In both the uranyl sulfate and nitric acid systems the protective coatings are composed of the same compounds, and it may be that those inhibitors that reduce corrosion in nitric acid will also be effective in uranyl sulfate systems. Further studies are necessary to determine whether this is true.

Of the two inhibitors investigated in uranyl sulfate solutions only molybdic acid showed some ability to retard the corrosion process, but its effect was not spectacular. Its action seemed to be independent of the oxygen concentration and very nearly independent of the initial concentration of the molybdenum. Molybdenum was removed from the solution during the corrosion process and must have been incorporated in the oxide film. In the future some of the films on the surface of the steel will be removed and analyzed microscopically and spectrographically.

Nearly all the experiments completed indicated an initially high corrosion rate that decreased with time. Such behavior was observed whether the steel was first subjected to nitric acid or to oxygenated uranyl sulfate solutions. Since an oxide of the same chemical composition was deposited on the surface of the steel in both cases and since the corrosion rate apparently depended on the completeness with which the steel was isolated from the solution, it seemed only logical that the corrosion rate should decrease as the film increased in thickness. Table 12 shows the initially high corrosion rate followed by a decreasing rate and indicates that, from the standpoint of total corrosion, nitric acid pretreatment has no advantages over no pretreatment in static tests.

The higher corrosion rate in the more concentrated uranyl sulfate solutions appeared to be closely related

to the ability of uranyl sulfate solutions to hold measurable amounts of chromium ions in solution. The data in Table 13 demonstrate this fact. The uranyl sulfate solution with 40 g of uranium per liter and a pH of 2.3 contained 10 ppm of chromium ions, and the solution with 315 g of uranium per liter and a pH of 1.4 contained 55 ppm. The sulfuric acid solution with a final pH of 1.4 had only 1 ppm. Hence, the pH of the solution was not the only factor that determined the chromium ion concentration of the solution. On the other hand, the pH did appear to have an effect on the amount of iron that remained in solution. Future experiments are planned to gain information about the two processes.

DYNAMIC CORROSION STUDIES

H. C. Savage
C. G. Heisig
R. A. Lorenz
D. Schwartz
J. H. Gross
R. E. Wacker

Test Facilities. For clarity, previously reported descriptions of test facilities have been repeated and expanded where necessary in this report.

Loops. The dynamic corrosion and solution stability test program for homogeneous reactor solutions is being carried out in a number of circulating test loops. The basic design of these loops is shown in Fig. 12. To date only solutions of uranyl sulfate of various concentrations and with various additives have been tested.

Circulation of the solution in the test loops is accomplished with a Westinghouse Model 100A, totally enclosed, centrifugal pump (see Fig. 13). In general, these pumps will deliver 100 gpm at a head of 250 ft and are designed to withstand system pressures to 2000 psi. The loops are made entirely of stainless steel and are designed to withstand operating conditions of 1000 psi and 250°C. Type-347 stainless steel is used in all sections that are in contact with the uranyl sulfate solution. Other types of 18-8 stainless steels – types 304, 316, etc. – are used on some parts that are not in direct contact with the recirculating solution or where welding is not required. The circulating lines are either 1- or 1 1/2-in. pipe, whereas the pressurizers are made of 4-in. pipe approximately 6 ft long.

All welding on the loops is now done by the heliarc process with close inspection control. To prevent weld metal burn-through, all work is backed up with helium during welding. The main inspection requirements are smooth weld surfaces inside and out with complete penetration and "Dy-chek" and x ray of the finished work to ensure sound welds. In loops B and C, which were made prior to this inspection procedure, the welds are very poor.

In addition to the welded joints a number of flanged joints are used in the loops for inspection ports and installation of the pressurizers and test sections. A specially designed joint that is now in use is shown in Fig. 14. This type of joint has the advantages of fabrication simplicity, material economy, and minimum cracks for solution hold-up; it has proved to be a very satisfactory, leak-tight joint.

The pressurizer used on the circulating loops has several functions. Under operating conditions the system pressure must be maintained in excess of the vapor pressure of the circulating solution to prevent boiling. This can be accomplished in two ways in the pressurizer. One method consists of heating the pressurizer to the temperature necessary for the required steam

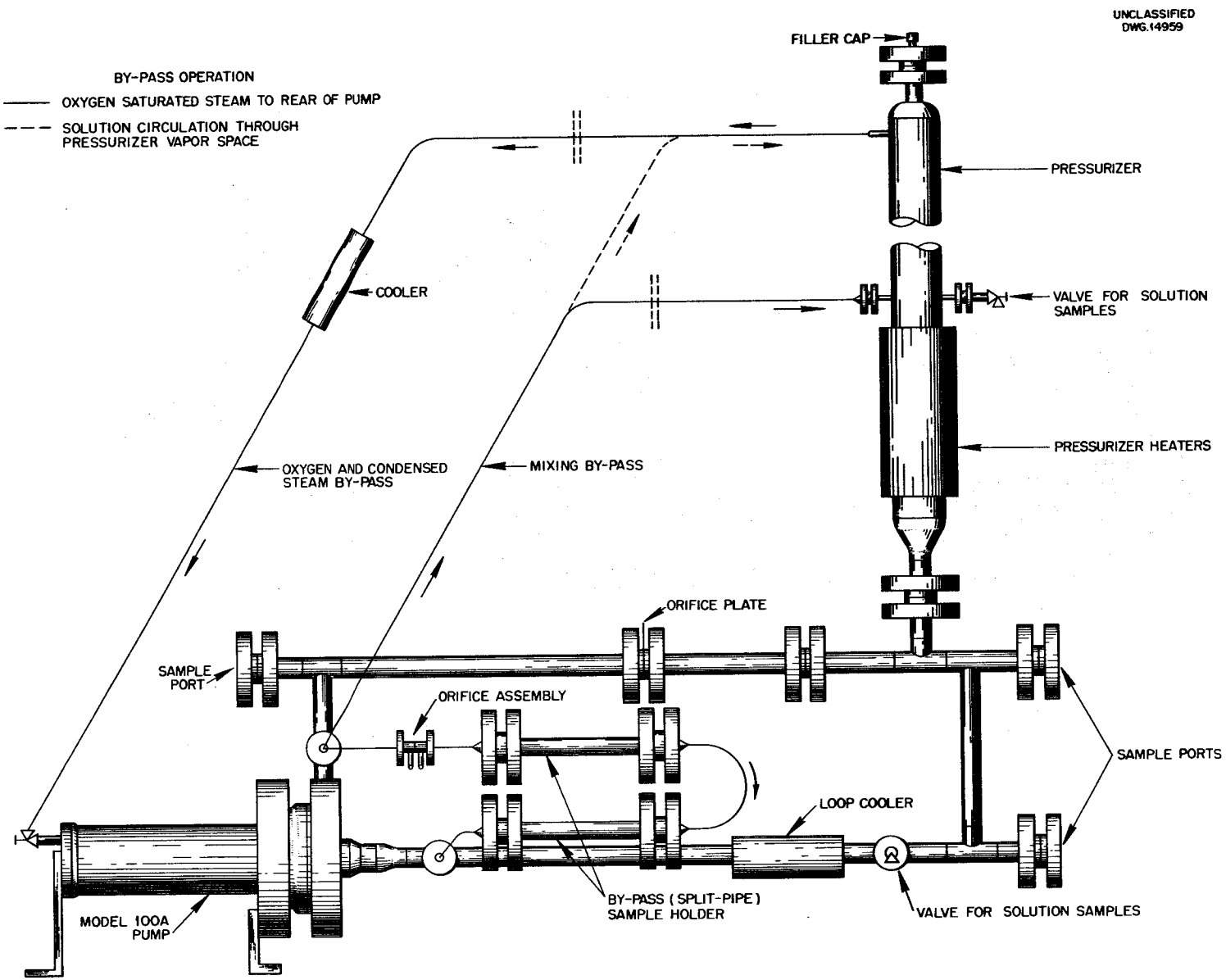

Fig. 12. Test Loop 100A.

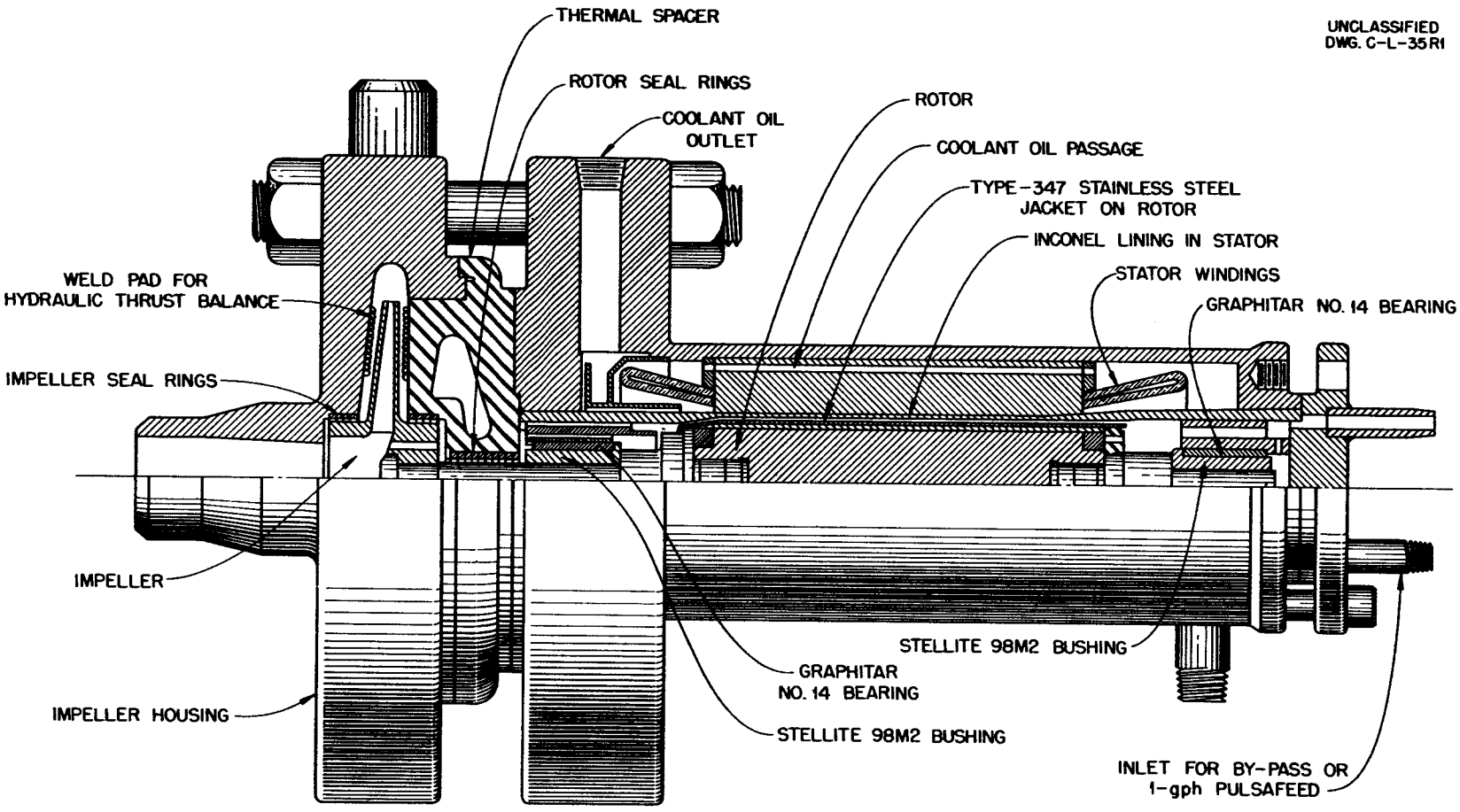

Fig. 13. Modified Westinghouse Model 100A Pump.

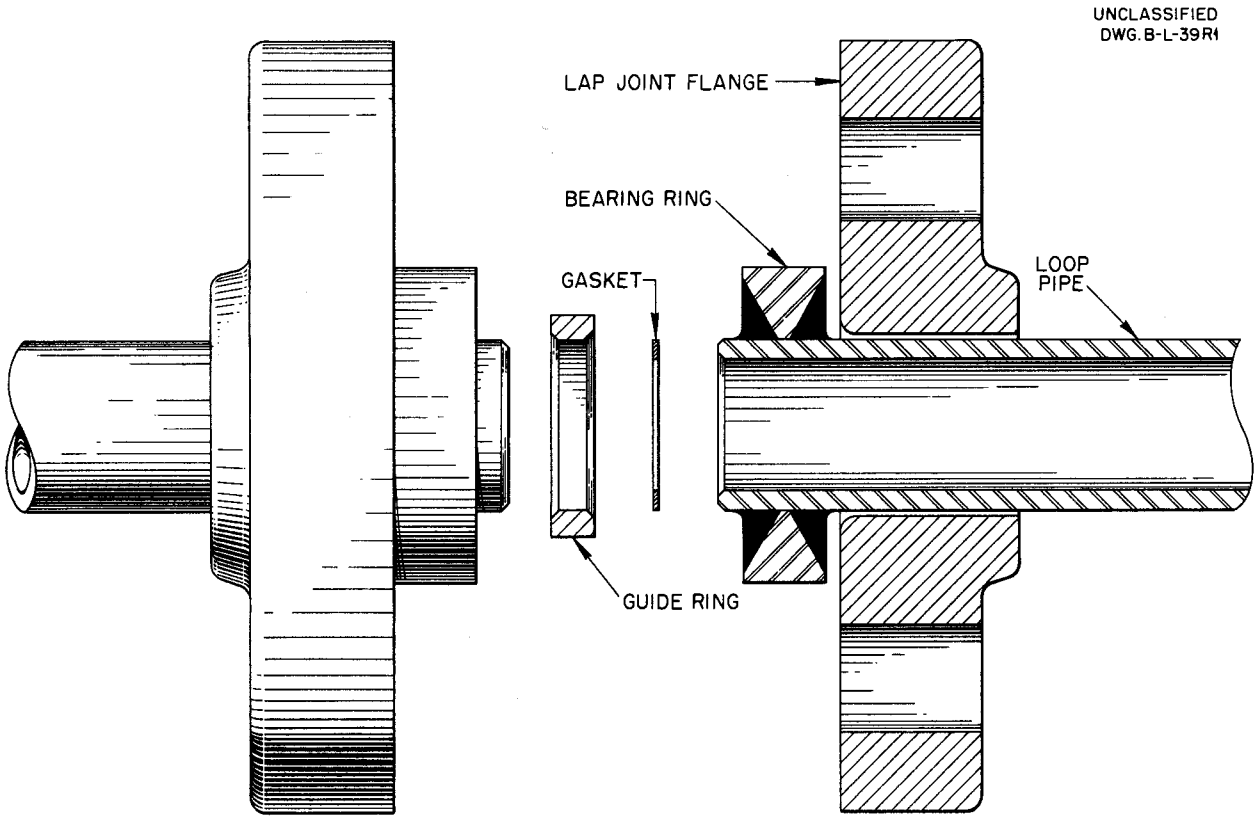

Fig. 14. Special Welding Stub Ends.

pressure with electric heaters embedded in an aluminum jacket cast on the external wall. A second method consists of introducing gas pressure into the vapor space of the pressurizer. In addition to system pressurization, the pressurizer provides free space for expansion of the solution in heating from room temperature to operating temperatures and functions as a reservoir for the excess solution needed for the large number of solution samples removed for analysis during operation.

There are no valves in the main circulating stream of the loops. However, auxiliary valves are needed for sampling, adding gas, and regulating flow through some of the by-pass lines. It was necessary to design and make a special valve, leak-tight on both the seat and packing sides at pressures up to 1000 psi, to satisfy the requirements of all stainless steel construction. The valve that is now in use is shown in Fig. 15. These valves are relatively easy to fabricate and can be welded or flanged into the loop as required. They have proved superior to the conventional bar-stock needle valves. All the materials are resistant to the corrosive action of the uranyl sulfate.

Solution Samplers. Samples of the uranyl sulfate solution are taken regularly during all operating periods, and special sampling equipment is required since the loops operate at 1000 psi and 250°C. A stainless steel sampling bomb of 30 to 60 cc vol is used. The bomb has a valve at each end and is connected to a valve on the loop through a side opening fitted with a standard 1/4-in. flared tube

fitting. A sample is obtained by closing the valves at the ends of the bomb and then opening the loop valve. As soon as the bomb is filled with solution, the loop valve is closed. After the solution in the bomb has cooled, the end valves are opened and the sample is removed.

Solution samples for gas analysis are obtained similarly, except that the bomb for obtaining them has no side opening. The evacuated bomb is connected to the loop valve through one of the end valves of the bomb, and the sample is taken by opening the loop valve and the bomb valve connected to it. As soon as the bomb has filled, these two valves are closed so that a known volume of solution and the gas it contains are sealed in the bomb. After cooling, the bomb is connected to an Orsat gas analyzer and the gas is transferred by steam distillation.

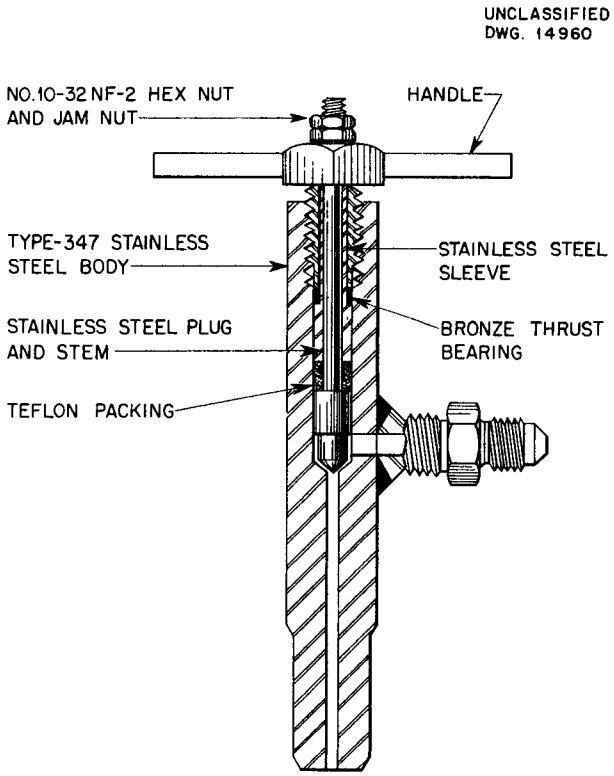

Fig. 15. Solution Sampling Valve.

Corrosion Sample Holders. To facilitate dynamic corrosion testing of various materials, by-pass sample holders have been incorporated in the loops. The by-pass units are connected across the pump head as shown in Fig. 12. The holders consist of a section of pipe with flanged openings at each end for installation of various specimen samples. The original purpose of the sample holders was to provide a section of material that could be removed for inspection and through which uranyl sulfate would flow in a manner similar to the flow in the main loop. Therefore a split length of material with a round bore was designed for installation in the by-pass holders. As the design progressed, it became obvious that these split sections could be adapted for use as holders for a large number of either plates or pins, and that by varying the cross-sectional area of the bore the effects of velocity might be studied. Accordingly, several types of split sections and specimens were designed. The bores, specimen size, and free area were sized so that approximately 15-gpm flow through the holders gave a maximum bulk velocity of approximately 25 ft/sec. The tapered bore holders were designed to give an eightfold increase in velocity from inlet to exit (a maximum range of approximately 10 to 80 ft/sec).

The types of split sections and specimens used are described in the following:

1. CYLINDRICAL BORE, NO TAPER. This section is used for studying corrosion and erosion in straight pipe sections of various materials.

2. ROUND PIN HOLDER, STRAIGHT BORE. This section is used for rough sorting of various materials in the form of round pins. Since the flow around the pins will be turbulent and directed against and around the pins, erosion

and corrosion will probably be abnormally high. The possibility of galvanic effects between the pins and holder has led to the search for a suitable insulating material at the points of contact.

3. FLAT PLATE HOLDER, STRAIGHT BORE. This section is used for obtaining semiquantitative data on the corrosion of various materials that show promise in experiment 1. Flow by the flat plates is more streamlined than in the pin holder since only small areas of the plates are subjected to the direct impact of liquid.

4. FLAT PLATE HOLDER, TAPERED BORE. This section is used to study the effect of velocity on corrosion and erosion rates. The same type of flat plate samples are used as in experiment 2.

The following typical assembly procedure is given to explain the functions of the various parts of the assembly (also see Fig. 16).

1. Selected and marked specimens are weighed, measured, photographed (if desired), and assembled in holders in such a way that the direction of flow past the specimens is known.

2. The halves of the split sections are assembled and clamped together with bands.

3. The end adapter is then fitted to the outer shell.

4. The sample holders are inserted so that the tapered end of the holder is snugly seated in the adapter.

5. Stainless steel gaskets, 0.020 in. thick, are slipped over the free end of sample holder. When the gasket is snug on the holder taper, the clearance between the outer-shell flange face and the gasket is approximately 0.015 to 0.020 inch.

6. The other end adapter is then put in place.

Westinghouse Pump. The Westinghouse, Model 100A, centrifugal pump used for circulating uranyl sulfate in the test loops has a 3-phase, 3400-rpm, squirrel-cage induction motor. The pump is totally enclosed, and the rotor operates in the solution being pumped. The electrical stator windings, cooled by circulating oil, are protected from the uranyl sulfate solution by a 0.040-in.-thick Inconel diaphragm. The rotor is covered with a stainless steel can. The journal bushings are of Haynes Stellite 98M2, the bearings are Graphitar No. 14, and the seal rings around the impeller hubs are tantalum. All other parts of the pump that are in contact with solution are fabricated of 18-8 stainless steels. As purchased from Westinghouse, the pump is equipped with titanium carbide journals and nickel gaskets, seal rings, and labyrinth rings. Since these materials are not resistant to the corrosive action of uranyl sulfate solution, they have been replaced.

Stainless steel or tantalum labyrinth rings in the thermal spacer that separates the pump from the motor prevent excessive mixing of the hot solution in the impeller housing with the cooler solution in the motor region. At a circulating-solution temperature of 250°C, the temperature of the solution in the motor and bearing region is approximately 80 to 110°C.

Tantalum seal rings are installed around the front and rear hubs of the stainless steel, closed impeller to reduce pumping loss. Since the thrust-bearing surfaces are small and will not carry a large thrust load, it is necessary to remove any thrust load by

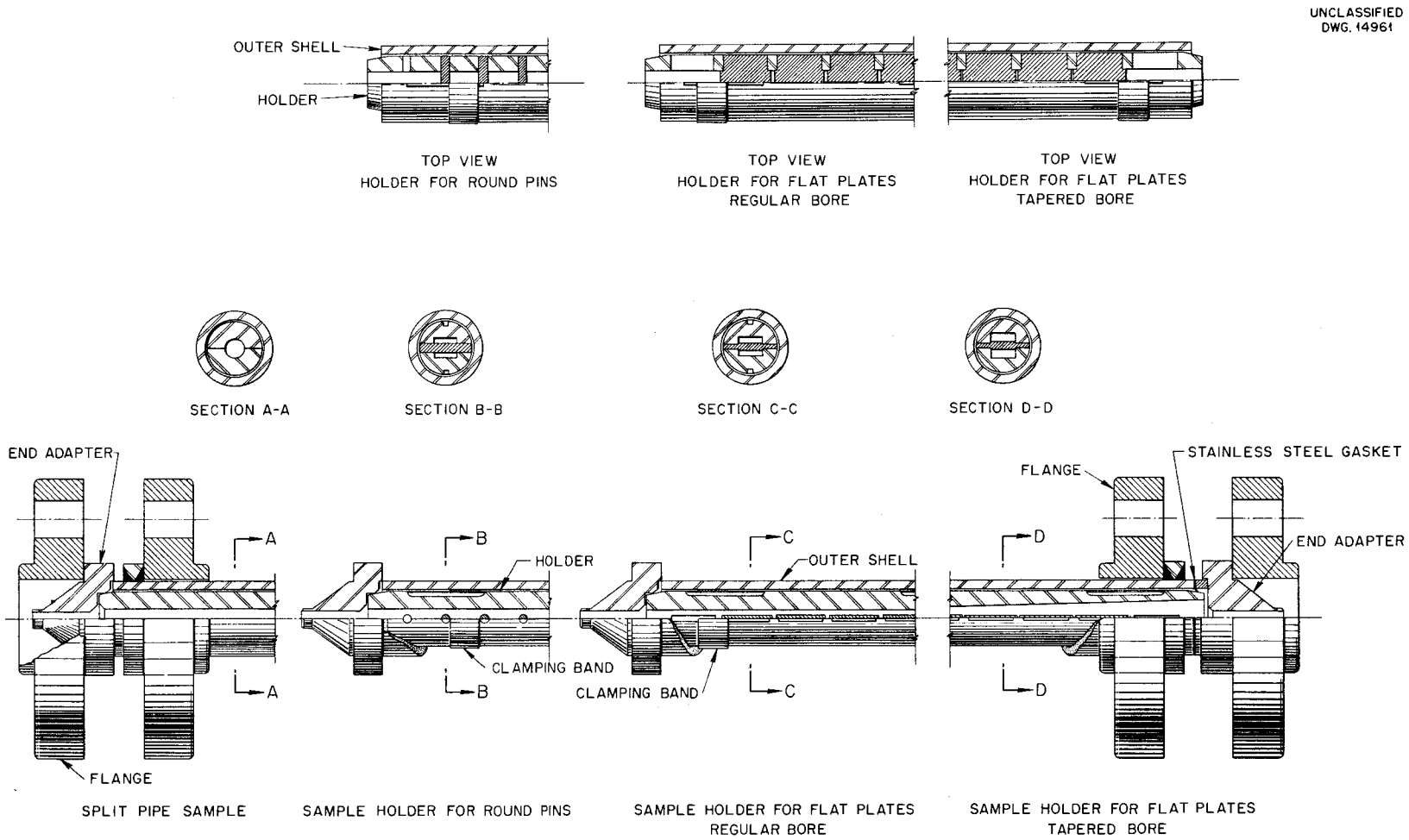

Fig. 16. Sample Holder Assembly.

hydraulic balance of the impeller. The thrust load is balanced by the combined action of the seal rings at the impeller hubs and radial weld pads or ribs on the thermal spacer and the impeller housing. Four pads, approximately 2 5/16 in. long, 1 in. wide, and 1/8 in. thick and made of weld metal deposited on the casing walls, are placed 90 deg apart on the front and rear impeller casing walls. The front and rear pads are 45 deg out of phase. Small holes drilled through the impeller hub tend to equalize the pressure on both sides of the impeller, whereas the weld pads increase the pressure between the shroud and casing as the impeller moves closer to the particular casing; the impeller, therefore, seeks an axial balance position. In practice, the position of the impeller, and thus the rotor, is changed by shimming or machining until the rotor rides free of the thrust-bearing surfaces. In all pumps there is 0.030 to 0.060 in. of freedom of movement of the rotor between the two thrust surfaces.

Approximately 14,000 hr of operating time has been accumulated on ten Model 100A pumps at system pressures of 500 to 1000 psi with solution temperatures up to 250°C. Operating time on individual pumps varies from a few hundred to more than 5000 hr on one pump. Various uranyl sulfate solutions with up to 300 g of uranium per liter have been used. In general, pump operation has been very satisfactory. The most frequent source of trouble has been loss of hydraulic thrust balance with resultant wear of either the forward or rear thrust-bearing surface. This loss of thrust balance, found to be the result of excessive corrosion of the 0.010-in.-thick stainless steel seal rings, has been virtually eliminated by the use of tantalum seal rings.

In going to higher concentrations of uranium in the uranyl sulfate solution, it became necessary to make modifications to prevent overloading of the pump motor. For uranyl sulfate solution with 300 g of uranium per liter, the solution density at 20°C is about 1.4 g/cc, compared with about 1.05 g/cc for a uranyl sulfate solution with 40 g of uranium per liter. Therefore at the higher concentration a corresponding increase must be made in the input power to the pump. Consequently, a series of tests was run on a Westinghouse, Model 100A, pump to determine its adaptability to solution densities up to 1.4 g/cc.

The pump was installed in a circulating loop and a series of pump characteristics measured (Fig. 17). The density-power relations were determined (Fig. 18) for two different flow rates. Solution density was varied by increasing the temperature of the circulated water and by additional runs with various concentrations of uranyl sulfate.

In order to pump solutions with densities to 1.4 g/cc without exceeding the power limits of the pump motor, the diameter of the pump impeller was reduced. Since the power varies approximately as the cube of the diameter and the flow is approximately proportional to the diameter, reducing the impeller diameter gave a large reduction in the input power at only slightly reduced flow rates. The diameter of an impeller was therefore reduced, first 3/8 in. and then 5/8 in. from the original 8 3/4-in. diameter.

With an impeller reduced 5/8 in. in diameter, another series of runs similar to those with the standard impeller was made. The pump characteristics (Fig. 17) show that reducing the diameter of the impeller caused

fairly large reductions in head and input power and small reductions in efficiency at corresponding capacities. The density-power relations are given in Fig. 19.

Test runs with a uranyl sulfate solution containing 300 g of uranium per liter are now being made by using an impeller with the diameter reduced 5/8 inch. The stainless steel impellers in the Model 100A pumps have been excessively corroded by uranyl sulfate solution, and since excellent corrosion results were obtained with titanium metal in the pin type of holders, a titanium impeller for the pump is being made.

Loop Operation. In addition to changing the solution in the loop, the operating conditions that may be varied are temperature, pressure, flow rate, and dissolved-gas concentration.

Physical Condition Control. The temperature of the pressurizer is controlled by electric heaters. The pump usually generates enough heat in circulating the liquid in the closed system to necessitate cooling the loop. A drip cooler is used in which the amount of cooling water is controlled by an air-operated valve. Loops with a large area exposed to air are insulated and provided with heaters similar to the pressurizer heaters. The heaters and coolers are operated by controlling pyrometers.

A loop superpressure of at least 200 psi, which is regulated either by pressurizer temperature or by gas pressurization with the addition of

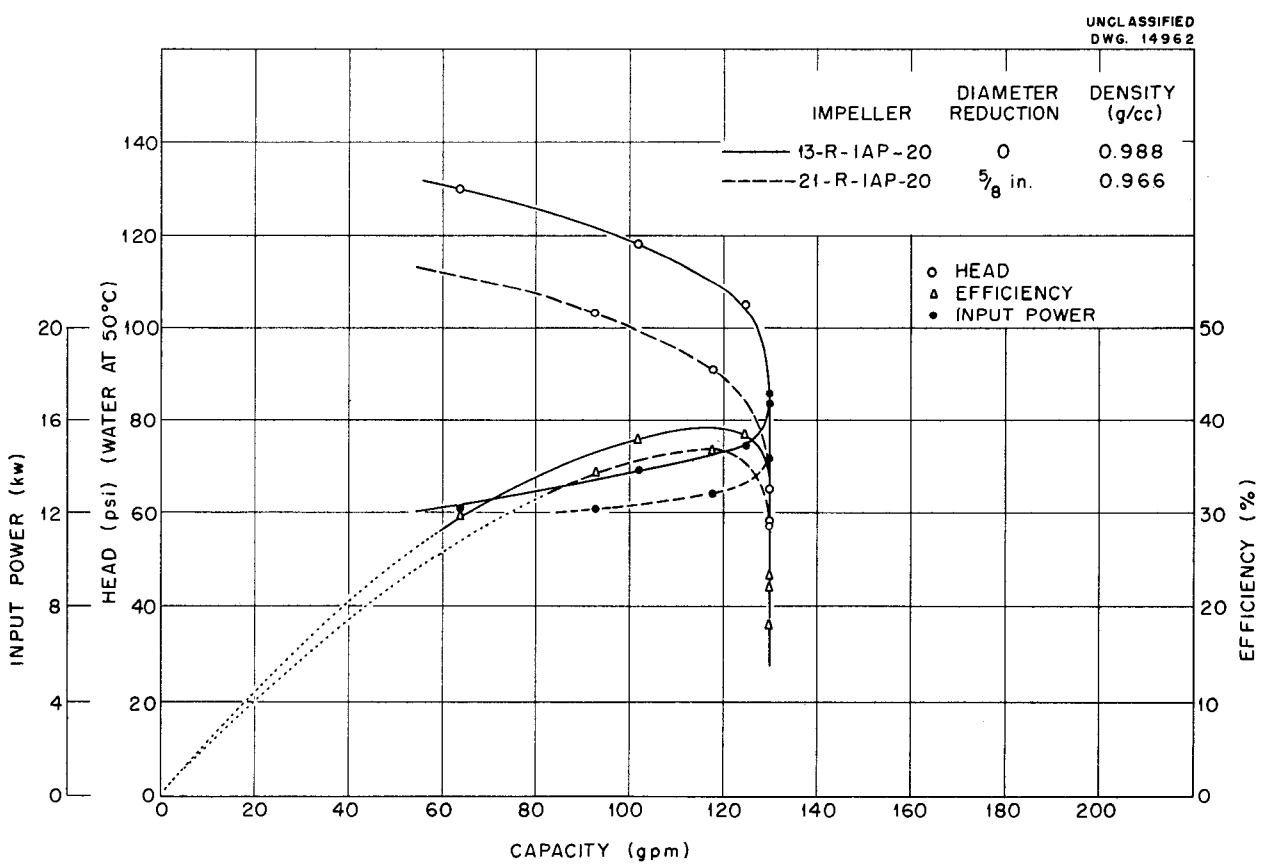

Fig. 17. Characteristics of Model 100A Pump. Loop F.

helium and/or oxygen, is maintained to prevent vapor binding of the impeller. When using gas pressurization the void space of the cold pressurizer is filled with gas to the required pressure from compressed-gas cylinders. Helium is used to dilute the oxygen when low dissolved-oxygen concentration is desired. A small amount of oxygen is added regardless of the method of pressurization in order to maintain solution stability.

Flow in the loop may be varied by changing the opening in the removable orifice-plate restrictor. Loops E and F have calibrated orifice plates in the line for measurement of flow. A differential-pressure cell is used to determine the pressure drop across the calibrated orifice. The by-pass sample-testing lines have calibrated orifice assemblies for measuring flow. A restrictor may be used in these lines to control the velocity through the sample holders. A wide range of fluid velocity is attainable with the 1-in. and 1 1/2-in. circulating lines in the loops that are now operating.

In order to protect personnel and equipment, safety cut-outs are used that operate on pump cooling-oil pressure, pump-case temperature, high loop temperature, high pressurizer temperature, and high and low pressure.

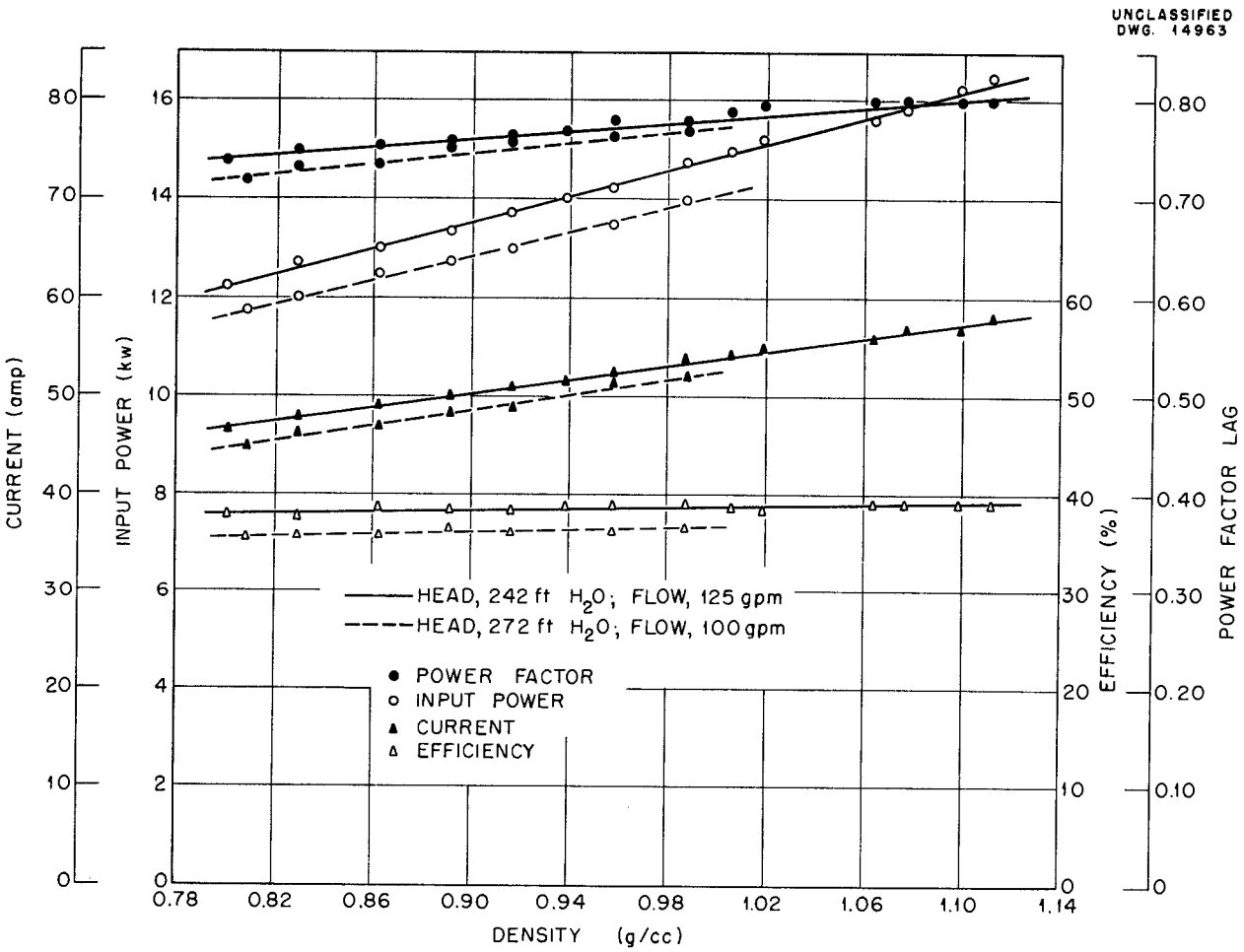

Fig. 18. Density-Power Relationship for Model 100A Pump with Standard Impeller. Loop F.

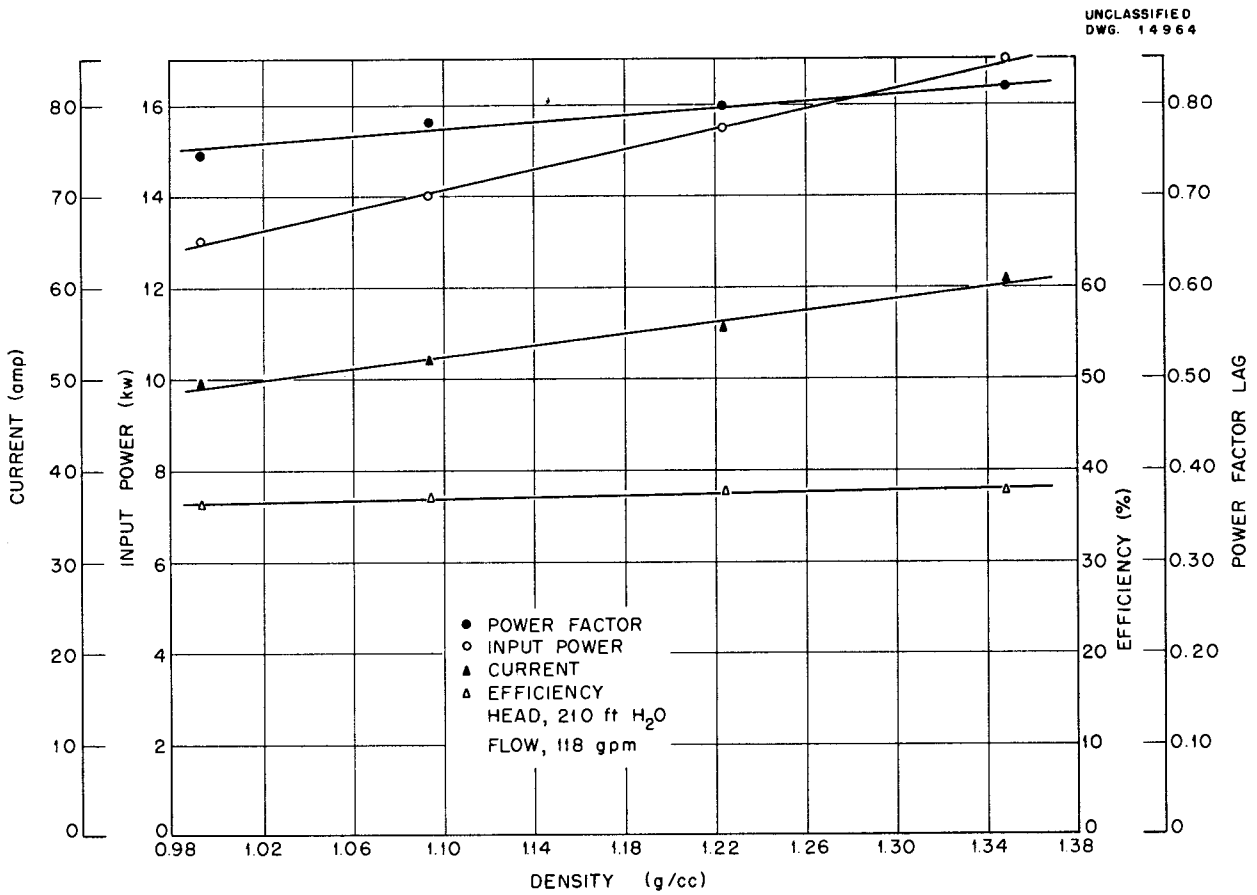

Fig. 19. Density-Power Relationship for Model 100A Pump with Impeller Reduced 5/8 in. in Diameter. Loop F.

Dissolved-Gas Control. The necessity of keeping a small amount of oxygen in the uranyl sulfate solution under operating conditions has been established. Adequate mixing of the solution with oxygen in the pressurizer vapor space is accomplished by manipulation of 1/4-in. stainless steel tubing by-passes. Several schemes have been used successfully.

One method for maintaining oxygen in solution is to connect a 1/4-in. tubing line from the top (vapor space) of the pressurizer to the lower pressure area in the rear of the pump (Fig. 12). Steam that is carrying oxygen is condensed by a cooling jacket on the line and clean water saturated with oxygen is produced. The stream passes through a regulating valve into the rear of the pump and thus to the circulating solution. This method has the advantage of supplying clean water to the pump bearings. To prevent concentration of the solution in the pressurizer, a small, flow-mixing by-pass is run from the pump discharge into the pressurizer liquid space. The amount of oxygen maintained in solution by this method is limited to the amount that can be dissolved in water and carried over at 1000 psi. If undissolved or excess gas is introduced to the pump through this line, bearing wear will result from poor lubrication. Also, the introduction of excess gas through the

rotor chamber to the impeller region results in gas binding of the pump. Therefore low oxygen pressures are used and the maximum oxygen concentration in solution is about 500 ppm. The low oxygen pressures used require that the pressurizer temperature be higher than the loop temperature in order to maintain system superpressure. Close control of the oxygen concentration is not possible with this method because of the above limitations and uncertainty in regulating the amount of solution flowing in the by-pass lines.

A second method is to increase the cold oxygen pressure in the pressurizer to 200 to 300 psi in contrast to 10 to 50 psi used in the first method. The by-pass to the rear of the pump is removed or closed off, and a 1/4-in.-tubing line is connected from the pump discharge to the top of the pressurizer (Fig. 12). This gives circulation of liquid through the gas-vapor space of the pressurizer, where the uranyl sulfate picks up oxygen, and back to the circulating line. The pressurizer and line temperatures are the same under these conditions. With this method oxygen concentrations up to 3000 ppm can be obtained. Lower oxygen concentrations are achieved by diluting the original oxygen in the pressurizer with helium. A fairly close control of dissolved oxygen concentration can be maintained with this method.

Status of the Loops. Nine circulating test loops have been constructed and put into operation, and three others are almost completed. The operating time on various loops varies from a few hundred hours on the newer loops to approximately 5000 hr on the older ones. The loops are operated continuously.

Loops A, B, and C have operating times of 3000 to more than 5000 hr with uranyl sulfate solutions. Some operating time on loop A has been with mixtures of hydrogen and oxygen. Proper shielding has been installed on this loop to protect personnel in the event of an explosion. Loops A, B, and C have 1-in. circulating lines; the remaining loops (E, F, J, K, L) have 1 1/2-in. circulating lines. Loop M has 1 1/2-in. carbon steel lines with a Westinghouse Model 30A pump (30 gpm at 100-ft head) and is being used to study corrosion of materials used in the reflector system of the HRE. The circulating liquid is water.

Loops B and C have been dismantled and sectioned for more detailed corrosion inspection. The new loops being installed have a number of different pipe bends and fittings with which to evaluate the effect of areas of high flow and turbulence.

Fuel System Test Results. The effects of oxygen concentration, hydrogen addition, and copper addition on the stability of fuel solutions has been studied. The number of new loops being put into service has increased, and to facilitate their use a standard preparational procedure has been developed.

Oxygen Concentration. Uranyl sulfate solution with 40 g of uranium per liter has shown stability at O_2 concentrations ranging in loop B from 50 to 600 ppm during approximately 4000 hr of operation at 250°C and in loop C from 600 to 3000 ppm during approximately 2300 hr at 250°C. An additional 1000 hr of operation with loop C was obtained at 150°C with the higher O_2 concentrations.[3] The loops were shut down and allowed to cool rather often during these

[3] J. H. Gross, H. C. Savage, C. G. Heisig, R. A. Lorenz, and R. E. Wacker, "Dynamic Corrosion Studies," *Homogeneous Reactor Project Quarterly Progress Report for Period Ending November 15, 1951*, ORNL-1221, p. 32.

experiments, and lost solution and O_2 were restored as necessary. (At present, there are no means for continuous gas addition, and leaks and consumption in corrosion cause a continual decrement in O_2 concentration between additions; hence, the concentrations of O_2 vary as shown above.)

No precipitation occurred in any of these experiments. During a large part of the time that loop B was operated a synthetic fission-product mixture was present, and for a brief period 1.5 g of copper(II) was added per liter of solution. Evidently the presence of these materials has no adverse effect on stability of the solution. It is now apparent that stability of the uranyl sulfate with 40 g of uranium per liter is assured with O_2 concentrations of at least 50 ppm. Actually, there have been several brief periods of operation with the solution containing fission products during which analyzed values of O_2 concentration were less than 10 ppm. However, it will not be possible to reduce the recommended minimum concentration until operating time at lower and better controlled O_2 concentrations has been accumulated. More complete understanding of the fundamental aspects of stabilization by oxygen is also required.

Stability of Uranyl Sulfate Solution with 300 g of Uranium per Liter. The stability of uranyl sulfate solution with 300 g of uranium per liter at 250°C has also been investigated. Since the corrosion rate is much higher at this concentration (see below), the operating time has been necessarily quite short. Loop F was run for 130 hr with 1000 to 1500 ppm of O_2, 84 hr with 700 ppm of O_2, 100 hr with 110 to 250 ppm of O_2, 53 hr with 60 to 120 ppm of O_2, 70 hr with 40 to 60 ppm of O_2, and 50 hr with 1000 ppm of O_2. There was no evidence of precipitation during these short periods. Comparing this with the experience with solutions containing 40 g of uranium per liter, it appears that the quantity of O_2 required for solution stability is independent of uranium concentration.

Hydrogen Addition. During the period covered by this report, loop A has been operated under an atmosphere of hydrogen and oxygen to determine the possible effect of hydrogen in various proportions on oxygen-stabilized uranyl sulfate solution with 40 g of uranium per liter. The operating temperature in the loop was 250°C. The lack of a method for continuous, closely controlled gas addition has seriously hampered the operation. During the first 400 hr, H_2 and O_2 were added in mole ratio $H_2/O_2 = 2$, at total cold gas pressures of 60 to 150 psig. The pressurizer was operated at 285°C, with a small stream of condensed steam plus entrained gas being returned to the loop via the back of the pump.

The data obtained in this manner were erratic. Both gases tended to disappear from the solution, with O_2 disappearing more rapidly than in the absence of H_2 on other loop runs. It was found necessary to renew the charge of gas daily. On several occasions, improper functioning of the gas circulation arrangement caused loss of gas in solution; when the O_2 concentration in the loop was zero, precipitation began.

To improve the reliability of gas distribution in the system, the condensate by-pass to the back of the pump was removed and a solution by-pass from the pump discharge to the pressurizer vapor space was installed. This modification required operation of the pressurizer at 250°C and maintenance of total cold gas pressure of 250 to 300 psig. Four hundred and

fifty hours of additional time have been accumulated in this manner. The charge of gas was renewed daily with H_2/O_2 mole ratios of 2, 4, and 6. During the day's operation, the ratio of the gases in solution increased as before. The onset of precipitation was evident on two occasions when no O_2 was found in solution, but no precipitation was observed at dissolved-gas ratios as high as $H_2/O_2 = 30$.

The unusually rapid disappearance of O_2 from solution (compared with behavior in the other loops) may be ascribed to recombination with H_2. The presence of H_2 does not seem to have any more direct effect than this on the stability of uranyl sulfate, even when H_2 is present in large excess.

Copper Addition. Short-term studies[3] on the effect of copper(II) added to fuel solutions containing 40 g of uranium per liter and fission products have been extended to 600 hr of operating time. Copper(II) was added as $CuSO_4$ at a concentration of 1.5 g of copper per liter, and O_2 concentration below 600 ppm was maintained. The behavior of this system was not unusual, except that the pH of the solution slowly assumed values of 2.1 to 2.2 rather than 2.4 to 2.7 as found in operation without additives.

Experiments also have been conducted with copper(II) in 0.1 *M* concentration (6.4 g of copper per liter) in UO_2SO_4 solution with 40 g of uranium per liter and O_2 concentration above 1000 ppm. This work was performed in loop L, a new loop prepared by pretreatment with oxygenated H_2O at 250°C, as described below. Three hundred hours of running time have been logged with four start-ups. There has been no precipitation, although the pH behavior of the solution has been significantly different from any encountered in a simple fuel solution.

Two new fuel solutions, made to the concentrations of uranium and copper given above, showed pH values of 2.50 and 2.55, respectively, at room temperature – entirely normal behavior for simple uranyl sulfate solutions of this concentration. When the first of these solutions was used in the loop, the pH rose to 3.4 as soon as the loop reached 250°C, and then in the course of 1 hr fell to 2.1. Through 40 more hr, the pH was at a value of 1.95; the run was then terminated because of a bearing burn-out. O_2 concentration ranged from 3000 ppm at the start to about 1500 ppm at the end. The pH of the solution drained from the loop (after several hours of cooling time) had risen to 2.4; however, the low pH values obtained on samples taken during the run (1.95 to 2.0) remained unchanged after a week at room temperature. No significant change in uranium concentration was noted at any time.

A second run was made with a new batch of fuel solution after thorough cleaning of the loop and 50 hr of additional operation with oxygenated H_2O (cleaning involved operation at approximately 150°C with 2% trisodium phosphate, followed by 5% HNO_3 for several hours). The previous behavior on start-up was repeated faithfully. After 4 hr of operation at 250°C, by which time the pH had fallen to 2.0, the loop was shut down for 16 hr and cooled but not drained. After restarting, the pH rose to 2.2 and quickly decreased to 2.0, where it remained. The procedure of shutting down and restarting was repeated later in the run with precisely the same result. The solution has not yet been drained from the loop.

No reasonable explanation for the behavior of this system has been advanced. A small-scale investigation of the chemistry of the system has been requested. The rather high,

general corrosion rate is described below.

Pretreatment with Oxygenated Water. With an increased number of new loops being put into service, a standard preparational procedure has been adopted. This involves cleaning by running with alternate charges of trisodium phosphate and 3 to 5% HNO_3 at temperatures below 150°C for periods of 2 to 12 hr, rinsing with water to a pH greater than 4.5, and then operating the loop at 250°C with water containing more than 1000 ppm of O_2 for several days. The procedure is also applied to any loop that has undergone precipitation or other drastic treatment before returning it to experimental use.

Corrosion. The practice of expressing general corrosion rates in terms of the increase in dissolved nickel per unit time per unit area of submerged surface has continued for lack of a more meaningful measure. The dubious character of numbers so devised has been clearly demonstrated by observations on loops B, C, and F during this period.

Erosion-promoted Attack. Loop C, which had displayed a general corrosion rate of less than 1 mpy for the preceding 1400 hr, developed a pin-hole leak at 3300 hr of total running time and was sectioned for inspection. The loop had operated with uranyl sulfate solution (40 g of uranium per liter) and O_2 concentrations above 600 ppm during all of its service. It ran at 150°C for about 1100 hr and at 250°C for the remainder of the time.

The leak terminating the life of this loop occurred as a result of very severe localized pitting in a welded cross that was part of the main pipe circuit. The section in question is shown in Fig. 20. This component was made by welding together four properly shaped pipe ends; it was made before institution of the present rigid inspection standards for welds and was not x rayed. It can be noted that both insufficient penetration and and excessive bleed-through took place in making these welds. Since analyses of various parts of this specimen showed that the welding material used was type-347 stainless steel, it was evident that the correct welding material has been used.

The pit that broke through was just downstream from the large lump of weld metal which bled through into the seam forming the lip of the inside of the turn for the main flow. It is quite likely that the initiation and development of this pit was, in large part, the result of the presence of severe turbulence or bubbling behind the protruding lump. The maximum depth of the pit approached the nominal wall thickness of the pipe.

Two other sections of this loop were subject to similar gross loss of metal. Figure 21 is a photograph of a tee in the main pipe circuit. This piece was made in the same manner as the cross described above, suffered from the same defects, and was attacked in the same fashion but to a lesser degree. Figure 22 shows the flow restrictor from loop C. At its original dimensions, the bulk velocity of fluid in the throat was in excess of 100 ft/sec. Heavy attack had increased the throat radius at least 0.100 inch. The three characteristic degrees of attack described previously[4] in connection with pin specimens are clearly seen in this flow restrictor. In the center region, originally of smallest diameter, unrestrained third-degree bare-metal attack took place.

[4] E. E. Bohlmann, J. H. Gross, C. G. Heisig, R. A. Lorenz, and H. C. Savage, "Dynamic Corrosion Studies," *Homogeneous Reactor Project Quarterly Progress Report for Period Ending August 15, 1951*, ORNL-1121, p. 42.

On either side of this region some film was maintained, and a considerably reduced but still unacceptable second-degree rate of removal occurred. First-degree attack, which involves removal of metal at a rate that may be acceptably low, occurred in the entrance and exit of the restrictor and in all wall sections of straight pipe. The attack at the entrance and exit of the restrictor is somewhat complicated by the contribution of some second-degree attack at the (poor) welds joining the restrictor to the main pipe. Pitting was enhanced in the transition zone between the areas of first- and second-degree attack, perhaps because of a local upset in the flow pattern when passing from rough to smooth wall.

At the time of failure of loop C, loop B had been operating for 5100 hr at 250°C with uranyl sulfate solution (40 g of uranium per liter) and less than 600 ppm of O_2. At about 3500 hr, an extensive deep pit was observed in a cross in loop B, and a decision was made to run the loop to failure with uranyl sulfate solutions containing fission products and low O_2 concentration. In the interest of safety of the operation, this decision was changed after the failure of loop C, and loop B was sectioned for examination at 5100 hours. The cross and tee corresponding to those of loop C are shown in Figs. 23 and 24. These parts were made in the same way and had the same defects as loop C. The pits produced were the same depth as

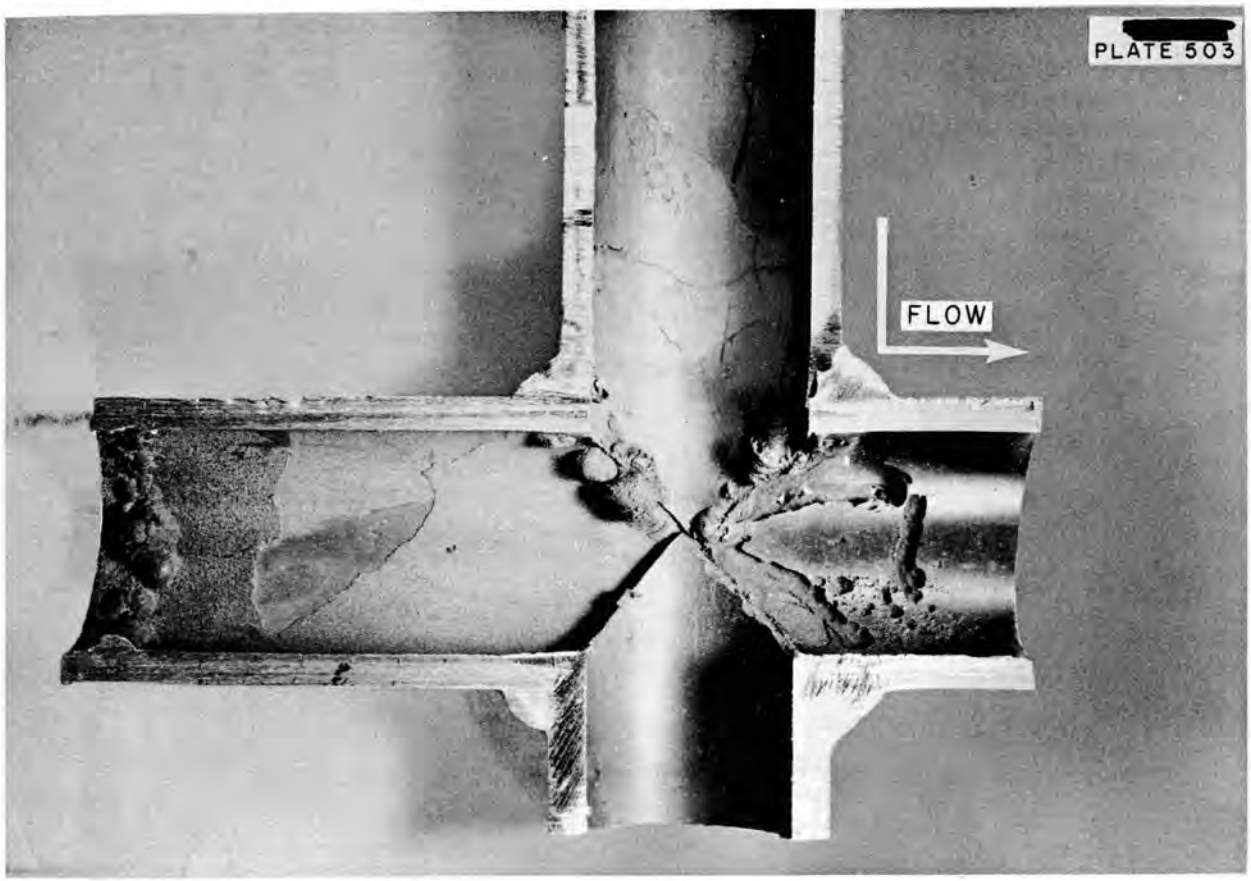

Fig. 20. Welded Cross in Loop C at 3300 Hours. Bulk velocity, ~40 ft/sec; UO_2SO_4 solution, 40 g of uranium per liter.

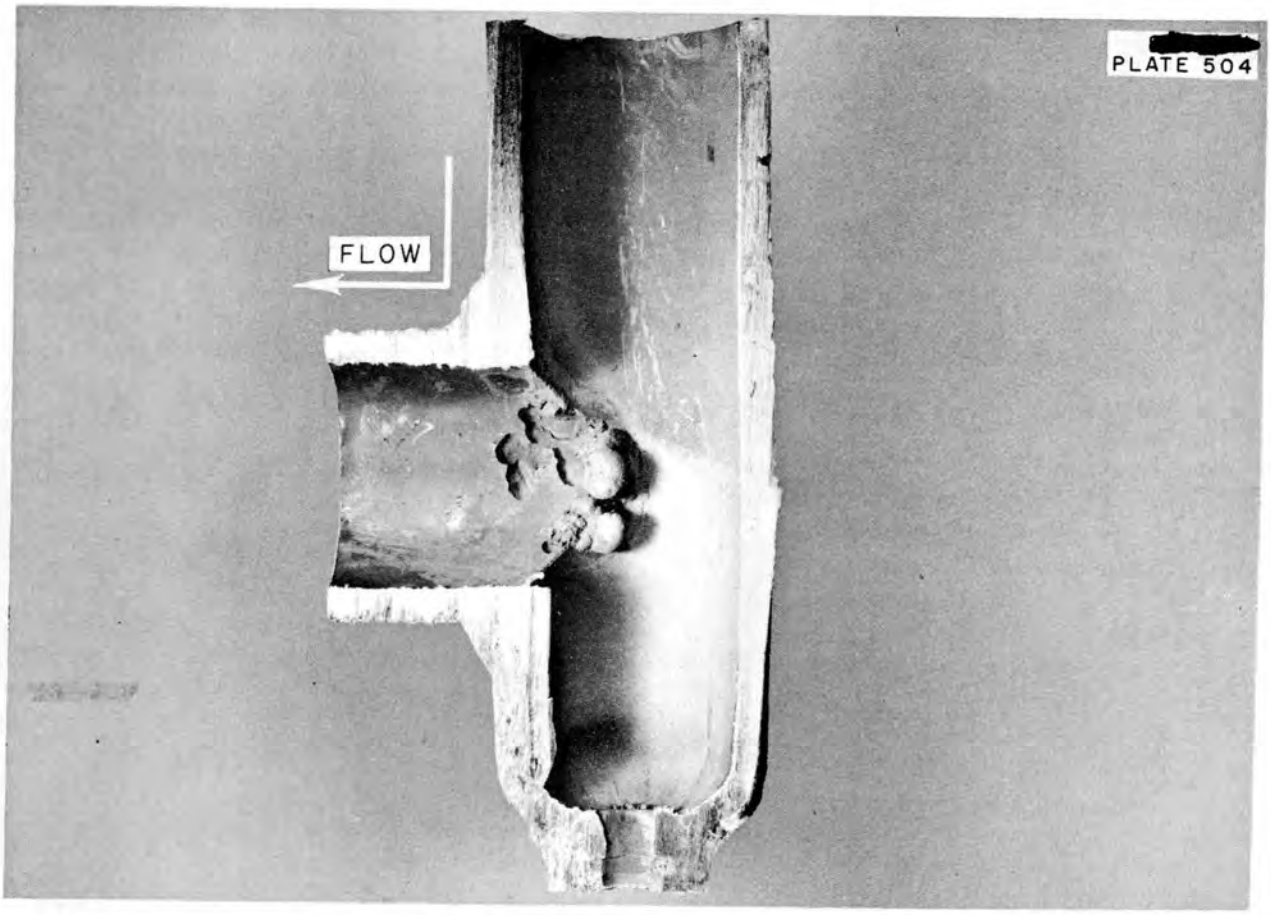

Fig. 21. Welded Tee in Loop C at 3300 Hours. Bulk velocity, ~40 ft/sec; UO_2SO_4 solution, 40 g of uranium per liter.

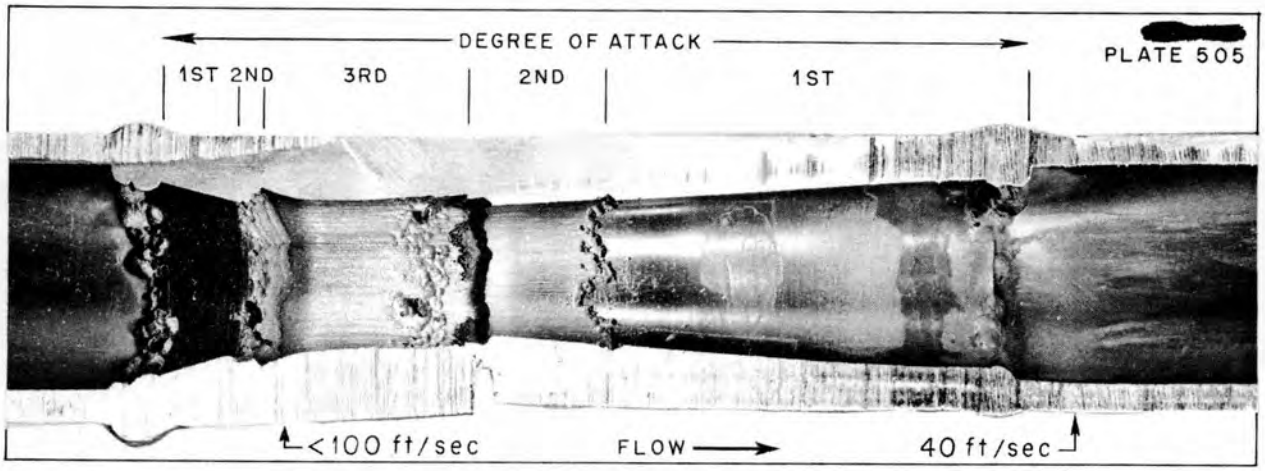

Fig. 22. Machined Flow Restrictor in Loop C at 3300 Hours. Maximum flow, 100 ft/sec; UO_2SO_4 solution, 40 g of uranium per liter.

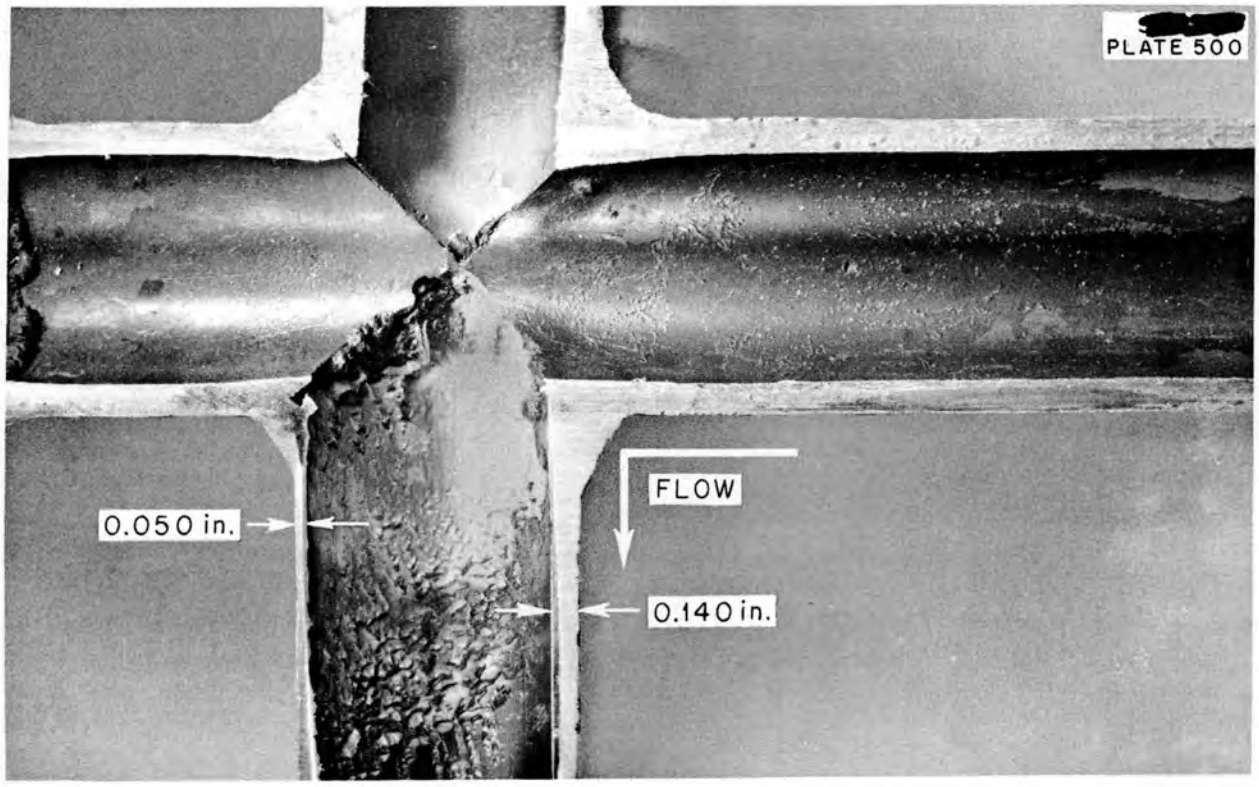

Fig. 23. Welded Cross in Loop B at 5100 Hours. Bulk velocity, ~40 ft/sec; UO_2SO_4 solution, 40 g of uranium per liter.

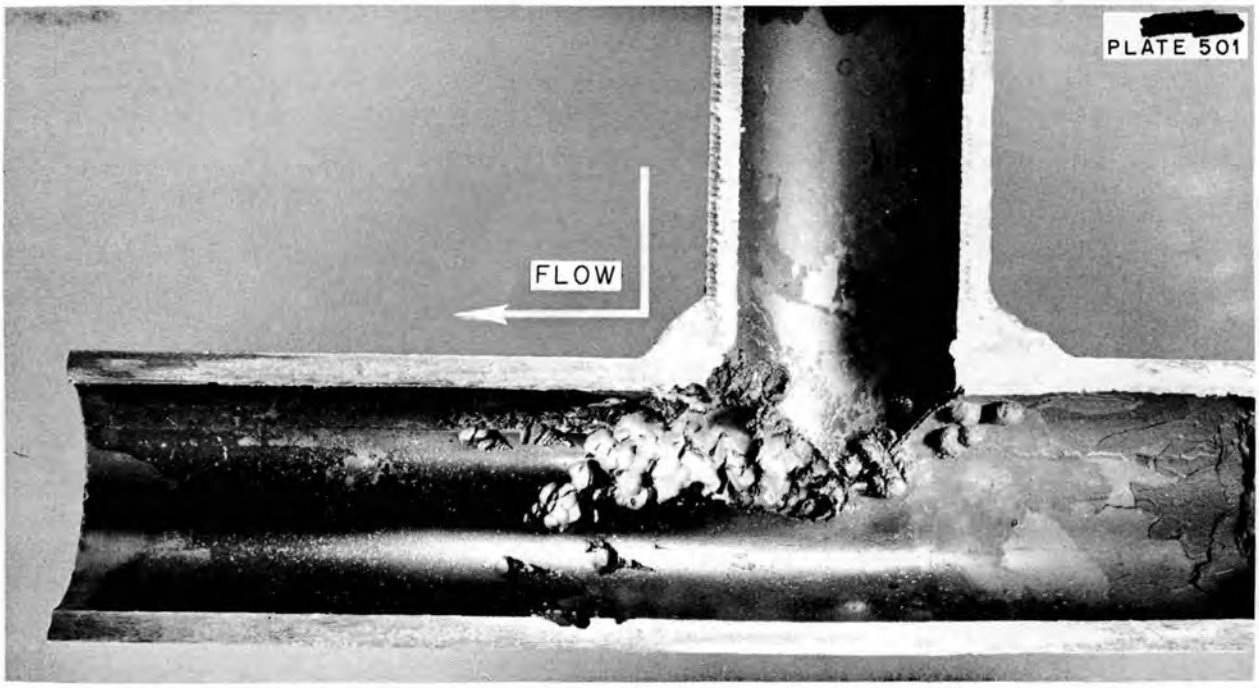

Fig. 24. Welded Tee in Loop B at 5100 Hours. Bulk velocity, ~40 ft/sec; UO_2SO_4 solution, 40 g of uranium per liter.

those of loop C (except that none actually came through the wall), but they had much greater areas and uniformity of depth. On the outside of the downstream leg of the main flow turn in the cross the wall thickness was reduced from 0.140 to 0.050 in. over several square centimeters. At the center of both X shaped welds joining the four legs, the pit depth was about 0.140 inch. The flow restrictor of loop B (not shown) was attacked similarly to that of loop C. The main flow of loop B passed through a pipe bend of 3 1/2-in. radius. The outer half of this bend is shown in Fig. 25. The wall was slightly roughened, but attack was by no means so serious as in the sharp turns. The longitudinal pipe seam that lies in the side of this bend was more heavily attacked than the remainder of the pipe wall.

Loops B and C showed general corrosion rates (during most of their operating life) of between 0.5 and 5 mpy. It is not practical to make an accurate measurement of the amount of metal removed in the severely attacked zones described above, but a very rough estimate indicates that these zones may account for one-third of the total removal of metal from the loop. On this basis alone it would seem reasonable to believe that real values of the corrosion rate in regions of smooth flow and lower velocity, such as straight pipe runs, will be acceptably low. However, in these loops about one-half of the of the submerged area is in the pressurizer, where the flow rate is essentially zero. If the low static corrosion rates (see following section on "Static Corrosion Studies") apply in the pressurizer, then there remains the possibility of a moderately high rate in straight runs of pipe handling flows of 35 to 45 ft/sec.

Corrosion of Uranyl Sulfate with 300 g of Uranium per Liter. Loop F has been used for studying uranyl

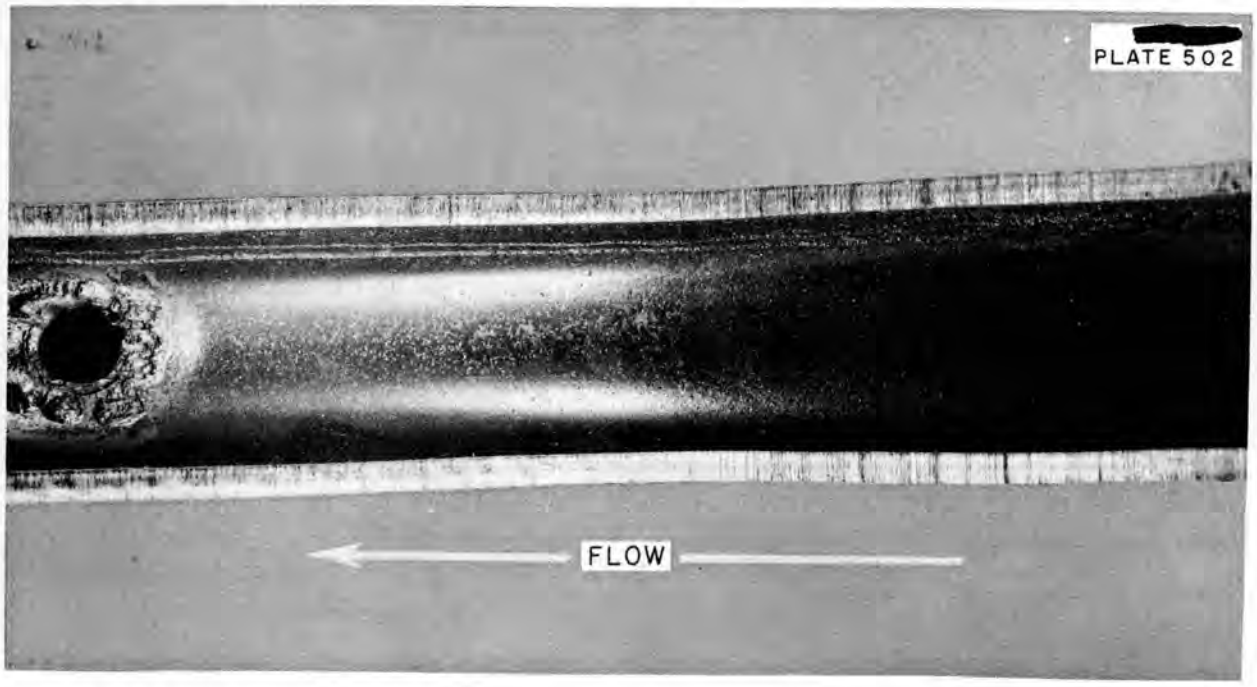

Fig. 25. Outer side of 3 1/2-in. Bend in Loop B at 5100 Hours. Bulk velocity, ~40 ft/sec; UO_2SO_4 solution, 40 g of uranium per liter.

sulfate solutions with 300 g of uranium per liter and various concentrations of O_2. The first 130-hr period of operation was with 1000 to 1500 ppm of O_2 at 250°C. The dissolved-nickel increment corresponded to a general corrosion rate of about 40 mpy, with solution of 150 g of stainless steel. Upon inspecting the loop, it was found that 53 g of metal had been lost by the pump impeller alone, whereas the pipe interiors presented a satisfactory appearance. Only one major pit was found outside the pump – in a flange weld zone adjacent to an orifice-plate flow restrictor.

It is perhaps significant that commercial forged tees were used in this loop, rather than the locally built welded fittings used in loops B and C. The interior finish of the commercial product is much better, and no pitting occurred in the initial period described.

Attack in the pump, however, was quite heavy. The impeller face showed deep pits, starting at small scratches and tool marks, that were usually greatly elongated in the direction of flow. The interior of the impeller and all sharp edges were pitted badly. The hydraulic positioning pads (built up of weld metal) were removed down to and below the base metal at their leading edges. Attack of this kind continued during further experiments with reduced O_2 concentrations to a total running time of 487 hr and a total impeller weight loss of 130 grams. Figures 26*a*, *b*, and *c* are photographs of a representative pit started from a scratch on the impeller. The photographs were made at 130, 287, and 487 hr of service, respectively, and are all at approximately 10X. Figure 27 is a general view of the impeller after 487 hours.

Pin Specimens. A set of pin specimens mounted in the holders described previously was in use on loop F during the first 130 hr of operation (Fig. 28); a duplicate set was in use on loop C during its last 540 hr of operation. The sets consisted of specimens of five different stainless steels and, in loop F, a titanium specimen. The bulk fluid velocity past the pins was 19 ft/sec in loop F and 28 ft/sec in loop C. In loop F, attack on the pins was of first, second, and third degrees, with weight losses ranging up to 160 mg/cm^2 in 130 hours. Agreement between duplicate specimens of the same alloy was fairly good, but because of the severity of the erosion-promoted attack it is not desirable to compare the various types of stainless steel on the basis of this test. Titanium again demonstrated exceptionally good behavior in the corrosive medium–there was no weight loss and no visible erosive damage.

The weight losses of the set of specimens in loop C were insignificant; almost all losses were less than 1 mg/cm^2 in 540 hr, although the bulk velocity in loop C was much higher than in loop F. Evidently susceptibility to erosive attack is a function not only of the fluid flow pattern but also of the concentration of the medium.

Copper. In the experiments with fuel solution containing copper(II), the general corrosion rate appeared to be significantly higher than in simple fuel solution. The apparent rate in loop L began at 14 mpy and has proceeded in the later stages at 5 to 10 mpy. In view of the brief experience with this solution and the peculiarities of its chemistry, no discussion of the increased corrosion rate will be given

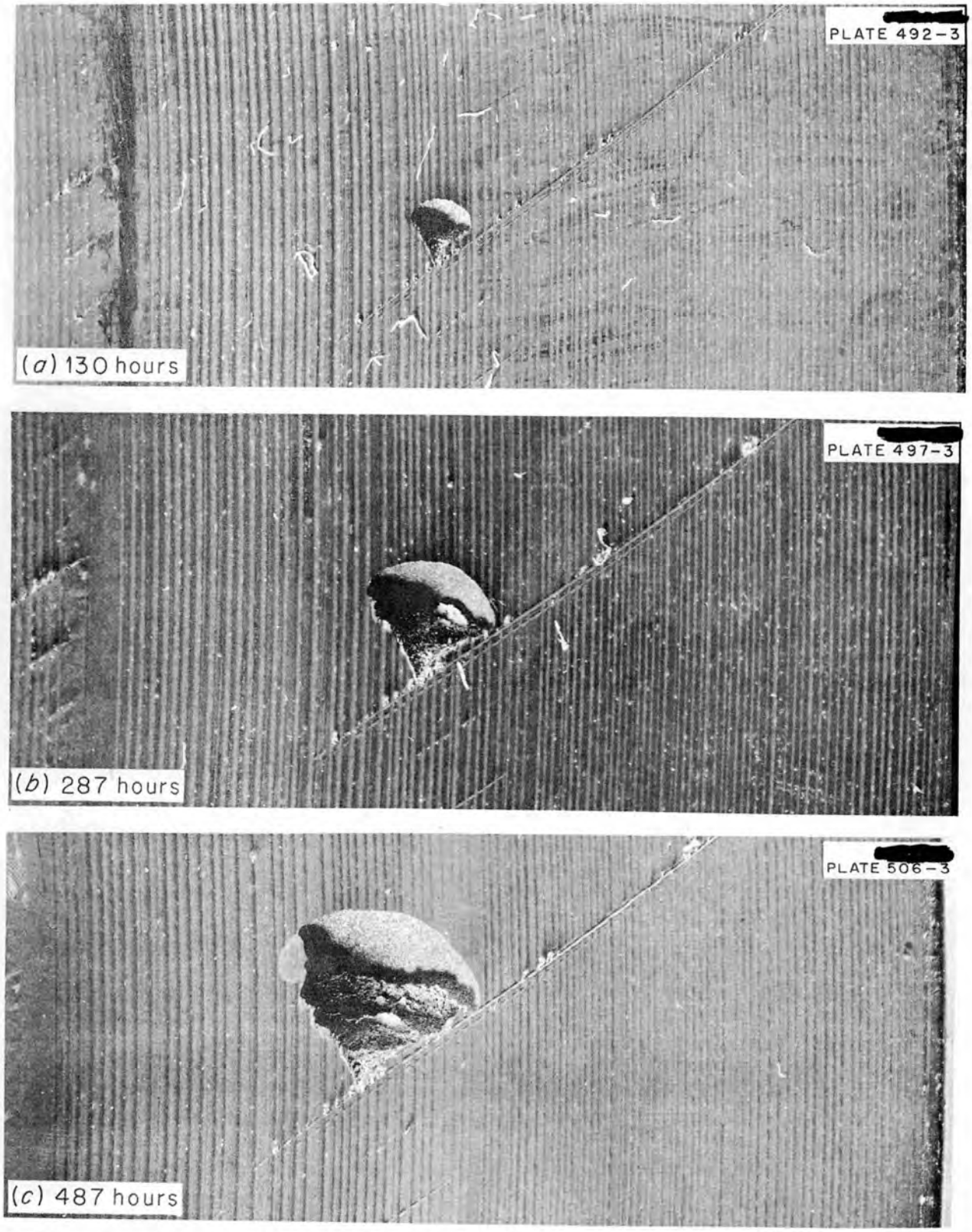

Fig. 26. Pit Growth in Pump Impeller. Loop F; UO_2SO_4 solution, 300 g of uranium per liter. ~10X.

[redacted]
PLATE 506

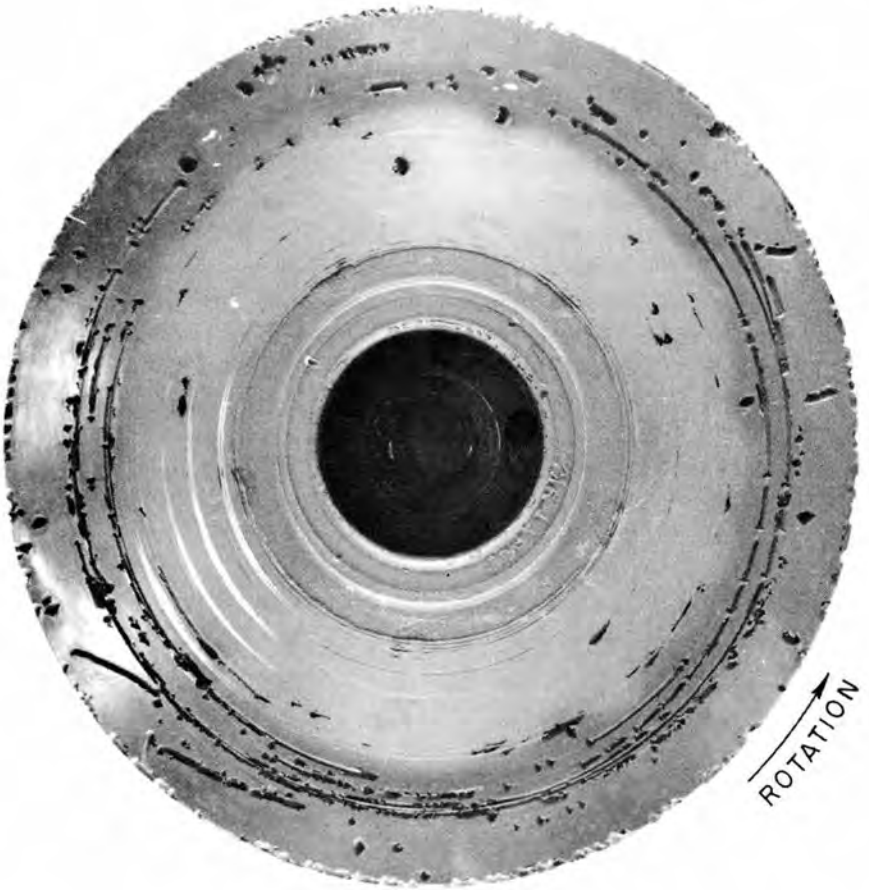

Fig. 27. Pump Impeller in Loop F at 487 Hours. UO_2SO_4 solution, 300 g of uranium per liter.

[redacted]
PLATE 491

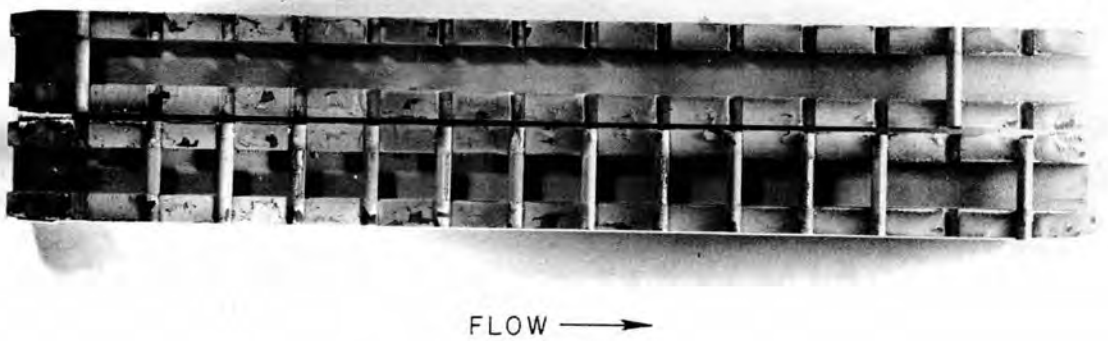

Fig. 28. Specimen Pins in Holder at 130 Hours. Loop F; UO_2SO_4 solution, 300 g of uranium per liter.

in this report. A set of pin specimens duplicating those of loops C and F are being tested in loop F.

Future Work. Loops are scheduled for operation with uranyl sulfate solutions containing 5, 100, and 200 g of uranium per liter during the next quarter. All the systems described above will be continued, although it may become necessary to interrupt or modify the work with uranyl sulfate solutions containing 300 g of uranium per liter because of the rapid destruction of equipment. The straight and tapered specimen holders will be put into service, and a program of detailed examination of various materials, surface preparations, velocities, and corrosive media will begin. A very low-flow, high-pressure gas-metering valve now being developed by the Instrument Section may be used in the H_2-O_2 experiments, in conjunction with a 1-gph let-down system, to improve the results of that investigation. Work on alternate fuels will begin when the new equipment is delivered.

STATIC CORROSION STUDIES

J. L. English S. H. Wheeler

Uranyl Sulfate Corrosion Studies. The investigation of the uranyl sulfate-type-347 stainless steel system operating in the presence of oxygen at 250°C has continued. The objective of these studies has been to correlate the effects of uranium and oxygen partial pressure on the corrosion behavior of type-347 stainless steel.

The uranyl sulfate solutions used contained from 40 to 300 and, in a few cases, 550 g of uranium per liter. The oxygen pressures investigated ranged from 25 to 650 psia. These pressures were obtained by the addition of calculated quantities of 35% H_2O_2 to the test solutions at the start of each test run. In determining the desired operating oxygen partial pressure at 250°C, the following factors were taken into consideration:

1. the amount of oxygen initially present in the test solution at room temperature,
2. the amount of oxygen present in the air space of the test autoclave containing the solution at room temperature,
3. the amount of oxygen dissolved in the test solution while operating at 250°C under the desired oxygen partial pressure,
4. the amount of oxygen necessary to produce the desired partial pressure in the vapor phase at 250°C.

In the absence of information on the solubility of oxygen in uranyl sulfate at elevated temperature, the solubility data for water were used.[5] These data are probably slightly in excess of values expected for uranyl sulfate solutions, since dissolved salts generally decrease gas solubilities.

The addition of hydrogen peroxide to uranyl sulfate solution at room temperature results in a nearly instantaneous and quantitative precipitation of uranium peroxide, UO_4, and sulfuric acid is produced as a secondary product. However, during the 1-hr period required to reach 250°C in the sealed test autoclaves, UO_4 undergoes thermal decomposition to UO_3, starting in the neighborhood of

[5] H. A. Pray, C. E. Schweickert, and B. H. Minnich, *The Solubility of Hydrogen, Oxygen, Nitrogen, and Helium in Water at Elevated Temperatures*, BMI-T-25, May 15, 1950.

slightly over 100°C with the liberation of oxygen. Total decomposition of UO_4 is practically complete at a temperature of 200°C. The UO_3 formed during the heating process reacts with the free sulfuric acid initially produced to re-form uranyl sulfate.

This method of producing oxygen partial pressures, although not completely satisfactory, has proved expedient for examination of oxygen effects on the corrosion of type-347 stainless steel. The reliability of this method is being checked against similar tests by using direct pressurization of the system with compressed oxygen gas.

The tests were conducted with solution volumes of 150 ml in stainless steel autoclaves. For these tests, the solution was replaced at the start of each run; in other tests now in operation, the original test solution was used continuously for the duration of the investigation. The initial surface condition of the autoclaves and the corrosion test specimens were the same at the start of all tests - lathe machined. The test specimens were machined from rolled 1 1/2-in.-OD bar stock to 0.5 cm in thickness and 3.0 cm in diameter. The exposed surface area of the individual specimens was approximately 20 cm^2. The surface area of the stainless steel autoclaves in contact with the test solution at 250°C was 225 cm^2. Thus, the total surface area to solution volume ratio was 1.6 cm^2/1.0 cc of solution.

The actual chemical analysis of the type-347 stainless steel test specimens was, in weight per cent:

carbon	0.08
chromium	18.0
nickel	10.2
manganese	1.2
silicon	0.6
niobium	0.99

Chemical analyses are not yet available on the type-347 stainless steel autoclaves.

Four partial pressures of oxygen, 75, 140, 265, and 650 psia, were investigated to test the effect of oxygen on the corrosion of type-347 stainless steel at 250°C in uranyl sulfate solutions containing 40 g of uranium per liter. The tests were operated singly because there were not enough autoclaves available for duplicate tests at the time of the study. The periods of continuous exposure were gradually extended as the tests progressed so that the order of exposure times was 48, 240, 240, 336, 336, and 504 hours. New test solutions were used at the start of each exposure period. A further breakdown of the calculated oxygen data at 250°C is given in Table 14.

TABLE 14

Calculated Oxygen Data

OXYGEN PRESSURE (psia)	SOLUBLE O_2 (ppm)	TOTAL O_2 INITIALLY PRESENT (mg)
75	405	180
140	775	370
265	1275	725
650	3710	1835

The tests were run for 1748 hr (10.4 weeks). Total uranium and dissolved-nickel content were determined for each test solution at the completion of a run, and pH measurements were made at room temperature on the exposed solutions. The corrosion test specimen weights were recorded in an as-removed-from-solution condition.

Data for the series of tests are given in Table 15. Uranium analyses are listed as the average of two determinations. The spread between duplicate uranium analyses on any one solution was less than 0.5 g per liter.

TABLE 15

Corrosion of Type-347 Stainless Steel in Uranyl Sulfate Containing 40 g of Uranium per Liter and Various Partial Pressures of Oxygen at 250 °C

CUMULATIVE TIME OF TEST (hr)	SOLUTION pH	TOTAL URANIUM (g/l)	DISSOLVED NICKEL (μg/ml)	CUMULATIVE WEIGHT LOSS (mg/cm 2)	CORROSION RATE[a] (mpy)
PRESSURIZED WITH 75 psia OF OXYGEN					
0	2.4	40.9	<1		
48	2.2	39.7	54	0.15	1.37
288	2.3	40.5	16	0.21	0.31
528	2.4	40.6	18	0.27	0.23
864	2.0	40.8	22	0.27	0.13
1200	2.0	40.5	1	0.25	0.09
1704	2.1	40.4	2	0.25	0.06
1772	2.4	40.6	2	0.24	0.06
PRESSURIZED WITH 140 psia OF OXYGEN					
0	2.4	40.3[b]	<1		
48	2.2	39.1	68	0.09	0.78
288	2.3	40.3	7	0.07	0.11
528	2.4	40.4	12	0.14	0.12
864	2.0	40.5	19	0.08	0.04
1200	2.0	40.1	2	0.08	0.03
1704	2.1	40.5	2	0.06	0.02
1772	2.4	40.2	4	0.04	0.01
PRESSURIZED WITH 265 psia OF OXYGEN					
0	2.4	39.8[c]	<1		
48	2.2	38.5	48	0.14	1.24
288	2.3	39.5	13	0.03	0.04
528	2.4	39.6	13	0.12	0.10
864	2.0	39.7	11	0.05	0.03
1200	2.0	39.5	2	0.06	0.02
1704	2.1	39.8	3	0.04	0.01
1772	2.3	39.9	7	0.03	<0.01
PRESSURIZED WITH 650 psia OF OXYGEN					
0	2.4	38.2[d]	<1		
48	2.2	37.2	43	0.09	0.83
288	2.3	38.1	26	0.04	0.06
528	2.4	38.3	21	0.10	0.08
864	2.0	38.0	16	0.07	0.03
1200	2.0	38.1	11	0.06	0.02
1704	2.1	38.6	27	0	0
1772	2.3	38.8	10	+0.07	

[a] Based on cumulative weight loss.

[b] Dilution effected by the addition of 2 ml of H_2O_2 to 148 ml of UO_2SO_4.

[c] Dilution effected by the addition of 4 ml of H_2O_2 to 146 ml of UO_2SO_4.

[d] Dilution effected by the addition of 10 ml of H_2O_2 to 140 ml of UO_2SO_4.

A graph of the as-removed cumulative weight changes for the four test specimens is shown in Fig. 29. Weight changes are plotted as a function of the exposure time. The weight loss vs. time curves are irregular, with the exception of the 75 psia oxygen test data. A steady loss in weight was observed on this specimen during the first 528 hr, after which time a constant but slight increase was apparent. The 650 psia oxygen test specimen showed a cumulative weight increase of 0.07 mg/cm^2 after 1772 hours. The over-all extent of weight variation for all specimens was within the range of +0.1 to -0.3 mg/cm^2. The bulk of the data fell within the 0 to -0.2 mg/cm^2 bracket.

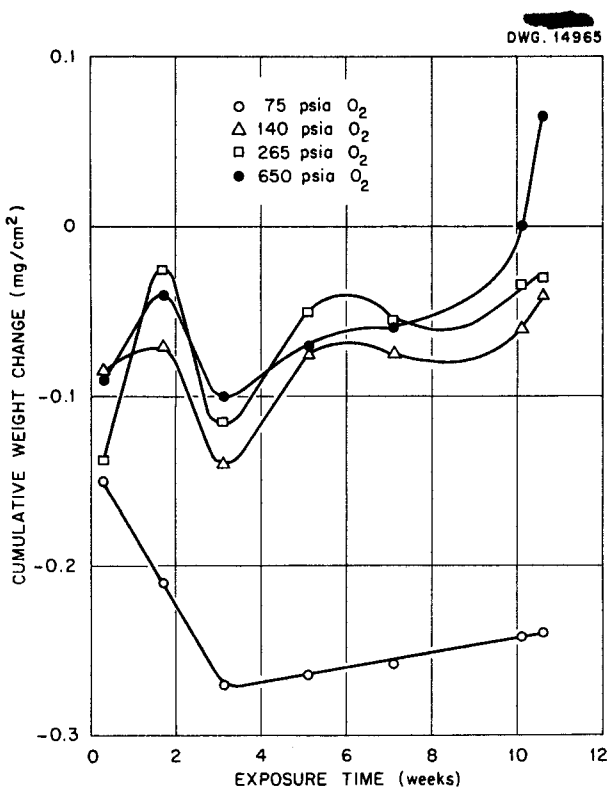

Fig. 29. Cumulative As-Removed Weight Changes on Type-347 Stainless Steel Exposed at 250°C to UO_2SO_4 Solution (40 g of uranium per liter).

Little change in appearance was observed on the specimens between the 48- and 1772-hr exposures; all were covered with rather thin, semilustrous, light-gray films that did not appear completely continuous upon microscopic examination at 200X. No evidence of localized corrosion attack was found on any of the specimens. Surfaces appeared slightly etched at the grain boundary regions.

An examination of the uranium analysis data in Table 15 shows one phenomenon that occurred in all four test solutions. At the end of the first 48-hr period in each test, the uranium content ranged from 1.0 to 1.3 g per liter less than the initial value. These were the only instances in which such deviations in uranium values were observed, and at this time the reason for the decrease is unexplained.

The test solutions were characterized by abrupt increases in dissolved nickel content during the first 48 hours. Subsequent exposure periods of 240, 336, and 504 hr showed a decided incremental decrease in nickel content as compared with the initial 48-hr values. Cumulative, dissolved-nickel values are shown in Fig. 30 as a function of the exposure time. The nickel values for the 75-, 140-, and 265-psia oxygen tests followed a similar trend – that is, a tendency to level off with increased exposure time. The test with highest oxygen pressure, 650 psia, gave results that indicated a nearly constant slope of the cumulative nickel vs. time curve after the initial 48-hr period. All curves exhibited slight "tails" upward for the final dissolved-nickel content obtained during the last 68 hr of testing. Since the tests were stopped at this point, it is not known whether the increased slope of these curves would have been significant had the tests continued.

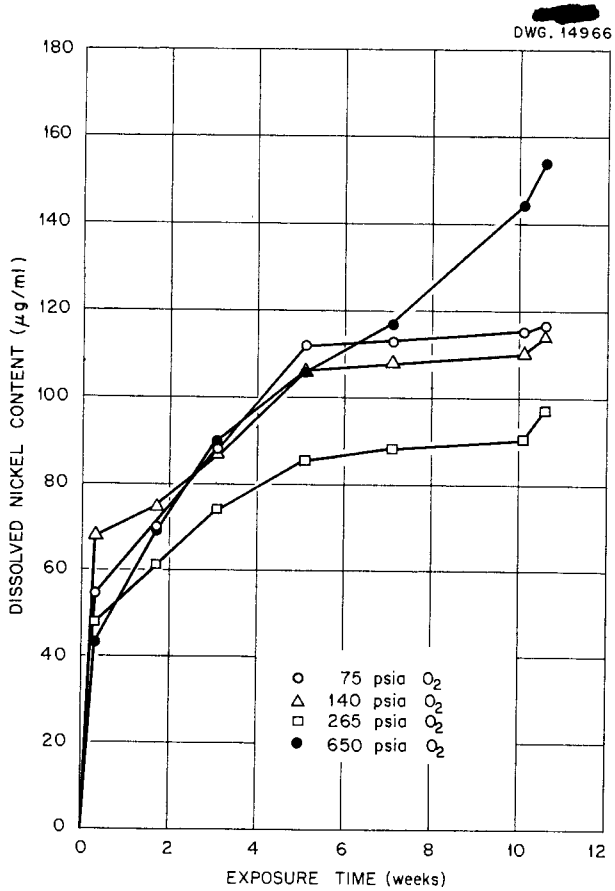

Fig. 30. Cumulative Increase in Dissolved Nickel Content in Oxygenated UO_2SO_4 Solution (4 g of uranium per liter) in Contact with Type-347 Stainless Steel at 250°C.

Although these data tend to indicate a more corrosive situation with the highest oxygen pressure, 650 psia, the results cannot be interpreted as conclusive since only single tests were involved. Physical and chemical variations in the initial surface condition of the autoclaves and specimens may introduce influencing variables. The dissolved-nickel data are summarized in Table 16.

Since the corrosion test specimens exhibited definite film formation on all surfaces as they were removed from the test solutions, it was obvious that the measured weight changes were not a true criterion of actual corrosion damage. Another evaluation of corrosion attack was obtained by the determination of the dissolved nickel content in the test solution. Nickel, unlike chromium and iron, which partially precipitate hydrolytically as oxides in uranyl sulfate solutions at 250°C, appears to remain dissolved in solution.[6] Therefore, assuming that corrosion attack on the stainless steel occurs uniformly, with metal being removed in the same proportion as the components present in the alloy, the corrosion rate can be calculated from the dissolved nickel value.

The observed corrosion rates listed in Table 17 were determined from the cumulative weight losses of the specimens removed from the test solutions. The calculated corrosion rates were based on the cumulative, dissolved nickel content in the test solutions. For the latter calculations, a total submerged surface area of 245 cm^2 and an average value of 10.5% for the nickel content of type-347 stainless steel were used. The accuracy of the analytical method for the determination of dissolved nickel in uranyl sulfate solutions was ±10%. A comparison of the observed and calculated data is given in Table 17.

The 48-hr corrosion rates as determined from dissolved-nickel data were considerably higher than those obtained from weight changes. A maximum rate of 3.57 mpy was obtained for the test with 140 psia of oxygen; rates for the other three tests ranged from 2.3 to 2.8 mpy. The final over-all rates, after 1772 hr, were similar in magnitude - 0.14 to 0.22 mpy. Thus, these data indicate no pronounced effect of oxygen content in the range

(6) "Effect of Variables on Corrosion: Series I," *op. cit.*, ORNL-1057, p. 57-58.

of 400 to 3700 ppm on the corrosion of rolled type-347 stainless steel in uranyl sulfate solutions containing 40 g of uranium per liter at 250°C.

Defilming methods were investigated for the removal of corrosion product films from the test specimens as means for further checking the validity of

TABLE 16

Dissolved-Nickel Content of Oxygenated Uranyl Sulfate Solutions Containing 40 g of Uranium per Liter in Contact with Type-347 Stainless Steel at 250°C

CUMULATIVE TIME OF TEST (hr)	DISSOLVED NICKEL (μg/ml)							
	75 psia OF O_2		140 psia OF O_2		265 psia OF O_2		650 psia OF O_2	
	Σ Ni	Δ Ni	Σ Ni	Δ Ni	Σ Ni	Δ Ni	Σ Ni	Δ Ni
0	<1		<1		<1		<1	
48	54	54	68	68	48	48	43	43
288	70	16	75	7	61	13	69	26
528	88	18	87	12	74	13	90	21
864	112	22	106	19	85	11	106	16
1200	113	1	108	2	87	2	117	11
1704	115	2	110	2	90	3	144	27
1772	117	2	114	4	97	7	154	10

TABLE 17

Comparison Between Corrosion Rates Determined by Observed Specimen Weight Losses and Those Calculated from Dissolved-Nickel Content for Type-347 Stainless Steel Exposed to Oxygenated Uranyl Sulfate Containing 40 g of Uranium per Liter at 250°C

CUMULATIVE TIME OF TEST (hr)	CORROSION RATES (mpy)							
	75 psia OF O_2		140 psia OF O_2		265 psia OF O_2		650 psia OF O_2	
	OBS.	CALC.	OBS.	CALC.	OBS.	CALC.	OBS.	CALC.
48	1.37	2.84	0.78	3.57	1.24	2.52	0.83	2.26
288	0.31	0.61	0.11	0.66	0.04	0.53	0.06	0.60
528	0.23	0.42	0.12	0.42	0.10	0.35	0.08	0.43
864	0.13	0.32	0.04	0.31	0.03	0.25	0.03	0.31
1200	0.09	0.23	0.03	0.23	0.02	0.18	0.02	0.25
1704	0.06	0.17	0.02	0.16	0.01	0.13	0	0.21
1772	0.06	0.16	0.01	0.16	<0.01	0.14		0.22

the dissolved-nickel method for determining corrosion rates. An electrolytic method using 5 wt % sulfuric acid was finally selected.[7] The test specimen was made the cathode and lead was used for the anode. The procedure consisted of heating the defilming solution, which contained 2 ml of Rodine inhibitor per liter of solution, to 75°C, and then, with the specimen in the solution, maintaining a cathodic current density of 20 amp/cm^2 for 3 minutes. By using this electrolytic method, the average weight loss of unexposed type-347 stainless steel specimens was determined to be 0.5 mg/cm^2, which is 2 to 5% of the total weight of a film actually removed by the stripping method. This average weight loss was applied as a blank correction to the over-all weight losses of the corrosion test specimens.

After sufficient blanks were run to demonstrate reproducible weight losses, the four corrosion test specimens were defilmed and corrosion rates were determined by using the corrected weight losses. A comparison with the rates obtained from the dissolved-nickel method is given in Table 18. All rates were based on the total exposure period of 1772 hours.

The results shown in Table 18 are in good agreement considering the numerous variables involved in the experiments, and they serve as a realistic check on the reliability of the dissolved-nickel method for determination of corrosion rates on type-347 stainless steel in uranyl sulfate solutions at 250°C.

Studies now in progress include the effect of oxygen on corrosion and solution stability of uranyl sulfate solutions containing 100, 200, and 300 g of uranium per liter in type-347 stainless steel systems at 250°C. The partial pressures of oxygen being used are 25, 75, 150, 265, 500, and 650 psia. The tests are operated in duplicate. Results and data will be reported in the next quarterly progress report.

Reflector Corrosion Studies. Corrosion data from a series of small-scale, 150-ml solution volume, autoclave tests at 200°C conducted during the past quarter are being evaluated and will be reported in the next quarterly progress report. The materials being tested are mild carbon steel and SAE-1030 and type-347 stainless steels. Exposures have been made in normal and heavy water containing approximately 70 ppm of oxygen and 300 ppm of trisodium phosphate. The effects of low and high concentrations of oxygen, 70 and 520 ppm, on the corrosion behavior of mild carbon steel have also been studied.

[7] B. B. Knapp, "Preparation and Cleaning of Specimens," *Corrosion Handbook* (H. H. Uhlig, ed.), Wiley, New York, 1951, p. 1080.

TABLE 18

Comparison of Corrosion Rates Determined from Weight Losses with Those Obtained by the Dissolved-Nickel Method

PARTIAL PRESSURE OF OXYGEN (psia)	CORROSION RATE (mpy)	
	BY WEIGHT LOSS	BY DISSOLVED NICKEL
75	0.14	0.16
140	0.12	0.16
265	0.10	0.14
650	0.17	0.22

RADIATION STABILITY

H. F. McDuffie, Group Leader

J. W. Boyle
W. E. Hill
J. F. Manneschmidt
D. M. Richardson
A. W. Smith
F. H. Sweeton
L. F. Woo
W. C. Yee

LONG-TERM EXPOSURES IN THE X-10 GRAPHITE PILE

As reported in the previous quarterly report,[1] two chromate-pretreated type-347 stainless steel bombs containing uranyl sulfate solution (40 g of uranium per liter, 93% enrichment) after 2900 hr of continuous irradiation in the X-10 graphite pile appeared to have maintained their stability, whereas two oxygen-pretreated bombs in the same reactor environment gave evidence of solution instability at 1400 hours. Specifically, one oxygen-pretreated bomb failed at 6:00 PM on September 21 and the other at 12:30 AM on September 24. One of the chromate-pretreated bombs ultimately failed at 8:00 AM on November 29 and the other at 8:00 AM on December 1, after a total of around 3100 hours. At the termination of the experiment on December 3, the small amount of residual gases remaining over the four bombs was collected, pooled, and analyzed. The gases were substantially all hydrogen, which was presumably derived from corrosion processes that ultimately reduced the uranium and caused failure of the solution.

Long-term exposures of uranyl sulfate solutions containing copper sulfate were initiated during the quarter. A copper sulfate concentration of 0.002 *M* was chosen to give reasonably high gas pressures over the solution at temperatures of 200 to 300°C. Three type-347 stainless steel bombs were pretreated with 2% chromic acid solution at 250°C for 18 hr; bomb 370 was then used without further treatment. The other two bombs, containing an unenriched uranyl sulfate solution, were subjected to a prerun in which they were heated to 250°C for 50 hr under pressure of oxygen or a hydrogen-oxygen mixture. The purpose of these variations in treatment was to ascertain whether the prerun might remove loose portions of the thick pretreatment film and leach out easily soluble components such as nickel; accomplishment of these tasks would make it easier to interpret analytical results obtained after irradiation. The results of 1250 hr of continuous irradiation in hole 60 of the X-10 graphite pile are summarized in Table 19. If bomb 371 continues to give satisfactory evidence of good behavior, these three experiments will be continued to a total time of 2000 hours. It is hoped that the results of nonirradiation corrosion experiments now in progress as part of the loop program will be of assistance in defining desirable experimental conditions for the next experiments.

SHORT-TERM EXPOSURES IN THE LITR

An interesting series of four experiments has been completed recently in the vertical experimental facility utilizing hole C-44 of the LITR in which the flux has been monitored as 1.3×10^{13} at a power level of 1000 kw. For each experiment, uranyl sulfate solution containing copper sulfate

(1) H. F. McDuffie *et al.*, "Radiation Stability," *Homogeneous Reactor Project Quarterly Progress Report for Period Ending November 15, 1951*, ORNL-1221, p. 35.

TABLE 19

Long-Term Exposures of Chromate-Pretreated Bombs in Hole 60

BOMB NO.	PRERUN	CONDITION AFTER 1250 HR
370	None	Solution failed at 240 hr
371	Oxygen	Solution apparently unchanged
372	Hydrogen + oxygen	Ambiguous behavior after 967 hr (leak or failure)

TABLE 20

Short-Term Exposures in the LITR

PRETREATMENT	PRERUN	EXPERIMENT NO.	ANALYTICAL DATA				
			URANIUM (mg)		COPPER (mg)		NICKEL (mg/ml)
			IN	OUT	IN	OUT	OUT
Chromate	Yes	V-7	199	184.4	9.49	4.46	0.37
Chromate	No	V-5	195	197.7	15.72	9.99	0.87
None	Yes	V-6*					
None	No	V-8*					

*Failed after 48 hr.

(40 g of uranium per liter, 93% enrichment; 0.03 to 0.05 *M* $CuSO_4$) was exposed for one week at an average flux of 1×10^{13} (power level of 800 kw). Of primary interest were comparisons between the behavior of chromate-pretreated and unpretreated type-347 stainless steel bombs and between bombs that had or had not been given a prerun treatment (heated under oxygen pressure in the presence of unenriched uranyl sulfate solutions containing copper sulfate prior to being loaded with the enriched solution for the irradiation). Table 20 gives the type of pretreatment and prerun chosen, together with relevant analytical data. The effect of pretreatment appears quite marked; the superiority of chromate-pretreated surfaces in these radiation tests at high flux and with copper in solution is quite analogous to the superiority of chromate-pretreated surfaces described above for solutions without copper at lower fluxes. The satisfactory operation of a static system for as much as one week at high flux levels (experiment V-5) is very encouraging when it is realized that nothing, short of terminating the experiment, can be done to correct any bad condition that might develop. Any indication of impending trouble (pH change, nickel build-up, etc.) in a reactor could be corrected or the reactor shut down before substantial damage had been incurred. The lower concentration of nickel found in experiment V-7, as compared with V-5, was anticipated as a result of the prerun. A substantial amount of additional experimental data will, however, be required before definite conclusions regarding corrosion rates can be justified.

During each experiment, data for describing the time dependence of total pressure as a function of total pressure were obtained at various temperatures. These data are treated in some detail in the section of this report on "Fundamental Radiation Chemistry Studies" in which it is shown that the behavior of experiment V-5 was consistent throughout the run, whereas experiment V-7 indicated that the recombination rate was decreasing. The analytical indication of loss of copper in experiment V-5 is at variance with the pressure data and is being rechecked. Some evidence for reversible formation of an insoluble substance when uranyl sulfate and copper sulfate solutions are heated above 200°C has been supplied by data from the corrosion loop program and from deliberate experiments by the solution chemistry group. This work is being followed very closely by the solution chemistry and the radiation groups.

LONG-TERM EXPOSURES IN THE LITR

During the past quarter facilities for use at hole HB-5 of the LITR were completed; dummy runs were carried out to check experimental handling procedures; and a trial run of a bomb containing pure water was carried out for one week as a final check on the performance of the control equipment. Removal of this irradiated assembly provided a relatively safe test for shielding and withdrawal techniques and indicated that no trouble should be expected with experiments using bombs containing uranyl solutions.

CONTROLS AND INSTRUMENTATION

W. M. Breazeale, Section Chief

A. M. Billings
D. G. Davis
L. P. Inglis
E. E. Mason
C. A. Mossman
J. E. Owens
L. R. Quarles
D. S. Toomb
W. P. Walker

Most of the work of the controls and instrumentation group during the past quarter consisted of observing the operation of the process instruments installed in the HRE. A number of adjustments, most of them minor, have been made. A discussion of the operating experience is given in the section of this report on "Status of the HRE." A list of major changes to controls and instrumentation, which made the circuit different from that described in ORNL-1094,[1] follows:

1. A safety interlock that now unconditionally dumps the reflector if the pressure is *both* more than 500 psi abolute and more than 150 psi above the fuel system pressure has been added to prevent application of excessive external pressure to the core.

2. Since the reflector level rises with consequent increase in reactivity when the circulating pump is cut off, a temporary interlock has been added to immediately dump the D_2O as soon as the pump stops. The interlock acts only when the reactor is in the "run" position. To avoid the possibility that the operator might try to refill the reflector with both heads of the D_2O pulsafeeder by returning the control to the "start" position and thus increase reactivity at an unsafe rate, another temporary interlock automatically dilutes the fuel when the control is in the "start" position. These interlocks will probably be removed after the critical experiments when the reactivity effect of changed D_2O level and safety plate position have been experimentally determined.

3. The original safety circuit that enabled the D_2O timer to drop the safety absorber plates at the same time the reflector was dumped is now considered an over-cautious feature, and the contact originating this operation has been removed.

A few instrument changes have been made, and the most important are the following:

1. An automatic controller has been installed in the oxygen system to enable the operator to maintain the oxygen concentration between close limits.

2. In recent off-gas tests, flashbacks occurred that started hydrogen and oxygen recombination in the fuel dump tank at the exit of the let-down line from the high-pressure system. A temperature alarm has been installed at this point to detect this danger and warn the operator that burning is taking place in the dome of the dump tank.

3. Investigation showed that the instability of the level indicator on the fuel dump tank was caused by temperature changes in the lines supporting the weigh tank. The weigh tank is being replaced by a float detector, similar to the one indicating the level in the pressurizer, which

[1] L. R. Quarles and W. P. Walker, *A Manual of HRE Control and Instrumentation*, ORNL-1094, Jan. 9, 1952.

will not be affected by temperature changes in the same way.

4. Tests are now being run on the Y-12 mockup in an effort to find a suitable valve for the pulsafeeder gas bleed in the fuel line. Although the tests are not finished, it appears that a 1/4-in. spline plug will be suitable.

Some development of instruments continues; the most important phases are the following:

1. The bellows-seal stainless steel control valves have a flexible joint in the shaft which allows a side thrust to deflect the main shaft and results in breakage of the plug in the seat. Two valves have been modified to provide a one-piece shaft, and tests indicate that the difficulty has been eliminated.

2. As has been reported, it is necessary to add oxygen to the high-pressure fuel system to reduce corrosion. The flow is very slow, approximately 10 cc/min at NPT. Measurement of this low flow rate is accomplished by determining the pressure drop across a 10-ft length of capillary tubing with a differential-pressure cell. A valve of conventional design is being used to control the flow, but the flow is so low that tolerances on the plug and seat are excessively close. A new coaxial valve has been designed for controlling the area through which the gas flows by heating the outer section of the coaxial assembly. Tests now in progress seem to indicate that this design is satisfactory.

3. A group of three all-welded differential-pressure cells has been received from The Foxboro Company. These cells have a range of 20 in. of water at a static working pressure of 1500 psi. All parts in contact with the liquid are type-347 stainless steel, and all joints are welded. Preliminary tests show exceptionally low hysteresis but a temperature coefficient that is higher than normal. One of these units is now installed in the HRE.

Work is continuing on the concentration indicator and control; some of this work is described in the following section. Automatic indication of concentration is particularly desirable for the boiling reactor, because the exact volume occupied by the fuel and moderator in the conventional boiling reactor designs is not known.

CHEMICAL CONCENTRATION DETERMINATION

W. H. Davenport, Jr.[2] R. H. Powell

A discussion of the use of the Densitrol for determination of uranyl sulfate concentrations can be found in an earlier quarterly report.[3] Since that report was written most of the effort has been directed toward improving and testing a Densitrol unit intended for operation at solution temperatures near room temperature.

Pyrex plummets have been shattered by sudden gas surges through the Densitrol tank, and thus the necessity for providing more rugged units is indicated. In addition, pyrex is badly corroded by high-temperature uranyl sulfate solutions. Stainless steel or titanium plummets will be sufficiently rugged and may make operation at higher temperatures feasible. Since density changes

[2] Present address: Chase Brass and Copper Company, Watertown, Connecticut.

[3] W. H. Davenport and R. H. Powell, "Chemical Control," *Homogeneous Reactor Project Quarterly Progress Report for Period Ending November 15, 1951*, ORNL-1221, p. 53.

in the neighborhood of a few parts in 10^4 are to be observed, the plummets should show no change in dimensions in going from atmospheric pressure to at least 1000 psi. In operation the plummets will be pressurized to an internal pressure approximating the normal reactor operating pressure, but the external pressure in the fuel system will, of course, not be maintained when the reactor is shut down.

Details of the method of pressurizing, testing, etc. will be given in a forthcoming report, but a brief summary of the results of the study can be given here. A 0.015-in.-wall type-347 stainless steel plummet was pressurized to 1800 psi without any detectable change in shape after the pressure was reduced. It was then sealed off with an internal pressure of 950 psi of nitrogen and stored for four months. At the end of this time some permanent warping was evident.

A titanium plummet was filled with argon to 1000 psi (at room temperature), and no warping was observed. It was then heated in an attempt to raise the pressure to 2000 psi to see whether a safety factor of another 1000 psi could be obtained; it ruptured at exactly 2000 psi (313°C). A photograph of the ruptured plummet is shown in Fig. 31. A second plummet has been constructed and will be tested at a somewhat lower peak pressure.

The effect of gas bubbles flowing through the tank containing the plummets was investigated. Bubbles appear to cling less to the pyrex floats than to the metal ones. Smooth plummets (without welded lips) appear to be affected least. These tests indicate that, unless the solution is gassing freely, not enough bubbles will cling to the surface of the float to cause a serious error in the readings. This work, in particular the studies of the effects of pressure and temperature, is continuing.

A low-temperature Densitrol unit with a pyrex plummet has been installed in the Y-12 mockup, but owing to the pressure of other work it has not yet been given an operational test. This unit will automatically record solution densities between 1.033 and 1.053 g/cc, corresponding to approximately 20 and 43 g of uranium per liter, and is compensated over the temperature range of 4 to 20°C.

UNCLASSIFIED
PHOTO 9871

Fig. 31. Rupture of 0.025-in. Titanium Tube Wall at 313°C and 2000 psi.

It is possible in principle to determine the concentration of uranyl sulfate in aqueous solution by measuring the absorption in the 4200-Å band. As a first step it will be necessary to find a cell material transparent to visible radiation, insoluble in uranyl sulfate solutions, and stable under neutron and gamma irradiation. In line with this, the absorbance curves of certain glasses have been measured before and after exposure in the X-10 graphite pile. Exposures were made at 250°C and an average flux (slow plus fast) of 7.3×10^{11} neutrons/cm^2/sec. The first exposure ended July 2, 1951, and the results were reported in a previous report.[4] The total irradiation was 5.4×10^{18} nvt. A second exposure beginning on July 23 gave an additional dose of 9.23×10^{18} nvt. The absorbance curves before and after exposure and after cooling are shown in Figs. 32, 33, 34, and 35. It is possible that a steady state condition may have been reached at 250°C, but the experiment was not arranged to determine this. Several tentative conclusions may be drawn.

1. Self-induced damage sets in soon when the glasses are reduced from 250°C inpile temperature to room temperature out of the pile.

2. The net damage is related to opposite effects of self-damage from induced activity and of the change in the rate of annealing of the glass at 250°C to room temperature, at which temperature the annealing rate is much slower.

3. Exposure of the irradiated glasses to ordinary light from a 150-watt tungsten light bulb can temporarily cure, at room temperature, the major net damage, but once the light source is removed the drastic self-damaging effect predominates.

4. The possibility exists that certain glasses and naturally transparent inorganic materials, and certain fused materials, can be made useful for inpile service or for low-pressure reactor service when a combination of high annealing temperature (250°C is not considered a true annealing temperature) and a light source are concurrently applied to these optical materials. Further, there is a suggestion that a steady state of radiation damage may be achieved early if temperature and light exposure are likewise controlled.

Certain materials such as fused spinel, fused sapphire, and fused titania possess remarkable corrosion resistance to 0.17 *M* uranyl sulfate at 250°C, and because of this feature alone they should be carefully examined for resistance to radiation damage and for possible reactor service such as optical windows, reactor liners, and electrical insulating materials in contact with uranyl sulfate.

English of the Reactor Experimental Engineering Division has investigated the chemical stability of these artificial gems in a 0.168 *M* uranyl sulfate solution at 100°C. He found that a sample of fused titania lost 0.48 mg/cm^2 in 1344 hr of exposure, a rate of 0.28 mpy, and fused, whereas sapphire lost 1.50 mg/cm^2, a rate of 0.92 mpy.

No further work was carried on during the past quarter on the method of concentration determination by measurement of changes in the *Q* and inductance of a coil immersed in the solution. The other approaches outlined above seemed more fruitful, and available manpower was concentrated on these investigations.

[4] W. H. Davenport, Jr. and R. H. Powell, "Chemical Control," *Homogeneous Reactor Project Quarterly Progress Report for Period Ending August 15, 1951*, ORNL-1121, p. 75-83.

UNCLASSIFIED
DWG. 14967

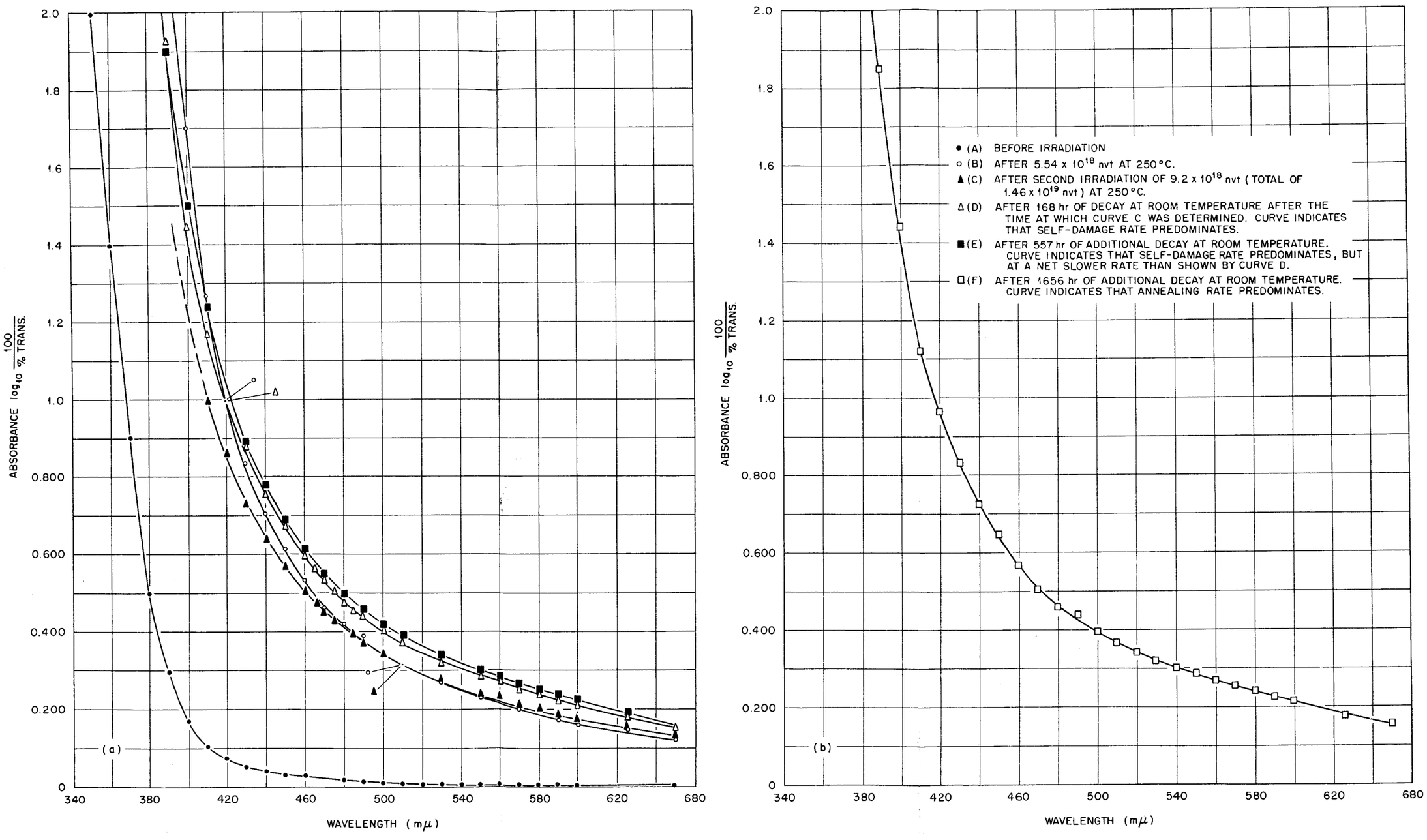

Fig. 32. Absorbance Curves of Radiation-Resistant Glass, ORNL-1M. Boron, very strong; cadmium, weak. For chemical composition of the glasses measured for Figs. 32, 33, 34, and 35 see ORNL-1221, Table 7, and L. Melnick *et al.*, *J. Am. Ceram. Soc.* **34**, 84 (1951).

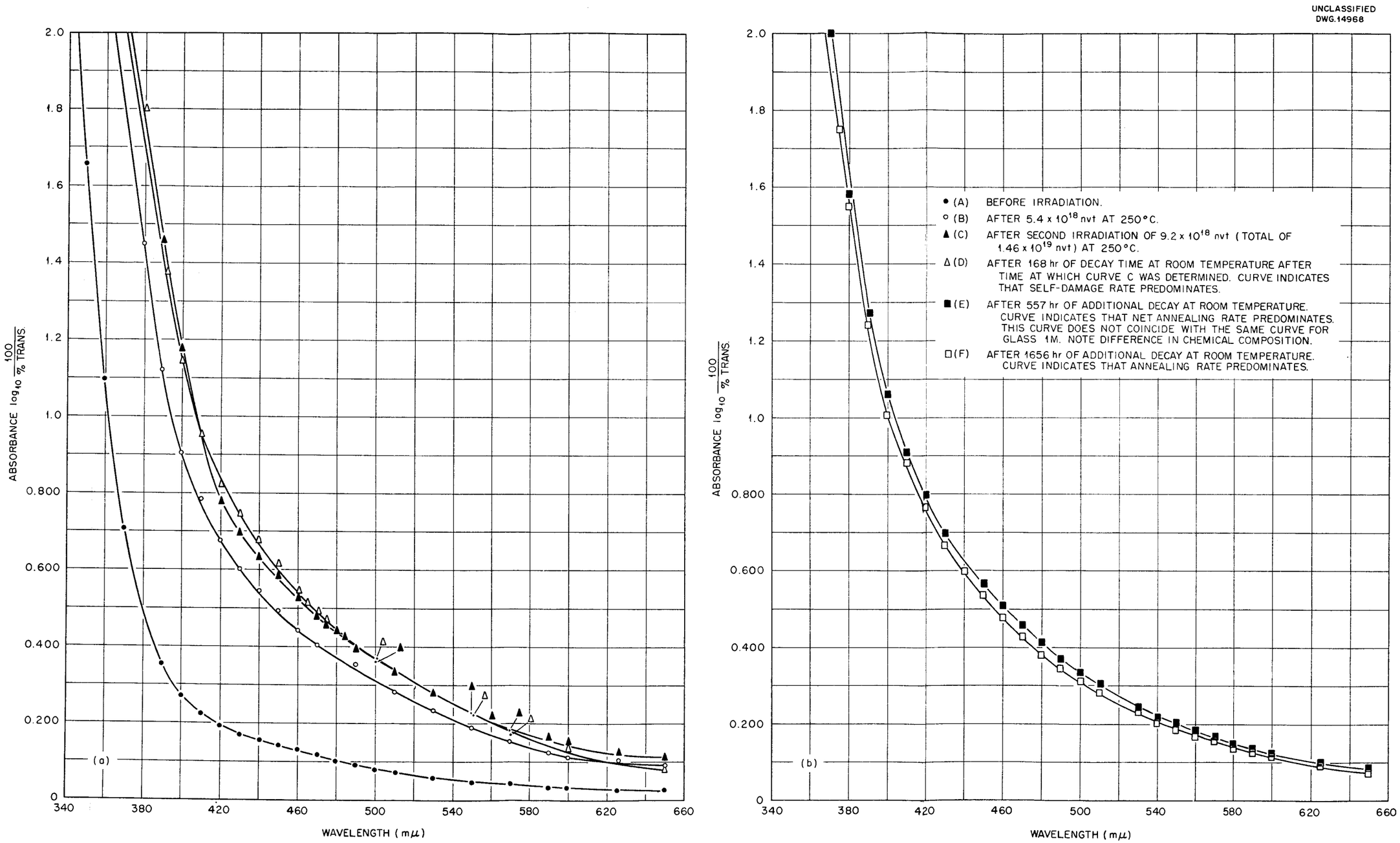

Fig. 33. Absorbance Curves of Radiation-Resistant Glass, ORNL-2M. Boron, trace; cadmium, strong.

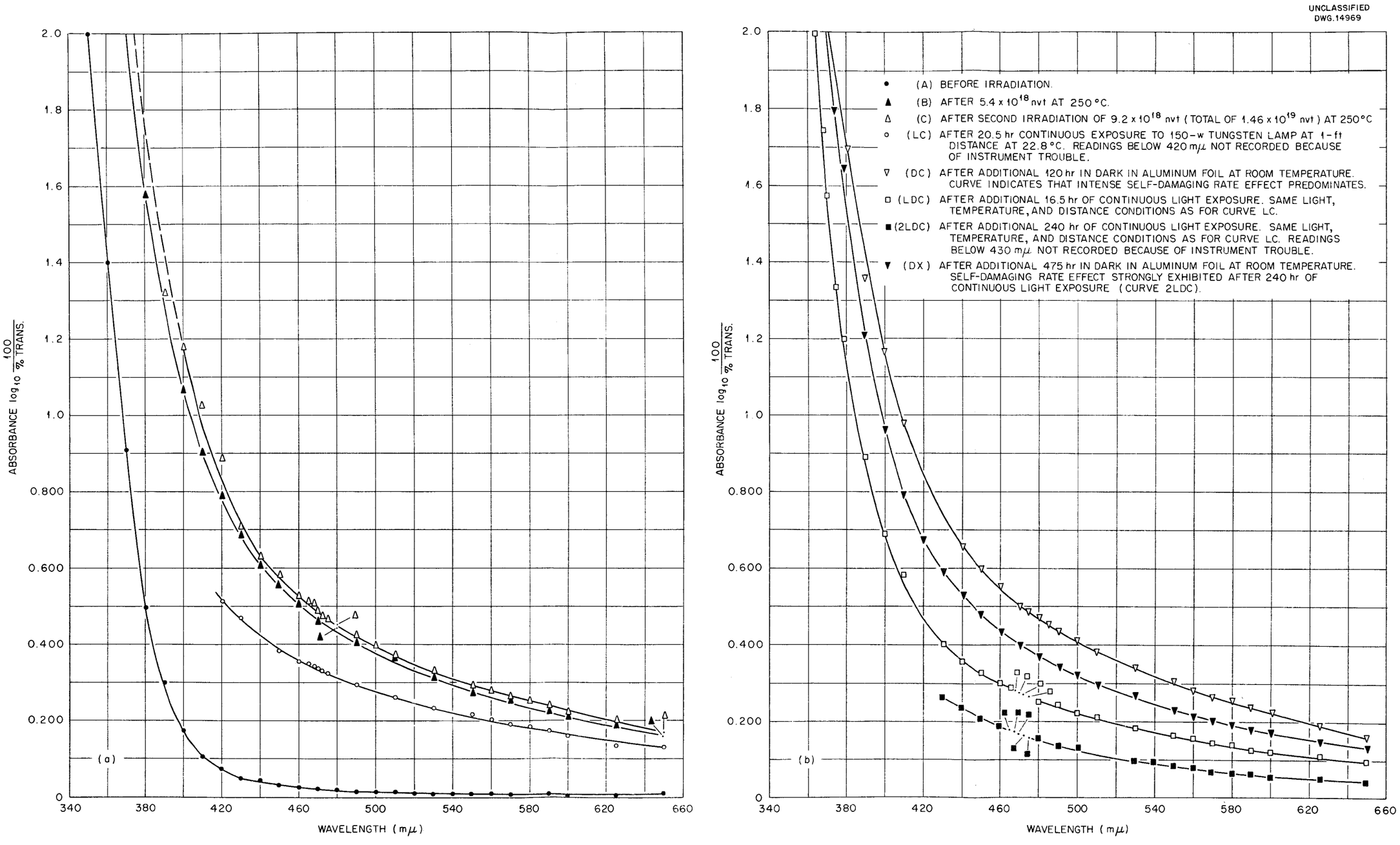

Fig. 34. Absorbance Curves of Radiation-Resistant Glass, ORNL-3M. Boron, moderate; cadmium, moderate.

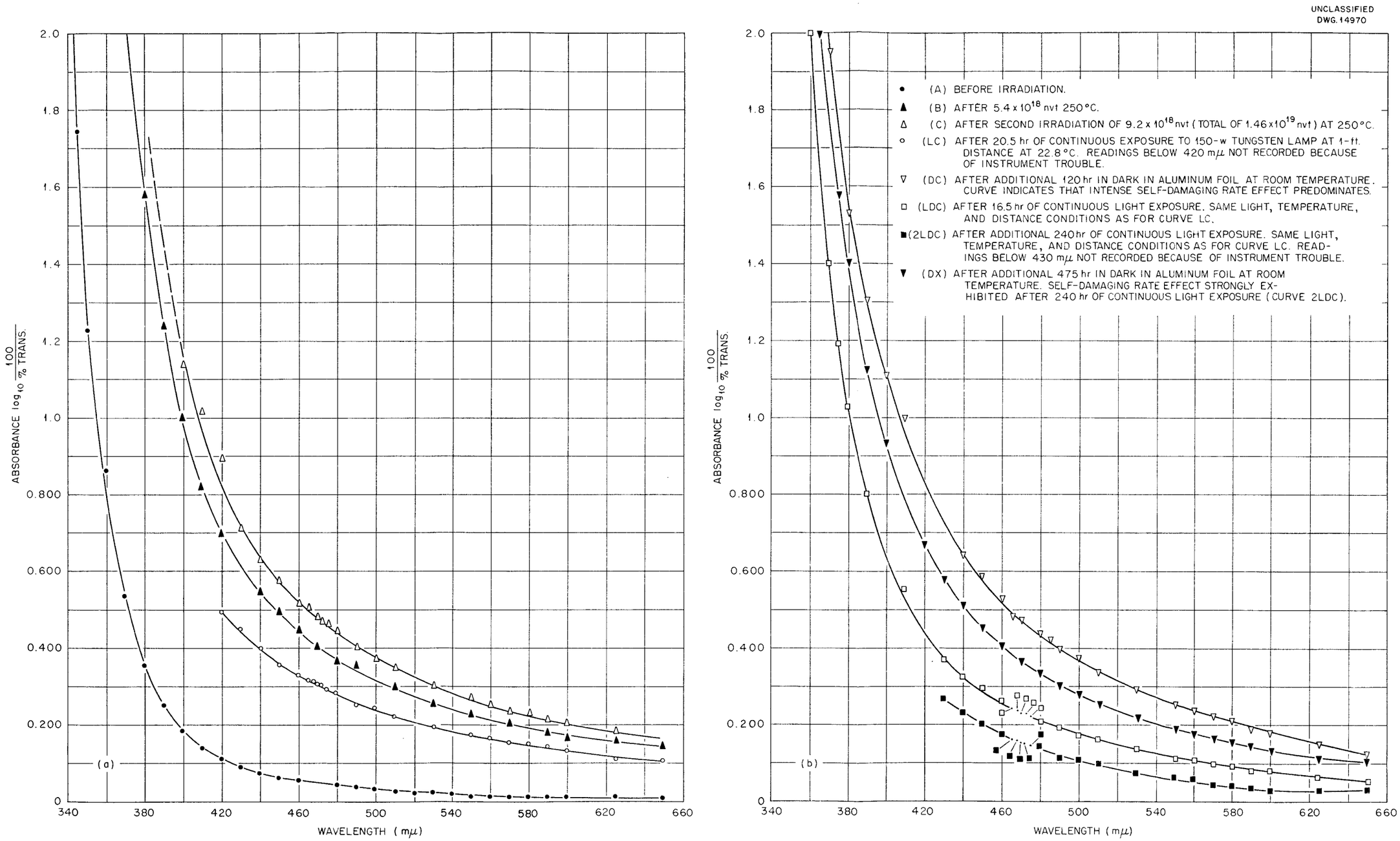

Fig. 35. Absorbance Curves of Radiation-Resistant Glass, ORNL-4M.

Part II

BOILING REACTOR AND SLURRY STUDIES

SLURRY AND BOILING REACTOR RESEARCH

R. N. Lyon, Section Chief

Alternative systems to the circulating solution for homogeneous reactors may consist of a circulating slurry, a boiling solution, or a boiling slurry. To date most of the research effort has been spent on the first two of these alternative systems, since it is believed that knowledge of all three systems can be gained most rapidly in this way.

SLURRY STUDIES

A. S. Kitzes R. B. Gallaher
W. Q. Hullings

Three types of uranium trioxide monohydrate have been investigated: amorphous, platelet crystals, and fine, rod-like crystals.

Considerable experience has been gained during the past quarter in pumping slurries.

Engineering studies of slurry systems continue to be hampered by a lack of uniformity in the oxide available for testing. Both platelet form and rod form are furnished in wide ranges of particle size, pH, and agglomerability – even the color varies from batch to batch. In spite of these variations, the caking and abrasion problems seem to have been eliminated in circulating systems with temperatures up to 150°F in the absence of radiation. The viscosity of various slurry concentrations has been measured, and design of equipment for slurry critical experiments has been outlined.

Loops. During the past quarter, several runs were made in the 150 to 110°C temperature-cycle loop previously described.[1] In making these runs, sampling techniques were greatly improved and reliable chemical analytical procedures for studying the abrasive and corrosive action of $UO_3 \cdot H_2O$ slurries during pumping were developed.

Slurries containing as high as 200 g of amorphous $UO_3 \cdot H_2O$ per liter of water were pumped through the stainless steel loop at a velocity of 10.5 ft/sec with a centrifugal pump. Samples were drawn off through a tube welded into the center of the vertical pipe leading from the discharge of the pump. Chemical analyses of duplicate samples taken periodically indicated reproducibility of results within experimental error. Conclusions drawn from available data indicate no evidence of erosion, corrosion, or caking in any part of the system.

Uranium trioxide monohydrate in crystal-rod form was circulated in the loop with similar results. Microscopic examination revealed a rounding of the crystal corners but no other change in the slurry.

A high-temperature slurry loop similar to the ones in which uranyl sulfate is now being circulated has been designed. It is anticipated that the loop will be in operation by June 1, 1952.

Uranium trioxide of varying concentrations will be circulated at velocities greater than 20 ft/sec with a Westinghouse Model 100A pump. The loop will operate at 250°C and 1000 psi. Abrasion, corrosion, and particle comminution or growth will be the properties initially studied.

Pumps. Amorphous uranium trioxide monohydrate slurries were circulated continuously by means of the 1.5-hp, fluid-bearing, canned-rotor pump at

(1) A. S. Kitzes, R. B. Gallaher, R. V. Bailey, W. Q. Hullings, and C. A. Gifford, "Slurry Pumping Studies," *Homogeneous Reactor Project Quarterly Progress Report for Period Ending August 15, 1951*, ORNL-1121, p. 155.

room temperature for approximately 1000 hr without detectable wear. The pump (described previously[2]) was then dismantled, and examination of the parts showed no visible or measurable wear or corrosion.

For the first 600 hr of operation, a slurry containing 100 g of UO_3 per liter of water was circulated through a stainless steel loop. Dry UO_3 was then added to bring the concentration of solids up to 200 g per liter. The pump circulated this slurry for the additional 400 hours.

The clearance between the rotors and cans of the motor was 0.010 inch. Microscopic examination of the solids showed that the oxide particles were reduced in size by the pumping operation.

(2) A. R. Frithsen and M. Richardson, "Canned Rotor Pump," *Aircraft Nuclear Propulsion Project Quarterly Progress Report for Period Ending June 10, 1951*, ANP-65, p. 170.

PHYSICAL PROPERTIES OF SLURRIES

Viscosity Measurements of $UO_3 \cdot H_2O$–H_2O Slurries. For proper engineering design of systems requiring the pumping of slurries, the viscosity, density, and other related physical properties of the slurries must be known as a function not only of the concentration of uranium but also of particle size.

Viscosity measurements for slurries of amorphous $UO_3 \cdot H_2O$ and water were made over a wide range of temperatures by measuring the pressure drop required to give a desired flow rate of slurry through a given length of tubing. The plasticity parameters were then determined from a plot of the shear diagrams. These data are shown in Table 21.

Apparent viscosities for $UO_3 \cdot H_2O$–H_2O slurries can be calculated by using

TABLE 21

Plasticity Parameters of Amorphous $UO_3 \cdot H_2O$ – H_2O Slurries

TEMPERATURE (°C)	SLURRY CONTAINING 290 g OF $UO_3 \cdot H_2O$ PER LITER OF H_2O		SLURRY CONTAINING 190 g OF $UO_3 \cdot H_2O$ PER LITER OF H_2O	
	COEFFICIENT OF RIGIDITY, η (lb/ft·sec)	YIELD STRESS, τy (lb/ft^2)	COEFFICIENT OF RIGIDITY, η (lb/ft·sec)	YIELD STRESS, τy (lb/ft^2)
40			0.0021	0.131
60				
70	0.0023	0.175		
80			0.0018	0.101
100	0.0021	0.146	0.0015	0.060
120	0.0018	0.065	0.0011	0.030
140	0.0016	0.065		

the parameters listed in Table 21 in the following equation:

$$\mu_e = \eta + \frac{D(\tau y)}{6V},$$

where

μ_e = apparent viscosity,

η = coefficient of rigidity (lb/ft·sec),

τy = yield stress (lb/ft^2),

D = diameter of pipe (ft),

V = velocity of slurry (ft/sec).

From the preliminary determinations of the plasticity parameters, it was found that the uranium trioxide slurries followed the law of plastic flow – a finite stress was required to initiate fluid shear. Additional tests are planned in which the plasticity parameters will be determined for varying particle sizes, concentration, and purity as a function of temperature.

Density. The densities of the slurries were usually calculated by using the following equation and assuming the density of dry $UO_3 \cdot H_2O$ to be 6:

$$d = V_1(d_1 - 1) + 1,$$

where

d = density of slurry (g/ml),

d_1 = density of $UO_3 \cdot H_2O$ = 6,

V_1 = volume fraction of uranium trioxide in slurry.

Absolute density measurements were made by using a pycnometer when accurate determination of density was necessary.

Sedimentation Rates. Settling rates are important factors in the operation of a slurry reactor, since criticality may be affected as uranium particles settle and cause decreased flow velocity and turbulence. A program has therefore been initiated to determine settling rates in $UO_3 \cdot H_2O$ slurries as a function of temperature, particle size, and concentration of oxide.

Preliminary data indicated that for 44-μ particles, the settling rates increased as the temperature of the system was increased, and the rate of fall was slower in concentrated slurries than in dilute ones. The increase in settling rate was found to be of the same order of magnitude as predicted by Stokes law for free-falling spheres. Determinations were made by observing the level of slurry in a 100-ml graduated cylinder. Reproducibility of the results obtained with different batches has been poor. This is undoubtedly caused by lack of uniformity in the batches of oxide. Plans have been made for determining the settling rate as a function of purity and particle size of the oxide.

Crystal Growth. Uranium trioxide crystals in the form of platelets grew when autoclaved at 250°C for 24 hr or longer in stainless steel bombs. The original crystals (average size 50 μ) grew to a maximum size of 500 μ and then split into smaller fragments approximately 100 μ in size. No evidence was found for the regrowth of the fragments.

Uranium trioxide crystals in the form of rods grew when autoclaved at 250°C for 24 hr or longer in stainless steel bombs, but the rate of growth was much less than for the platelets.

In 24 hr, the rods increased in size from 1 to 3 μ in diameter and 5 to 6 μ in length to 4 μ in diameter and 15 to 17 μ in length. It was also found that the small rods tended to agglomerate to form "clumps" 100 μ in diameter.

Criticality Experiments. In cooperation with the criticality group, critical experiments have been outlined for systems using uranium trioxide slurries of varying concentrations. Critical heights as a function of water moderation, turbulence, and settling of the oxide particles will be determined for a reactor of constant diameter.

Slurry will be forced into the reactor - an aluminum tank 12 in. in diameter and 24 in. high - through a tangential opening near the bottom of the tank and agitated to cause turbulence. A known height of water will surround the reactor and act as the reflector. The height at which the reactor goes critical will be measured with a special level indicator, which is being fabricated by the ORNL Instrument Department. Equipment for the criticality determinations is now being designed. The date for the first experiment has been tentatively set for July 1, 1952.

BOILING REACTOR STUDIES

As reported last quarter, the Los Alamos reactor, Supo, was operated under boiling conditions and much of the doubt regarding the stability of a boiling reactor was removed. However, these tests provided no quantitative basis for predicting the possible productivity of a reactor that is actually designed to boil. Also, because of the presence of a large stainless steel coil in the Supo reactor core, the response to sudden increases in reactivity of a reactor without large surfaces for bubble nucleation could not be determined. Several programs to help in settling these questions are currently under way.

Power Density Experiment (W. S. Brown). Equipment has been designed for an experiment to determine the maximum power density attainable in a boiling liquid at high pressures. Liquid will be heated in a pressure vessel to 2000 psi, and then a rupture disk will release the pressure and allow the liquid to flash through an orifice to atmospheric pressure. Temperature and pressure measurements will be recorded during the escape time to provide values for use in a heat balance determination on the vessel. The heat released per unit time will be determined from the heat balance. Knowing the volume of liquid present at any time will make it possible to determine the power density in kilowatts per liter. The pressure vessel has been constructed and the rupture disks and flanges have been received. Assembly of the equipment has begun.

Expected Density of Boiling Solutions (P. C. Zmola). Density variation and circulation calculations were based on an idealized flow pattern within a cylindrical boiling reactor. It was postulated that the boiling liquid flows upward in the center, liberates a substantial part of the vapor at the top surface, and flows downward in an annular region along the wall of the containing vessel. There is some experimental evidence to suggest the realism of this flow pattern. Other postulations and simplifications were made.

1. Uniform power generation was assumed.

2. The bubbles were considered as being small relative to the scale of

the flow pattern so that the fluid could be considered homogeneous.

3. All vapor was assumed to be generated within the liquid.

4. The cross-sectional areas of rising and downcoming regions were considered equal.

5. Average values were used for the density in the rising and downcoming regions.

6. Steam table values were used for the physical properties of the fluid.

The core fluid will circulate under steady-state conditions at such a rate that the natural-convection driving force resulting from the density difference between the rising and downcoming regions will be balanced by the flow resistance of the system. Equations for both the driving and resisting systems have been written as expressions for the maximum rising velocity, U_{max}. The expression for the driving system is

$$U_{max} = \frac{q_0''' V_0}{h_{fg} A_3} \frac{v_{fg}}{(1 - \eta)} \cdot \left[\frac{\frac{2(1 - \eta)}{\gamma} - (3 + \eta)}{4} + 1 \right].$$

The expression for the resisting system is

$$U_{max} = \sqrt{\frac{2_g h_0}{K} \gamma} .$$

In these two expressions

V_0 = total volume of reactor at operating temperature and pressure but zero power,

h_0 = height of fuel at reactor operating temperature and pressure but zero power,

q_0''' = power density based on V_0,

A_3 = cross-sectional area of the rising region,

h_{fg} = heat of vaporization (latent heat),

$v_{fg} = v_g - v_f$ = difference between specific volume of saturated vapor and liquid,

η = fraction of the bubbles remaining in the fuel stream for each pass near the top surface,

$$\gamma = 1 - \frac{\rho_i}{\rho_0} = 1 - \frac{2 + \left[\frac{1 + 3\eta}{1 + \eta}\right] \left[\frac{1 - D}{D}\right]}{2 + \left[\frac{3 + \eta}{1 + \eta}\right] \left[\frac{1 - D}{D}\right]},$$

ρ_i = mean density of fluid in core region,

ρ_0 = mean density of fluid in annular downcoming region,

D = ratio of average density to liquid density at operating condition, $(1 - D)$ is equal to the fraction of density decrease,

K = loss coefficient (number of velocity heads - flow resistance loss),

g = gravitational constant.

This system of equations has been plotted in Fig. 36 for the special case of a cylindrical reactor 20 ft in diameter and 20 ft high producing 470 megawatts (~2.6 kw per liter). The abscissa is equal to the fraction of density decrease from the saturated liquid condition, $(1 - D)$, and the ordinate is the maximum rising velocity, U_{max}. For a given operating pressure and loss coefficient, the fraction of density decrease, maximum rise velocity, and circulation factor can be determined.

It should be noted that since the specific power enters the driving force expression linearly, the graphs can be easily modified to give results for other values of total power or power density. A scale is provided on Fig. 36 for this purpose.

The calculations indicate the following:

1. The mean density is strongly dependent on the hydrodynamic losses in the system.

2. It is not essential that all bubbles become disengaged at the top surface for every circulation pass of the fuel. The effect of only

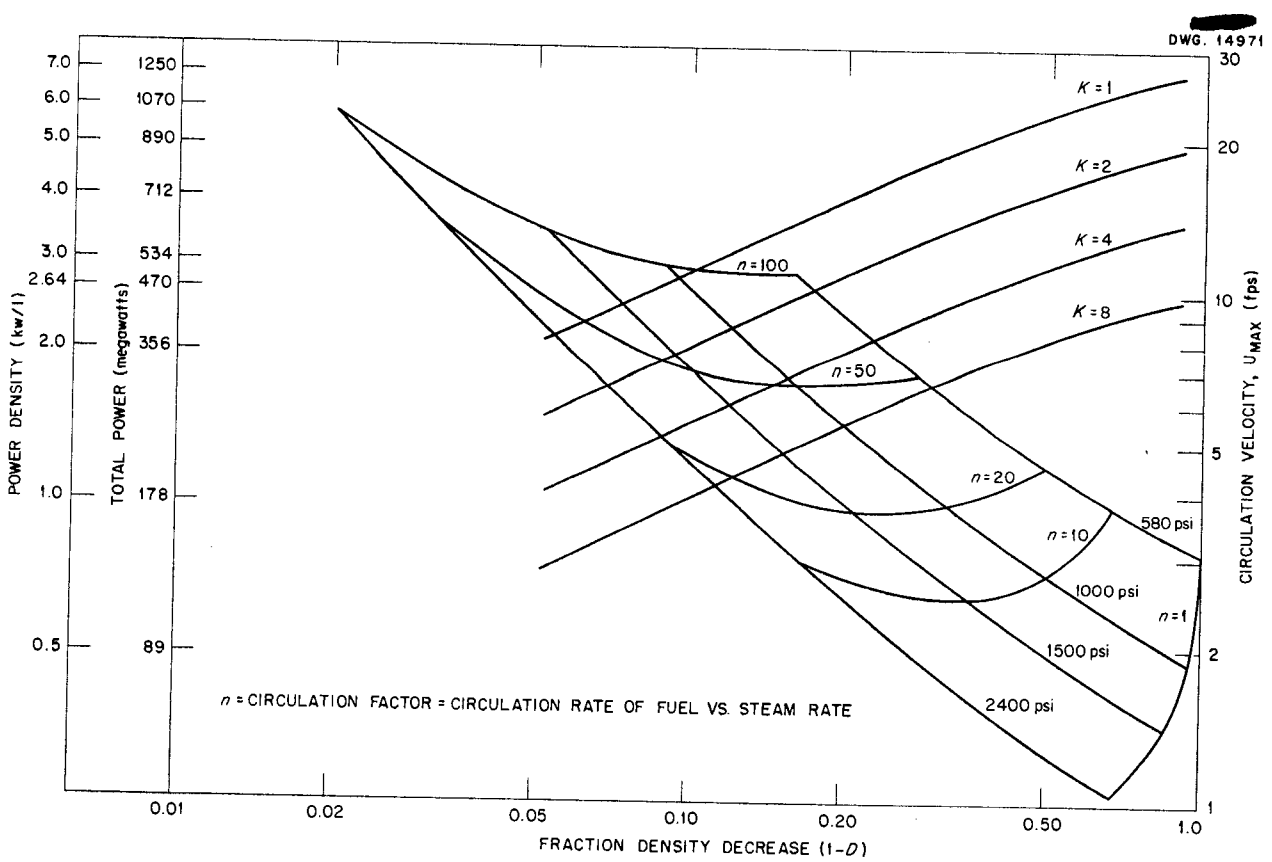

Fig. 36. Performance Chart for Circular Cylinder Boiling Reactor. Diameter, 20 ft; $\eta = 0$.

part of the bubbles being removed per pass requires a decrease in hydrodynamic resistance to maintain the same mean density.

3. Attention must be directed toward the problem of steam separation from the top surface of the fuel. At present it is not clear whether steam separation or decrease in mean fuel density will set the upper specific power limit.

Volume Boiling of Aqueous Solutions (R. F. Larson, J. D. Roarty). During the past quarter apparatus have been assembled to study volume boiling in a weak electrolytic solution. Boiling is generated by electrical resistance heating of the solution contained between two stainless steel plates that are immersed in approximately 25 liters of solution containing 0.25 g of potassium hydroxide per liter. The back surface of the stainless steel plates is enameled with a coating that is a good electrical insulator and on which bubbles form with difficulty. Hence, the electrical field is localized in the region between the stainless steel plates.

The purpose of this study is to measure the average bulk density of the boiling liquid at atmospheric conditions as a function of the specific power. The average bulk density is required in evaluating the driving force for natural circulation in a boiling solution. Another quantity of interest that this experiment might yield is a direct measurement of the velocity of the circulating boiling solution as a function of specific power. The circulation rate will have an important influence on the solution density and will enable the data obtained in this experiment to be used with the theoretical results of the preceding discussion.

To measure the average bulk density of the solution in the boiling region, air will be bubbled slowly through two glass tubes submerged at different levels in the solution. Equalization of the air flow in each tube will be determined by noticing the time rate of bubbles leaving the end of the glass probes. A differential manometer will be connected across the glass tubes, which serve essentially as pressure probes. By observing the differential height of the manometer reading with and without bubbles present in the test region, it is hoped that the ratio of the average bulk densities with and without boiling can be ascertained. Preliminary test results indicate uncertainty in the precision and adaptability of this method for density determinations.

Survey of the Experience of Boiler Manufacturers (R. F. Larson, P. C. Zmola). Problems associated with a boiling reactor were discussed with representatives of the Babcock and Wilcox Company, Foster Wheeler Corporation, and Combustion Engineering Superheater, Inc. It is the consensus of these manufacturers that the required conditions for a useful reactor are not impossible or even necessarily difficult to attain, but operating experience is not in existence to support the extrapolation.

Combustion Engineering has in the past built two steam generators in which heat is obtained by electrical resistance heating in the water itself. After a short discussion, it was concluded by the group that these units do not bear any greater similarity to a boiling reactor than does an ordinary steam generator.

Studies on the Promotion of Boiling by Fission in Superheated Uranium Solutions (R. J. Goldstein). The first phases of the experiment to

study the promotion of boiling by fission has been completed, and indications are that for reasonable superheats fission recoils are not good bubble promoters.

A sample of uranyl sulfate solution was heated in an oil bath until it became superheated. The sample was then placed in a neutron beam from the X-10 graphite pile to observe the effect of fission in the metastable system. For the maximum superheat obtained, approximately 16°F, no boiling was observed when the liquid was irradiated. The maximum thermal flux was measured in the solution as approximately 10^6 neutrons/cm^2/sec. With the sample used, this flux would give a fission density of 400 fissions/cm^3/sec.

It was originally theorized that fission fragments, or to be more exact, the track of high energy release where the fragments are slowed and stopped, would act as excellent nuclei for bubble formation. The effect was not thought of as cumulative, but rather that only one fission recoil track would be required for the formation of a bubble; the density of tracks in the liquid was of no great importance.

One possible explanation for the lack of bubbles in the exposed sample is that the superheat required for bubble formation from a track is greater than the 16°F obtained. At no time during the tests in the Pile Building were the samples capable of withstanding a superheat greater than 18°F, except one in which the superheat is believed to have been raised to about 35°F for an extremely short time. This compares with values of 24°F superheat obtained when the background flux is virtually zero. In the Pile Building there is sufficient background to produce several fissions in the sample every minute. Thus, if bubbles can be started by a fission recoil track at some superheat, Δt, sustaining a superheat greater than Δt in the Pile Building for more than a short time would not be expected. This may explain the anomalous behavior of the sample mentioned previously. However, the difference in superheat attained in the laboratory compared with that attained in the pile may merely be the result of unintended differences in cleaning technique and operating procedure or some other nonnuclear effect.

The only positive conclusion that can be drawn is that a single pair of fission tracks of low densities of fission are not nuclei for bubble formation in a uranyl sulfate solution containing 40 g of uranium per liter when the superheat is less than 16°F. Future experiments are planned to find the effect of fission on solutions that are superheated more than 16°F.

Boiling Reactor Kinetics (P. R. Kasten). A thorough investigation of the equations of motion is necessary in studying boiling reactor stability and therefore is a prerequisite to an extensive experimental program. Hence, attention has been directed to the development of kinetic equations applicable to a reasonable physical system. Once these equations are obtained, the time behavior of the system will be studied for various disturbances from equilibrium conditions.

The nuclear power equations have been presented in a previous HRE quarterly report[3] and can be written as

$$\frac{dP}{dt} = \lambda_0 [k(1 - \beta) - k_c] P + \sum_i \lambda_i c_i , \quad (1)$$

(3) "Reactor Physics," *Homogeneous Reactor Experiment Quarterly Progress Report for Period Ending November 30, 1950*, ORNL-925, p. 78.

$$\frac{dc_i}{dt} + \lambda_i c_i = \lambda_0 \beta_i k P , \qquad (2)$$

where

P = nuclear power of reactor,

t = time,

$\lambda_0 = \frac{1}{\tau k_{c0}}$,

τ = average lifetime of prompt neutrons,

k = material multiplication constant,

k_c = k required for criticality,

k_{c0} = k_c evaluated under initial conditions,

β = fraction of delayed fission neutrons,

c_i = concentration of ith group of delayed neutron emitters,

λ_i = decay constant of ith group of delayed neutron emitters,

β_i = fraction of fission neutrons in ith group of delayed neutrons.

A cylindrically shaped active region appears to be a reasonable starting point for this investigation. Under this condition, the characteristic equation

$$k_c = 1 + B^2 M^2 \qquad (3)$$

becomes

$$k_c = 1 + \frac{k_{c0} - 1}{1 + A}\left[\left(\frac{\rho_0}{\rho}\right)^2 + A\right], \qquad (4)$$

where

$$A = \left(\frac{\pi R}{2.405\ L_0}\right)^2 ,$$

R = equivalent radius of cylinder,

L_0 = equivalent fluid height under initial conditions,

ρ = fluid density of reactor,

ρ_0 = ρ evaluated under initial conditions, as developed in ORNL-1062[4] under the assumption of uniform fluid density.

The material k will be assumed to vary stepwise or linearly with time or both. Thus,

$$k = k_0 + ct . \qquad (5)$$

To complete the mathematical system, a relation between ρ and P is required, where

$$\rho = \rho_l - f_v(\rho_l - \rho_v) \qquad (6)$$

and

ρ_l = density of liquid,

ρ_v = density of vapor,

f_v = fraction of vapor in reactor core.

[When water is used as the solvent, only the density of the water will affect the critical reactor size if the volume of water displaced by the fuel is negligible. This is true for concentrations below 100 g of uranium per 1000 kg of water (U as UO_2SO_4).]

(4) J. M. Stein and P. R. Kasten, *Boiling Reactors: A Preliminary Investigation*, ORNL-1062, Nov. 23, 1951.

In Eq. 6, ρ and ρ_v are functions of pressure as given in tables of thermodynamic properties of the liquid and vapor. f_v is a function of the volume of vapor in the reactor core, which is dependent on the nuclear power and pressure. Hence, in order to relate ρ to P, the correspondence of p and f_v with P needs to be established.

The physical system is considered to consist of the elements indicated in Fig. 37.

UNCLASSIFIED
DWG. 14972

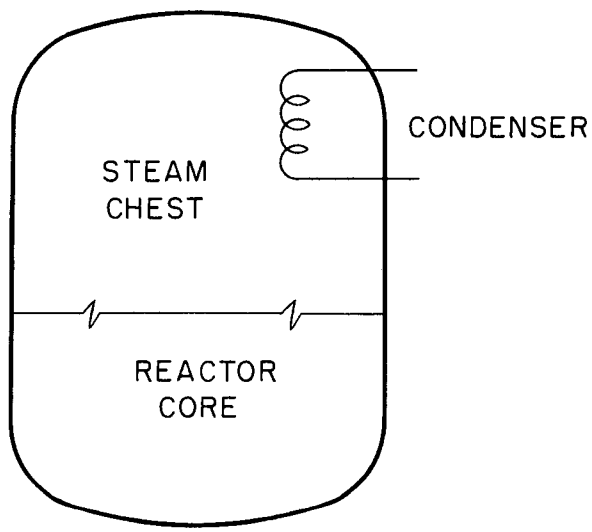

Fig. 37. Diagram of Reactor.

The following nomenclature will be used:

V_0 = total volume of reactor,

V_s = volume of steam chest,

V_b = volume of vapor in reactor core,

$V_{st} = V_b + V_s$,

V_l = volume of liquid in core,

M_0 = total mass of reactor fluid (liquid and vapor),

M_s = mass of vapor in steam chest,

M_b = mass of vapor bubbles in core,

$M_{st} = M_s + M_b$,

M = mass of reactor core liquid.

The volume occupied by the uranium salt in the system will be negligible, so

$$V_0 = V_{st} + V_l ,$$

$$M_0 = V_{st}\rho_v + V_l\rho_l ,$$

and hence

$$V_{st} = \frac{V_0\rho_l - M_0}{\rho_l\rho_v} = F_1(p) , \qquad (7)$$

where $F_1(p)$ is a function of the pressure, p, and is defined in Eq. 7 and in the nomenclature:

$$f_v = \frac{V_b}{V_b + V_l} . \qquad (8)$$

The heat content, H, above that of the saturated liquid of all the vapor bubbles within the core is now considered. Clearly,

$$H = V_b h_{fg}\rho_v , \qquad (9)$$

where

h_{fg} = energy required to vaporize a unit weight of the saturated liquid.

Since $h_{fg}\rho_v$ and $V_l = V_0 - V_{st}$ are functions of pressure alone, f_v can be stated as

$$f_v = \frac{H}{H + F_2(p)}, \tag{10}$$

where $F_2(p) = h_{fg}\rho_v(V_0 - V_{st})$.

The time rate of change of H is dependent upon the rate at which energy forms vapor bubbles and how quickly vapor leaves the core. Reasonable assumptions for the above are that the rate at which vapor is formed is proportional to the liquid superheat, and the rate of vapor removal is proportional to the vapor volume within the core. With these conditions,

$$\frac{dH}{dt} + \lambda H = K(T - T_s), \tag{11}$$

where

T = temperature of liquid,

T_s = temperature of the liquid in equilibrium with the pressure,

λ = reciprocal mean residence time of vapor in core,

K = effective heat transfer rate per degree of superheat.

Neglecting heat losses through the vessel walls, it follows that

$$\alpha \frac{dT}{dt} = P(t) - K(T - T_s), \tag{12}$$

where $\alpha = c_p V_l \rho_l \approx$ constant.

From Eq. 12,

$$T = \frac{1}{\alpha}\int_0^\infty e^{-(K/\alpha)x}[P(t - x) + KT_s(t - x)]\, dx = \frac{1}{\alpha}[q + Kg], \tag{13}$$

where

$$\dot{q} + \frac{K}{\alpha} q = P(t), \tag{14}$$

$$\dot{g} + \frac{K}{\alpha} g = T_s. \tag{15}$$

Hence Eqs. 11 and 12 become

$$\frac{dH}{dt} + \lambda H = \frac{K}{\alpha}[q + Kg - \alpha T_s], \tag{16}$$

where q and g are described in Eqs. 14 and 15.

It yet remains to find p as a function of P. This can be done by considering an energy rate balance on the total mass of steam, which is dependent upon P_c – the power removed by the condenser. From the heat transfer equation,

$$P_c = UA[T_s - \overline{T_w}] = c_p G[T_w(\text{out}) - T_w(\text{in})], \tag{17}$$

where

U = over-all heat transfer coefficient,

A = area available for heat transfer,

T_s = temperature of steam in vapor chest,

$\overline{T_w}$ = average temperature of cooling water in condenser coil,

$T_w(\text{in})$ = temperature of cooling water into condenser,

$T_w(\text{out})$ = temperature of cooling water out of condenser,

G = mass flow rate of cooling fluid,

c_p = specific heat of cooling fluid,

considering

$$\overline{T_w} = a\frac{T_w(\text{out}) + T_w(\text{in})}{2},$$

where

a = factor to compensate for linear averaging of $\overline{T_w}$,

$$P_c = \frac{UA}{1 + \frac{UAa}{2c_pG}}[T_s - aT_w(\text{in})] = F_3(p). \quad (18)$$

Since pressure has little effect on the enthalpy of a given mass of vapor, the desired relation between p and P is

$$\frac{dH_{st}}{dp}\frac{dp}{dt} = K(T - T_s) - F_3(p)$$

$$= \frac{K}{a}[q + Kg - aT_s] - F_3(p), \quad (19)$$

where $H_{st} = V_{st}h_{fg}\rho_v = F_4(p)$.

The above equations, together with the initial conditions, complete the mathematical system for $\rho = \rho(p,H)$, where p and H are related to the nuclear power. However, the solution of these equations is very difficult because they are nonlinear. Also, the nonlinear characteristics vary because F_1, F_2, F_3, and F_4 are dependent upon operating conditions. For short periods of time following a reactivity increase, these kinetic relations become less involved, and a particular case has been extensively investigated.[4] Also, a linearized version of the kinetic equations has been investigated by T. A. Welton.[5] Both reports indicate that although boiling reactors appear stable, more detailed exploration is needed to determine the conditions that assure stability. At present the F_i functions are being evaluated for initial pressures of 15 to 150, 580, and 1000 psia, and with this information the stability of the reactor and the effects of various parameters will be studied by solving the equations with a suitable differential analyzer. The results will be compared with those obtained when the equations of motion are simplified by assuming T_s constant and $T = T_s$. The effect of the delayed neutrons will also be investigated, particularly the error introduced by replacing the usual delayed-neutron equations by equations that consider a steady source (which simplifies the equations to a great extent). By such methods it is hoped that stability conditions can be defined for various operating conditions and also that future stability questions can be answered by simplified, approximate equations.

Small-Scale Boiling Reactor Experiment (W. M. Breazeale, R. B. Briggs, J. W. Brown, W. S. Brown, R. J. Goldstein, D. T. Jones, P. R. Kasten, R. F. Larson, C. G. Lawson, J. R. McWherter, P. C. Zmola). Although the foregoing experiments and analyses will aid in establishing the relationships between the variables that control the characteristics of a boiling reactor, it has become evident that a complete definition of these relationships can be obtained with

(5) T. A. Welton, *Comments on the Proposed Boiling Reactor Program*, ORNL CF-51-11-163, Nov. 27, 1951.

assurance only by studying the operation of an actual boiling reactor. With this in mind a small, temporary, chain reacting unit has been proposed, the preliminary design is nearing completion, and a feasibility report is currently being prepared. The apparatus for the proposed experiment is referred to as the Teapot, and, in general, it will consist of a cylindrical (17 1/2 in. in diameter and variable in height), unreflected, homogeneous reactor containing a solution of enriched uranyl sulfate in normal water as fuel and moderator. The equipment will be run under bulk-boiling conditions with the nuclear power supplying all the energy for vapor formation. It will be constructed for temporary use only and is in no way intended as a permanent facility.

The Teapot experiment is designed to answer some questions fundamental to the feasibility and to the design and construction of large-scale homogeneous boiling reactors. The following important points will be studied.

1. The stability of a boiling reactor under a variety of operating conditions will be investigated. Stability for certain conditions has been demonstrated by successful boiling of the Los Alamos water boiler, but operation with higher power densities and void volume may be quite different. Besides stability under normal conditions, the effect of sudden changes in δk will be studied. The degree of damping of the perturbations will indicate the inherent safety of boiling reactors.

2. The maximum power density attainable for the reactor as a function of pressure will be determined. Geometry, solution concentration, absence of a reflector, and absence of any baffles to control and direct circulation will of course affect the absolute value of the power density, but the effect of pressure and reasonable values of power density for a large-scale reactor will be available from the test data.

Points of secondary interest will also be investigated.

1. The prompt-neutron generation time and the effective number of delayed neutrons will be ascertained. This information will be of use in evaluating the kinetic equations for the Teapot.

2. The vertical flux distribution along the core axis will be obtained.

3. The maximum power density will be determined as a function of the height of the fuel in the core. This will indicate the effect of mean bubble time in the liquid on power density.

In addition, the Teapot experiment will give experience in the design and operation of a boiling reactor. Knowledge of the problems associated with this type of reactor should prove invaluable in future experimental and developmental work.

The working fluid will be a solution of uranyl sulfate in normal water. The uranium will be enriched (93.4% U^{235}) and the hydrogen-to-uranium ratio will be 400, which corresponds to a concentration of 59 g of U^{235} per kg of solution.

The Teapot is designed to sustain pressures of 150 psi and a thermal power load of 250 kw (4 to 5 kw per liter of solution). The design is simple because of the relatively low pressure specification, and yet it will be possible to operate over a large enough range to obtain pertinent data. The reactor will not necessarily

be expected to operate at the design power, even at 150 psi, because of the nuclear characteristics of the boiling system. Even if it is capable of developing 250 kw, this load would be applied for only a short period of time. Many experiments can be performed at low pressure – a small power density will give a relatively large void volume.

The Teapot experiment should be completed within one year after the acceptance of the feasibility report on its construction. Although operation of the reactor may continue over a period of several months, most of the important data should be obtained in the first week or two of operation.

The reactor and most of its auxiliary equipment, except the instrument and control panel, will be placed in a concrete pit under ground level to decrease the cost of shielding. The relative locations of the various equipment can be seen on the flow sheet, Fig. 38. The core of the reactor will be in one compartment of the large pit, which will be separated from the dump tanks below and the valves, pump, and other equipment alongside by several feet of concrete. Therefore operating personnel will be able to enter the "valve compartment" in cases of emergency when the reactor is not in operation and all fuel has been flushed out of the main system. Approximately 7 ft of Barytes concrete will be required for overhead shielding.

Some distance from the core there will be a vent tank and auxiliary dump tanks for holding the fuel from the main system. The vent tank will be buried in the ground and kept at approximately atmospheric pressure. Gas will be bled from it through an activated charcoal adsorber to the atmosphere.

Almost all controls will be operated from the instrument and control panel that will be separate from the reactor and the vent tank.

An initial assembly of the actual reactor components will be constructed and run under simulated operating conditions, and after the preliminary tests the equipment will be moved to the Teapot location for final installation.

Mechanical Design. The type-347 stainless steel core tank, as currently designed, is cylindrical in shape with a 17 1/2-in. ID and 1/4-in. wall thickness. The tank length is approximately 6 ft, and it has standard 18-in. dished heads. The design pressure of the core is 250 psi with a corrosion allowance of 1/16 inch.

A 1-in.-ID thimble extending the entire length of the tank will be located along the core axis. This thimble would at various times act as a receptacle for (1) the neutron source during start up, (2) instruments for measuring the vertical flux distribution in the core, and (3) a poison that can be introduced in the core to study the kinetics of the reactor.

Heat Exchangers. The main heat exchanger will be a partial condenser of 1-in.-OD stainless steel tubing with a heat transfer area of 15 ft^2. The condenser will be located in the top part of the core tank and will condense most of the steam generated in the core. Condensate, returning by gravity, will be directed toward the periphery of the core by a set of baffles. Cooling water connections will be made through the top of the tank.

A heat exchanger, located after the recombiner, will be used to condense

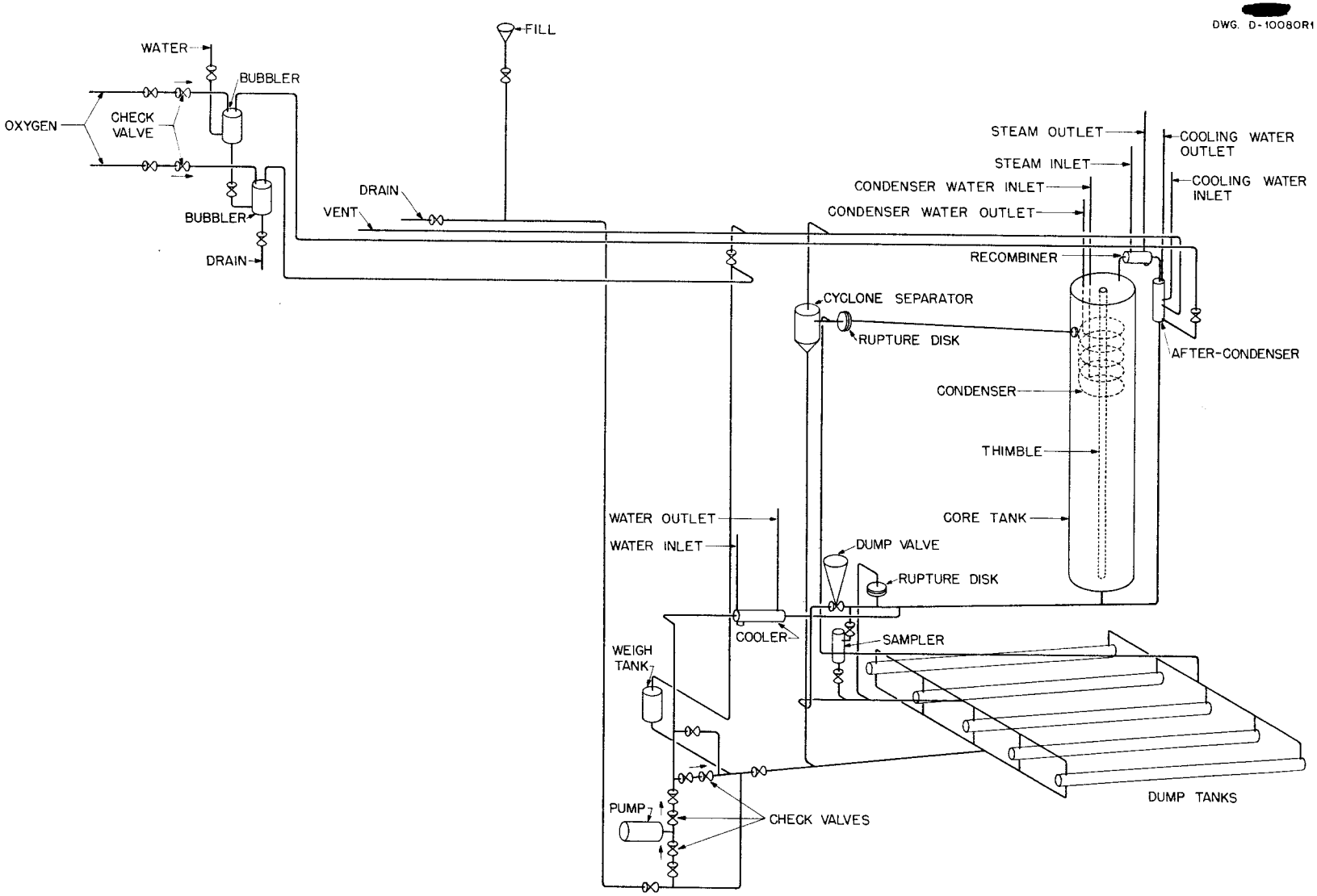

Fig. 38. Flow Diagram of Teapot Experiment.

the recombined hydrogen and oxygen and the steam not condensed in the main condenser. This total condenser will have a heat transfer area of 3 ft^2.

A cooler will be placed in the core-to-weigh tank fuel line to prevent flashing of solution when removing it from the high-pressure core. It will be fabricated in the form of a coil of 1/4-in. stainless steel tubing and will have a heat transfer area of 1 1/2 ft^2.

Feed System. A bellows type of positive-displacement pump has been selected for pumping the solution to the core tank. The pump has a displacement of 100 ml and will be manually operated to give a maximum flow rate of 0.5 gpm. The pump will be in operation only to increase the amount of solution in the core. The principal advantage of this type of pump is the control afforded when approaching critical.

A weigh tank will be provided in the system for weighing the solution in the core. It will be similar to the weigh tank used in the HRE.

Recombiner. A catalytic recombiner using platinized alumina pellets is planned for recombination of all hydrogen and oxygen formed in the core. Circulation through the recombiner would be assured by the decreased pressure at the total (after) condenser.

Corrosion. Oxygen will be dissolved in the condensate from the total condenser to decrease the corrosion rate and to keep the uranium in solution. It is believed that an absorber may be required below the total condenser to assure saturation of the condensate with oxygen.

Sampler. Present plans call for incorporating a device for sampling the radioactive solution when the reactor is shut down.

Flushing System. Provisions have been made for removing the fuel solution from the main system and flushing the pit to decrease the activity. Auxiliary dump tanks will be provided to contain the hot solution during the flushing operation.

Dump Tanks. In the present design, the main dump tanks are five 4-in.-ID and 6-ft-long containers made of type-347 stainless steel tubing.

System Piping and Valves. Nearly all piping in the Teapot will be 1/8-in. type-347 stainless steel. Fulton Sylphon 1/8-in. type-347 stainless steel valves with air actuators are to be used in the system. For emergency purposes a 2-in. stainless steel valve with the bonnet and stem assembly modified for air operation will be used to give a quick dump of the solution in the core. This valve will be opened automatically by a high flux of short period in the reactor and can also be controlled manually.

Rupture Disks. Two 2-in. type-347 stainless steel rupture disks will be provided on the Teapot to relieve excessively high pressure quickly. One will be located in the liquid region (set to rupture at 200 psi) and the other in the vapor space (set to rupture at 300 psi).

Instrumentation. The proposed instruments for neutron flux measurements at the reactor are:

1. two fission chambers with amplifying system sealer and count rate meter to be used during start-up and shutdown,

2. two 3-in. parallel-circular-plate ion chambers with amplifiers and

recorder to provide power level indication and act as safety chambers to prevent prohibitive power levels,

3. one 4-in. compensated ion chamber with log N amplifier and period circuit to provide log power and period readings and to open the dump valve if reactor period is too small,

4. boron-coated thermopiles and foils to give an indication of the axial flux distribution in the core.

The proposed standard process instruments are:

1. thermocouples to measure all pertinent temperatures,
2. a Baldwin pressure cell to measure core pressure,
3. Bourdon gages modified with Giannini pots to give remote readings for all other pressures in the systems,
4. a Baldwin load cell to measure the weight of solution in the weigh tank,
5. flowmeters to measure cooling-water flow.

SLURRY FUEL STUDIES

F. R. Bruce, Section Chief
J. O. Blomeke L. E. Morse
J. P. McBride

URANIUM TRIOXIDE CHEMISTRY

Uranium Trioxide Allotropy. Uranium trioxide monohydrate that has been heated in water at 250°C assumes either of three crystal habits: rods that are 1 to 5 μ in diameter and 10 to 30 μ long; thin translucent platelets, 6 to 50 μ along each edge; and finally, large octahedrons, which are several hundred microns along each edge.

X-ray-diffraction studies reveal that both the rods and platelets have an orthorhombic structure and are a mixture of alpha uranium trioxide monohydrate and beta uranium trioxide monohydrate, as reported by Zachariasen.[1] The bipyramids are found to have a triclinic structure. Although the exact relationship between these three forms is not as yet fully understood, there is some evidence that the presence of uranyl ion plays an important role in determining the type of crystal ultimately formed.

The rods are identical to a gamma uranium trioxide monohydrate reported by Vier,[2] and they are formed by decomposition of uranium peroxide dihydrate. These crystals are normally bright yellow and uniform in size. They have a pronounced tendency to grow upon digestion at 250°C until they are approximately 5 μ in diameter and 30 μ long. At this point, attained after about 70 hr of digestion, the rate of growth appears to decrease rapidly. The concentration of soluble uranium in an aqueous slurry of these rods is less than 10 ppm when the rods are initially formed, and this concentration does not greatly increase upon digestion periods of several hundred hours. On the other hand, if the rods are broken down by grinding, or other types of attrition, platelets are formed at 250°C, and there is an accompanying increase in the soluble uranium to 40 to 50 ppm. Since the transition of any crystal modification to a more soluble one is not believed likely, it is felt that the high observed solubility is caused by the presence of soluble uranium as uranyl nitrate carried down by occlusion in the rods. It is believed that the true solubility of the platelets is in the neighborhood of 2 to 3 ppm. The rods have desirable characteristics for slurry use. At a concentration of 250 g of uranium per liter they form a very flocculent type of precipitate and are easily redispersed by mild agitation after heating at 250°C and standing for periods as long as 30 days at room temperature.

Because of the generally encouraging picture presented by uranium trioxide rods, it was believed desirable to investigate thoroughly the preparation of this material and to formulate a flowsheet suitable for use in preparing quantities large enough for engineering studies and further laboratory experiments. This investigation was completed, and a flowsheet was presented for the preparation of 1-kg quantities of uranium trioxide monohydrate rods.[3]

---

(1) W. H. Zachariasen, *X-Ray Diffraction Studies of Miscellaneous Uranium Compounds*, MDDC-1152, June 1946.

(2) D. Vier, *Thermal Stability of Certain Oxide Hydrates in H_2O*, A-1277, May 26, 1944.

(3) J. O. Blomeke, *The Preparation of γ-$UO_3 \cdot H_2O$ from Uranyl Nitrate*, ORNL CF-51-12-67, Dec. 12, 1951.

The platelet form of uranium trioxide monohydrate is normally obtained upon digestion at 250°C of washed Mallinckrodt uranium trioxide, as well as from the digestion of fragmented rods. Mallinckrodt uranium trioxide, prepared by calcination of uranyl nitrate, normally contains a nitrate concentration of about 0.1% after exhaustive washing. The platelets upon digestion at 250°C grow at a rate comparable with that of the rods and eventually approach a size of 50 to 60 μ along their edges. They are not so bright a yellow as the rods, and their slurries pack to a higher bulk density and are not so easily redispersed after settling. When they are broken down mechanically, they assume their original form upon further digestion.

Bipyramids are obtained when either the rods, platelets, or Mallinckrodt uranium trioxide is digested at 250°C in the presence of several hundred parts per million of soluble uranium. The bipyramids appear to be identical to a delta uranium trioxide monohydrate reported by Vier.[2] Little is known of the stability of these crystals beyond the fact that they grow in water at 250°C. At the present time it is felt that the bipyramids are too large to be of use in a slurry reactor, since very violent agitation is required to maintain them in a homogeneous suspension. After grinding in a micronizer, further digestion of the bipyramids results in their conversion to platelets.

From the most recent data, it is concluded that the rod form of uranium trioxide represents a stable modification only in the absence of uranyl ion. In the presence of a small amount of uranyl ion, the rods are transformed upon heating to the platelets. In the presence of large amounts of uranyl ion, the platelets, in turn, are transformed to the bipyramids. It has been shown that sodium ion and nitrate ion do not play a significant part in the conversion of one form to another.

Considerably more experimental work must be done before the exact relationship of these three crystal forms can be determined and the relative merits of slurries made from each established in a more quantitative fashion.

Valence State Studies. In order to study the effect of partial pressures of hydrogen and oxygen on the equilibrium valence state of uranium in uranium oxide slurries, samples of the various oxides were heated in stainless steel at temperatures between 100 and 250°C for varying lengths of time.

Uranium dioxide oxidized to uranium trioxide in the presence of oxygen gas. The extent of this oxidation was dependent on the oxygen pressure and seemed to occur independently of the partial pressure of hydrogen. For example, a uranium dioxide slurry under an oxygen pressure of 202 psi was 75% oxidized in 16 hr at 250°C, whereas with an oxygen pressure of 378 psi the slurry was 82% oxidized in the same time. A uranium dioxide slurry under 63.5 psi of hydrogen and 61.5 psi of oxygen was 78% oxidized in 24 hours. With a hydrogen pressure of 63.5 psi and an oxygen pressure of 175 psi, this slurry was 91% oxidized in 24 hr (Table 22).

The extent of oxidation of U_3O_8 to uranium trioxide was found to be dependent both upon temperature and oxygen pressure. The presence of a partial pressure of hydrogen did not seem to inhibit markedly the oxidation of the uranium. Thus, after heating a U_3O_8 slurry under 51.8 psi of hydrogen and 25.9 psi of oxygen for 24 hr at 150°C, 63.2% of the uranium was oxidized. After heating at a temperature of 225°C for the same length of

time under 67 psi of hydrogen and 33.5 psi of oxygen, the uranium was 92.6% oxidized. Increasing the pressure of oxygen from 17.5 to 175 psi increased the degree of oxidation of the uranium from 75.2 to 96.8% (Table 23).

TABLE 22

Oxidation of UO_2 Slurries Upon Heating Under Varying Partial Pressures of Hydrogen and Oxygen

HEATING CONDITIONS		GAS PRESSURE		URANIUM OXIDIZED (%)
TEMPERATURE (°C)	TIME (hr)	H_2 (psi)	O_2 (psi)	
200	48	63.5	31.8	64.9
250	16		202	74.5
	16		378	82.2
	24	70	61.5	78.4
	24	70	175	91.4

TABLE 23

Oxidation of U_3O_8 Slurries on Heating for 24 hr Under Varying Partial Pressures of Hydrogen and Oxygen

TEMPERATURE (°C)	GAS PRESSURE		URANIUM OXIDIZED (%)
	H_2 (psi)	O_2 (psi)	
150	51.8	25.9	63.2
170	59.5	29.8	71.7
200	63.5	31.8	90.1
225	67	33.5	92.6
250		35	88.0
	175	35	85.1
	70	17.5	75.2
	70	175	96.8

It is interesting to note that the uranium trioxide monohydrate formed by the oxidation of U_3O_8 in a slurry at 150 to 170°C was entirely orthorhombic rods, whereas at 250°C the product formed was entirely plates. At the intermediate temperatures of 200 to 225°C the material was a mixture of the rods and the plates and at 250°C was mostly plates. A sample of U_3O_8 heated in water at 100°C, exposed to air, was about 85% oxidized in three weeks, and the product was orthorhombic rods.

When a slurry of uranium trioxide rods was heated at 250°C under varying pressures of hydrogen and oxygen, it was found that the slurry was unchanged by a stoichiometric mixture of hydrogen and oxygen, in the ratio of water, and was only very slightly reduced by a tenfold excess of hydrogen over the stoichiometric (Table 24).

TABLE 24

Reduction of UO_3 Slurries at 250°C Under Varying Partial Pressures of Hydrogen and Oxygen

HEATING TIME (hr)	GAS PRESSURE		URANIUM REDUCED (%)
	H_2 (psi)	O_2 (psi)	
20	263	26.3	0.5
	378	None	1.39
24	70	35	0
68	527	26.3	0.4

It is concluded from these studies that uranium trioxide is the stable equilibrium form when slurries of uranium oxide are heated in aqueous solutions at elevated temperatures since uranium dioxide is oxidized, even in the presence of excess hydrogen, to uranium trioxide; U_3O_8 is oxidized to UO_3, also in the presence of excess hydrogen; and uranium trioxide itself remains stable in the presence of excess hydrogen (Table 23).

Copper Sulfate Catalysis of Hydrogen and Oxygen Recombination. Preliminary experiments were carried out to evaluate the effectiveness of copper sulfate as a homogeneous catalyst for the recombination of hydrogen and oxygen over uranium trioxide slurries. Slurries containing 83.5 g of uranium trioxide rods in 0.05 *M* copper sulfate solution were heated at 250°C in a rocking autoclave under varying pressures of hydrogen and oxygen. After heating for 2 hr under hydrogen and oxygen pressures of 350 psi each, recombination was 50% complete, and after heating for 17 hr the recombination was 80% complete. When a slurry was heated at 250°C under 175 psi of oxygen and 350 psi of hydrogen for 200 hr, the recombination was 86% complete. Samples of these slurries were filtered, and a yellow filtrate that showed a high qualitative test for uranyl and sulfate ions and negative tests for copper ion was obtained. This filtrate had a pH of 4.0. Under the microscope this slurry appeared to consist of a mixture of small, rather uniform, reddish-brown plates and larger crystals resembling the triclinic uranium trioxide modification. These crystals were badly mixed and grown together. In some slurries that were heated for shorter periods of time, large, blue crystals were formed that are believed to be intermediate in the formation of the brown plates. It is postulated that uranium trioxide reacts with copper sulfate according to the following equation:

$$2\ UO_3 + CuSO_4 = CuUO_4 + UO_2SO_4\ .$$

At room temperature and at 100°C, there was no detectable reaction between uranium trioxide and copper sulfate after four days' time.

From these results it is apparent that copper sulfate catalyzes the recombination of hydrogen and oxygen over uranium trioxide slurries, and most of the recombination takes place during the early stages of heating. Upon further heating, the copper ion is removed from solution by formation of the insoluble $CuUO_4$. Thus, it appears that copper sulfate is not a promising material for the recombination of hydrogen and oxygen in slurry systems.

The use of copper oxide as a catalyst for the recombination of hydrogen and oxygen was investigated. As would be expected in the absence of copper ions, very little recombination occurred. After heating a mixture containing 5 g of uranium trioxide monohydrate and 0.5 g of copper oxide, intimately ground together, for 24 hr at 250°C the pressure decreased only from 1100 to 1000 psi. The filtrate from this slurry was colorless and had a pH of 6.0. The solids, apparently uranium trioxide monohydrate rods, were colored with a microcrystalline, reddish-brown material.

Deuterates of Uranium Trioxide. A preliminary study of the deuterates of uranium trioxide was initiated. As a result of this study, it was concluded that uranium trioxide gives identical reactions with deuterium oxide and with water and that no significant difference exists between the deuterates and the hydrates. Anhydrous uranium trioxide was mixed with deuterium oxide to form uranium trioxide dideuterate. This slurry was filtered, transferred to a vacuum desiccator, and dried for 2 hours. The product was then ignited to U_3O_8, and the formula for the original compound was found to be $UO_3 \cdot 1.9\ D_2O$, which corresponds to the similar dihydrate. Uranium trioxide monodeuterate prepared by the digestion of uranium trioxide in deuterium oxide at 100°C for two days was found to have the composition $UO_3 \cdot 1.01\ D_2O$,

which corresponds to a similar monohydrate. Uranium trioxide monodeuterate was also prepared by heating uranium trioxide dideuterate at 250°C for 20 hours. This material was found to have the composition $UO_3 \cdot 0.82\ D_2O$, which corresponds to preparations of the rods in a normal water system that analyzes 0.81 to 0.90 H_2O.

NO_2 and HNO_3 Vapor Oxidation of U_3O_8. As reported by Katz and Gruen,[4] NO_2 gas passed over U_3O_8 at 300 to 325°C slowly oxidizes the material to form a brick-red uranium trioxide. Similarly, nitric acid vapor, obtained by bubbling nitrogen or air through nitric acid at 70°C, yields a bright-red uranium trioxide. Both the above forms are hydrated more slowly in cold water than the usual uranium trioxide. With water at 100°C they hydrate to form uranium trioxide monohydrate, and with water at 250°C they form uranium trioxide monohydrate platelets. All these hydrates have a greenish tinge, which indicates a trace of unoxidized U_3O_8; however, the amount is very small. These compounds show no advantage over other forms of uranium trioxide for slurry purposes, and the plates formed at 250°C seem to be identical to those obtained from Mallinckrodt uranium trioxide.

Preparation of Uranium Trioxide by Oxidation of U_3O_8. In the preparation of uranium trioxide monohydrate by thermal decomposition of uranyl nitrate it is difficult to remove the last traces of nitrate by prolonged washing or by heating the anhydrous oxide in air at 500 to 600°C. Since it has been found that soluble uranium is an important constituent in influencing the transition of rods to platelets and bipyramids, a pure form of uranium trioxide is desired.

A potential method for preparing uranium trioxide free of nitrate ion is the high-temperature oxidation of U_3O_8 by oxygen, as reported by Sheft and Fried.[5] This preparation was explored by first precipitating ammonium diuranate and igniting it to U_3O_8 by heating at 450°C in air. The U_3O_8 was then heated at 750°C at an oxygen pressure of 850 psi. After three days of heating, only partial conversion of the black U_3O_8 to the yellow, microcrystalline uranium trioxide was indicated. The oxide was returned to the autoclave and heated at 750°C with 400 psi of oxygen for three more days. X-ray analysis showed this oxide to be somewhat similar to that obtained by heating Mallinckrodt UO_3 at 600°C in air for 100 hours. The uranium trioxide prepared by the oxidation of U_3O_8 still contained 0.16% nitrate ion by weight, and water slurries of this oxide heated at 250°C for 60 hr did not appear to be substantially different from a control prepared from Mallinckrodt oxide. On the basis of this work it is concluded that the oxidation of U_3O_8 is not a promising method for the preparation of pure uranium trioxide.

RADIATION CHEMISTRY

Two slurry irradiation experiments have been carried out at 250°C in hole 12 of the X-10 graphite pile. Both samples were composed of 30 ml of slurry containing 250 g of uranium per liter as uranium trioxide monohydrate rods, and they were exposed in unpretreated type-347 stainless steel bombs with capillary tubing and thermocouples attached. The first sample contained normal uranium and it was irradiated at full pile flux; the second contained 93.4% enriched material and was exposed to about one

[4] J. J. Katz and D. M. Gruen, "Higher Oxides of the Actinide Elements. The Preparation of Np_3O_8," *J. Am. Chem. Soc.* 71, 2106 (1949).

[5] I. Sheft and S. Fried, *Preparation of UO_3*, ANL-4181, July 13, 1948.

half the maximum pile flux. In both cases transfer of irradiated solids from the bombs to glassware was incomplete, which indicated that some caking occurred along the inside surfaces of the bomb. The unsatisfactory recovery of uranium in these experiments makes the results qualitative rather than quantitative, but they are nevertheless indicative of what occurs during slurry irradiation (Table 25).

Upon irradiation, the concentration of uranium in the supernatant increased from an original 3.3 mg/l to 80 mg/l for the natural uranium slurry and 445 mg/l for the enriched uranium slurry. Qualitative tests performed on the supernatant showed the presence of several parts per million of nitrate ion. Microscopic examination of the slurries revealed that extensive particle size degradation occurred during irradiation, and it is believed that the soluble uranium and nitrate ions originally occluded within the uranium trioxide crystals were released by this mechanism. Moreover, in the case of the enriched uranium slurry, some transformation of rods to platelets was observed, and it was previously shown that this transition is promoted by the presence of soluble uranium.

The corrosion of stainless steel during slurry irradiation resulted in iron concentrations of 58 and 111 mg/l for the natural uranium and enriched uranium slurries, respectively, compared with initial iron concentrations of 18 and 1 mg/l. This unexpectedly high corrosion rate is attributed to the bombs not being pretreated and to the presence of soluble uranyl nitrate, which would be expected to enhance corrosion.

In the natural uranium and enriched uranium slurries, tetravalent uranium increased on irradiation to 11.2 and 3.2%, respectively, from an initial low value of less than 0.1%. Since irradiation of nitrate ion yields nitrite ion, which is a good reducing agent, reduction of uranium is ascribed to the presence of the original nitrate impurity.

Equilibrium gas pressures of 330 and about 3000 psia were observed for the natural uranium and enriched uranium slurry, respectively. Although these pressures were much higher than anticipated, they are about a factor of 10 lower than those predicted for a similar solution containing no recombination catalyst. It is believed that the appreciable gas pressure developed over these slurries may be explained, in part, by the presence of the soluble uranium.

In future experiments pretreated bombs will be employed in irradiation experiments, and great care will be taken to wash the uranium trioxide free of all nitrate ion. Further experiments are awaiting the development of a bomb in which it will be possible to stir the slurry as well as cool it during its irradiation in the pile. It is intended that hole 11, which is presently being used by the Argonne National Laboratory, will be redesigned during April to accommodate this work.

PARTICLE SIZE GROWTH IN UO_3 SLURRIES

Since particle size is an important factor in determining settling rates, redispersability, and power required for circulating slurries, a study of particle size changes in uranium trioxide slurries has been initiated. A determination of particle size growth at 100°C was made by using the platelet modification of uranium trioxide monohydrate. The oxide was micronized prior to dispersion in water, and

TABLE 25

Summary of Irradiation Experiments 1 and 2

OBSERVATION	EXPERIMENT 1 NATURAL URANIUM		EXPERIMENT 2 93.4% ENRICHED URANIUM	
	UNIRRADIATED CONTROL	SAMPLE AFTER IRRADIATION	BEFORE IRRADIATION	AFTER IRRADIATION
Radiation time (hr)		136		250
Recovered volume (ml)	70	25		19
Total recovered U (mg/ml)	250	84.4		46.0
Soluble U in supernatant (mg/ml)	0.0033	0.08		0.445
U^{+4} in slurry (%)	0.1	11.2	0.1	3.2
Fission products in supernatant (%)		5		19.6
Corrosion				
Fe (μg/ml)	18	58	1	111
Ni (μg/ml)	1	4.4	1	2.7
Cr (μg/ml)	2.2	12	1	1.9
Equilibrium gas pressure (psia)		330		3000
pH	5.4	5.6	5.6	5.9
Crystal habit	Rods of 20 to 30 μ	Rods of 20 to 30 μ and fragments	Rods of 15 to 20 μ	Rods of 20 to 30 μ, fragments and platelets
Settling	Total in 5 min	Total in 30 min	R* = 0.1 in 5 min	R* = 0.86 in 5 hr
Color	Bright yellow	Dark yellow	Bright yellow	Dark yellow
Gas composition** (%)				H_2, 64.8 O_2, 32.4 CO_2, 1.3 Inerts, 1.5

*R = ratio of volume of settled solids to total volume.

**Analysis made by W. F. Kieffer.

particle size determinations were made by centrifugal sedimentation with sodium polyphosphate as a deflocculant. The results are shown in Table 26. In this table it is apparent that the smallest particles (those less than 1 μ) disappear very rapidly; that there is a steady increase in the amount of material between 1 and 4 μ; and, finally, that the formation of the largest sized particles (those greater than 4 μ) is slow.

TABLE 26

Particle Size Growth in Hydrated Uranium Trioxide-Water Slurries at 100°C

Slurry Composition: 250 g of uranium per liter as micronized platelets

Conditions: refluxed at 100°C with stirring

WEIGHT PER CENT OF PARTICLES LESS THAN STATED SIZE	PARTICLE SIZES (microns)				
	HEATING TIME (hr)				
	0	1	2	4	24
10	0.2	1.0	1.0	1.0	1.4
25	0.4	1.2	1.2	1.6	1.8
50	0.6	1.3	1.8	2.4	2.5
75	1.0	1.6	2.6	2.4	3.0
90	1.7	2.8	4.0	4.1	4.1

STUDIES OF NORMAL URANYL PHOSPHATE SLURRIES

Normal uranyl phosphate has previously been considered as a possible slurry fuel. The solids in slurries containing 250 g of uranium per liter as uranyl phosphate occupy about 80% of the total volume, presumably owing to the needle-like structure of the crystals, forming, upon settling, a brush-pile type of structure. It was of interest to know whether aqueous slurries of this material heated at 250°C would still retain this very low bulk density. Uranyl phosphate was prepared from uranyl ammonium phosphate by heating in 1 *M* HNO_3 at 98°C until conversion was complete:

$$3(UO_2)_2NH_4PO_4 \overset{HNO_3}{\rightleftharpoons} (UO_2)_3(PO_4)_2 + 3NH_4^+ + PO_4^{\equiv} .$$

The uranyl phosphate, being less soluble at 98°C, precipitates out and shifts the equilibrium, as written, to the right.

Particle size determinations were made on the uranyl phosphate slurries both before and after heating for various periods of time at 250°C (Tables 27 and 28). In the case of uranyl phosphate, both as prepared and when micronized, there was no appreciable change in the volume of

TABLE 27

Thermal Stability of Normal Uranyl Phosphate Slurries

Composition: 250 g of $(UO_2)_3(PO_4)_2 \cdot 5H_2O$ per liter

Conditions: heated at 250°C in sealed quartz tubes in a rocking autoclave; settled at room temperature for 24 hours

HEATING TIME (days)	SEDIMENTATION RATIO*
0	0.80
3	0.79
7	0.80
14	0.81

*Ratio of volume of settled solids to total volume.

settled solids after heating, even though some particle size growth did occur and some reduction of hexavalent uranium to tetravalent uranium took place. The pH of the uranyl phosphate slurry was 3.95. Heating decreased the pH to 3.0, which suggests that more thorough washing would be required to remove the acid carried over from the conversion step.

TABLE 28

Thermal Stability of Micronized Normal Uranyl Phosphate

Composition: 250 g of micronized $(UO_2)_3(PO_4)_2 \cdot 5H_2O$ per liter

Conditions: heated at 250°C in sealed quartz tubes in a rocking autoclave

WEIGHT PER CENT OF UPN PARTICLES LESS THAN STATED SIZE	PARTICLE SIZE (microns)			
	HEATING TIME (days)			
	0	4	11	15
10	1.64	3.84	3.72	3.05
25	2.41	5.28	6.26	5.6
50	4.29	6.73	10.5	11.2
62.5	4.95			
Sedimentation Ratio	0.76	0.74	0.73	0.73

PREPARATION OF UO_3 BY SPRAY CALCINATION

A Harvard type of spray calciner[6] was constructed and operated in an attempt to produce uniformly sized, submicron particles of uranium trioxide from uranyl nitrate solutions. Four preliminary runs were made in the spray calciner, and conversions of 26, 82, 53, and 79% to uranium trioxide were obtained. No correlation was found between operating conditions and the fraction of the uranyl nitrate converted to the trioxide. A microscopic examination of the product indicated that it was neither uniform nor submicron sized. This failure to meet specifications was attributed to inadequacies of the equipment. It is not felt that the apparatus described is adequate for the preparation of samples of uranium trioxide for laboratory purposes.

SLURRY EQUIPMENT STUDIES

A small boiler of 1-liter capacity equipped with a 3-kw electric resistance heater has been installed for testing the boiling characteristics of uranium trioxide slurries at 250°C. Operational tests indicated that the cooling coils of the boiler were overdesigned from the standpoint of the present type of heating arrangement and a very uneven, on-off type of control resulted when water was used in the coils. Further tests are being carried out with humidified air as a coolant. It is proposed to use this equipment for the study of foaming in boiling slurries and to explore the possibility of minimizing or eliminating foaming by chemical methods. In addition, it may be used for studies of the effect of power input on the average density of the slurry fuel.

A laboratory-scale fluid energy mill has been received from the Micronizer Company for use where little contamination of the product with extraneous materials is essential. The mill employs superheated steam, compressed air, or nitrogen gas for the refinement of uranium trioxide particles to submicron sizes by an attrition process.

(6) L. Silverman, M. W. First, G. S. Reichenback, Jr., and P. Drinker, *Final Progress Report*, NYO-1527, Feb. 1, 1950.

Part III

GENERAL HOMOGENEOUS REACTOR STUDIES

ISHR DESIGN

R. B. Briggs, Section Chief

R. E. Aven
J. O. Bradfute
R. H. Chapman
P. N. Haubenreich
C. E. Klotz
T. H. Pigford

A predesign report is being prepared that will describe the intermediate-scale homogeneous reactor that is proposed as a second step in the development of homogeneous reactors for producing fissionable materials and power. The following is a condensation of the portions of the report that have been completed or are being developed.

If the physics, chemistry, and engineering of the aqueous homogeneous systems were well understood, this second step could be the design and construction of a full-scale reactor to operate at a power near 1000 megawatts and produce about 200,000 kw of electricity. Such a reactor could produce 1 kg of plutonium a day from slightly enriched uranium and would require 50 to 100 tons of D_2O. The entire plant would cost between 100 and 200 million dollars.

However, the physics, chemistry, and engineering are not well understood. There is a good possibility that the aqueous homogeneous systems can be operated without control or safety elements by depending upon the temperature coefficient for regulation and by varying the concentration of the uranium in the fuel solution or slurry as the shim control. This type of operation will be attempted in the HRE, where many but not all the physics questions can be answered. Operation on a somewhat larger scale in a system geometrically and hydrodynamically similar to the production reactors may be required to establish answers to many of the problems of kinetics of control.

The chemistry of the aqueous homogeneous systems is less known than the physics. Uranyl sulfate and uranyl fluoride solutions and uranium oxide slurries are the useful fuel systems based upon nuclear cross-section considerations. It is now known that uranyl sulfate is stable – that is, the uranyl ion does not reduce and the uranium does not precipitate as an oxide if the oxygen concentration in the solution is maintained at a sufficiently high level. Dynamic corrosion tests with uranyl sulfate solutions containing enough oxygen to prevent reduction of the uranyl ion show that it may be possible to design a circulating system of type-347 stainless steel that will operate satisfactorily for several years with a fuel solution containing 40 g of uranium per liter. A design for obtaining smooth flow and a minimum of disturbances is required, but even with such a design, localized corrosion resulting from unexpected conditions could result in equipment failures. The corrosion picture at the higher concentrations of uranium desirable for more economical plutonium production is less encouraging. In order to obtain satisfactory equipment-life, it may be necessary to use titanium or zirconium, which have demonstrated corrosion resistance superior to that of the stainless steels in comparable dynamic and static corrosion tests, for constructing the high-pressure and high-temperature circulating system.

Less is known of corrosion of materials in uranyl fluoride solutions and in uranium oxide slurries than in uranyl sulfate. Static corrosion tests

seem to indicate that stainless steels are corroded more by uranyl fluoride than by uranyl sulfate solutions, so no relief from corrosion difficulties could be expected to result from a change to uranyl fluoride fuel. In recent tests there was some indication that erosion in uranium oxide slurry systems may be negligible, but too little information is available to permit a realistic comparison of the uranyl sulfate solution and uranium oxide slurry systems.

Processing of the fuel solutions or slurries is being studied on a small scale. Several flow sheets are being evaluated. The recommended process will depend upon the reactor fuel and the state of the fission products and plutonium in the fuel. At present the solubility of plutonium in the uranyl sulfate solutions appears to be so low at 250°C that plutonium will precipitate as an oxide long before reaching the operating concentration that has been considered as normal. Continuous filtration may be required to remove the plutonium, or it may adhere to the walls of the equipment. Some of the fission products may precipitate; others may remain in solution. Ion exchange and electrolytic processes have been suggested as parts of the chemical cycles, but experience is lacking in the processing of representative solutions at the proper activity levels.

The engineering of aqueous homogeneous reactors is in an early stage of development. Circulating very highly radioactive solutions at high temperatures and pressures is new. Pumps must be developed to handle large volumes of solution with little or no leakage and a minimum of maintenance. Large, high-pressure valves may be required. Fabrication of large vessels and pipes with walls several inches thick is difficult if the material must be stainless steel and may be even more difficult if they must be made of titanium or zirconium or lined with those materials. Thousands of cubic feet of deuterium and oxygen may have to be recombined each hour unless internal catalysts, such as copper, prove feasible.

Equipment maintenance is probably the major engineering problem. If ordinary maintenance procedures were applicable, the problems would be relatively simple; however, the equipment is expected to be so intensely radioactive that it must be serviced and replaced by remote-control methods. Thus, a premium is placed upon reliable equipment and experience in design and equipment maintenance.

Because of the uncertainties of the aqueous homogeneous systems and the lack of experience, the design and construction of a pilot plant, in which the nuclear, chemical, engineering, and economic feasibilities can be demonstrated at a cost which is small relative to that of the production units, is considered to be the logical second step. The requirement that the reactor be a pilot plant and that it be constructed and operated at a small relative cost implies that the reactor itself be relatively small and that the power level be relatively low. A normal operating power near 50 megawatts has been selected as the one that will permit a significant increase in size compared with the HRE and a reasonable extrapolation to the larger reactors. A homogeneous reactor to operate at this power level might be constructed at a cost of 10 to 15 million dollars. Since this reactor would be intermediate in size and power between the HRE and a production reactor, it is designated as the ISHR, or Intermediate-Scale Homogeneous Reactor.

A rather general study of the characteristics of plutonium producers

led to the conclusion that designing, building, and operating a reactor with a core 6 ft in diameter at a power of 48 megawatts would provide the experience and information necessary for economical extrapolation to a production scale. Predesign work in progress on the ISHR is devoted to the development of a general conceptual design for the reactor. *The purpose of this design is to point out the information available today and the information that must be obtained before the reactor can be designed in detail and constructed.*

BASIS FOR SELECTION OF REACTOR SIZE

As a first step in selecting the size and suggesting a design for the prototype, the following requirements have been specified.

1. The response to changes in reactivity must be similar so that once the control characteristics of the ISHR are demonstrated extrapolation to the production reactor can be made with assurance.

2. The hydrodynamics of flow in the core must be similar to those of the production reactor.

3. Mechanical components must be designed so that representative experience will be obtained in design, operation, and maintenance of equipment.

4. The chemistry of fuel solutions and reactor materials and the process for plutonium extraction must be such that extrapolation to the production process will be possible.

The basis for establishing similitude in the ISHR has been reported previously.[1] Pertinent general information regarding the production reactor and the 6-ft-dia core finally selected for the ISHR are presented in Table 29.

CONTROL

In evaluating the similarity of control of the ISHR and the production reactors the possibilities of purely nuclear oscillations and oscillation resulting from the coupling of the core and pressurizer have been studied. Also, pressure and power surges have been calculated for the several reactors by assuming disturbances to the reactivities of the systems.

For small disturbances in the reactivity of a reactor, the short-time kinetic behavior has been described by Stein[2] and Welton[3] in terms of the constants:

τ = prompt generation time (sec),

β = fraction of delayed neutron,

ω_N^2 = rate of decrease of prompt rise rate if reactor continues to operate at power but heat removal is discontinued (sec^{-2}),

α = linear damping coefficient for pressurizer system (sec^{-1}),

ω_H^2 = squared circular frequency of pressurizer oscillation (sec^{-2}).

The term ω_N^2 depends upon the temperature coefficient of reactivity at constant pressure, $\partial k/\partial T$, the specific power, P_0/V, the heat capacity and

(1) J. A. Lane, *A Comparative Survey of the Feasibility and Economics of Aqueous Homogeneous Reactors for the Large Scale Production of Plutonium and U-233*, ORNL-1096.

(2) J. M. Stein (ed), "Physics," *Homogeneous Reactor Experiment Report for the Quarter Ending February 28, 1950*, ORNL-630, p. 21; "Reactor Physics," *Homogeneous Reactor Experiment Feasibility Report*, ORNL-730, p. 48.

(3) T. A. Welton, "Over-all Stability of the HRE," *Homogeneous Reactor Project Quarterly Progress Report for Period Ending November 15, 1951*, ORNL-1221, p. 65.

density of the fluid, $C\rho$, and the prompt generation time, as follows:

$$\omega_N^2 = \frac{\left(\frac{\partial k}{\partial T}\right)\left(\frac{P_0}{V}\right)}{C\rho\tau} .$$

To achieve nuclear stability it is desirable that the return of power to equilibrium be considerably overdamped. If the time behavior is e^{pt}, then p satisfies the equation

$$p = \frac{1}{2}\left[- \frac{\beta}{\tau} \pm \sqrt{\left(\frac{\beta}{\tau}\right)^2 - 4\omega_N^2}\right] .$$

For no oscillations to occur as the power returns to equilibrium

$$\left(\frac{\beta}{\tau}\right)^2 > 4\omega_N^2 .$$

If the inequality is reversed, the power will oscillate the number of cycles determined by the relative values of the two terms. Values of $(\beta/\tau)^2$ and $4\omega_N^2$ are plotted in Fig. 39. Whether nuclear oscillations are important depends upon whether a disturbance is reinforced by "feedback" from the external circulating system. Investigation of detailed

TABLE 29

General Characteristics of Aqueous Homogeneous Plutonium Producers

	DESIGN I	DESIGN II	DESIGN III	DESIGN IV	DESIGN V
Core diameter (ft)	6*	10	15	20	30
Core volume (liter x 10^{-3})	3.2	15	50	120	400
Power level (megawatts)	48	630	2000	4000	8900
Specific power in core (kw/l)	15	42	40	33	22
Maximum pressure (psia)	1000	1000	1000	1000	1000
Fuel	UO_2SO_4	UO_2SO_4	UO_2SO_4	UO_2SO_4	UO_2SO_4
Moderator	D_2O	D_2O	D_2O	D_2O	D_2O
Uranium concentration (g/l)	250	550	155	115	93
U^{235} concentration (%)	3.5	2.4	1.1	0.88	0.74
Average flux in core (neutrons/cm^2·sec x 10^{-13})	5.2	7.2	36	54	72
Exit temperature of solution (°C)	250	250	250	250	250
Pumping rate (gpm x 10^{-3})	20 to 5	100	240	420	940
Temperature rise in core (°C)	9.4 to 38	23	32	36	36
Residence time in core (sec)	2.6 to 10.4	2.2	3.3	4.4	6.7
Gas bubble volume (% of core)	0.4 to 1.6	0.9	1.4	1.6	1.6

*ISHR core.

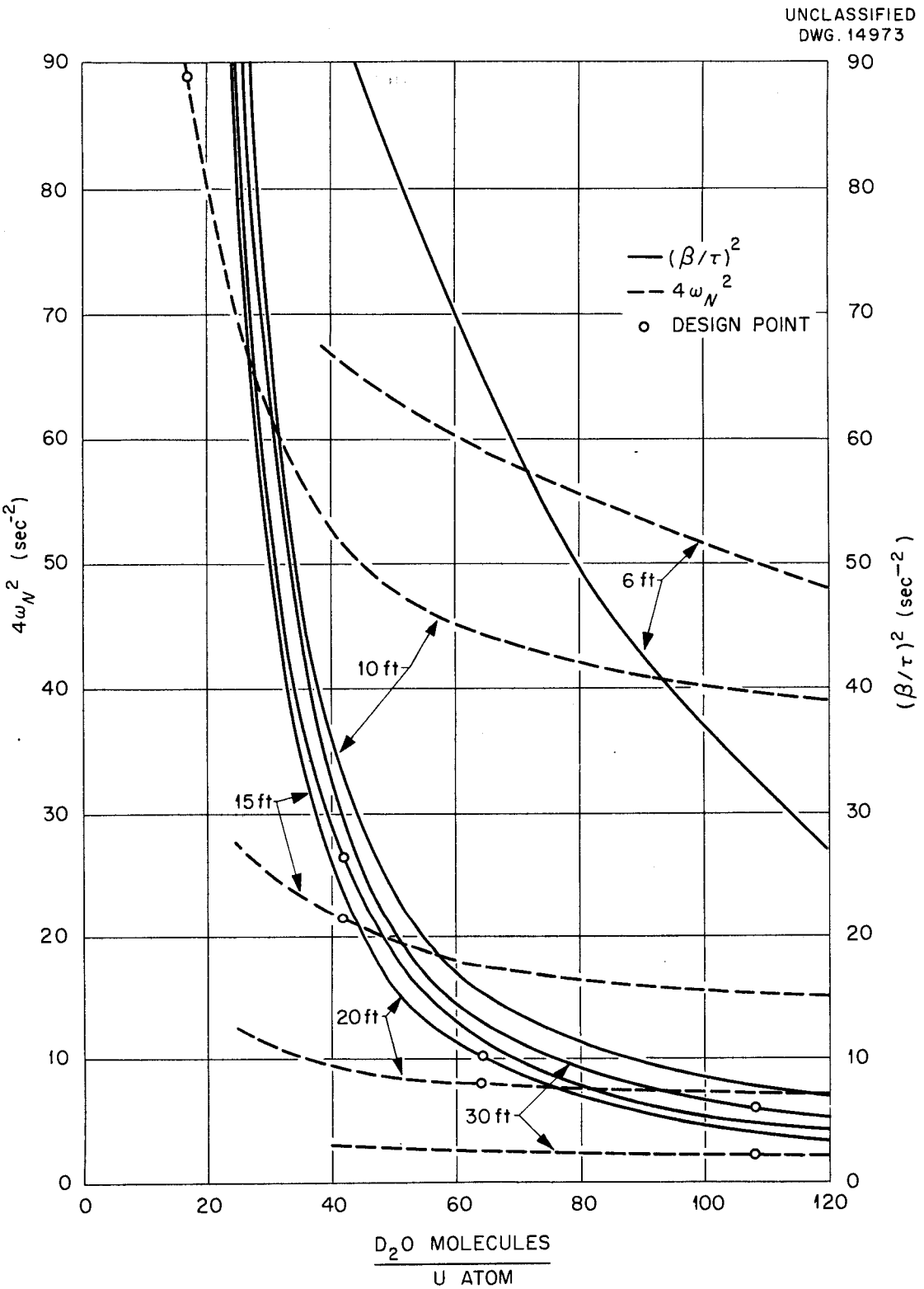

Fig. 39. Comparison of Factors Affecting Stability.

designs is required to evaluate this effect.

The general stability condition, which is of greater interest, involves the build-up of oscillations between the core and pressurizer. Such oscillations are initiated as fluid is expelled from the core during a power surge. Their amplitudes vary with time as e^{qt}, with q given by

$$q = \frac{1}{2}\left[\frac{\omega_N^2\left(\frac{\beta}{\tau}\right)}{\left(\frac{\beta}{\tau}\right)^2 + \omega_H^2} - \alpha\right],$$

where the first term may be described as the antidamping coefficient, K, and the second term as the damping coefficient.

Values for K and α have been calculated for a standard pressurizer system applied to the reactors of Table 29, and the ratio α/K, which should exceed unity for a stable system, is plotted in Fig. 40. In most instances α/K is satisfactorily large; however, in instances where it approaches a value of 1 under the conditions selected, improved ratios can be obtained by modifying the design to change α and/or ω_N^2, since they depend only upon the mechanical characteristics of the system.

In addition to examining the basic nuclear and mechanical stability of the systems, maximum pressures and specific powers have been estimated under conditions of sudden increases in reactivity for the several reactors (Table 29). The reactivity rise considered was that resulting from a sudden increase of 5% in the average density of the fuel and moderator in the core. This change is equivalent to a reduction in temperature of 30°C or the replacement by fuel solution of a volume of gas equal to 5% of the core volume. Table 30 contains the results of the calculations for the reactor-pressurizer systems.

The data presented in Tables 29 and 30 and Figs. 39 and 40 indicate that information regarding the control of

TABLE 30

Comparison of Characteristics of Reactors with a Step Change in Reactivity Introduced

	DESIGN I	DESIGN II	DESIGN III	DESIGN IV	DESIGN V
Core diameter (ft)	6	10	15	20	30
Initial specific power (kw/l)	15	42	40	33	22
Reactivity change	0.0265	0.0104	0.0083	0.0065	0.0046
Maximum specific power (kw/l)	4500	1390	296	139	57
Maximum pressure rise (psi)	2000	190	14	5	2
Maximum temperature (°C)	275	273	271	270	270
Time to attain maximum power (sec)	0.07	0.1	0.3	0.6	1.1
Time to attain maximum pressure (sec)	0.07	0.1	0.2	0.2	0.2

the 6-ft-dia reactor can be extrapolated with assurance to the larger sizes. Similar characteristics were obtained for 7- and 8-ft-dia cores. Although they could be operated at lower enrichments, the lower specific power obtained at a total power of 50 megawatts and the longer residence times in the core with a maximum flow of 20,000 gpm made them appear less satisfactory. A 4-ft-dia core was also considered; however, the minimum required fuel enrichment was estimated to be 19%, which is considered too high to be acceptable.

HYDRODYNAMICS

Stability of the reactors is expected to depend upon the flow patterns in the core, but the form of this dependence is not well understood. Generally, zones of stagnation are to be avoided. A desirable flow pattern would be one that permitted a reasonable estimate

UNCLASSIFIED
DWG. 14974

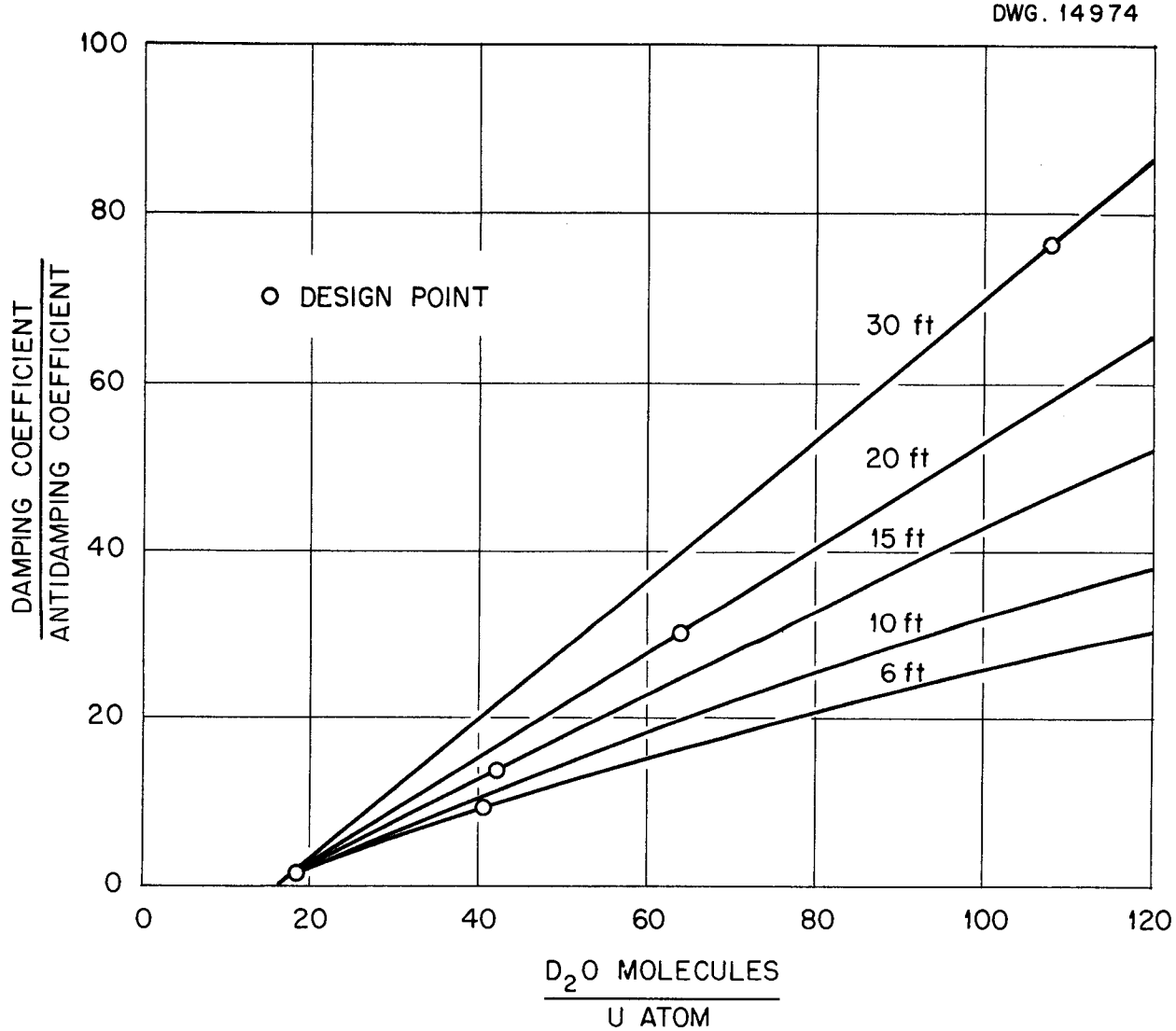

Fig. 40. Comparison of Coefficients Affecting Core-Pressurizer Stability.

to be made of temperature, gas, and concentration gradients in the core. However, the hydrodynamics problem in selecting a core size for the ISHR is not one of specifying the flow pattern, but one of assuring that information obtained from the prototype can be extrapolated to larger reactors.

Two types of flow are being considered. One is a vortex type of flow in which fluid is introduced into the core through an inlet tangential to the sphere at the equator and is withdrawn at the poles. The other is an axial type of flow with the fluid introduced at one end of the core and withdrawn at the other. Important parameters for comparison of cores of different sizes are believed to be the Reynolds number for axial flow and the Reynolds and Froude numbers for rotational flow. For the purpose of this comparison, the Reynolds number has been defined as

$$Re = \frac{V\rho}{D\mu}$$

and the Froude number as

$$Fr = Dv\,\frac{\omega_R^2}{g}$$

where

V = volumetric velocity of fluid (ft^3/sec),

ρ = density (lb/ft^3),

μ = viscosity ($lb/ft \cdot sec$),

D = diameter of sphere (ft),

Dv = diameter of forced vortex in center of sphere (ft),

ω_R = angular velocity of forced vortex (sec^{-1}),

g = gravitational constant (32.2 ft/sec^2).

Typical values are presented in Table 31. The Reynolds number may be a factor of 2 to 10 less in the 6-ft core than that in the large cores. With Reynolds numbers of 10^6 to 10^7, as found here, this extrapolation should not be difficult. Froude numbers, which are considered to be a measure of the characteristics of the vortex, can be duplicated in the small core.

MECHANICAL COMPONENTS

Mechanical similitude of the prototype and the production reactors is desired to obtain experience with the full-scale equipment under actual operating conditions. This involves the use of a 20,000-gpm circulating system, which appears satisfactory for the control and hydrodynamics studies. Variation of the flow through the range 5,000 to 20,000 gpm has been suggested as desirable for facilitating the investigation of the effects of variations in flow, temperature rise, and gas concentration upon control.

TABLE 31

Comparison of Reynolds and Froude Numbers

	DESIGN I	DESIGN II	DESIGN III	DESIGN IV	DESIGN V
Core diameter (ft)	6	10	15	20	30
Reynolds number x 10^{-7}	0.12 to 0.47	1.3	2.3	3.4	5.1
Froude number	16 to 250	147	100	73	47

CHEMICAL CONSIDERATIONS

Chemical similitude involves the use of representative temperatures, metals, fuel concentrations and solutions, plutonium concentrations, and radiation levels. The plutonium production rate in the 6-ft core is expected to be 0.6 atoms per fission compared with 1.0 in the producers. In all other chemical considerations, conditions in the ISHR will essentially duplicate those proposed for production operations.

BASIS FOR FAVORING SPHERICAL CORE

A first consideration in reactor design is the core. The question of spherical core vs. cylindrical core has been re-examined, and it seems clear that the spherical shape is to be preferred, at least for large vessels. Table 32 shows a comparison of cylinders with spheres having the same geometrical buckling. Because there is an important advantage in reduced wall thickness and reactor volume favoring the spheres when large vessels are required, the sphere was selected as the core shape for the ISHR to preserve the geometrical similarity dictated by the hydrodynamics considerations.

Criticality of the 6-ft-dia sphere has been investigated by two group methods which took into account the effect of the steel shell and the use of a D_2O reflector with a stainless steel or zirconium core tank. Although the accuracy of the calculations is debatable, they indicate that little is to be gained by reflecting the core unless the core tank can be made of zirconium or can be very thin. Results of the calculations are shown in Fig. 41. Considering the effect of the steel shell, the enrichment required for operation with 250 g of uranium per liter of UO_2SO_4 at 250°C appears to be nearer 2.5% than the 3.5% reported in Table 29. Reflecting the core with D_2O complicates the reactor design considerably without providing an important decrease in required enrichment, so the ISHR considered in the predesign report will have no reflector other than the steel shell.

HEAT PRODUCTION IN THE REACTOR SHELL

The selection of the proper shell thickness for the reactor depends upon the maximum allowable working stress permitted in the vessel. This value has been specified as 10,000 psi. The two important stresses are the

TABLE 32

Comparison of Spheres and Cylinders with Equal Buckling

RATIO OF CYLINDER DIAMETER TO SPHERE DIAMETER	RATIO OF CYLINDER HEIGHT TO CYLINDER DIAMETER	RATIO OF CYLINDER WALL THICKNESS TO SPHERE WALL THICKNESS	RATIO OF CYLINDER VOLUME TO SPHERE VOLUME
0.92	1	1.84	1.17
0.81	2	1.62	1.59
0.79	3	1.58	2.20
0.77	∞	1.54	∞

pressure or hoop stress arising from the internal pressure and the thermal stress arising from the temperature difference across the wall thickness. The temperature difference results from the flow into the core of the heat produced by the absorption of gammas within the shell.

Sources of Heat. Heat is produced by absorption of core gammas and absorption and scattering of neutrons in the shell.

Core Gammas. The heat produced by the absorption of core gammas within the shell is given as a function of shell thickness in Fig. 42. Table 33 gives the source, energy, and current of core gammas entering the shell.

Absorption and Scattering of Neutrons in Shell. The fast neutron current entering the shell has been calculated to be 1.92×10^{12} fast neutrons/cm^2·sec and the thermal neutron current has been calculated to be 2.1×10^{12} thermal neutrons/cm^2·sec. Since the radius of the sphere is large, slab geometry has been assumed for all the absorption processes to simplify the calculations. The heat production curves are presented in Fig. 42.

Inelastic scattering of fast neutrons is assumed to result in the production of one 1-Mev gamma for each collision. The absorption of fast and thermal neutrons in steel is assumed to produce one 7-Mev capture gamma for each absorption. Heat is calculated as being produced where

[redacted]

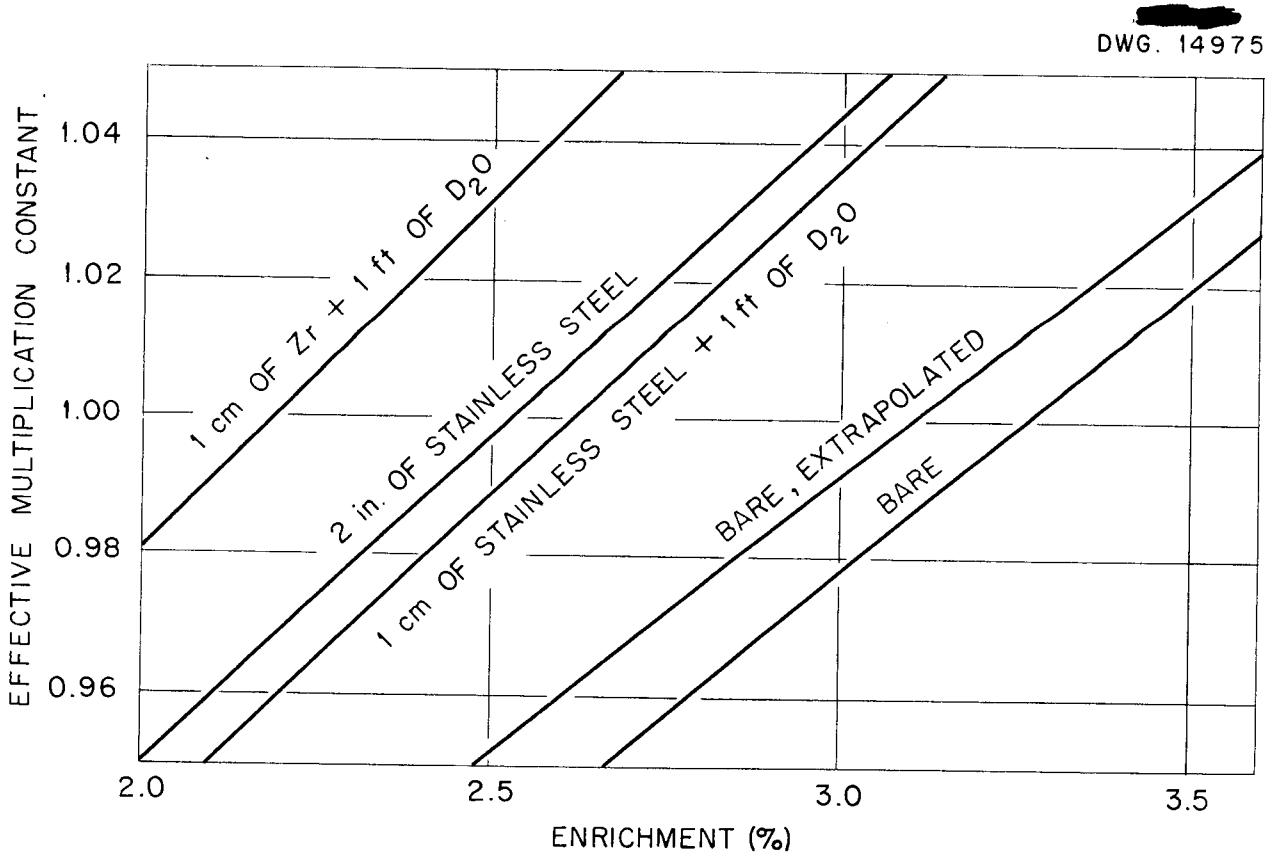

Fig. 41. Effective Multiplication Constants for a 6-ft Reactor with Various Reflectors. Operating conditions: 250°C, 250 g of uranium per liter.

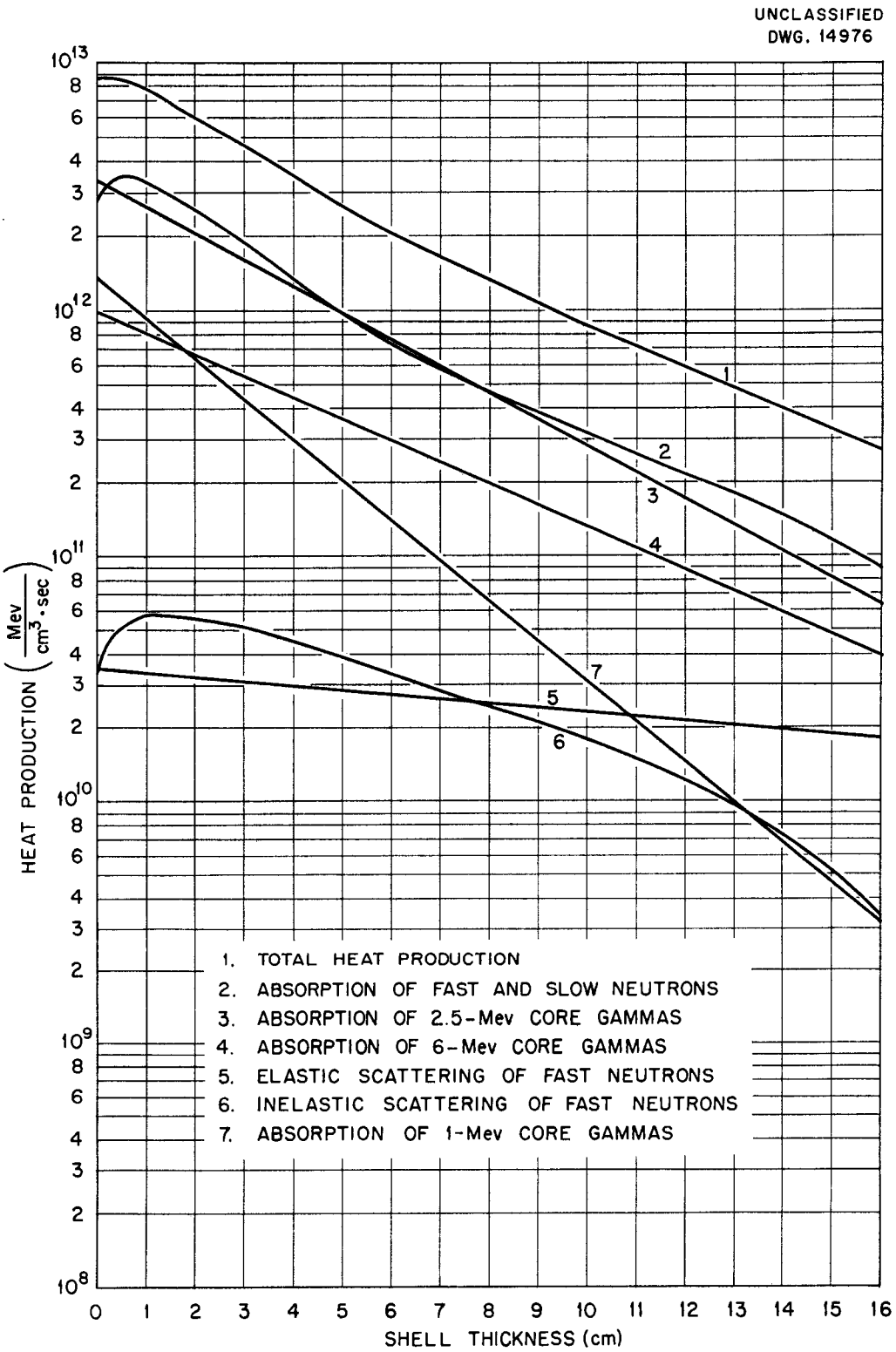

Fig. 42. Heat Production in Reactor Shell.

TABLE 33

Source, Energy, and Current of Core Gammas Entering the Shell

SOURCE	AVERAGE ENERGY (Mev)	DISTRIBUTION OF PRODUCTION	CURRENT ($\gamma/cm^2 \cdot sec$)
Uranium and sulfur capture	6	Same as the thermal-neutron flux distribution	8.164×10^{12}
Prompt fission gammas	1	Same as the thermal-neutron flux distribution	3.57×10^{12}
Fission products	2.5	Uniform throughout core	5.41×10^{12}

the gammas are absorbed, so the heat production function depends upon the thickness of steel and its neutron- and gamma-ray absorbing properties. The curves presented in Fig. 42 for a 16-cm-thick shell were found to be representative for thicknesses greater than 4 centimeters. Heat production per cubic centimeter is less in thinner shells.

Total Heat Production. The total heat production curve in Fig. 42 can be represented by the equation

$$H = \left(5.0e^{-0.184x} + 5.7e^{-0.438x} - 2.0e^{-3.35x} \right) 10^{12} ,$$

where

H = total heat production rate ($Mev/cm^3 \cdot sec$),

x = distance from inner surface of shell (cm).

This heat production function is being used to estimate the temperature distribution and thermal stress in the reactor shell.

SHIELDING STUDIES

Work has been started on designing a shield for the ISHR. Shielding requirements for the reactor compartment, induced radioactivity in the external system, and leakage of radiation through pipes in the shield are being investigated.

Reactor Shield. Barytes concrete was the first material to be studied for the reactor shield, since its properties are fairly well known and it appears to offer an economical shield. Following procedures outlined by Blizard,[4] the required thickness was calculated for a spherical shield of all barytes concrete immediately surrounding the reactor pressure shell. This geometry requires the thickest shield, so the calculated thickness will be a conservative value for any other geometry. It was found that the shield thickness was determined by secondary gammas from neutron capture in the shield, with the gammas from the core contributing less than 1% of the total radiation. The dosage from fast neutrons would be insignificant beyond 6.5 feet.

Because of the importance of secondary gammas in the all-barytes shield, calculations were made for concrete containing 1% boron in the form of colemanite, $Ca_2B_6O_{11} \cdot 5H_2O$. Results are shown in Fig. 43.

(4) E. P. Blizard, *Introduction to Shield Design*, ORNL CF-51-10-70, Jan. 30, 1952.

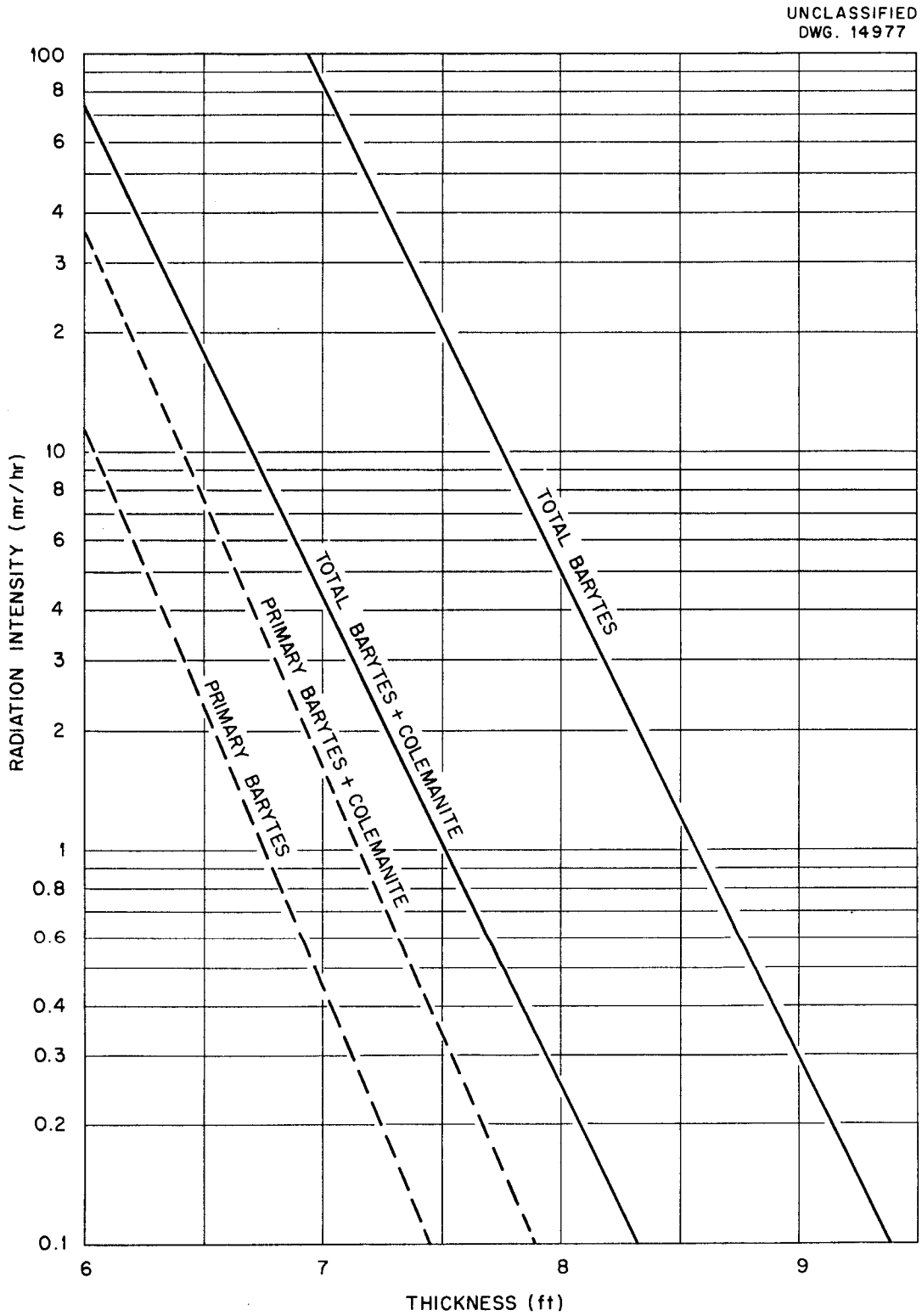

Fig. 43. Effect of Boron in Barytes Concrete.

In a shield containing colemanite, more than 98% of the neutrons would be captured in boron and the production of gammas in the shield would be effectively reduced. The primary radiation from the core would be greater owing to a decrease in concrete density, but the total amount of radiation would be reduced. Results indicate a saving of 1 ft in shield thickness by the addition of 1% boron.

Induced Radioactivity in Equipment. Induced radioactivity in the external system was found to be mainly from delayed neutrons. If three or more feet of shielding separated the equipment from the core, the capture of leakage neutrons from the core would be less than 1% of the total. The reason for the high value of delayed-neutron capture lies in the large size of the piping considered. More delayed neutrons would be emitted because of the large volume; there would be a greater probability of the neutrons being thermalized before reaching the steel walls and there would be some multiplication that would increase the number.

Figure 44 shows the induced radioactivity based on outside surface area in a 20-in. schedule-80 pipe. The upper limit is shown in which all the neutrons leaking from the fuel solution are assumed to be captured in the pipe, either on the first pass or after being scattered back by the shield. The lower limit, considering only those neutrons captured on first pass through the pipe walls, is 14% of the upper limit.

Results show that the most serious source of induced radioactivity is Co^{60}. Cobalt, which does not ordinarily appear in analyses of stainless steel, is present in so-called pure nickel (electrolytic) to the extent of 0.30 to 0.50%. The results shown in Fig. 44 are based upon a cobalt content of 0.50% of the nickel and an irradiation time of two years.

Gamma-Ray Leakage Through Pipes. In maintaining equipment for large reactor systems containing many pumps and heat exchangers it may be desirable to isolate one group of equipment for servicing while the reactor and remainder of the system continue to operate. With this type of operation, intensely radioactive solution would fill pipes leading to the shut-off valves between the isolated equipment and the core. Calculations have been made to estimate the gamma leakage through empty pipes of the ISHR following shut-off.

It was assumed in the calculations that the core was full of fuel and that the system was operating at 50,000 kw. Fuel was kept from the loop by means of gate valves on either side of the core (inlet and outlet).

The pipe was assumed to be 20 in. in diameter and straight from valve to receptor; the gamma flux was computed to be 1.3×10^{11} gammas/cm^2·sec at 5 ft from the valve and 3.5×10^{10} gammas/cm^2·sec at 10 feet. With two 90-deg bends between the source and the receptor, the radiation was computed to be 2.5×10^5 gammas/cm^2·sec at 5 ft and 2.0×10^4 gammas/cm^2·sec at 10 feet. These calculations did not consider penetration of shield (in a straight line) between source and receptor. With penetration considered, radiation at 5 ft was raised by a factor of 10^5 and at 10 ft by a factor of 10^2. Additional calculations and design studies are being made to develop tolerable conditions.

HYDROGEN-OXYGEN EXPLOSIONS

A study is being made of the hazard from a possible explosion of the hydrogen and oxygen generated in the

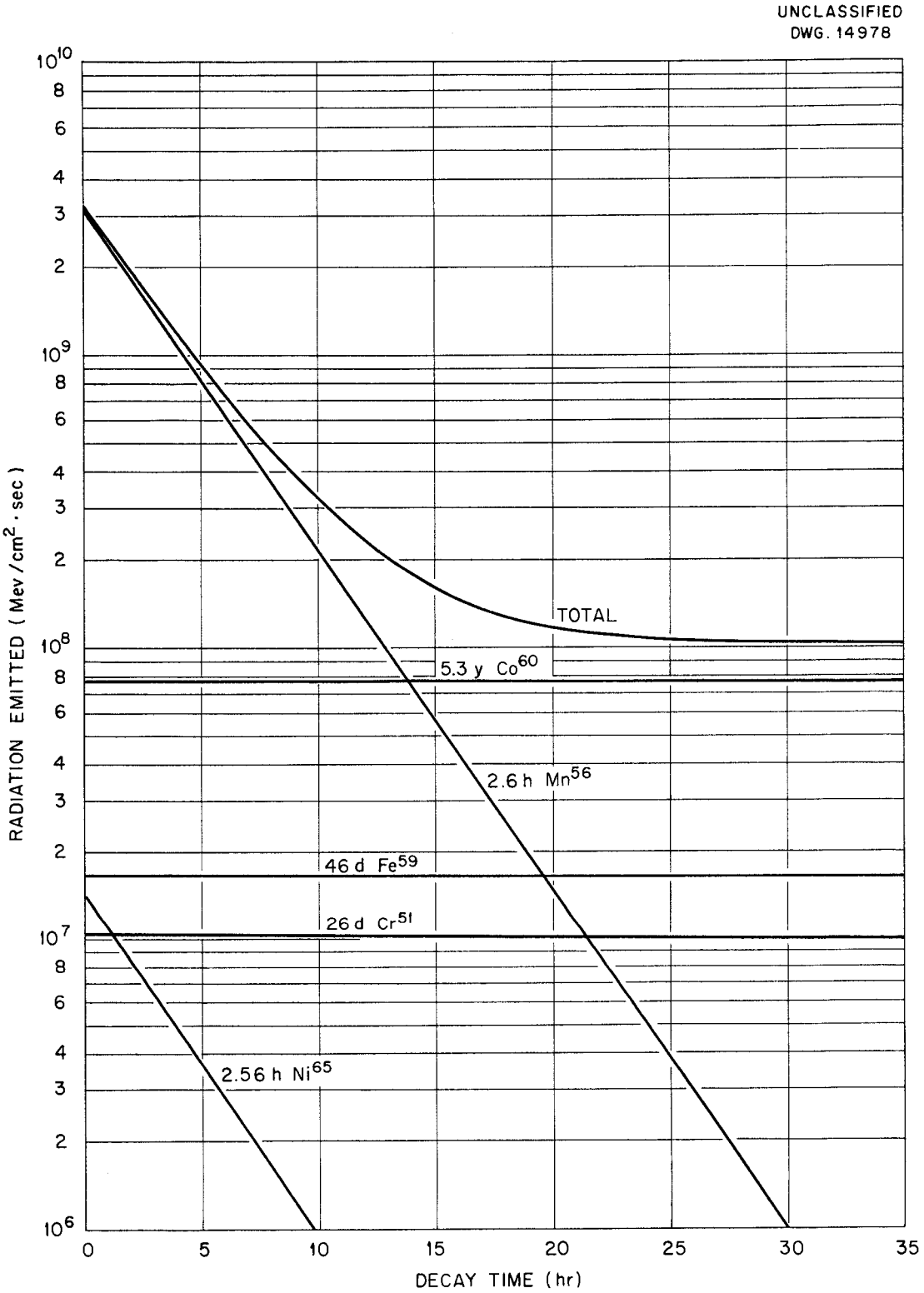

Fig. 44. Induced Radioactivity in Type-347 Stainless Steel.

core vessel of the ISHR. Assuming that the fuel contains no catalyst, such as copper sulfate, to effect recombination of dissociation gases as they are formed, a stoichiometric mixture of hydrogen and oxygen will be liberated at the rate of 0.9875 lb moles/min when the reactor is operating at a power level of 48 megawatts.

If it were found necessary to operate at a pressure of 1000 psia to minimize the volume of gas in the core, explosive mixtures would be present in the system. Explosions may possibly occur in the core vessel and in auxiliary equipment such as the gas-liquid separator, piping, and the recombiner system. A chemical explosion may occur by one of two distinct processes:

1. deflagration or smooth burning, which is controlled by chemical reaction rate and is characterized by a relatively low velocity of flame propagation,
2. detonation, which is largely a hydrodynamic phenomenon and is characterized by a shock wave that travels through the unburned gas at a velocity greater than sonic velocity.

The pressures generated during detonation are usually on the order of twice those generated from deflagration. Shock waves in the surrounding medium of noncombustibles may accompany deflagration, but such waves are unstable and tend to decay to normal compression waves as they progress through the medium.

Explosions in the Core Vessel. In calculating the volume of gas that will be present in the reactor core the following assumptions were made:

1. The partial pressure of water vapor in the dissociation gas is equal to the vapor pressure of water over an aqueous solution containing 250 g of uranium per liter of uranyl sulfate at 250°C and 1000 psia.

2. At every point in the core the gas and liquid move at the same local linear velocities.

3. (*a*) The liquid moves through the core in slug flow, with negligible back mixing, or (*b*) the liquid in the core is completely mixed, so that the average concentration of gas in the core is equal to the concentration of gas in the effluent liquid.

Assumption 3(*b*) leads to twice the gas volume in the core as assumption 3(*a*). Gas volumes calculated for a 6-ft-dia core and for the expected range of liquid flow rates are shown in Table 34.

For predicting the pressure that may result from a deflagration of the

TABLE 34

Total Volume of Hydrogen, Oxygen, and Water Vapor in ISHR Core at 250°C and 1000 psia

LIQUID FLOW (gal/min)	GAS VOLUME FOR SLUG FLOW (ft^3)	GAS VOLUME FOR PERFECT MIXING (ft^3)
5,000	1.802	3.60
20,000	0.450	0.901

gas in the core, it is first assumed that the explosion occurs at constant volume. On this basis the explosion pressure is calculated to be 3960 psia. If a shell thickness of 2.5 in. is assumed, the resulting tensile stress is 14,250 psi. If it is further assumed that the deflagration is accompanied by a shock in the surrounding fuel and that the deflagration has occurred at a point such that the shock reaches the wall without attenuation, the stress may momentarily be on the order of 30,000 psi. Even though this is near the yield point in tension for type-347 stainless steel, which for static loading is 30,000 to 37,000 psi at 250°C, there appears to be little danger of rupture or plastic flow. Also, an additional factor of safety may be present because metals usually exhibit higher yield points for dynamic loading than for static loading. Furthermore, the above assumptions are extremely conservative, as will be shown in the following discussion.

At the pressures assumed the compressibility of liquid water is appreciable, and it is reasonable to expect that during a deflagration the liquid will be compressed and the spherical shell will expand isentropically so that the combustible mixture will expand as it burns. In calculating the deflagration pressures that would result it is assumed, as a worse possible case, that all the gas in the core would be ignited, and no gas or liquid would escape from the core. Taking into account the work performed by the gas in compressing the liquid and expanding the shell, the pressures and stresses shown in Table 35 are obtained. Calculated curves for explosion pressures and resulting stresses at various gas volumes are shown in Fig. 45.

Even if the tensile stresses are doubled to allow for shock reflection, the predicted stresses are still below the elastic limit of type-347 stainless steel.

If the reactor were operated with vortex flow in the core, the total gas volume in the core should be somewhat less, for the same liquid flow rate, than the volumes listed in Table 34. The volume occupied by the gas in the forced vortex should be small (0.13 ft^3 for a 2-in.-dia vortex tube in a 6-ft sphere), and the centrifugal action should decrease the gas holdup in the liquid. Therefore deflagration pressures should be on the order of 2000 psia.

TABLE 35

Calculated Pressures for Deflagration Accompanied by Isentropic Compression of Liquid and Expansion of Shell

For a spherical shell 6 ft in diameter and 2.5 in. thick

INITIAL GAS VOLUME (ft^3)	GAS-TO-LIQUID VOLUMETRIC RATIO	EXPLOSION PRESSURE (psia)	TENSILE STRESS (psi)
0.450	0.00405	1705	6,130
0.910	0.00811	2080	7,480
1.802	0.01619	2530	9,100
3.60	0.0328	3035	10,900

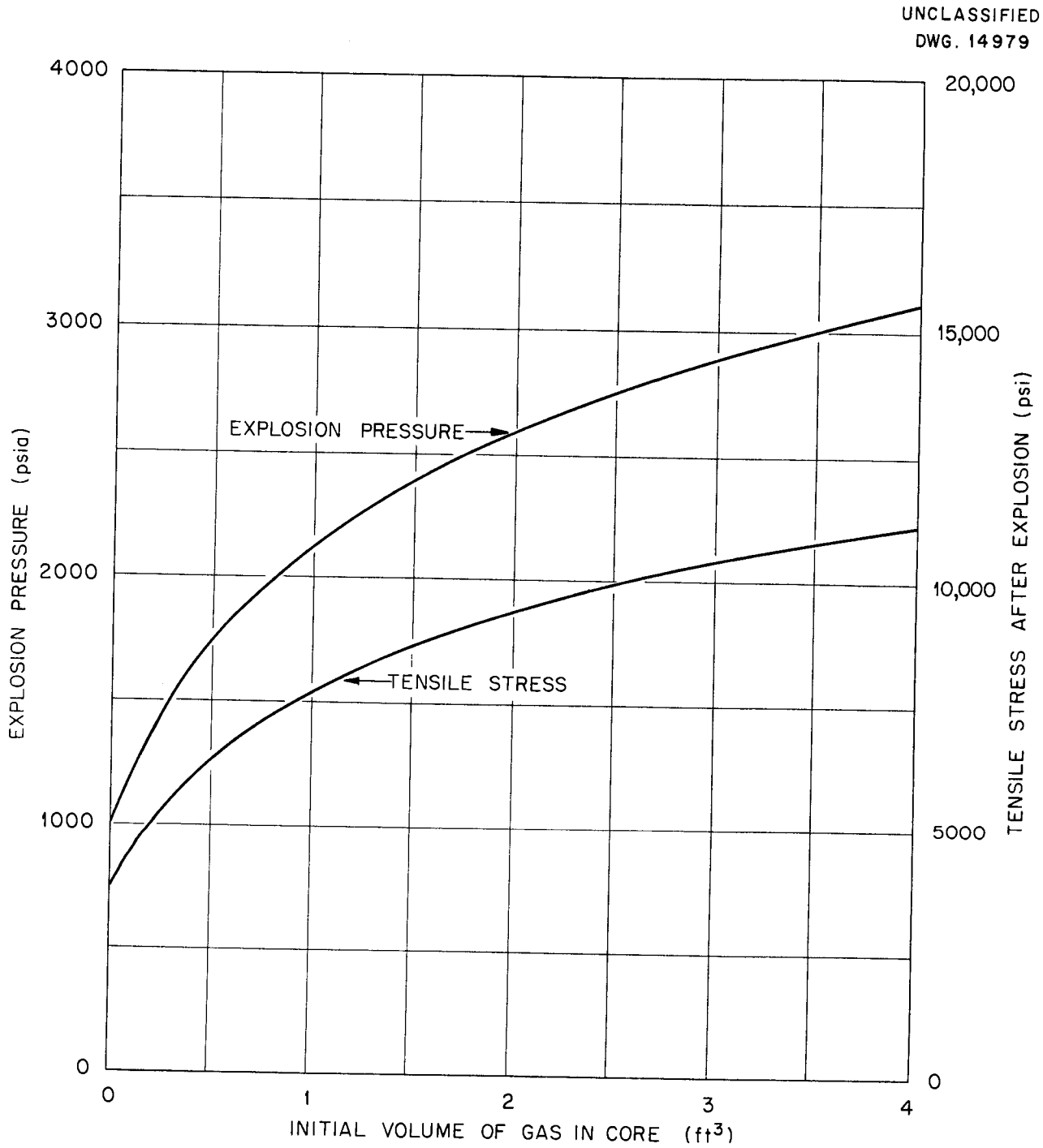

Fig. 45. Pressures and Stresses Resulting from Explosions in Core of ISHR.

However, there exists the possibility of a detonation wave progressing longitudinally through the forced vortex. The velocity of a stable detonation wave traveling through this combustible mixture is calculated to be 6,950 ft/sec, with a resulting impact pressure of 13,140 psia. A high local shearing stress would exist momentarily at the top or bottom

of the vortex tube when the detonation wave reached the end of the tube. In this region, however, the vessel would probably be strengthened by supporting members or it might be connected to piping that would absorb the detonation impact.

Although the hazard from possible detonation in the forced vortex does not appear to be great, it is possible that detonation may be prevented by installing in the vortex tube some obstruction such as a series of baffles or a wire helix[5] to dissipate the energy of the shock wave and cause the combustion process to degenerate to a deflagration.

Explosions in Other Parts of the System. Since in the case of a deflagration in the core the change in gas volume caused by vessel expansion is small compared with that from compression of liquid, the deflagration pressures shown in Table 35 and Fig. 45 should apply to any other part of the reactor system in which the initial pressure, temperature, and gas-to-liquid volumetric ratios are nearly the same. For a cylindrical gas separator 20 in. in diameter and operating in vortex flow, the vortex tube may be about 4 in. in diameter. The resulting gas-to-liquid volumetric ratio would be much higher than those listed in Table 35, so it may be concluded that the deflagration pressure in this unit would be on the order of 3000 to 4000 psia.

If the separator were constructed of 20-in. schedule-80 pipe, which is being considered for the main liquid-flow lines for the ISHR, the stresses resulting from deflagration would be on the order of 30,000 psi, which is near the elastic limit for type-347 stainless steel. It may be advisable, therefore, to construct the separator and other auxiliary equipment to handle the combustible gases from piping for heavier duty.

The detonation velocity and impact pressure would be the same for the gas-liquid separator as those listed previously for the case of detonation in the core vessel.

It may be generalized that in the equipment for handling the combustible mixture from the gas-liquid separator the pressure will increase roughly by a factor of 4 upon deflagration and by a factor of 10 upon detonation, provided the combustible mixture is of the same composition as that issuing from the core. If the amount of water vapor in the mixture is reduced by condensation because of cooling in the lines, the deflagration and detonation-impact pressures will increase. In the limiting case with no water vapor present in the mixture, the pressure will increase approximately sevenfold upon deflagration and twentyfold upon detonation. It is important, then, to maintain the vapor lines at a temperature sufficient to prevent condensation unless the equipment is small enough that it can easily be designed to withstand these pressures.

Safety Precautions for the Recombiner System. In the previous discussion it was assumed that explosion had been initiated by some unspecified means. Since the reactor temperature of 250°C is considerably below the temperature for auto-ignition, which, for this mixture, is estimated to be of the order of 600°C, there appears to be little opportunity for igniting the gas in the core and separator other than by propagation of a flame upstream from the recombiner system. Such propagation may be prevented by installing a suitable flame arrester between the separator and recombiner.

[5] B. Lewis and G. von Elbe, *Combustion, Flames and Explosions of Gases*, p. 612, Academic Press, New York, 1951.

There are two physical properties of the combustible mixture that are useful in specifying the characteristics of a flame arrester. The first property is the laminar (or normal) flame velocity, which is the velocity of propagation of a flame front relative to and normal to the unburned gases when all factors of flow and turbulence are removed. The laminar flame velocity for the combustible mixture issuing from the reactor at 250°C is estimated to be about 15 ft/sec. The other property is the quenching distance, which is the minimum diameter of a tube through which a flame will propagate under laminar conditions. When a laminar flame tries to propagate through an opening of diameter less than the quenching distance, heat and chain carriers are lost to the walls and unburned gas more rapidly than they can be replenished by chemical reaction, and combustion ceases. The quenching distance for this combustible mixture is estimated to be about 0.0007 inch.

Unless detonation occurs, the velocity of flame propagation in a practical combustion system is only about three times the laminar flame velocity. This suggests that a device in which the linear velocity of the unburned gas is many times the laminar flame velocity would be an effective flame arrester. A safe design of such an arrester would be a critical-flow nozzle, valve, or orifice upstream from the recombiner. The velocity of the gases through such an arrester would be unaffected by the fluctuations in pressure that would be expected to occur in the recombiner, provided the pressure upstream of the arrester is always greater than twice the downstream pressure.

Although the critical-flow velocity may not be sufficient to prevent a detonation wave from passing upstream through the flame arrester, it is possible that the energy of the detonation wave would be so dissipated when the wave met the standing shock wave just downstream of the arrester that the detonation would degenerate into a normal compression wave which could go no further upstream. A critical-flow arrester would fail to function if an explosion occurred in the equipment downstream of the arrester that was sufficient to cause the flow through the arrester to become subcritical and decrease momentarily to the velocity of flame propagation. Hence, it would be necessary to use, in series, another arrester operating on a principle other than velocity or to provide a pressure relief downstream of the critical-flow arrester.

The simplest design of a quenching-flame arrester would be a screen with holes of a diameter less than the quenching distance. However, if a flashback and pressure surge were to occur, hot combustion gases would be forced through the holes with little cooling and could easily ignite the combustible mixture upstream of the arrester. Therefore an effective quenching-flame arrester must provide cooling surfaces of high thermal conductivity and heat capacity so that during a flashback the temperature and chain-carrier concentration of the gases at some point in the arrester will remain lower than the values critical for ignition of the unburned gas. These criteria may be satisfied by a series of fine-mesh wire screens, one or more sintered-metal disks, a section packed with fine metal shot, or a drilled block that has been drawn so that the diameter of the holes is on the order of the quenching distance.

The choice of a critical-flow or quenching-flame arrester, or a combination of the two, depends upon the allowable pressure drop upstream of

the recombiner system. Either type of arrester would have an advantage over the steam-blanket system used for the HRE in that it could be designed to arrest flames in stoichiometric mixtures of hydrogen and oxygen containing no water vapor and would require no auxiliary control system.

ENGINEERING STUDIES OF COMPONENTS

C. B. Graham, Section Chief

J. S. Culver
J. A. Hafford
C. W. Keller
R. J. Kedd
H. J. Kraig
J. I. Lang
L. B. Lesen
W. L. Ross
I. Spiewak
P. N. Stevens
D. Taylor
R. H. Wilson
C. D. Zerky

STEAM TURBINES AND GENERATORS

It is particularly important to the reactor equipment designers to know as early as possible the optimum pressure and temperature of the steam to be generated in the main heat exchanger. This requires an optimization of conditions that takes into account manufacturing and operating problems of the turbine generators. A preliminary investigation of suitable turbines and generators for the large-scale homogeneous reactors has been started. As a result of a discussion with one of the large manufacturers, several significant points developed, and the manufacturer offered to investigate the problems in greater detail. Other manufacturers are to to be consulted in the near future.

It is highly probable that a standard turbine, 125,000 kw, for example, with minor alterations can be used with a 200-psig saturated steam supply. The usual turbine is designed with a high-pressure unit and a low-pressure unit on the same shaft. By eliminating the high-pressure unit and using only the low-pressure turbine, a 60,000- to 80,000-kw (electric output) unit results. If larger single units are desired, the high-pressure unit may be replaced by a second duplicate low-pressure unit to give a total output of 120,000, to 160,000 kw. The principal problem encountered in supplying this unit with 200 psi of saturated steam is that of blade erosion in the later stages because of excessive moisture in the steam. The blades are usually reinforced with Stellite to reduce the erosion. In large central stations operated with 10 to 12% moisture in the exhaust, blade repairs are required after 20 to 30 years of service. No experience has been cited where large units were run with about 18% (theoretical) moisture in the exhaust, but it is the tentative opinion of the manufacturer that a standard unit can be modified to give reasonable blade life (certainly five years and probably 10 to 15 years).

Until actual experience is obtained, it is expected that the first unit will operate at 1800 rpm, since low speeds are conducive to long blade-life; it will have extra Stellite on the blades; it will be altered to promote moisture removal in the later stages; and provision will be made for connecting a line-pressure steam reheater at a later date, if needed. The capacity and final details of the unit will depend on condenser water temperature, etc. and thus upon location. One, two, or three regenerative heating stages may be used, depending on a comparison of the cost of heater installation to the value of increased efficiency and the amount of lower temperature heat available from the reactor as a by-product. A standard electric generator can be used.

TEST LOOP FOR 4000-gpm PUMP

A Byron Jackson 4000-gpm centrifugal pump manufactured for the Westinghouse Atomic Power Division has been obtained for use in the test loop previously described.[1] This canned-rotor, 1800-rpm pump was operated by WAPD for 1800 hr in water at approximately 300°C under 2000 psi of pressure. During operation the only significant difficulty encountered was that small clearances between the rotor and the can caused them to rub after only a slight amount of bearing wear. After this trouble was corrected at WAPD, no further difficulty was encountered over a period of several hundred hours. The pump was received from WAPD in good operating condition. The other major items for the loop and auxiliary components are on order, and it is anticipated that delivery will be completed by early fall of this year.

Since the pump was designed for use with hot water, a few parts in the impeller end of the pump will have to be replaced to permit operation with homogeneous reactor fuel solutions. Should long-term or ISHR operation become desirable, major alterations would probably be required, such as modification of the design of the pump rotor by incorporating self-aligning, all-metal bearings and by increasing clearances between the rotor and can. Replacement of the type-18-8W stainless steel shaft, and possibly the cast type-347 stainless steel impeller housing and other smaller parts, would probably be necessary to ensure adequate long-term corrosion resistance. These alterations cannot be recommended until the fuel-corrosion problems are studied further.

It is now tentatively planned to operate the pump at variable speed by rewiring, as a variable-frequency power source, two of the motor-generator sets left in the experimental area when the electromagnetic process equipment was removed. In addition to supplying data on points of wear and on the suitability of large, water-lubricated radial and thrust bearings, the test loop of the 4000-gpm pump will afford the first opportunity for studying corrosion and erosion effects in larger pipe sizes. Design of the loop system is such that with minor changes it can be used for slurry pumping studies, if this becomes desirable.

The test loop for the 4000-gpm pump will be fabricated from 10-, 8-, and 6-in. stainless steel pipe, and at least one flange joint in each size will be used. Auxiliary components for maintaining satisfactory operation will provide cooling of the loop and a flow of condensate water for flushing fuel solution from the motor and bearing chamber of the pump. The condensate water will be obtained by taking a small stream of the solution to atmospheric pressure, flashing a portion to steam, and condensing the steam. Two small, high-pressure piston pumps will return the condensate to the main pump and the remainder of the solution to the loop. The returning solution will pass through an oxygen dissolver to supply sufficient oxygen to the system and maintain solution stability. The oxygen dissolver will be similar to the one used on the HRE.

Adequate instrumentation will be provided to maintain continuous operating conditions, collect some test data, and protect personnel and equipment from hazardous operating conditions or equipment failures.

---

(1) J. R. McWherter, J. Brown, W. L. DeRieux, J. D. Maloney, and W. L. Ross, "Pump Loop Design," *Homogeneous Reactor Project Quarterly Progress Report for Period Ending November 15, 1951*, ORNL-1221, p. 18-20.

MAIN PUMPS AND VALVES

The first phase of work on a contract with the Allis-Chalmers Mfg. Co. for the design and fabrication of a 20,000-gpm, totally enclosed, canned-rotor pump has been completed with their submission of preliminary designs of several types of pumps. The second stage, consisting of detailed design, has been started.

A similar contract is being negotiated with the Worthington Pump and Machinery Corporation for the design and development of a 20,000-gpm pump with a standard motor. An internal water-lubricated bearing will be used in this pump. High-pressure water will be supplied to the center of the bearing where the flow divides and a portion of the water flows into the impeller chamber. The remaining water will flow along the shaft toward the motor, and its pressure will be lowered to atmospheric. The water will then be pumped back to the bearing. An essentially conventional, contact seal will be provided at the low-pressure point on the shaft where it will be well out of the high radiation field. Thus the departure from known industrial practice in this pump is in the bearing design. Accordingly, Worthington is preparing a full-scale mockup bearing and seal test to establish feasibility of this design.

Although the development of a satisfactory pump of this type is somewhat less assured than the canned-rotor pump development and would take a longer time, its success would probably give advantages over the canned-rotor pump in initial and maintenance costs. In an effort to eliminate the cumbersome water system for the high-pressure-water bearing and also to make possible the use of conventional external bearings, preliminary discussions have been initiated with the Byron Jackson Co. for the development of a high-pressure mechanical shaft seal. If a seal of this type can be developed, which appears doubtful at this time, convential pumps would become feasible. Evidence now available indicates that any of these 20,000-gpm pumps would be capable of pumping either a slurry or a solution.

The preliminary designs from Allis-Chalmers allow comparison of four kinds of totally enclosed pumps. The different designs of 20,000-gpm pumps that develop a 200-foot head may have axial, mixed, or centrifugal flow, depending on the synchronous speed of the motor and the kind of impeller that is chosen. A comparison of some of the pertinent preliminary information for these pumps is given in Table 36. The over-all efficiencies are based on the assumption that a hydraulic type of bearing and a motor with a metal seal between stator and armature, similar to the Westinghouse Model 100A pump, will be used.

Table 36 shows that the 1200-rpm centrifugal unit has the best efficiency. Its relative fluid velocities are more favorable than for the higher speed pumps, since lower velocities generally cause less corrosion - or erosion, if a slurry is used. Velocity data are not available for the 900-rpm unit, but the impeller velocity would be expected to be lower and the casing velocity higher than at 1200 rpm.

The 3600-rpm pump is most advantageous with regard to the ease of manufacturing. This is especially true if forged construction must be used. Generally, construction of the others becomes more difficult as casing diameter increases.

TABLE 36

Comparison of 20,000-gpm, 200-ft Head Pumps

	AXIAL-FLOW PUMP	MIXED-FLOW PUMP	CENTRIFUGAL-FLOW PUMP	CENTRIFUGAL-FLOW PUMP
Synchronous rpm	3,600	1,800	1,200	900
Brake hp	1,570	1,415	1,380	1,435
Over-all efficiency (%)	69	78	78.7	76.5
Operating power (kw)	1,310	1,160	1,149	1,182
Power cost per year 0.5¢/kwh	$57,500	$51,000	$50,500	$52,000
Cost difference per year	$7,000	$500	0	$1,500
Shape and relative size	See Fig. 46*a*	See Fig. 46*b*	See Fig. 46*c*	See Fig. 46*c*
Maximum fluid velocity relative to				
Impeller (ft/sec)	225	104	76	
Casing (ft/sec)	70	52	56	
Normal thrust (down) (lb)	20,400	1,550	1,880	
Motor efficiency (%)	90	91.5	89.7	90.5
Power factor	0.91	0.84	0.80	0.796
Motor cooling-water head loss (psi)	123	193	375	695
Rotor diameter (in.)	8.1	10.7	10.8	16.3
Wearing-ring speed (ft/sec)	248	138	95	

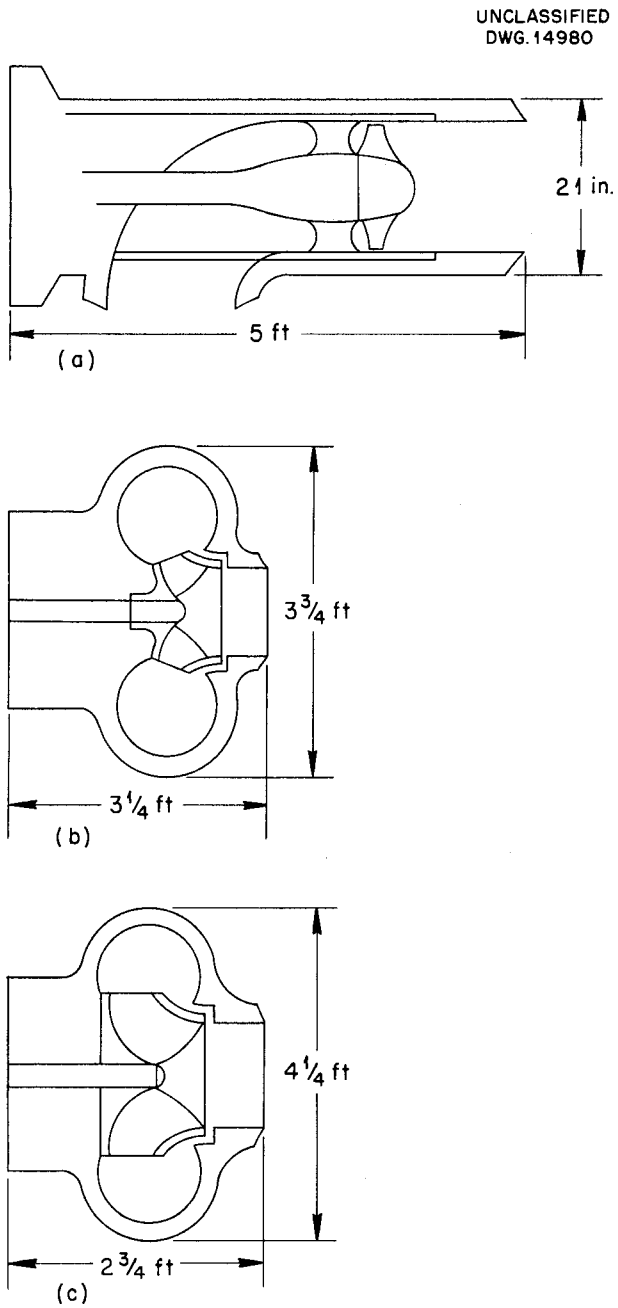

Fig. 46. Shapes and Relative Sizes of 20,000-gpm, 200-ft Head Pumps. See Table 36.

MAIN HEAT EXCHANGER

Large heat exchangers for future reactors have been discussed with The Lummus Co. of New York, who have agreed to submit a preliminary design and cost estimate. More recently, tentative specifications have been submitted to the A. O. Smith Corp. of Milwaukee for their consideration. When design criteria have been agreed upon, several companies will be asked to submit preliminary bids. The following are tentative specifications.

1. CONDITIONS ON CORROSIVE LIQUID SIDE

Circulation rate at 250 °C	20,000 gpm
Heat transfer	190,000 Btu/sec
Entering temperature	250 °C
Working pressure	1000 psi
Pressure drop	20 to 40 psi
Corrosion allowance	~0.030 in.

Material: type-347 stainless steel, all welded construction

Properties of liquid:

density	1.22 g/cc
viscosity	0.445 lb/hr·ft
specific heat	0.785 Btu/lb·°F
estimated thermal conductivity	0.35

2. CONDITIONS ON BOILING WATER SIDE

Working pressure: 200 psig, design for 600 psi maximum

Material: iron pressure shells

Provide entrainment separator in steam draw-off, if needed, to produce essentially dry steam

As a result of preliminary discussions with The Lummus Co., the following tentative design features appear feasible and practical. Steam would be removed from a horizontal boiler drum approximately 25 ft long

and 7 to 9 ft in diameter. Several vertical, U-tube, heat exchangers would be arranged approximately 5 ft below and to one side of the drum. Boiler water would be circulated, by convection, from the boiler drum over the exchanger tubes and back into the drum. The heat exchanger tube sheet would be at the bottom, so that the fuel solution would enter at the bottom, circulate up through the stainless U-tubes and back down, and leave from the lower end of the exchanger. A pressure drop of 20 psi appears to be adequate.

Four exchangers 4 ft in diameter and 15 ft high would be required. The probability that two or three units larger in diameter may be more economical is being considered. Seamless tubes 1/2 in. in diameter would be welded to the tube sheets. The advisability of using double tube sheets is questionable because of stresses resulting in the tubes. Since steam removal from the drum should be accomplished with minimum entrainment, a small drum, and little loss of pressure, considerable discussion also centers about the method for removing steam. However, at this stage of the design, it appears that a 200,000-kw heat exchanger can be constructed with the use of essentially proved industrial practice.

It should be noted that the above design is well suited to shielding, because the exchangers can be heavily shielded but the steam drum may be lightly shielded. Also, a minimum of shielded floor space is required, and the over-all height is reasonable.

ISOLATION VALVES

In order for continuous operation of a large homogeneous reactor to be obtained, it would be desirable to provide a multiplicity of separate circulating systems that could be isolated if trouble developed. A stand-by system (or systems) could be used to replace the isolated system. To accomplish this, two large valves, about 20 in., would be required in each circulating system. The valves should provide sufficient closure to permit draining of the isolated system, which would require that they be remotely operated, have zero leakage of the hot solution past the seat after the isolated section has been drained, and be dependable. The principal problems encountered in developing a valve for this purpose are: corrosion, galling of parts, wire drawing at the seat, and external leakage of the solution.

A double-disk, gate valve, Fig. 47, seems to be the most feasible for meeting the requirements. The valve would be provided with a gas bleed for removing any trapped gases and a means for flushing the fuel solution from between the disks before draining the isolated section. To reduce the galling tendency, the disks would be

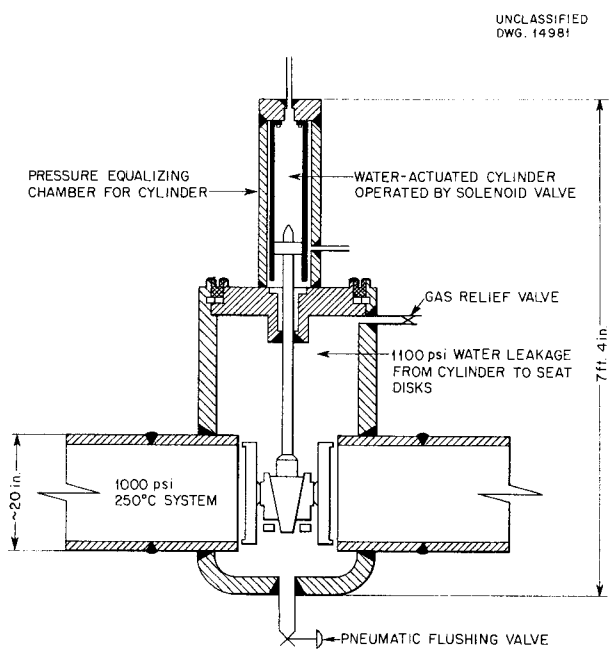

Fig. 47. Isolation Valve.

moved horizontally into position against the seats without any wedging action of the disks, and seating would be effected by high-pressure water injected between the disks. Only water (or D_2O) could then leak into the isolated system.

Wire drawing at the seats is not considered to be a serious problem unless the valves are to be closed against high pressure for extended periods. The use of a hard, corrosion-resistant alloy for these faces would be desirable; but no suitable material has yet been found. If slurry is used, Stellite would probably be satisfactory.

The valves could be operated by three alternate methods. First, a high-pressure-water operated piston drive integral with the valve could be provided to inject water into the system between disks through the stem bearing (Fig. 47). Second, a sealed motor drive integral with the valve could be used with high-pressure water injected as a bearing lubricant and as the source for the seating pressure for the disks. Third, a conventional operating mechanism removed from the valve could be provided. High-pressure water would be injected into the stuffing box to prevent external leakage of the fuel solution and provide the high-pressure water between the disks for seating pressure.

The valves are designed so that only minor changes would be required for adapting them to a slurry reactor. If increased freedom in the use of materials were not needed, the valve would probably be designed to wipe the seats when closing. Several manufacturers who expressed a desire to design and produce these valves include Jenkins Bro., Darling Valve & Mfg. Co., Crane Co., and Chapman Valve Mfg. Co.

MISCELLANEOUS ADDITIONAL VALVES

A large check valve, approximately 20 in., may be required for each circulating system to prevent back flow when a pump is shut down. Also, a number of special, remotely operated, smaller valves will be required for by-passing large valves for pressure equalization, drain and fill valves, control valves for the hydraulic system, chemical process valves, etc. These may be hydraulically, solenoidally, or pneumatically operated. Since the problems in developing these valves are not anticipated to be so difficult as in the large valves, very little, other than generalized discussions with several valve manufacturers, has been done to date.

HRE RECOMBINERS

The design of future reactors has not progressed to a point where recombiner design criteria can be established, and therefore development of large recombiners has not been started. The Aerojet Engineering Corp. of Los Angeles has expressed an interest in conducting design and developmental work if a flame type of recombiner is desired, and they have considerable related experience that may be utilized.

SMALL CANNED-ROTOR PUMP

The Allis-Chalmers Mfg. Co., on its own initative, has developed a 5-gpm canned-rotor pump to work against a head of 35 ft of water. This pump features hydrostatic bearings and all stainless steel construction at relatively low cost. Preliminary tests at the factory are promising, and Allis-Chalmers has offered to loan the pump for test with fuel. Rather wide usage of this pump can be

made for test loops, inpile experiments, general chemical applications, liquid metal experiments, etc. However, for some time this pump will be available in only a limited variety of capacities.

ISHR FUEL FEED PUMPS

Development of fuel feed pumps for large reactors will be started as soon as capacity requirements are known. Instead of the pulsafeeder pump used in the HRE, which is probably not suitable for the larger reactors because of capacity limitations, a multistage centrifugal pump may be preferred. The Byron Jackson Co. has built a 22-stage, 10-gpm, high-head pump that might be altered to serve this purpose. The major alterations required would be changes in bearing materials and development of a suitable, leak-proof driving means. Numerous other manufacturers have built similar pumps.

BEARINGS FOR 100-gpm PUMP

The 100-gpm pumps are equipped with Graphitar bearings that are aligned by means of a light press fit in the motor housings. Because of the low viscosity of the lubricating fluid (water), the bearings must be very accurately aligned with the journals. Misalignment causes very slight wear of the Graphitar to take place until a sufficiently lubricated surface develops. Any distortion of the pump parts during operation will cause additional wear.

The chemical properties of the fuel and a desire to increase bearing life have provided some incentive for replacing Graphitar bearings with Stellite. There is also some reason to believe that metal bearings will be better than Graphitar if slurry is pumped. Metal bearings, when misaligned, are more susceptible to scoring and therefore have been line-lapped after installation. This operation is expensive and does not permit the interchange of bearings between various pumps.

An experimental self-aligning bearing was tested in a 100-gpm pump. The bearing was made of Graphitar in a stainless steel housing and employs a "universal-joint" type of tilt ring to carry axial thrust and a narrow rocker ring to support radial loads. The entire assembly can be used without alteration of the pumps. The bearing ran for 138.2 hr under normal conditions (temperature about 100°C) with no observable wear on the radial surfaces. Very slight signs of local wear resulting from misalignment were occasionally observed in "press-fit" Graphitar bearings after the first few hours of operation. Because of the apparent absence of wear, it appears that the experimental bearing aligned itself as intended. Stellite 98M2 is being installed to replace the Graphitar, and the bearing will be tested again.

The thrust balancing pads in the impeller housing of the 100-gpm pump promote corrosion because of the turbulence they create. In order that the pads may eventually be eliminated, a large, tapered, land thrust bearing that embodies both radial and thrust surfaces in one assembly has been built. Self-alignment is accomplished fundamentally in the same manner as described for the bearing. This unit may be mounted in the rotor chamber with minor alterations to the pump. Both radial and thrust journals were made of Stellite No. 1, which was heliarc welded on a stainless steel blank. The bearing was run twice for 24 hr and failed both times because of overheating of the radial bearing.

Observation of the bearing surfaces after seizure showed that the bearing self-aligned and that the thrust surfaces took the heavy applied thrust load without undue wear. The reason for the failure of the radial face cannot be explained by past experience with simple radial sleeve bearings. It is believed that the seizure condition can be relieved by increasing the longitudinal flow of the lubricant to the radial surface of the bearing.

Certain impregnated-graphite materials are reputed to be superior for poorly lubricated bearings or shaft seals; therefore corrosion tests have been completed on silver- and babbitt-impregnated graphite supplied by Byron Jackson. The tests show that the silver-impregnated graphite will corrode more than the babbitt-impregnated graphite at any concentration of fuel and temperature, but it is still feasible for use at low fuel concentration (about 20 g of uranium per liter) at 100 °C. Byron Jackson, General Electric, and the Naval Experimental Engineering Station recommend the silver-impregnated graphite for water- or steam-lubricated bearings and noncorrosive conditions. Specific applications for this material have not been determined.

The shaft and journals of the Byron Jackson pump to be used in the 4000-gpm loop are made of type-322 stainless steel (18-8W). This material is being used rather generally because it may be hardened by a nitriding process called malcomizing. An investigation of its corrosion resistance has been started to estimate the life of the pump parts and to determine future uses for the material. The studies consist of dynamic loop tests, bomb tests, and static insolution tests.

Thus far, it has been observed that type-322 stainless steel, although not advised for high-temperature and/or high fuel concentration service, will probably stand up in low temperature (100 °C), low concentration fuel. Unfortunately, the malcomized samples have not been tested because of a lack of facilities, but they are not expected to be so resistant to corrosion as the untreated material. Since water will be injected into the rotor chamber of the 4000-gpm pumps and the chamber will be cooled, the type-322 stainless steel parts may be expected to last for some time unless concentrated fuel gets into this chamber. If tests with malcomized material are negative, positive measures will have to be taken to guard against fuel contamination of the rotor chamber.

REACTOR CORE DEVELOPMENT AND GAS SEPARATORS

The difficulty encountered in developing a satisfactory flow pattern in the HRE core is indicative of what may be expected in developing larger homogeneous reactors. The HRE core cannot be scaled up directly because of the excessive pressure drops and velocities that would result. A program now under way has as its objective the development of a suitable core for the ISHR and ultimately for industrial-scale homogeneous reactors.

The study is being conducted to obtain as much information as possible from small models that are relatively easy to build and operate. The information will then be used in building an 8-ft core, which represents the upper limit of an intermediate-size core vessel. The intermediate tests will provide data, some of which cannot be obtained on a small scale,

for the final design of reactor vessels.

The characteristics required of the core are:

1. feasibility and economy in construction,
2. stability of flow and adequate heat removal from all points,
3. low pressure drop (preferably less than 15 psi),
4. low gas holdup,
5. velocities near the walls consistent with corrosion problems.

Two general types of configuration are being considered. The first is a vessel with tangential inlets that give the fluid in the reactor core a rotating motion. This type of flow will produce low gas holdup and possibly effect gas removal in the core. The gas is collected in a vortex void that lines up with the outlets, which are located at the poles of the vessel. The HRE core is of this type. A thorough study of this type of flow in small models is being made at the University of Tennessee; supplementary data are being obtained at ORNL. Work has also begun on an 8-ft sphere that will utilize rotating flow.

The second type of flow, classed under the general title "straight through," is accomplished with designs in which little or no effort is made to rotate the liquid. In general, the straight-through flow is characterized by lower pressure drop and higher gas holdup than the rotating type. The straight-through investigation is still in the small model stage. It is possible that the flow distribution in this type of core can be adjusted to produce essentially ideal temperature distribution. Adjustment of flow distribution in the rotating type is difficult. It has not yet been definitely proved that the temperature distribution in either type would be acceptable.

Rotating Type Cores - Small Models. Investigation has been made of the flow through a 12-in. steel sphere with four 2-in. tangential inlets and two 2-in. polar outlets (Fig. 48). The sphere is equipped with plastic windows for visual observation of the vortex and possible stagnant regions.

The visual results were encouraging. The vortex lined up well with the outlets and was stable at flows ranging from 10 to 130 gpm with various inlet and outlet combinations. At low flow rates, where gravitational forces tend to become important, the vortex assumed a conical shape but remained well oriented and stable. Studies of flow pattern with potassium permanganate indicated that there was no stagnant region (a characteristic of HRE models), probably because of the higher ratio of radial-to-tangential velocity components in the present model and the use of multiple connections.

Figure 49 is a plot of the over-all pressure drop through the sphere as a function of flow rate. The ordinate is the product of the number of inlets and the pressure drop. The "predicted" line shown is of the form:

$$N\,\Delta P = \frac{V_0^2}{2\pi^2 g_c R_1^4}\left[\left(\frac{R_s}{R_2}\right)^2 - 1\right], \qquad (1)$$

where

N = number of inlets,

ΔP = pressure drop (ft of water),

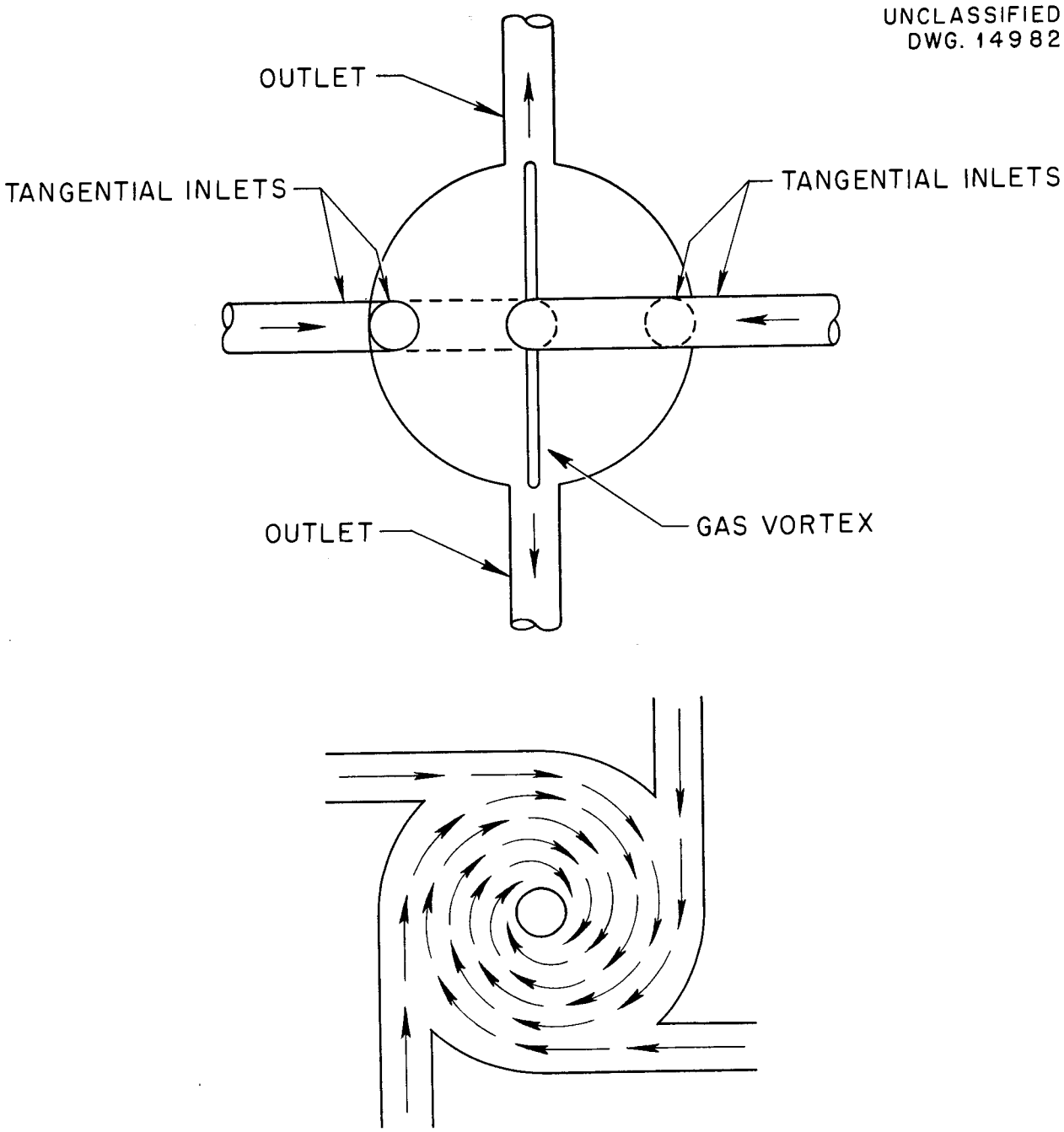

Fig. 48. Rotating Flow Model.

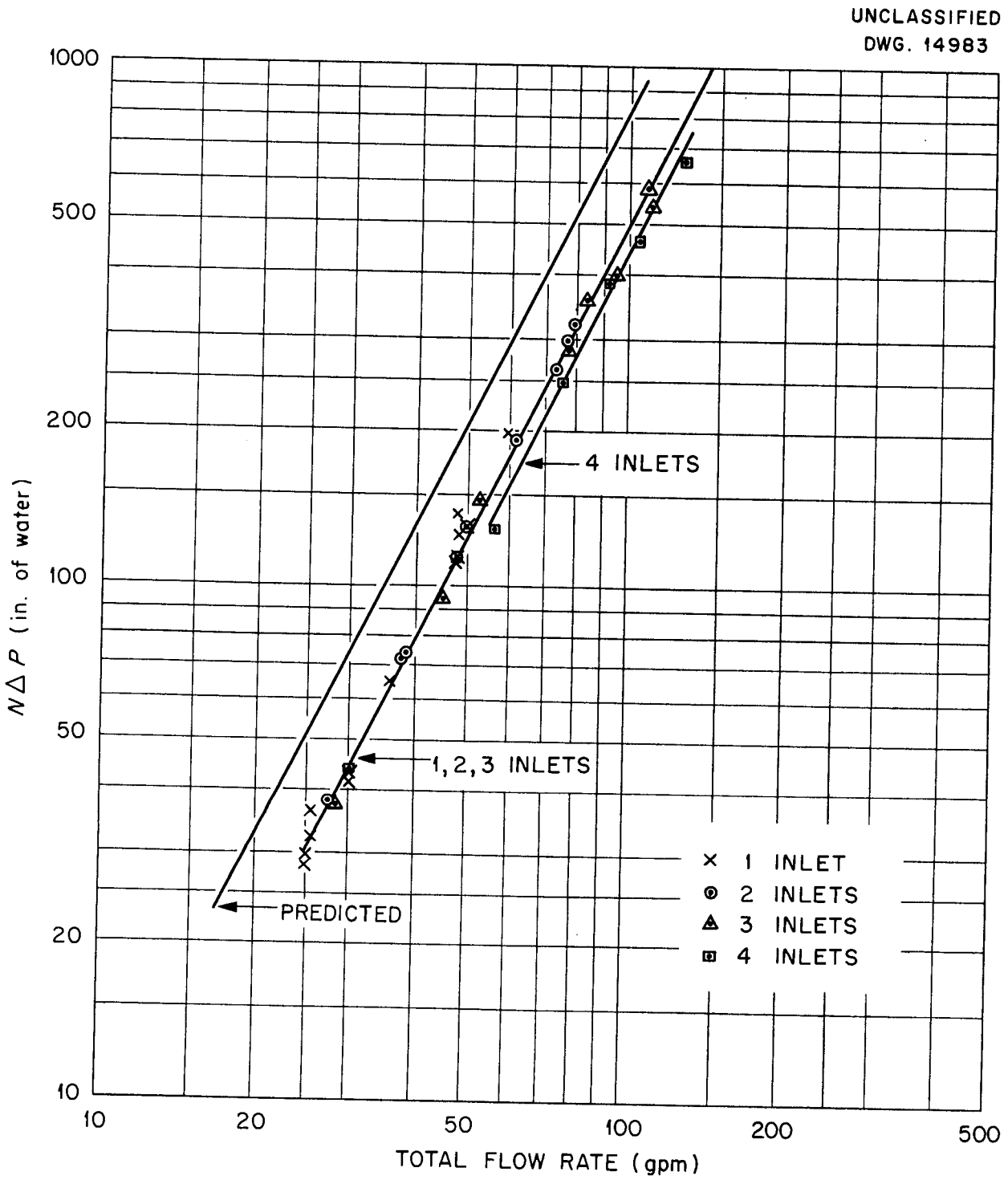

Fig. 49. Over-all Pressure Drop vs. Flow Rate for 12-in. Sphere.

V_0 = flow rate through the sphere (ft^3/sec),

g_c = gravitational constant (32.17 ft/sec^2),

R_1, R_2, and R_s are the radii in feet of the inlets, outlets, and sphere, respectively.

This equation is the theoretical expression for one inlet, assuming a free vortex and that the pipe velocity is equal to the tangential velocity at the equator. The correction term, N, introduced for multiple inlets is empirical. It can be seen that the correlation is 40% higher than the experimental data for one, two, and three inlets. This is similar to the results reported by the University of Tennessee for small glass spheres.[2] Data for four inlets are 12% below the data for one to three inlets.

Figure 50 is a plot of the pressure drop from the inlet to a point on the wall at a radius of 2.44 inches. The ordinate is again $N\,\Delta P$. The predicted line shown is of the same form as in the previous plot, with the point radius used in place of R_2. The data are seen to be considerably lower than expected, and furthermore there is a separate line for each number of inlets.

The inference from these data is that there is an abnormally large pressure drop near the outlet. The cause is not clear. Further work on this problem will be done primarily at the University of Tennessee. Future plans for the 12-in. sphere at ORNL include the testing of inserts in the inlets and outlets to obtain better understanding of the behavior of the outlet.

[2] "Nature of Liquid Flow Within a Spherical Container," *Homogeneous Reactor Project Quarterly Progress Report for Period Ending August 15, 1951*, ORNL-1121, p. 187.

However, at least on an empirical basis, the over-all pressure drop can be estimated as a function of flow rate and sphere geometry. According to Eq. 1, p. 189, ORNL-1121,[3] the University of Tennessee suggested that

$$\Delta P = \frac{\rho V_0^2}{2\pi^2 g_c R_1^4}\left\{\frac{1}{N_1}\left[\left(\frac{R_s}{R_2}\right)^2 - 1\right] + \frac{1}{N_2^2}\left(\frac{R_1}{R_2}\right)^4\right\}, \quad (2)$$

where

ΔP = pressure drop from inlet to outlet of the sphere (lb force/ft^2),

ρ = liquid density (lb mass/ft^3),

V_0 = total liquid flow rate (ft^3/sec),

R_1 = radius of inlet pipe (ft),

R_2 = radius of outlet pipe (ft),

R_s = radius of sphere (ft),

N_1 = number of inlet pipes,

N_2 = number of outlet pipes,

g_c = gravitational conversion factor (lb mass·ft/sec^2·lb force).

This is adjusted by inserting an empirical constant:

$$\Delta P = \frac{\rho V_0^2}{2\pi^2 g_c R_1^4}\left\{\frac{a}{N_1}\left[\left(\frac{R_s}{R_2}\right)^2 - 1\right] + \frac{1}{N_2^2}\left(\frac{R_1}{R_2}\right)^4\right\} \quad (3)$$

[3] *Ibid.*, p. 189.

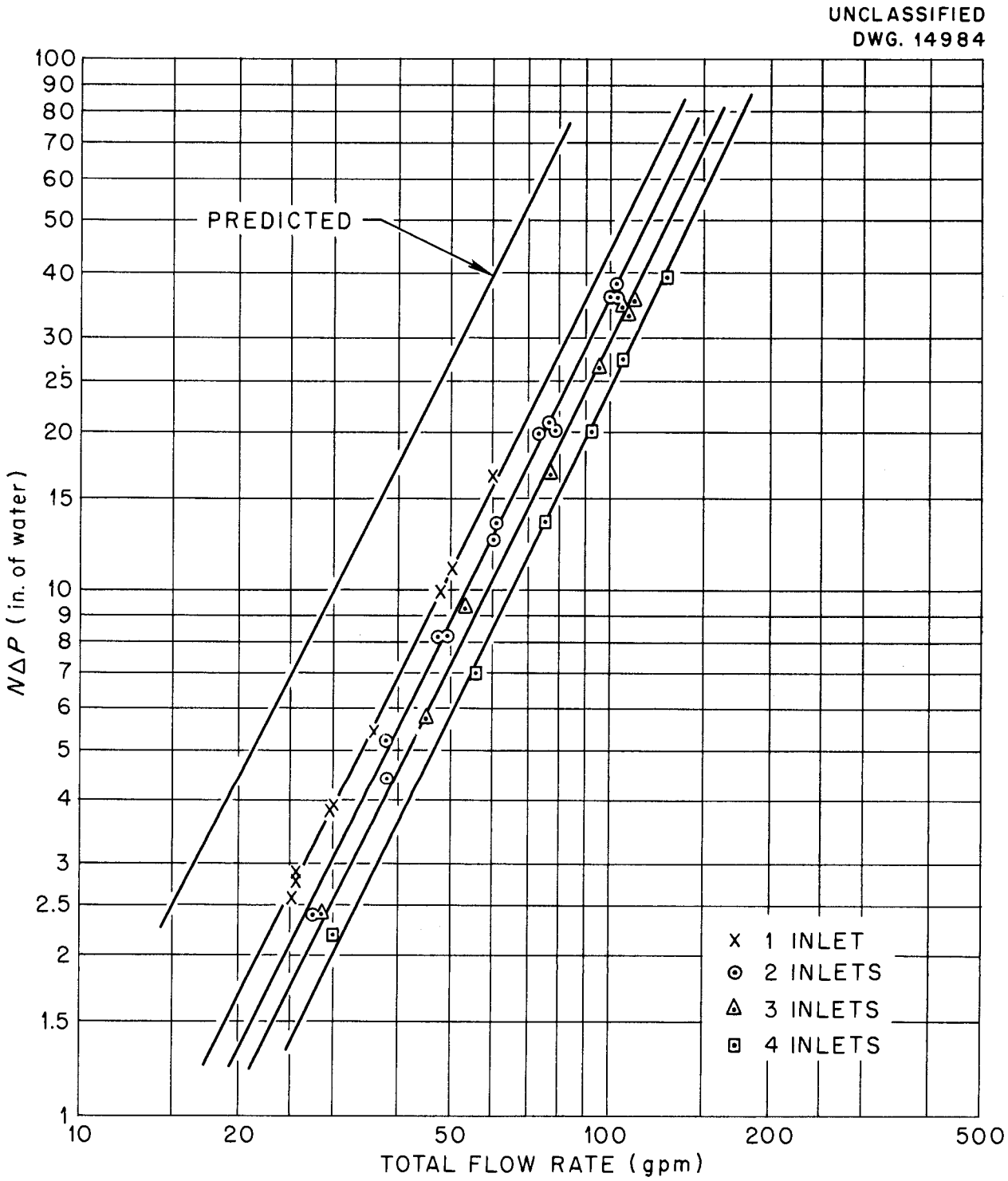

Fig. 50. Pressure Drop from Inlet to Wall Top at Radius of 2.44 in. vs. Flow Rate for 12-in. Sphere.

where a is a constant that depends on the number of inlets. The constant is evaluated directly from the data for one to four inlets. Values for five and six inlets are extrapolated. It is suggested that Eq. 3 be used to estimate the pressure drop for rotational-type reactor cores. It is as yet only a tentative correlation, but it will yield conservative predictions of ΔP.

Number of Inlets	1	2	3	4	5	6
Constant, a	0.6	0.6	0.6	0.53	0.46	0.40

Straight-through Cores. Preliminary model study of straight-through flow was carried out in a cylindrical plastic section 12 in. in diameter by 12 in. long (Fig. 51*a*). Both ends of the cylinder are connected to 4-in. pipe by means of 90-deg conical diffusers. At both ends of the cylinder there are flanges for mounting baffles or plates. Provision is made for gas or dye injection into the cylinder and into the upstream pipe to enable visual observation of flow patterns.

Operation of the equipment, without inserted obstructions, revealed that there was a strong jet through the center with stagnation near the walls. This would tend to produce overheating everywhere but at the central axis of a reactor. This condition has to be corrected either by production of slug flow with a velocity contour close to the flux gradient or production of good turbulent mixing to keep the reactor close to isothermal.

The most promising flow distribution has been obtained with a plate inserted across the cylinder at the inlet (Fig. 51*b*). A number of plates with drilled entry holes of 3/16 to 1 1/4 in. and solidity ratios of 0.83 to 0.99 have been tried. Solidity is the ratio of metal area to total plate area. Flow behavior around the plates is as follows: Strong eddies circulate between a region of well-defined jets near the plate and provide adequate mixing. The jets gradually lose their kinetic energy to the turbulent eddies and so lose their identity. Then the turbulence decays, according to theory, by a power function in going downstream until slug flow is approximated when steady state is reached. The distance from the plate of the transition region is increased by higher solidity ratios and by larger spacing between holes.

In a reactor, this approximate geometry can be attained by drilling entry holes in a thermal shield or by using multiple parallel inlets. The maximum solidity ratio is governed by pressure drop and corrosion limitations that limit liquid velocities. Because the corrosion picture is not yet clarified, this maximum is not known but it is believed to be between 0.8 and 0.9 for a 15-ft vessel.

At this time the well-mixed turbulent flow appears more promising than slug flow. In the cylindrical model, slug flow has been characterized by stagnant liquid near the cylinder walls, which sometimes had a low, downward velocity, while the main flow was up. Good mixing can be achieved by maintaining the entire vessel in the jet and transition regions. For a large reactor with a limited solidity ratio, perhaps 20 to 40 inlet pipes spaced to cover the lower hemisphere would be necessary. The outlet configuration is less important; a smooth conical outlet diffuser is apt to be sufficient.

Listed below are other ideas that have been tested:

1. A plate with drilled holes gave the flow a rotational component

UNCLASSIFIED
DWG. 14985

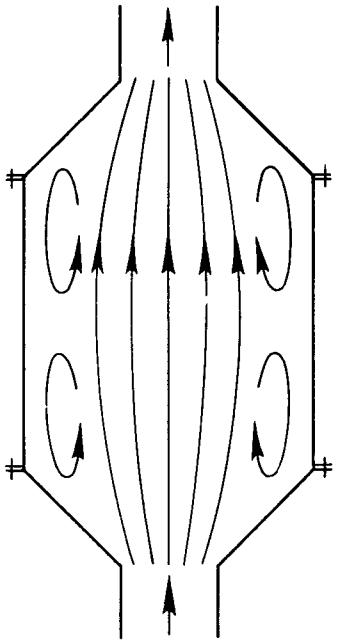

(*a*) Cylindrical Straight–through Model

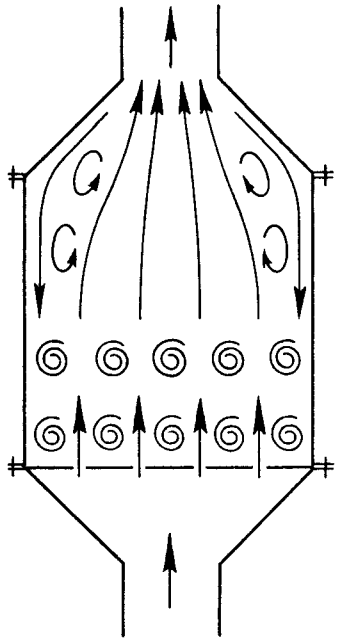

(*b*) Model with Plate Distributor

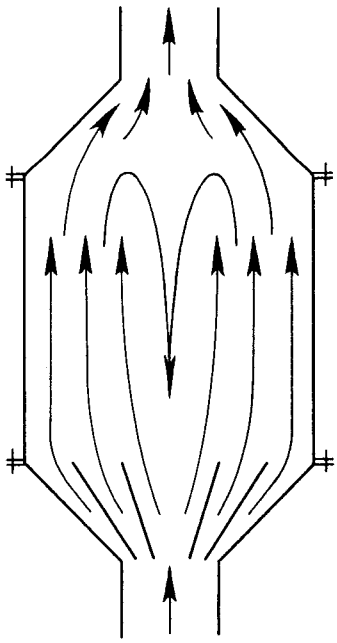

(*c*) Model with Conical Diffuser

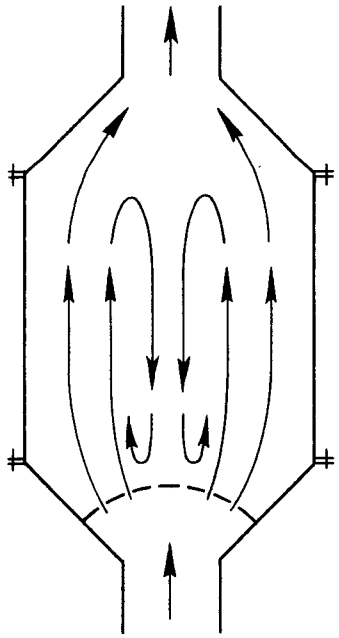

(*d*) Model with Shower Cap

Fig. 51. Reactor Core Models.

and produced a strong updraft at the center, which was surrounded by a "doughnut" of stagnant liquid. Flow was satisfactory elsewhere, except that the central updraft used more than its share of the flow. The use of vanes might be possible for producing good rotating slug flow.

2. Placing four concentric cones in the inlet expansion (Fig. 51*c*) resulted in rapid flow along the outside wall with stagnation and downflow at the center. Removal of the center cone did not help the situation.

3. Inserting a plastic shower-cap at the apex of the inlet cone (Fig. 51*d*) also produced strong flow along the wall and poor flow at the center. Aligning the cap to give good angular flow distribution was difficult, partly because of leaks at the intersection of the cone wall and the cap.

4. Removing the side stream at the cone wall (Fig. 52*a*) by cutting some small holes in the conical section was intended to promote flow through the entire cone instead of just having a jet at the center, but no observable effects were obtained.

Another promising model is a 9-in. glass sphere with an inlet at the top and two outlets, in the northern hemisphere parallel, to the inlet (Fig. 52*b*). A flask commonly employed in chemical laboratories was used as the model. The mixing appeared quite uniform; however, the model was not geometrically similar to large or intermediate homogeneous reactors in that the connections were small.

Two 18-in. spherical models that will incorporate the best ideas obtained in the above work are planned. One will utilize multiple inlets in the southern hemisphere and a single outlet at the north pole (Fig. 52*c*). The second will have an inlet at the north pole and four outlets in the northern hemisphere (Fig. 52*d*). These models will be scaled to the best current visualization of a 15 ft core and will operate at 1000 to 2000 megawatts.

Eight-Foot Sphere. Design is proceeding on a 50,000-gpm loop to be used for studying the flow characteristics of an 8-ft sphere. The first model will have two tangential inlets of 24-in. pipe and two polar outlets of 30-in. pipe and will be used to study the rotational flow pattern. Provision will be made for measuring liquid velocities with Pitot tubes, observing pressure gradients, looking for stagnant regions with dye or by conductivity techniques, studying gas removal, and evaluating the temperature distribution to be expected in the sphere if it were operating as a reactor. The system is scheduled for operation this summer.

A second pair of 8-ft hemispheres has been purchased, and provision will be made in the 50,000-gpm system to test the best alternate flow system developed from the small-scale models.

Gas Separators. If a rotational flow pattern is used in the ISHR core, gas will probably be removed from a vortex at the core outlets or in the outlet pipes close to the core. This plan for gas removal will be tested in the 50,000-gpm, 8-ft model. The low-pressure drop across the core that is desired implies lower relative rotational velocities in the vortex than are used in the HRE. Because of this and the larger average path that a bubble must travel, gas removal will be less efficient in this core than in the HRE.

If a straight-through core is used in the ISHR, gas must be removed in the external system; therefore two

devices for removing gas from liquid flowing in a pipe are being investigated, and models are under construction. These devices differ principally in the method of rotating the fluid. In one, the flow pattern is established by forcing liquid through a scroll, which is similar to forcing liquid backward in a centrifugal pump (with no impeller).

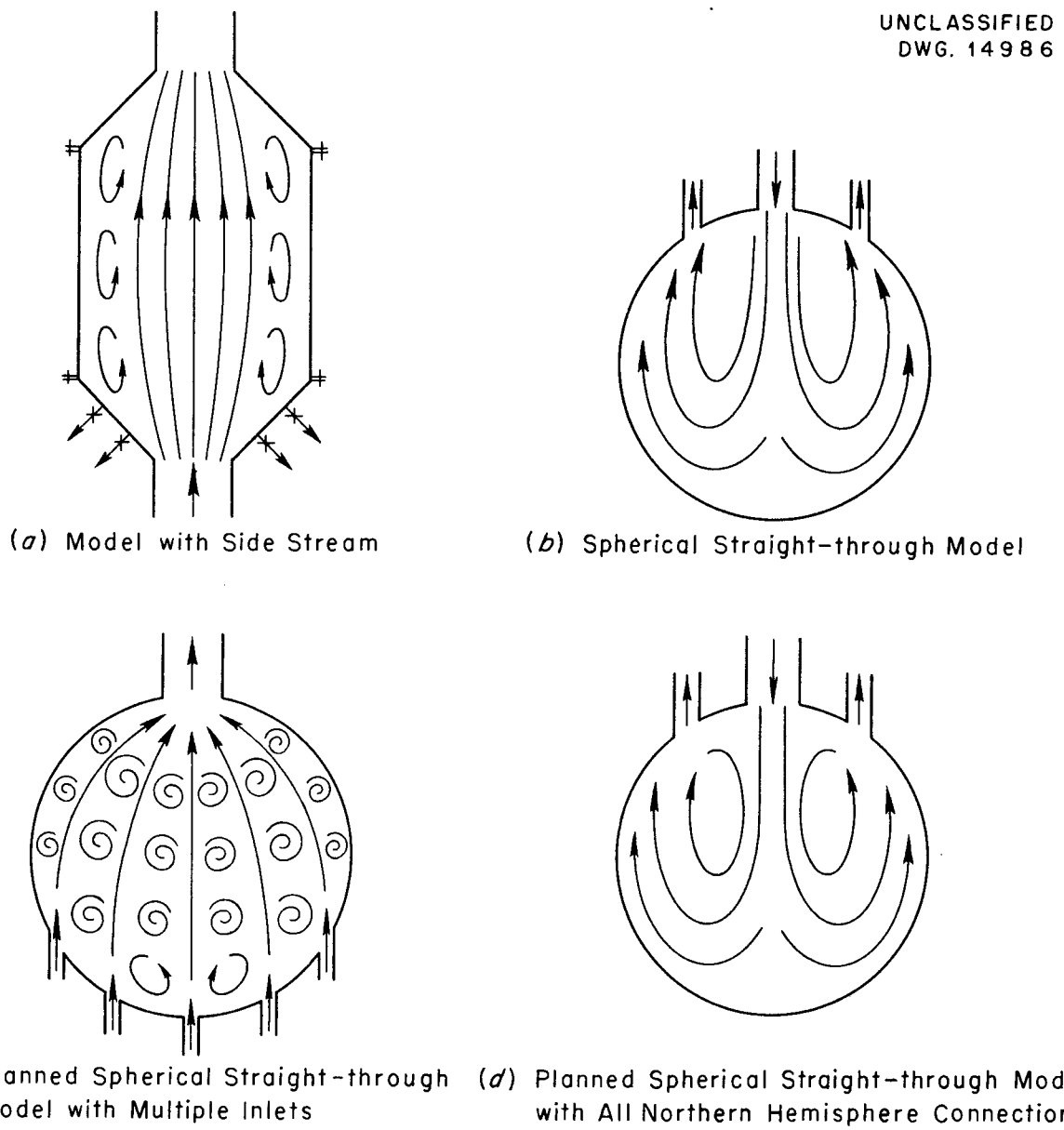

Fig. 52. Reactor Core Models.

In the second device, vanes are used in the line to set up rotation.

Velocity traverses will be made in these models, and gas removal and pressure drops will be investigated. As a result of these experiments a full-scale separator may be built and tested in the 50,000-gpm system. It is believed that a separator featuring low pressure drop and little or no additional fuel holdup can be built into the line between the core and heat exchanger for the ISHR.

FUNDAMENTAL RADIATION CHEMISTRY STUDIES

H. F. McDuffie, Group Leader
J. W. Boyle W. F. Kieffer
E. L. Compere M. D. Silverman
H. H. Stone

GAS PRODUCTION FROM URANIUM SOLUTIONS AND SLURRIES

Uranyl Sulfate. The initial rate of gas production for pure uranyl sulfate solutions has been determined as a function of temperature, concentration, and isotopic enrichment. This phase of the work is almost completed and has been reported in detail.[1] To summarize briefly, the rate of gas production under constant neutron flux decreases with an increase in uranyl sulfate concentration and a decrease in enrichment (U^{235} content). The rate of gas production is independent of temperature between 30 and 250°C.

The reason for the decrease in G (molecules of H_2 produced per 100 ev expended in solution) with an increase in uranyl sulfate concentration ($G = 1.7$ at 1 g of uranium per liter and $G = 0.5$ at 800 g of uranium per liter) has received some thought. To determine whether the change is related to some characteristic of the uranyl ion or to some less specific property, such as mass of solute, two solutions were made consisting of mixtures of UO_2SO_4 and Cs_2SO_4. Cs_2SO_4 was chosen because (1) cesium is an alkali metal and would be expected to behave as an inert material; (2) the ratio of Cs to SO_4 in Cs_2SO_4 is 265.8:96 and the ratio of UO_2 to SO_4 in UO_2SO_4 is 267:96, so that in relation to SO_4 the cation mass is very nearly equal. By comparing the last two columns in Table 37, it can be seen that G is diminished with an increase in uranium concentration but is not changed when an equivalent mass, such as cesium ion, is added.

The experiment showed that the decrease in G with increase in uranyl

[1] H. F. McDuffie, et al., "Radiation Stability," *Homogeneous Reactor Project Quarterly Progress Report for Period Ending November 15, 1951*, ORNL-1221, p. 117-123; J. W. Boyle, "Gas Production in Aqueous Reactor Solutions," *Chemistry Division Quarterly Progress Report for Period Ending December 31, 1951*, ORNL-1260.

TABLE 37

Gas Production from Solutions Containing UO_2SO_4 and Cs_2SO_4

CONCENTRATION OF URANIUM (mg of U per ml) (93% enriched) I	CONCENTRATION OF Cs_2SO_4 (mg of Cs_2SO_4 per ml) II	CONCENTRATION OF URANIUM EQUIVALENT TO Cs_2SO_4 (mg of U per ml) III	G OBSERVED FOR SOLUTION OF COMPOSITION COLUMN I + II	G OBSERVED FOR SOLUTION OF COMPOSITION COLUMN I + III
4.03	0	0	1.66	1.66
6.74	155.3	102.2	1.63	1.32
6.23	324.2	213.3	1.64	1.06

sulfate concentration is specific for uranyl ion and does not depend on mass of solute cation.

The interest in Cu^{++} ion as a possible pressure inhibitor in homogeneous reactors prompted examination of solutions of UO_2SO_4 with added Cu^{++} ion to determine whether the copper depressed the rate of gas formation. It was found that Cu^{++} did not decrease the rate of gas formation; rather, it increased the rate slightly, as was predicted.[2] The decrease in equilibrium pressure over fissioning UO_2SO_4 solutions containing copper is caused by a chemically induced back reaction – the recombination of hydrogen and oxygen gases to form water. Table 38 shows that the gas production is actually increased by adding Cu^{++}. The experiments were carried out in silica ampoules, and chromate pretreated stainless steel was present in only the last experiment. Two ampoules were prepared with stainless steel present; in one the metal was completely submerged and in the other it was half in the gas phase and half in the solution. The two ampoules gave the same results.

Uranyl Nitrate. The Los Alamos water boiler,[3] the first homogeneous reactor built in this country, gave satisfactory service from the start. The present Supo model[4] has a gas recombination system[5] that lends itself readily for obtaining gas production data. The reactor is charged with uranyl nitrate solution containing approximately 76.2 g of uranium per liter, 88.7% enrichment. This solution is not very different from solutions used by Handley and Boyle in determining *G* values for uranyl nitrate solutions in the X-10 graphite pile. Table 39 gives a comparison of *G* values for uranyl nitrate solutions obtained at the two different sites.

(2) A. O. Allen, T. W. Davis, G. V. Elmore, J. A. Ghormley, B. M. Haines, and C. J. Hochanadel, *Decomposition of Water and Aqueous Solutions Under Pile Radiation*, ORNL-130, Oct. 11, 1949.

(3) "An Enriched Homogeneous Nuclear Reactor" (Los Alamos Scientific Laboratory of the University of California), *Rev. Sci. Instruments* **22**, 489 (1951).

(4) L. D. P. King, *The Los Alamos Homogeneous Reactor, Supo Model*, LA-1301, Feb. 7, 1952.

(5) M. E. Bunker, R. P. Hammond, L. D. P. King, J. A. Leary, and W. R. Wykoff, *Gas Recombination System of the Los Alamos Homogeneous Reactor*, LA-1337, Mar. 6, 1952.

TABLE 38

Effect of Dissolved Copper on Gas Production from UO_2SO_4 Solutions

Concentration: 40 g of uranium per liter, 93% enriched

COPPER CONCENTRATION (*M*)	TEMPERATURE (°C)	*G* VALUES
	120	1.52
0.05	120	1.61
0.03	120	1.56
0.03	190	1.55
0.03	210	1.54
0.03	210	1.56*

*Type-347 stainless steel present.

TABLE 39

Comparison of *G* Values for $UO_2(NO_3)_2$ Solutions

REACTOR	SOLUTION COMPOSITION	TEMPERATURE OF SOLUTION (°C)	*G* VALUE
X-10	42.3 g of uranium per liter, 93.2% enriched	100	1.50
Supo	76.2 g of uranium per liter, 88.7% enriched	70	1.47
Supo	76.2 g of uranium per liter 88.7% enriched	70	1.31

The irradiations at X-10 were made in silica ampoules. The hydrogen produced was measured and analyzed on a vacuum line, and the energy was calculated from calorimetric data[6] for gamma and fast-neutron heating and it was monitored for slow-neutron (fission) heating. The fission energy released in the ampoule was derived from the expression

$$\overline{nv}t\sigma_f N_0 E = \Sigma ev$$

where $\overline{nv}$ is the slow neutron flux, t is the time of irradiation in seconds, σ_f is the fission cross section for U^{235} (546×10^{-24} cm^2), N_0 is the total number of atoms of U^{235} in the ampoule, and E is the energy released per fission, 165 Mev.

The two values for the Supo reactor were calculated by different methods. The value of 1.47 was obtained from hydrogen-oxygen recombination in the catalytic beds and was equivalent to 0.55 moles of H_2O per kwh of reactor operation. The value of 1.31 was determined from the volume of make-up water (0.49 moles of H_2O per kwh) necessary to keep the reactor operating at constant volume prior to the installation of the recombination system.

It is significant that *G* values determined under such drastically different conditions for similar solutions give results in such good agreement. The agreement gives confidence to the extrapolations for gas production data in the present homogeneous reactor studies. From studies on uranyl sulfate solutions, a slight lowering of *G* values in going from 42.3 to 76.2 g of uranium per liter would be expected, but *G* should not be affected by the two different enrichments, 93.2 and 88.7%.

Uranyl Fluoride. It is planned to study the UO_2F_2 system more thoroughly next quarter. Preliminary data indicate that *G* values may be somewhat higher for UO_2F_2 solutions than for UO_2SO_4. A batch of enriched UO_2F_2 has recently been received for these studies.

Uranium Oxide Slurries. Fundamental silica ampoule studies of gas production from uranium oxide slurries are planned for next quarter to supplement the slurry-irradiation program now being carried out cooperatively with the Chemical Technology Division

[6] D. M. Richardson, *Calorimetric Measurement of Radiation Energy Dissipated by Various Materials Placed in the Oak Ridge Pile*, ORNL-129, Oct. 1, 1948.

(discussed in more detail in the section of this report on "Slurry Fuel Studies").

PEROXIDE STUDIES IN URANYL SULFATE SOLUTIONS

Irradiations of both natural and enriched uranyl sulfate solutions have been made in the X-10 graphite pile by two groups of investigators at ORNL - Boyle and Kieffer, and Ghormley, Hochanadel, Stewart, and Sworski. In these experiments the uranium concentration was varied from 0.00168 to 3.39 *M*, the enrichment from 0.71 to 93.2%, and the temperature from 30 to 120°C. Analyses of the gases produced during bombardment were made by these workers. Experiments by the second group indicate that the peroxide produced during bombardment is approximately equivalent to the excess hydrogen found from gas analysis when analyses for both are run at the same time.

The data obtained from a total of 45 such experiments have been correlated by assuming that the analysis for excess hydrogen gas gives the amount of peroxide present.

$$(2H_2O \rightsquigarrow H_2 + H_2O_2)$$

On the basis of the estimated amount of peroxide and the known concentration of uranium, calculations were made to determine whether the solubility product of uranyl peroxide,

$$K_{S.P.} = 1.3 \times 10^{-3} \pm 15\%,$$

had been exceeded during the experiments. Although the effects of sulfate complexing, activity coefficients, and a temperature coefficient of solubility were neglected, the experimental results confirm the calculated values for precipitation. In three experiments at 100°C, in which precipitation was observed, calculations showed that the solubility product had been exceeded by a factor of 4. Duplicate experiments at 120°C failed to give the precipitates expected from the calculations. Six experiments, indicated by calculations to be borderline cases, did not show precipitation.

In every experiment checked, some thermal decomposition of peroxide must have occurred in the time interval (at least 10 min) between removal of the sample from the pile and observation; furthermore, considerable time elapsed (several days) before gas analyses were completed on the bombarded samples. Hence, the results reported for peroxide formation always tend to be low.

Out-of-pile experiments on peroxides have been devised to simulate pile conditions. By controlling the rate of addition of hydrogen peroxide to uranyl sulfate solutions at various temperatures, it should be possible to approximate the rate of formation of peroxide in pile-bombarded solutions. Some data are available on the temperature dependence of uranyl peroxide decomposition and the solubility product of uranyl peroxide at room temperature. However, little is known about the decomposition of hydrogen peroxide in uranyl sulfate solutions or about the temperature coefficient of uranyl peroxide solubility. In order to separate these two factors, rate experiments are being conducted under conditions that avoid uranyl peroxide precipitation.

Standard techniques in kinetics are being employed in the experiments. Analyses for hydrogen peroxide are made with standard ceric sulfate by using a back titration with ferrous sulfate and orthophenanthroline as an indicator. Solutions of these reagents as low as 0.002 *N* have been employed

satisfactorily in the presence of uranyl sulfate. Experiments thus far have been conducted in 0.0045 to 0.17 *M* uranyl sulfate solutions at 78°C in which the initial hydrogen peroxide concentration has been varied from 4×10^{-4} to 5×10^{-3} *N*.

The pertinent data are given in Table 40, and the results of several typical experiments are shown in Fig. 53. Examination shows that the rate is first order with respect to peroxide concentration and apparently independent of uranyl sulfate concentration from 0.0175 to 0.176 *M*. The rate constants, *k*, in the fourth column of the table have been calculated on this basis using the equation

$$\frac{d(H_2O_2)}{dt} = k(C_{H_2O_2}) .$$

There is an apparent decrease in the rate constant at 0.0045 *M*. The

TABLE 40

Decomposition of Hydrogen Peroxide in Aqueous Uranyl Sulfate Solutions at 78.0°C

EXPERIMENT	UO_2SO_4 CONCENTRATION (*M*)	INITIAL H_2O_2 CONCENTRATION ($M \times 10^3$)	k ($sec^{-1} \times 10^4$)
A	0.162	3.84	4.70
B	0.162	4.37	5.07
C	0.162	4.32	4.78
D	0.176	1.02	4.60
E	0.162	4.95	4.90
F	0.0486	4.08	6.00[a]
G	0.0486	4.60[b]	
H	0.0497	3.80	6.39[c]
J	0.0497	4.02	5.97[c]
K	0.0526	1.24	4.94
L	0.0526	1.27	5.05
M	0.0176	0.976	5.29
N	0.0176	1.14	5.30
O	0.0175	1.37	5.26
P	0.0178	0.496	4.09
Q	0.0178	0.420	4.07
R	0.0045	0.380	3.35
S	0.0045	0.463	4.26
AA	0	5.19	0.0685
BB	0	4.72	0.0748

[a] Supersaturated solution.
[b] Heavy precipitation.
[c] Small precipitation.

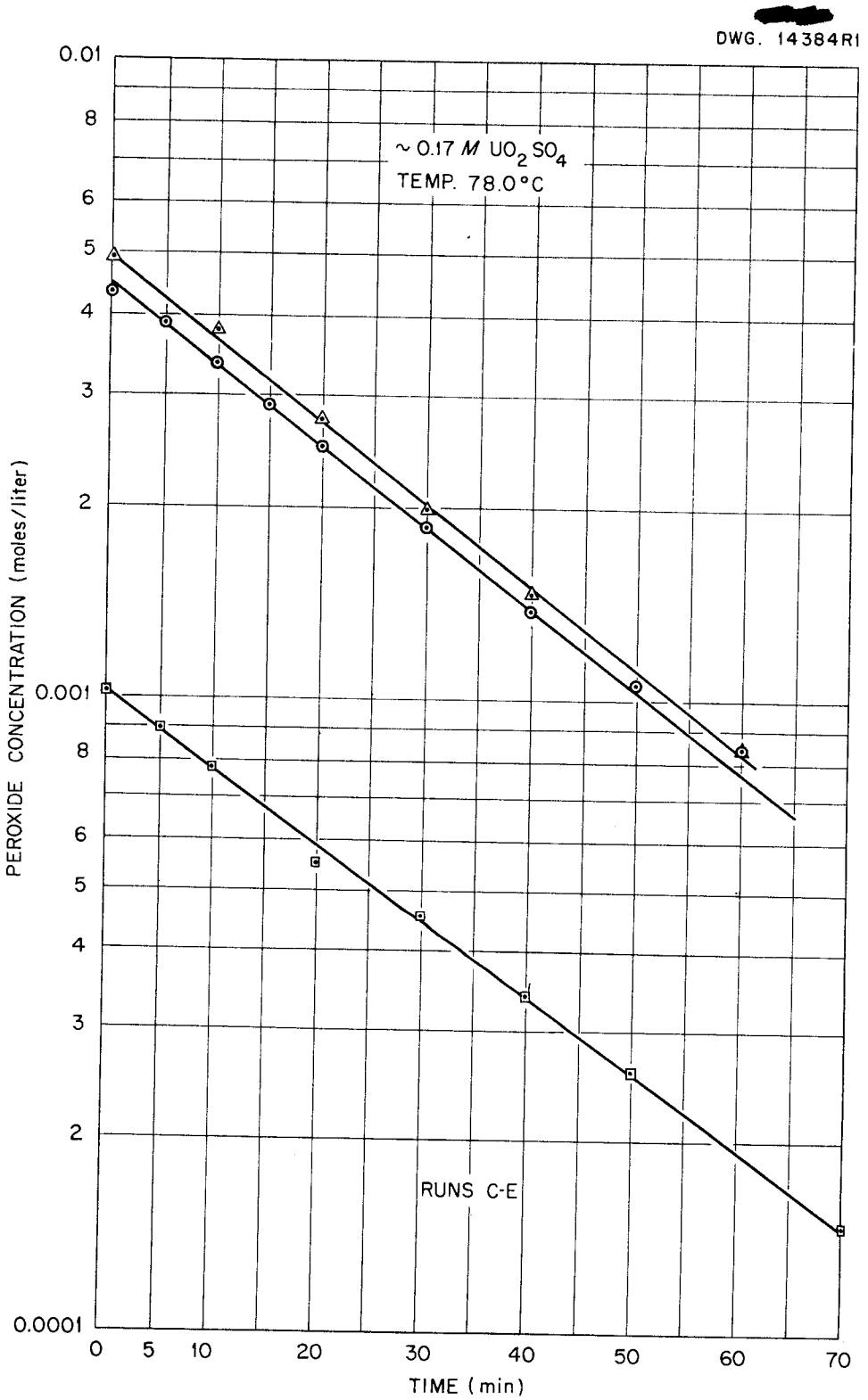

Fig. 53. Decomposition of Hydrogen Peroxide in Uranyl Sulfate Solutions.

large difference between this value and that for pure water (7×10^{-6}) suggests catalytic activity by uranyl sulfate or its ions.

The maximum allowable hydrogen peroxide concentration in solution has been limited by the solubility of uranyl peroxide formed according to the reaction

$$UO_2^{++} + H_2O_2 \rightleftharpoons UO_4 + 2H^+$$

in which the pH of the solution has been established by the uranyl sulfate concentration. It should be possible, however, by lowering the pH to increase the allowable peroxide concentration so that more nearly equal peroxide-uranium ratios can be investigated. Although there has been some variation in pH (2.5 to 3.3) with no apparent effect on the rate constant, no attempt has yet been made specifically to check the effect of hydrogen ion, or the individual uranyl and sulfate ions; these are to be investigated shortly, along with variations in temperature.

HOMOGENEOUS RECOMBINATION OF HYDROGEN AND OXYGEN IN AQUEOUS SYSTEMS

Studies of the solution recombination of hydrogen and oxygen without radiation are being made to evaluate the rate constants and other kinetic factors influencing the process in the presence of various catalysts. Uranyl sulfate solutions, frequently with the addition of copper sulfate catalyst, have been used. Work during the past quarter has demonstrated that:

1. The recombination rate is dependent on the first power of the copper concentration.

2. The reaction appears to be first order in hydrogen and independent of oxygen concentration at the 2:1 hydrogen to oxygen level.

3. The rate is not affected by type-347 stainless steel surfaces.

4. The observed rates are influenced by the slow diffusion of gas into the solution.

All factors thus far found to influence the observed rates have been successfully described mathematically in a kinetic equation.

The out-of-pile technique employed involves adding a 2:1 hydrogen-oxygen mixture to a 30-ml type-347 stainless steel bomb containing the solution, closing the system, and observing the rate of pressure drop after thermostating at the desired temperature (usually 250°C).

The rate equation for homogeneous recombination of hydrogen and oxygen in solution may be written:

$$dN_{H_2}/dt = [k_U + k_{Cu}(Cu)] \times V_{soln} \times (H_2)$$

where

dN_{H_2}/dt = moles of hydrogen recombined per hour,

k_U = first-order rate constant for recombination due to uranyl sulfate (hr^{-1}),

k_{Cu} = catalytic recombination rate constant for copper [(moles of copper per liter)$^{-1}$ hr^{-1}],

(Cu) = copper concentration (moles of copper per liter at reaction temperature),

(H_2) = dissolved hydrogen concentration (moles of H_2 per liter),

V_{soln} = volume of solution (liters).

This is adapted to the experimental system by the following equation:

$$\frac{d}{dt} \ln (\pi - A) = F_G F_D \; [k_U + k_{Cu}(\mathrm{Cu})]$$

where

π = total observed pressure (psia),

A = pressure of steam, inert gases, excess oxygen (psia),

F_G = geometric factor – ratio of moles of H_2 dissolved at saturation to total moles of H_2 in system,

F_D = diffusion term – ratio of moles of dissolved H_2 under dynamic reaction conditions to moles of dissolved H_2 at saturation.

Calculated values for the term F_G have been confirmed on the basis of experimentally determined material balances for hydrogen in the system. Thus the evaluation of this term is comparatively sound. The remaining minor uncertainties involve gas solubility coefficients in the solution (data from BMI-T-25[7] for pure water were used), small but unheated external volumes in the apparatus, etc.

It was observed that a half-filled cylindrical bomb showed a much faster recombination rate when placed in a horizontal position than when in the vertical position. These and other experiments were brought into agreement by the introduction of a diffusion term F_D in the rate equation. In unagitated bombs it appeared that the rate of diffusion of gas into the solution was slow enough that recombination caused a significantly lower dissolved gas concentration to exist in the lower levels. The use of estimated diffusion coefficients in a mathematical treatment based on this viewpoint led to an evaluation of F_D, which gave consistent rate constants for the various unagitated experiments. Transient terms in F_D were shown to have minor effect under the particular conditions considered, and a steady-state solution for F_D was used. The general effect of the transient terms will be developed further for possible application under conditions of very rapid reaction.

The use of rocking and other methods of agitating the bombs has given rate constants that approach those obtained from unagitated bombs with the F_D correction, and this technique is being developed. The theoretical value of F_D may be somewhat lower than that observed, since natural convection, which would tend to assist in the transfer of gas from the vapor plane throughout the liquid, may exist to some extent in the bombs. Also, the degree of agitation attainable with present laboratory equipment appears capable of completely removing the diffusion effect.

The uranyl sulfate rate constant, k_U, appears to be independent of the uranium concentration in uranyl sulfate containing 40 g of uranium per liter and above. At somewhat lower concentration the value falls off. This appears to resemble somewhat the behavior of the thermodynamic activity of uranyl sulfate (at other temperatures), and there seems to be a good possibility of correlating thermodynamic and catalytic activity when data become available.

The rate of recombination in the presence of copper is much greater than in the uranyl sulfate solution described above. The recombination

[7] H. A. Pray, C. E. Schweickert, and B. H. Minnich, *The Solubility of Hydrogen, Oxygen, Nitrogen, and Helium in Water at Elevated Temperatures*, BMI-T-25, May 15, 1950.

rate has been found to depend on the first power of copper concentration, and consequently the copper term is written k_{Cu}(Cu). Values of k_{Cu} at 250°C have been calculated from experimental data to be in the range 5000 to 6300 (moles of copper per liter)$^{-1}$ hr^{-1}. However, some adjustment of these values may be made after a firmer evaluation of F_D has been achieved.

Cobalt and zinc ions have been tested as recombination catalysts and found to have little or no catalytic activity.

Further work is visualized as developing a firmer evaluation of F_D or eliminating the need for it by sufficient agitation, exploring the effect of temperature on the recombination rate owing to copper and uranyl sulfate, correlating the thermodynamic and catalytic behavior of uranyl sulfate, and exploring the behavior of other systems – for example, uranyl fluoride and copper fluoride – and of other possibly catalytic substances, such as cerium, manganese, thallium, tin, vanadium, titanium, iodine, bromine, etc.

GAS KINETICS OF INPILE RADIATION STUDIES

C. H. Secoy

Theory. In a closed system that contains a water solution of fissionable atoms and a vapor space when exposed to a thermal neutron flux, water molecules along the fission-recoil tracks are dissociated to form free radicals that in turn may interact to re-form H_2O molecules or to form hydrogen and hydrogen peroxide molecules. Hydrogen peroxide will, of course, thermally decompose to yield oxygen and water. The over-all result is the production of a 2:1 hydrogen-oxygen gas mixture.

The rate of production of hydrogen in such a system has been shown to be independent of temperature (or very nearly so) and proportional to the fission density in the solution. The yield is often expressed by the quantity G, defined as the number of molecules of hydrogen produced per 100 ev of absorbed energy. The production at a particular flux, ϕ, and for a solution containing $[U^{235}]$ moles of U^{235} per liter can be expressed by

$$K = \frac{\phi\sigma_{235}E[U^{235}]G}{100} ,$$

moles of H_2 per liter per second, (1)

where E = 168 Mev (the fission recoil energy per fission).

Simultaneously with the production of gas, and apart from the recombination of free radicals in the fission-recoil track, a molecular recombination of hydrogen and oxygen occurs. The rate of recombination depends on the temperature of the system, the concentration of hydrogen in solution, and the presence of certain ions that serve as homogeneous catalysts. The rate of recombination of hydrogen is given by the expression

$$\frac{-d[H_2]}{dt} = K_s[H_2] , \qquad (2)$$

in which the bracketed quantities indicate concentrations in moles per liter, and K_s is the solution molar rate constant. If it is assumed that no concentration gradients exist in the solution, Eqs. 1 and 2 combine to give the net change of hydrogen concentration as

$$\frac{d[H_2]}{dt} = K - K_s[H_2] . \qquad (3)$$

From a consideration of the solubility of hydrogen and oxygen and the relative gas-to-liquid volumes in the system, it is possible to relate hydrogen concentration to the partial pressure of hydrogen and oxygen in the system, and Eq. 3 can be written as

$$\frac{dP}{dt} = K_1 - K_2P. \qquad (4)$$

Equation 4 is the simplified equation, the form of which has been proved correct by the data from a number of inpile experiments. According to Eq. 4 a plot of dP/dt vs. P should yield a straight line, with the intercept on the dP/dt axis being the production rate, K_1, and the slope of the line representing the recombination rate constant, K_2. The effect of increased temperature (or any other factor that accelerates the recombination) is to yield lines of increased slope. If, on the other hand, factors affecting the recombination rate remain unchanged but the production rate is changed (e.g., by precipitation of uranium from solution), the slope of the line will remain unaltered but the dP/dt intercept will change. The intercept on the P axis ($dP/dt = 0$) gives the steady-state pressure of the system (Fig. 54).

Equation 4 has been found correct in its general form and the effects just mentioned are in agreement, at least qualitatively, as described. However, before a quantitative treatment is possible the details must be examined more carefully. Of first consideration will be the procedure

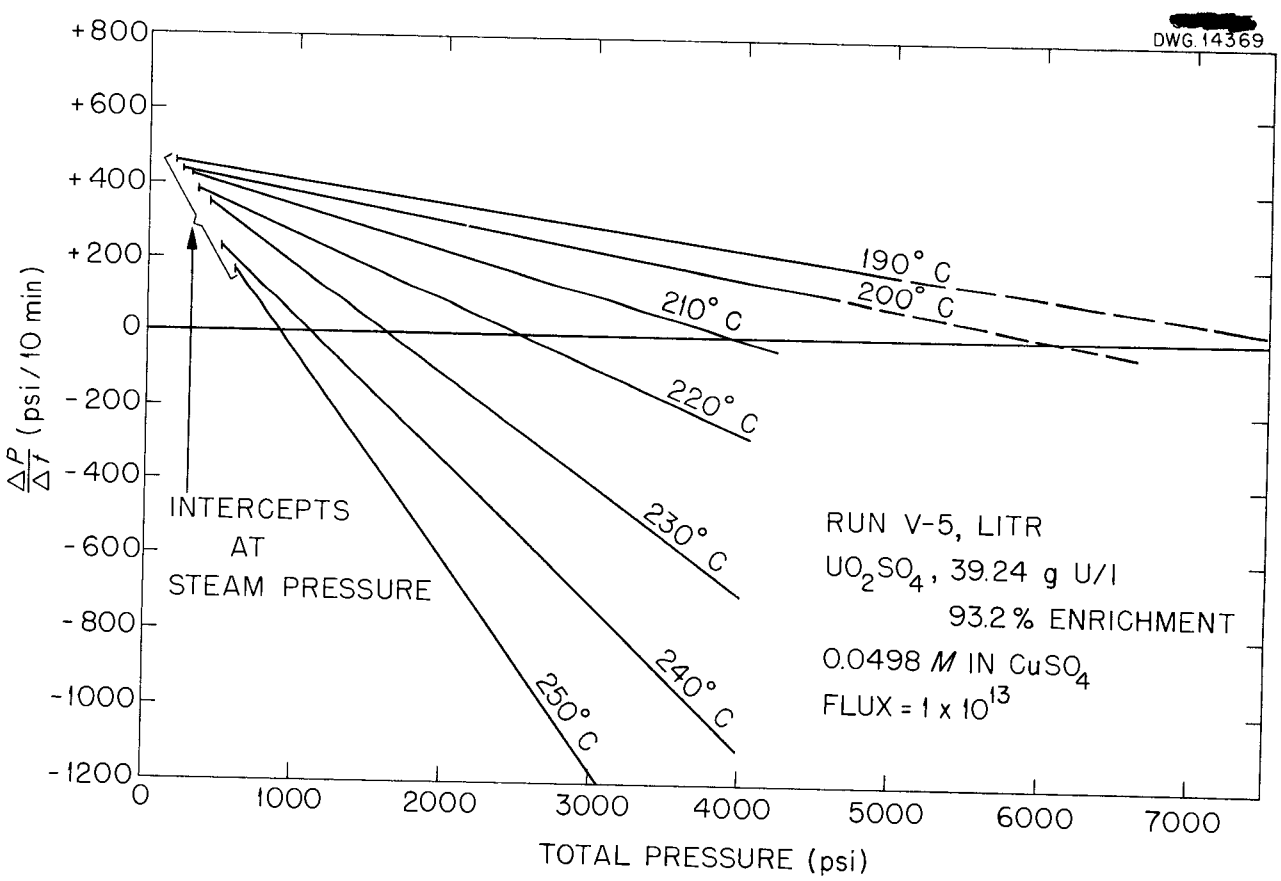

Fig. 54. Relationship Between $\Delta P/\Delta t$ and P at Various Temperatures.

in transforming Eq. 3 to Eq. 4 and second, the effect of concentration gradients as a result of finite diffusion rates.

It will be assumed that the gas obeys the ideal gas law, Henry's law, and Dalton's law. Thus it is possible to write for each gas

$$N_{gi} = \frac{P_i V_g}{RT}, \tag{5a}$$

$$N_{li} = \frac{P_i V_l}{\alpha_i}, \tag{5b}$$

$$P = P_{H_2} + P_{O_2}. \tag{5c}$$

Also, since two moles of hydrogen are produced (or recombined) with one mole of oxygen,

$$N_{H_2} = 2N_{O_2}, \tag{6a}$$

$$\frac{dN_{H_2}}{dt} = 2\frac{dN_{O_2}}{dt}. \tag{6b}$$

By multiplying Eq. 3 by V_l, the liquid volume, and assuming that all reaction takes place in the liquid phase,

$$\frac{dN_{lH_2}}{dt} = \frac{dN_{H_2}}{dt} = V_l K - K_s N_{lH_2}. \tag{7}$$

From Eqs. 5a and 5b

$$N_{H_2} = N_{gH_2} + N_{lH_2} = \left[\frac{V_g}{RT} + \frac{V_l}{\alpha_{H_2}}\right] P_{H_2},$$

$$N_{O_2} = N_{gO_2} + N_{lO_2} = \left[\frac{V_g}{RT} + \frac{V_l}{\alpha_{O_2}}\right] P_{O_2}. \tag{8}$$

Taking the derivative,

$$\frac{dN_{H_2}}{dt} = \left[\frac{V_g}{RT} + \frac{V_l}{\alpha_{H_2}}\right] \frac{dP_{H_2}}{dt} \equiv Q_{H_2} \frac{dP_{H_2}}{dt},$$

$$\frac{dN_{O_2}}{dt} = \left[\frac{V_g}{RT} + \frac{V_l}{\alpha_{O_2}}\right] \frac{dP_{O_2}}{dt} \equiv Q_{O_2} \frac{dP_{O_2}}{dt}. \tag{9}$$

From Eq. 5c

$$\frac{dP}{dt} = \frac{dP_{H_2}}{dt} + \frac{dP_{O_2}}{dt}. \tag{10}$$

Proper substitutions from Eqs. 6b, 9, and 10 into Eq. 7 yields:

$$\frac{dP}{dt} = \left[\frac{1}{Q_{H_2}} + \frac{1}{2Q_{O_2}}\right] (V_l K - K_s N_{lH_2}). \tag{11}$$

Partial expansion of Eq. 11 and further substitutions from Eqs. 5c, 6a, and 8 yield,

$$\frac{dP}{dt} = \left[\frac{1}{Q_{H_2}} + \frac{1}{2Q_{O_2}}\right] V_l K - \frac{V_l P K_s}{\alpha_{H_2} Q_{H_2}}. \tag{12}$$

An expression for K was given in Eq. 1, and K_s can be expressed as equal to $k_{Cu}[Cu]$ when the experiment is carried out in the presence of cupric ions. All other quantities in Eq. 12 are known constants or can be determined in the course of an experiment. Values of Henry's constant, α, have not been determined for the salt solution but have been measured for hydrogen and oxygen in water.

The effect of diffusion on the rate processes must also be considered. For simplification, any radial diffusion gradients (in a cylindrical

bomb) will be neglected and the x axis will be considered to lie along the axis of the cylinder. In a volume element of unit cross section and depth dx, four processes are occurring. In time dt they are:

1. production $= K\,dx\,dt$,
2. diffusion in $= -D\dfrac{dc}{dx}\,dt$,
3. diffusion out $= -D\left[\dfrac{dc}{dx} + d\left(\dfrac{dc}{dx}\right)\right]dt$,
4. reaction $= -\dfrac{d(c\,dx)}{dt}\,dt = kc\,dx\,dt$.

The net over-all change in moles of hydrogen is given by the combination of the four terms integrated over the length of the bomb, L, and multiplied by the cross-sectional area, A. This gives,

$$\frac{dN_{H_2}}{dt} = A\int_0^L K\,dx + D\,d\left(\frac{dc}{dx}\right) - kc\,dx\,. \quad (13)$$

If c were not a function of x, i.e., if there were no diffusion gradient, Eq. 13 would readily integrate to give Eq. 12. In order to express c as a function of x, the steady-state case is considered:

$$K\,dx + D\,d\left(\frac{dc}{dx}\right) - kc\,dx = 0\,. \quad (14)$$

Dividing by dx and transposing gives

$$D\frac{d^2c}{dx^2} = kc - K\,. \quad (15)$$

Defining y as the difference in concentration from the steady-state concentration, $y = c - K/k$, and substituting, the equation becomes,

$$\frac{d^2y}{dx^2} = \frac{k}{D}y\,,$$

and the solution is

$$y = A_1\,e^{-\sqrt{k/D}\cdot x} + A_2\,e^{+\sqrt{k/D}\cdot x}\,. \quad (16)$$

At $x = 0$ (the liquid-gas interface) $y = y_0$ and therefore,

$$y_0 = A_1 + A_2\,. \quad (17)$$

A second boundary condition is obtained since regardless of whether the system is above or below the steady state, y must always decrease with increasing x. Therefore, A_2 must be zero and,

$$y = y_0\,e^{-\sqrt{k/D}\cdot x} = y_0\,e^{-x/\lambda}\,. \quad (18)$$

A diffusion factor, F_D, is defined by,

$$F_D \equiv \frac{\bar{y}}{y_0} = \frac{\int_0^L y\,dx}{\int_0^L dx} = \frac{\lambda}{L}(1 - e^{-L/\lambda}), \quad (19)$$

in which $\bar{y}$ is the mean effective value of the concentration difference from steady-state concentration. λ is the distance in which the concentration falls off by a factor e and can be referred to as the diffusion length. When L is large in comparison with λ, which is true in this application, $F_D \cong \lambda/L$.

The relation between y and the partial pressure of hydrogen is given by,

$$P_{H_2} = \alpha_{H_2}C_0$$

$$P_{H_2} - P_{H_2(ss)} = \alpha_{H_2}(C_0 - C_{ss})$$

$$= \alpha_{H_2}y_0\,. \quad (20)$$

Returning now to the nonsteady-state case,

$$\frac{dN_{H_2}}{dt} = \int_0^L -V_l \; K_s \; y \; dx \; . \qquad (21)$$

The steps in solving this equation and converting to the pressure variable are completely analogous to those given above and will not be repeated. The final equation is,

$$\frac{dP}{dt} = 36\phi\,\sigma_f E\,[U^{235}]\,V_l G F_D \left[\frac{1}{Q_{H_2}} + \frac{1}{2Q_{O_2}}\right] - \frac{V_l F_D}{\alpha_{H_2} Q_{H_2}} \cdot P \left[\sum k_i C_i^{m_i}\right] . \qquad (22)$$

The molar rate constant for the ith ion is k_i, the concentration is C_i, and the order of the recombination reaction for the ith ion is m_i. This quantity is summed for all ionic species having an effect on the reaction rate. All other quantities in Eq. 22 have been defined above. It should be pointed out that in the derivation of Eq. 19 for F_D, entrance effects at the liquid-gas interface have been ignored and that transient effects and eddy diffusion have been neglected. Equation 19 can hardly be expected to hold well in the inpile experiments in which much internal heating occurs. In fact, the experiments indicate that the mixing is about ten times better than that given by simple diffusion.

Experiments. Equation 22 can be applied to the pressure data obtained from inpile irradiation studies for two purposes. First, the solution molar rate constant can be calculated from the steady-state pressure; second, the gas production rate can be calculated from the extrapolated dP/dt value at $P = 0$, provided the diffusion factor is known.

Cupric Ion Molar Rate Constant. The cupric ion has been shown to have a very high specific rate effect in comparison with uranyl ion, and in the experiments to be described the effect of the uranyl ion can be neglected. At the steady state $dP/dt = 0$, and upon rearrangement and cancellation of common terms Eq. 22 yields,

$$k_{Cu} = Q_{H_2} \left[\frac{1}{Q_{H_2}} + \frac{1}{2Q_{O_2}}\right] \frac{36\phi\sigma E\,[U]\,G\alpha_{H_2}}{[Cu]P_{ss}} \; . \qquad (23)$$

In the temperature range 190 to 260°C being considered, the solubilities of H_2 and O_2 are nearly the same and no serious error is introduced by setting $Q_{H_2} = Q_{O_2}$. This gives

$$k_{Cu} = \frac{54\phi\sigma E\,[U]\,G\alpha_{H_2}}{[Cu]P_{ss}} \; , \; hr^{-1} . \qquad (24)$$

Table 41 gives the experimentally determined steady-state pressures for two experiments that were carried out in the X-10 graphite pile and two in the LITR. The copper concentration differed in the experiments from 0.002 M in experiment 371 to 0.05 M in experiment V-5. The calculated values for k_{Cu} given in Table 41 were plotted on semilogarithmic paper against $1/T$ in Fig. 55. Also shown are values of k_{Cu} at three temperatures that were obtained from out-of-pile experiments. The calculated energy of activation is 23 kcal, and

TABLE 41

Cupric Ion Molar Rate Constant

TEMPERATURE (°C)	α_{H_2} (psi/mole/liter)	P_{ss} (psia)	k_{Cu} (hr^{-1})	REMARKS
Experiment 363				
194	15,000	2000	495	
209	13,200	860	1010	Hole 12, Graphite Pile
229	10,800	300	2380	$\phi = 5 \times 10^{11}$
239	9,800	185	3500	[U] = 0.16 *M*
249	8,700	103	5580	[Cu] = 0.009 *M*
259	7,750	60	8530	
Experiment 371				
210	13,100	3400	1140	
215	12,500	2420	1530	Hole 60, Graphite Pile
222	11,700	1806	1920	$\phi = 5 \times 10^{11}$
226	11,250	1448	2310	[U] = 0.16 *M*
230	10,800	1148	2800	[Cu] = 0.002 *M*
236.5	10,000	894	3320	
241	9,530	649	4360	
Experiment V-5				
190	15,400	7668	467	
200	14,300	5855	567	Hole C-44, LITR
210	13,100	3598	846	$\phi = 1 \times 10^{13}$
220	11,900	2140	1290	[U] = 0.1557 *M*
230	10,800	1205	2080	[Cu] = 0.0498 *M*
240	9,650	595	3770	
250	8,600	304	6570	
Experiment V-7				
210	13,100	4873	1060	
220	11,900	3104	1510	Hole C-44, LITR
230	10,800	1414	3000	$\phi = 1 \times 10^{13}$
240	9,650	890	4260	[U] = 0.158 *M*
250	8,600	428	7890	[Cu] = 0.0299 *M*
260	7,650	305	9850	
Out-of-Pile				
190			244	Mean of 3 experiments range 226 to 258
220			1349	Mean of 3 experiments range 1246 to 1450
250			5365	Mean of 11 experiments range 4860 to 6310

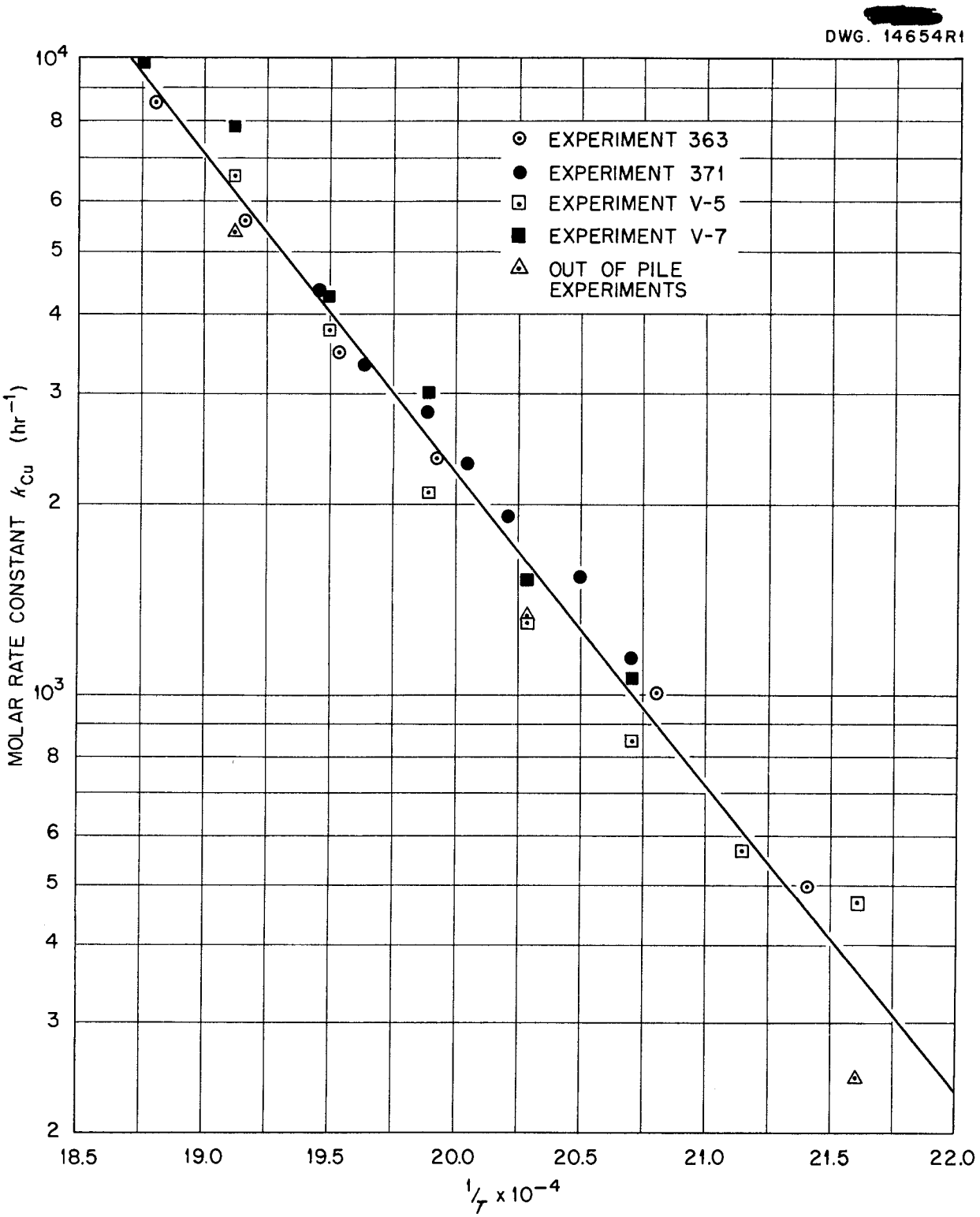

Fig. 55. Molar Rate Constant for Cupric Ions vs. Reciprocal of Absolute Temperature.

k_{Cu} can be expressed as a function of temperature by,

$$2.3 \log k_{Cu} = \frac{-23,000}{RT} + 30.88 \ . \quad (25)$$

Although there is considerable scatter to the points in Fig. 55, the data are considered quite satisfactory owing to the experimental difficulties and the approximations involved in the calculation. The values of α_{H_2} were obtained from BMI-T-25[7] and apply to the solubility of hydrogen in water. When data for the solubility in the appropriate solution become available, the values of k_{Cu} must be corrected accordingly.

The fact that the three points from out-of-pile experiments all lie below the line in Fig. 55 is not believed to be evidence for the existence of a radiation effect on the reaction rate since they also lie within the range of variation of the inpile results. In the calculation of k_{Cu} from the out-of-pile experiments, the application of the geometric correction factor, Q, is necessary, and the diffusion factor, F_D, must either be applied or diffusion effects eliminated by adequate agitation of the vessel. Some uncertainty is involved in the Q factor in estimating the volume of the external system. In the experiments cited the bombs were agitated and no diffusion factor was used. There remains an element of uncertainty as to whether the agitation was adequate to ensure complex mixing. The degree of agreement of the results with the inpile data indicates that neither of these factors is seriously in error.

Diffusion Factor, F_D. As previously mentioned, if a true value of the "mixing coefficient" for an inpile experiment is available, values of G (the gas production) could be calculated from the dP/dt value at $P = 0$. Equation 19 was derived for the diffusion factor from simple diffusion theory, but there remains the question of whether simple diffusion can account for the actual mixing obtained in an experiment. Since a dependable value of G has been obtained by other experiments, a comparison of theoretically calculated diffusion factors (Eq. 19) and experimentally determined mixing factors appears in order.

Table 42 gives the values of the required mixing factors, designated $F_D{}^*$, for experiments V-5 and V-7 calculated from the dP/dt intercepts using G = 1.5 molecules H_2 per 100 ev. Values of F_D calculated by Eq. 19 are given for comparison. The only available data for D, the diffusion coefficient, are those of Ipatiev and Teodorovich[8] for the diffusion of gases in water, and these were used in the calculation of F_D. Values of the mixing factor and the diffusion coefficient as a function of temperature are shown graphically in Fig. 56.

The conclusions from these calculations are: (1) Mixing is actually about ten times better than that which would result from simple diffusion alone; it is about 70% of perfect mixing at 200°C and becomes less complete at higher temperatures. (2) The mixing factors other than pure diffusion are relatively temperature independent as indicated by the similarity in shape of the curves of Fig. 56. The first conclusion seems reasonable in view of the complexity of thermal gradients in the system and the possibility of actual bubble

[8] V. N. Ipatiev, Jr. and V. P. Teodorovich, "Diffusion of Gases in Liquids under Pressure. II. Effect of Temperature on the Diffusion of Gases in Liquids under Pressure," *J. Phys. Chem. (U. S. S. R.)* **10**, 712-718 (1937).

[redacted]

DWG. 14655R1

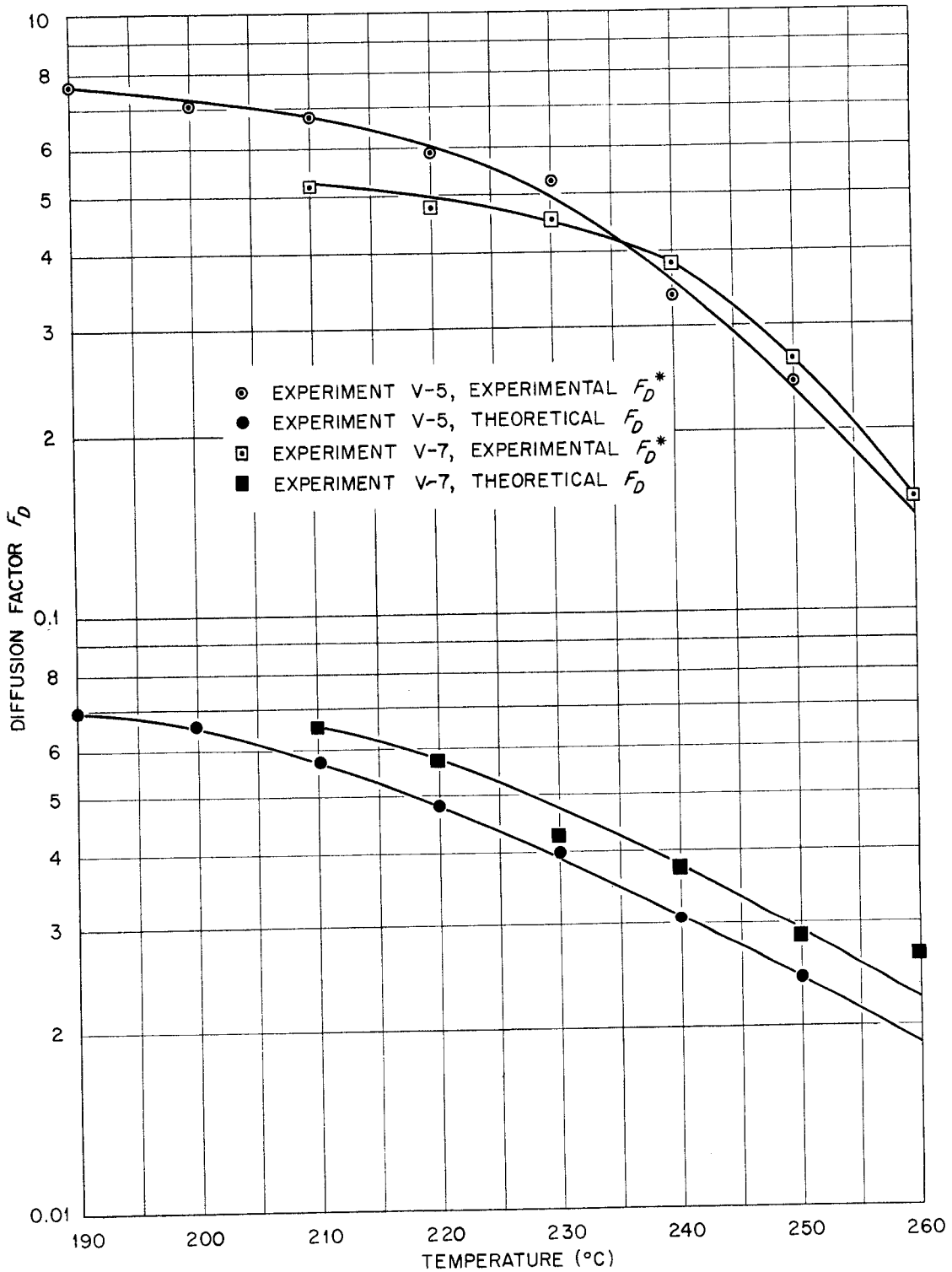

Fig. 56. Experimental and Theoretical Diffusion Factors for Experiments V-5 and V-7.

formation; both factors give rise to increased mixing. Furthermore, there is no obvious reason why these factors should display much variation over the temperature range employed.

In conclusion emphasis should be given to the practical application of the concepts advanced here, particularly as exemplified in Eq. 4, in the interpretation of pressure data during the course of an experiment. The nature of a dP/dt vs. P graph indicates immediately the state of affairs in the system. This has proved a most useful tool in the experimental program and is expected to continue to do so.

TABLE 42

Calculated Mixing Coefficients and Diffusion Factors

TEMPERATURE (°C)	$(dP/dt)_{P=0}$ (psi/hr)	MIXING FACTOR $F_D{}^*$ FOR $G = 1.5$	DIFFUSION FACTOR F_D
Experiment V-5			
190	2748	0.765	0.069
200	2610	0.707	0.066
210	2550	0.673	0.057
220	2292	0.589	0.048
230	2100	0.526	0.040
240	1380	0.337	0.031
250	1008	0.240	0.024
Experiment V-7			
210	2045	0.514	0.065
220	1941	0.457	0.057
230	1894	0.451	0.042
240	1636	0.380	0.037
250	1159	0.262	0.028
260	690	0.152	0.026

SOLUTION CHEMISTRY

W. L. Marshall, Group Leader

R. D. Brown
H. O. Day, Jr.
J. S. Gill
E. V. Jones
K. S. Warren
H. W. Wright

PLUTONIUM SOLUBILITIES IN URANYL SALT SOLUTIONS

K. S. Warren H. W. Wright

Stability of Plutonium Sulfate in Uranyl Sulfate Solutions. The investigation of the stability of plutonium(IV) sulfate in aqueous uranyl sulfate has continued. Previous experiments to determine the amount of plutonium remaining in solution after heating uranyl-plutonium sulfates for various periods of time and at several temperatures[1] showed that equilibrium was not attained so rapidly at the lower temperatures; therefore a determination of reaction rates appeared desirable.

A stock solution containing about 0.5 g of plutonium(IV) per liter of UO_2SO_4 (650 g of uranium per liter) was prepared in a manner similar to that used in preparing 1.26 *M* UO_2SO_4. Small amounts of the stock solution were sealed in glass ampoules and placed in an aluminum heater for desired periods of time and then removed, centrifuged, and analyzed. Details of this procedure were described previously.[1] The data obtained at 100, 110, 125, and 150°C were plotted (Fig. 57), and the reaction rate, k, for each temperature was calculated. It appeared that first-order reaction treatment of the data was applicable, at least as a first approximation. From the straight line derived from log k plotted vs. $(1/T)$, the energy of activation was calculated to be about 31 kilocalories. This value for the energy of activation of the hydrolysis reaction applies specifically to plutonium dissolved in 2.73 *M* UO_2SO_4 heated in pyrex glass ampoules with no more oxygen present than was originally contained in the enclosed air above the liquid sample. Future studies are planned in which other types of containers, lower concentrations of uranium, and higher concentrations of oxygen will be the variables.

Stability of Plutonium Ion in Uranyl Fluoride Solution. A solution containing 0.53 g of plutonium(IV) per liter of uranyl fluoride solution was prepared from plutonium peroxide and a solution of uranyl fluoride containing 398 g of uranium per liter. An exploratory investigation of the stability of the plutonium(IV) ion in this type of solution was conducted at 130°C in the same manner that the sulfate solutions had been studied previously. Plutonium precipitated from solution, behaving similarly to the sulfate under these conditions, as may be observed from the data in Table 43.

The linear relationship between the logarithm of the concentration of the plutonium ion and time indicated by the data suggests a first-order reaction. During attempts to prepare a suitable sample for the stability investigation, a light-yellow precipitate that has not been identified was obtained in every case.

[1] W. L. Marshall, R. D. Brown, H. O. Day, J. S. Gill, E. V. Jones, K. S. Warren, and H. W. Wright, "Solution Chemistry," *Homogeneous Reactor Project Quarterly Progress Report for Period Ending November 15, 1951*, ORNL-1221, p. 97.

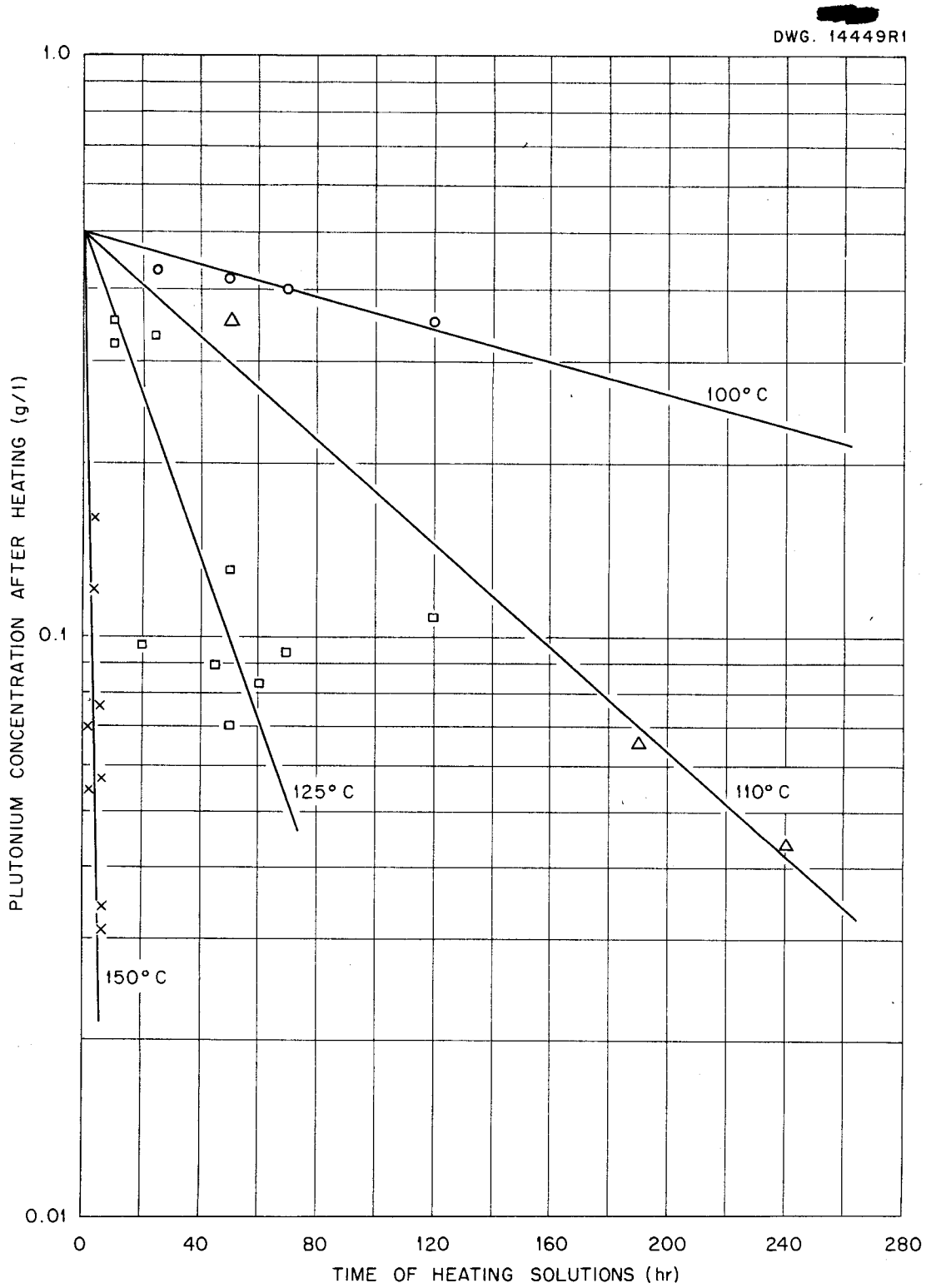

Fig. 57. Change of Concentration of Plutonium Sulfate in 2.73 *M* Uranyl Sulfate During Heating at Various Temperatures.

TABLE 43

Stability of Plutonium Ion in Uranyl Fluoride Solution

TIME OF HEATING AT 130°C (days)	AMOUNT OF PLUTONIUM REMAINING IN SOLUTION (g/l)
0	0.53
0.75	0.34
5	0.04
10	0.006

Effects of Radiation on the Valence State of Plutonium. Little is definitely known concerning the ability of intense gamma-radiation fields to produce valence changes of plutonium ions in solution. A few experiments were planned for the purpose of studying this subject, since it would have a direct bearing on the homogeneous reactor program. Samples of plutonium(III) and plutonium(VI) were prepared by electrolyzing plutonium sulfate in a glass cell with platinum electrodes. A current density of 0.55 ma/cm^2 of electrode surface was used, and the solution was not stirred. Portions of the electrolyte were removed from the anode and cathode compartments and sealed in pyrex glass ampoules. These ampoules were irradiated for 67 hr in a gamma field at 12,000 r/min. After irradiation the samples were kept at room temperature for three days before opening and diluting with 0.1 *M* H_2SO_4. Absorption measurements were made on the diluted samples with a Beckman quartz spectrophotometer. An inspection of the absorption curves showed that while the high and low valence states of the control samples tended to "drift" back to the original IV state while standing under room conditions, the valence states of the irradiated samples changed even more rapidly to the more stable IV state. It is desired to repeat this experiment at least once before arriving at more quantitative conclusions.

It is planned to conduct plutonium solubility investigations in stainless steel bombs, and, if warranted, in titanium bombs. There is considerable interest in the effect of oxygen on the solubility of plutonium because of recent work by Tomlin of the Chemical Technology Division. A stainless steel bomb has already been fabricated for the first of this new series of investigations.

A second irradiation study is being made in connection with plutonium valence changes. The elapsed time between irradiation and absorption analysis will be held to a minimum to eliminate "postirradiation" drifts that may be in opposition to the effects of the gamma radiation itself.

A plutonium-uranyl phosphate solution is being prepared for solubility investigations similar to those made with the corresponding sulfates.

CALCULATED FISSION-PRODUCT BUILDUPS AND EXPERIMENTAL SOLUBILITIES OF FISSION-PRODUCT MIXTURES IN URANYL SULFATE SOLUTIONS

J. S. Gill W. L. Marshall

In order to provide a basis for an investigation of fission-product solubilities and to be able to eliminate certain fission products from solubility consideration, the actual expected amounts were calculated for a typical reactor. Continuous operation of the reactor for one month and for one year were chosen for the calculations, since these times should be much in excess of actual processing intervals. The behavior of fission products in the relative amounts indicated by these calculations is being studied at 250°C in uranyl sulfate solutions.

Calculations. Fission-product buildups were calculated for a 50 kw/liter reactor running continuously at this power for the times specified,

with all fission chains producing a given element being considered. The chains, together with fission yields, were obtained from data of the Plutonium Project.[2] Standard equations involving buildups of stable and unstable isotopes were used; however, approximations were made where no significant change would occur in the final summation for a given element. The calculated values are given in Table 44 for both no gaseous fission-product removal and for 100% removal. The actual amounts should be between these two limits and will depend on the percentage of gaseous fission-product removal during reactor operation. To determine buildups for other power levels, the values in Table 44 should be multiplied by the appropriate power ratio – that is, for a 25 kw/liter reactor, the buildups would be halved.

[2] L. A. Pinck and G. E. Hilbert, "Behavior of Certain Fluorene Compounds Containing Trivalent Carbon and Tetravalent Nitrogen," *J. Am. Chem. Soc.* 68, 2411-2442 (1946).

Experiments. Synthetic mixtures of chlorides or nitrates of ten of the solid fission products with highest yield (Ce, Zr, Cs, Mo, Ru, Ba, Sr, La, Nb, and Y) were fumed to dryness with a 1:1 HNO_3-H_2SO_4 mixture. An amount of the dry mixture equivalent to one year's production, assuming no gas removal, was added to 0.125 and 1.25 *M* UO_2SO_4 solutions, respectively, and the resultant solutions were heated to 250°C. These experiments were conducted in titanium bombs with platinum

TABLE 44

Calculated Solid Fission-Product Buildups for a Homogeneous Reactor Continuously Operated at 50 Kilowatts per Liter

ELEMENT	FISSION-PRODUCT BUILDUP IN OPERATION FOR ONE MONTH (g/l)		FISSION-PRODUCT BUILDUP IN OPERATION FOR ONE YEAR (g/l)	
	WITH NO GAS REMOVAL	WITH 100% GAS REMOVAL	WITH NO GAS REMOVAL	WITH 100% GAS REMOVAL
Cerium	0.2	0.06	2	0.7
Neodymium	0.2	0.07	2	0.8
Zirconium	0.2	0.08	2	0.6
Cesium	0.1	0	2	0
Molybdenum	0.1	0.1	1	1
Ruthenium	0.1	0.1	1	1
Barium	0.09	0.0001	0.8	0.001
Strontium	0.08	0.007	0.8	0.1
Lanthanum	0.07	0	0.7	0
Praseodymium	0.04	0	0.6	0
Niobium	0.04	0.004	0.5	0.1
Yttrium	0.04	0	0.3	0
Technetium	0.03	0.03	0.5	0.5
Rubidium	0.03	0.007	0.3	0.01
Promethium	0.02	0.02	0.2	0.2
Rhodium	0.006	0.006	0.3	0.3

filters; the apparatus was initially developed by Zemel and Stoughton and has been described in earlier reports. The solutions were filtered at 250°C from the solid, and the various soluble components were determined by separation tracer and spectrographic techniques.

The variation in analytical data between the individual runs and between the tracer and spectrographic data is quite marked, and for this reason the individual values will not be reported until more consistent results are obtained. It does appear justifiable, however, to say that Ce, Zr, Ru, Ba, and Nb will be the first of the elements studied to precipitate. Interaction of these elements, or others, with the reactor surfaces was not considered.

FISSION-PRODUCT SOLUBILITIES IN URANYL SULFATE SOLUTIONS

E. V. Jones

Cesium Sulfate. The silica tube synthetic method has been applied in the study of the solubility of cesium sulfate in 0.126 and 1.26 *M* UO_2SO_4 as a function of temperature. A partial report on this work and on other solubility studies has appeared previously.[3]

The corrected data are given in Table 45 and are shown in Fig. 58 along with the data of Lietzke and Stoughton[4] for cesium sulfate solubility in water. The extremely low solubility for cesium sulfate in 1.26 *M* UO_2SO_4 has been noted and will be investigated further.

Cadmium Sulfate. The solubility of cadmium sulfate in 1.26 *M* UO_2SO_4 has been studied as a function of temperature using the synthetic method, and the data are given in Table 46 and shown in Fig. 59. For comparison purposes, the solubilities by Lietzke and Stoughton[4] and Benrath[5] in water and in 0.126 *M* UO_2SO_4 are included in Fig. 59.

[3] Marshall, Brown, Day, Gill, Jones, Warren, and Wright, *op. cit.*, ORNL-1221, p. 99.

[4] M. H. Lietzke and R. W. Stoughton, *The Measurement of the Solubility of Fission Product Sulfates at High Temperatures and Pressures*, ORNL-970, March 13, 1951.

[5] A. Benrath, F. Gjedebo, B. Schiffers, and H. Wunderlich, "Solubility of Salts and Salt Mixtures in Water at Temperatures Above 100°," *Z. anorg. allgem. u. Chem.* **231**, 285 (1937).

TABLE 45

Solubility of Cesium Sulfate in Uranyl Sulfate Solutions

SOLUBILITY IN 0.126 *M* UO_2SO_4		SOLUBILITY IN 1.26 *M* UO_2SO_4	
TEMPERATURE (°C)	Cs_2SO_4 (wt %)	TEMPERATURE (°C)	Cs_2SO_4 (wt %)
53.8	64.19	167.7	0.30
61.6	66.00	178.5	0.33
77.3	67.12	187.3	0.37
84.2	67.55	214.8	0.44
104.8	68.58	245.3	0.49
140.2	70.07	285.6	0.54
177.5	71.66	288.6	0.78*
228.6	73.48		

*Two liquid layers, much undissolved.

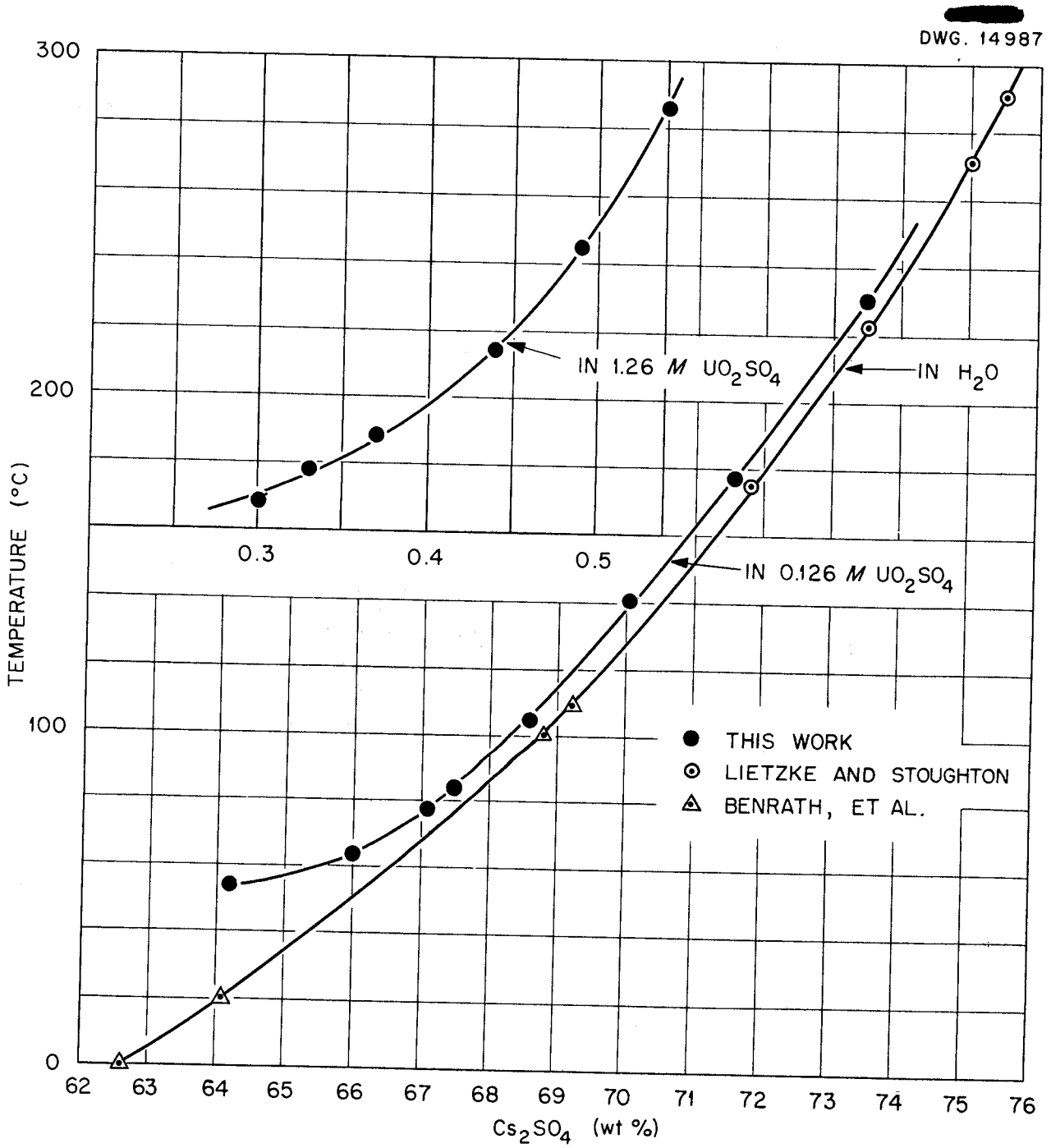

Fig. 58. Solubility of Cs_2SO_4 in UO_2SO_4 Solutions.

Cadmium sulfate shows a negative temperature coefficient of solubility and considerable supersaturation. The temperatures recorded are those at which the last crystals dissolved on very slow cooling.

Silver Sulfate. The solubility of silver sulfate is being studied in 0.126 and 1.26 *M* UO_2SO_4 by the synthetic method. Silver sulfate shows a positive temperature coefficient of solubility. In 0.126 *M* UO_2SO_4, a

[redacted]

DWG. 14988

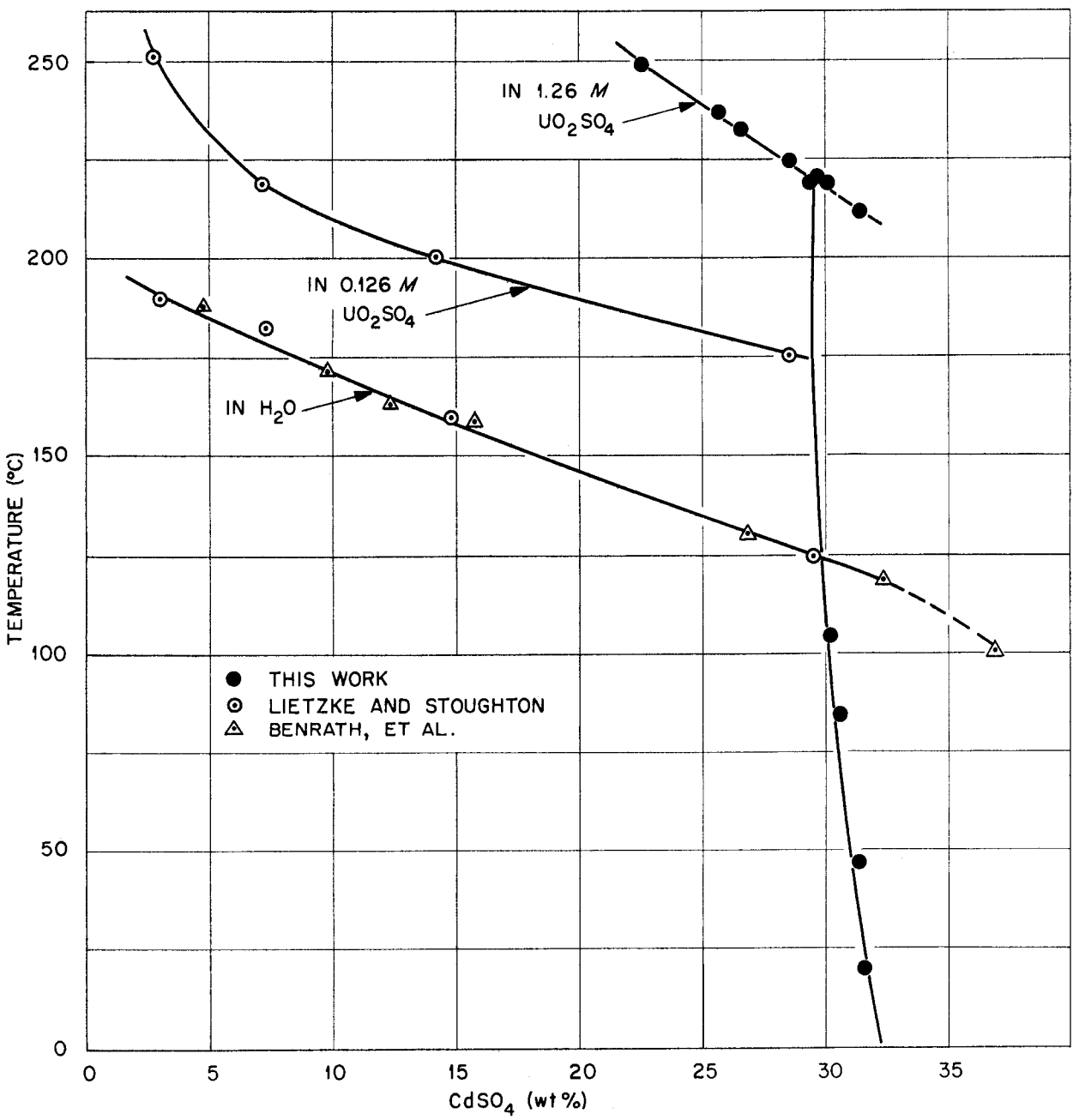

Fig. 59. Solubility of $CdSO_4$ in UO_2SO_4 Solutions.

reversible reaction occurs at about 150°C that yields a reddish precipitate, and plans are made to investigate the nature of this red product.

TABLE 46

Solubility of Cadmium Sulfate in 1.26 *M* Uranyl Sulfate

TEMPERATURE (°C)	$CdSO_4$ (wt %)
21	31.62
47.8 (209)*	31.33
84.2	30.50
102.9 (215.8)*	30.12
215.8	29.37
216.8	29.69
220.8	28.68
228.7	26.54
230.6	25.83
244.3	22.51

*Double solubility points.

At present there is some uncertainty in the data. For this reason, the completed work will not be reported until next quarter.

Interpretation of Data. Solubility data for $Y_2(SO_4)_3$, $La_2(SO_4)_3$, Cs_2SO_4, $CdSO_4$, Ag_2SO_4, and $Ce(SO_4)_2$ in water, and in 0.126 and 1.26 *M* UO_2SO_4 were studied. These data were obtained from the current investigation by Lietzke, Zemel, and Stoughton of ORNL and previously published data on studies in water. The data have been plotted using the van't Hoff isochore,

$$\frac{d \log N}{d\left(\frac{1}{T}\right)} = -\frac{\Delta H}{2.3R} .$$

In most cases the plots yielded straight-line relationships. Differential heats of solution obtained for the fission-product sulfates (in the saturated solution) are given in Table 47. Values of log ΔH for a given fission-product solubility were plotted against concentration. In all of these salt systems the slope was positive.

TABLE 47

Some Differential Heats of Solution of Fission-Product Sulfates in Water and Uranyl Sulfate Solution Above 100°C

SALT	ΔH_{soln} (kcal/mole)		
	IN H_2O	IN 0.126 *M* UO_2SO_4	IN 1.26 *M* UO_2SO_4
$Y_2(SO_4)_3$	-27	-16	-9
$La_2(SO_4)_3$	-23	-12	-8
$CdSO_4$	-17	-14	-5.4
$Ce(SO_4)_2$	-10	-6.9	
Ag_2SO_4	+1.1	+2.3	+3.7
Cs_2SO_4	+0.20	+0.20	+1.5

TWO-LIQUID-PHASE TRANSITION TEMPERATURES FOR THE DEUTERIUM OXIDE-URANYL SULFATE AND URANYL FLUORIDE SYSTEMS

E. V. Jones

Two-liquid-phase transition temperatures were determined for various concentrations of uranyl sulfate and uranyl fluoride in deuterium oxide. For purposes of comparison, similar measurements were made in normal water for both the sulfate and fluoride systems.

Experiments. Uranyl sulfate was prepared by Lietzke and Griess[6] at ORNL by adjusting a sulfuric acid–Mallinckrodt uranium trioxide solution

(6) M. H. Lietzke and J. C. Griess, "Preparation of Pure Uranyl Sulfate for Experimental Purposes," *Homogeneous Reactor Project Quarterly Progress Report for Period Ending August 15, 1951*, ORNL-1121, p. 124.

to the stoichiometric ratio. Approximately anhydrous uranyl sulfate was prepared by dehydrating the salt at 350°C with a dried air stream as prescribed by Mansfield of the Chemical Technology Division. Analysis for uranium indicated 97.6% anhydrous UO_2SO_4. This solid was dissolved in 99.8% D_2O to make the required UO_2SO_4-D_2O solutions. The UO_2SO_4-H_2O solutions were made using both dehydrated UO_2SO_4 and $UO_2SO_4 \cdot 3H_2O$ solid. No transition temperature difference was noted between samples.

Uranyl fluoride prepared at Y-12 was dried at 135°C to give 99.9% UO_2F_2. This solid was dissolved in 99.8% D_2O and also in H_2O to make the respective solutions.

Experimental runs were made in 4-mm-ID silica tubing in rocker apparatus similar to that used in previous solubility studies. The Brown temperature recorder and thermocouple was calibrated both by potentiometric methods and by melting points of naphthalene (79°C), tin (232°C), and bismuth (271°C).

Results. The data for uranyl sulfate are shown in Table 48 and Fig. 60. Two significant results were obtained: first, the two-liquid-phase appearance temperature was lowered about 10 deg in D_2O as compared with the water system, with the minimum critical solution temperature for the D_2O system being 275°C; second, the values obtained in water are about 10 deg below those previously reported for this system,[7] i.e., 285°C instead of 295°C for the minimum critical solution temperature.

One explanation that could be given for the differences between past and present results in water is that prior to July, 1951 all uranyl sulfate used in the work was prepared by the acetone

[7] C. H. Secoy, "The System of Uranyl Sulfate-Water. II. Temperature-Concentration Relationships Above 250°," *J. Am. Chem. Soc.* **72**, 3343-5 (1950).

[redacted]

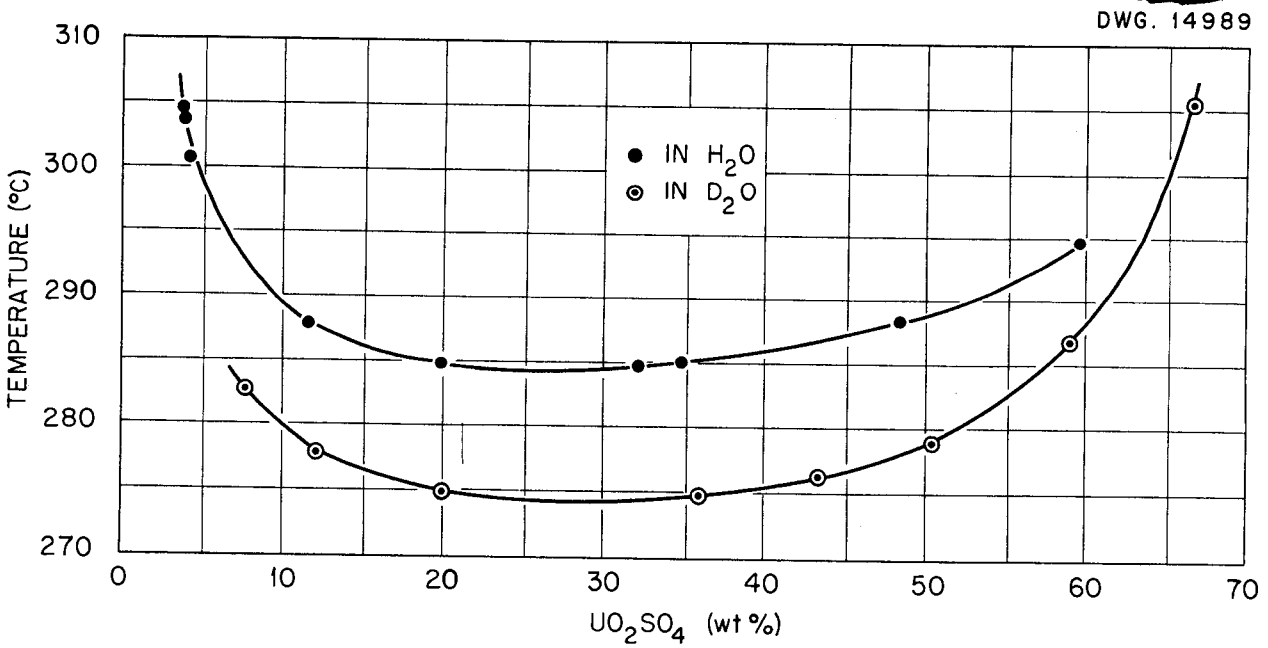

Fig. 60. Two-Liquid-Phase Region of UO_2SO_4 in H_2O and D_2O.

TABLE 48

Two-Liquid-Phase Appearance Temperatures for Uranyl Sulfate in Water and in Deuterium Oxide

IN H_2O		IN D_2O	
TEMPERATURE (°C)	UO_2SO_4 (wt %)	TEMPERATURE (°C)	UO_2SO_4 (wt %)
304.7	3.77	282.7	7.80
303.7	3.88	277.7	12.07
300.8	4.02	274.7	20.03
287.6	11.56	274.7	36.05
284.7	20.01	276.3	43.53
284.7	32.15	278.8	50.54
285.0	34.90	286.6	59.02
288.1	48.28	305.5	66.46
294.5	59.34		

precipitation process.[8] Several variables were introduced to test this explanation and the possibility of uranyl sulfate decomposition upon drying at 275°C. Two runs were made with uranyl sulfate solution prepared at Y-12, three runs were made with uranyl sulfate solution prepared by Lietzke and Griess, and two runs were made with acetone-precipitated uranyl sulfate. A final run was made after adding one drop of acetone to the Lietzke-Griess uranyl sulfate solution. The results are given in Fig. 61. No temperature effect is indicated from the use of other samples of uranyl sulfate prepared by stoichiometric combination of uranium trioxide and

[8] L. Helmholz and G. Friedlander, *Physical Properties of Uranyl Sulfate Solutions*, LAMS-30, Dec. 15, 1943.

[redacted]

DWG. 14990

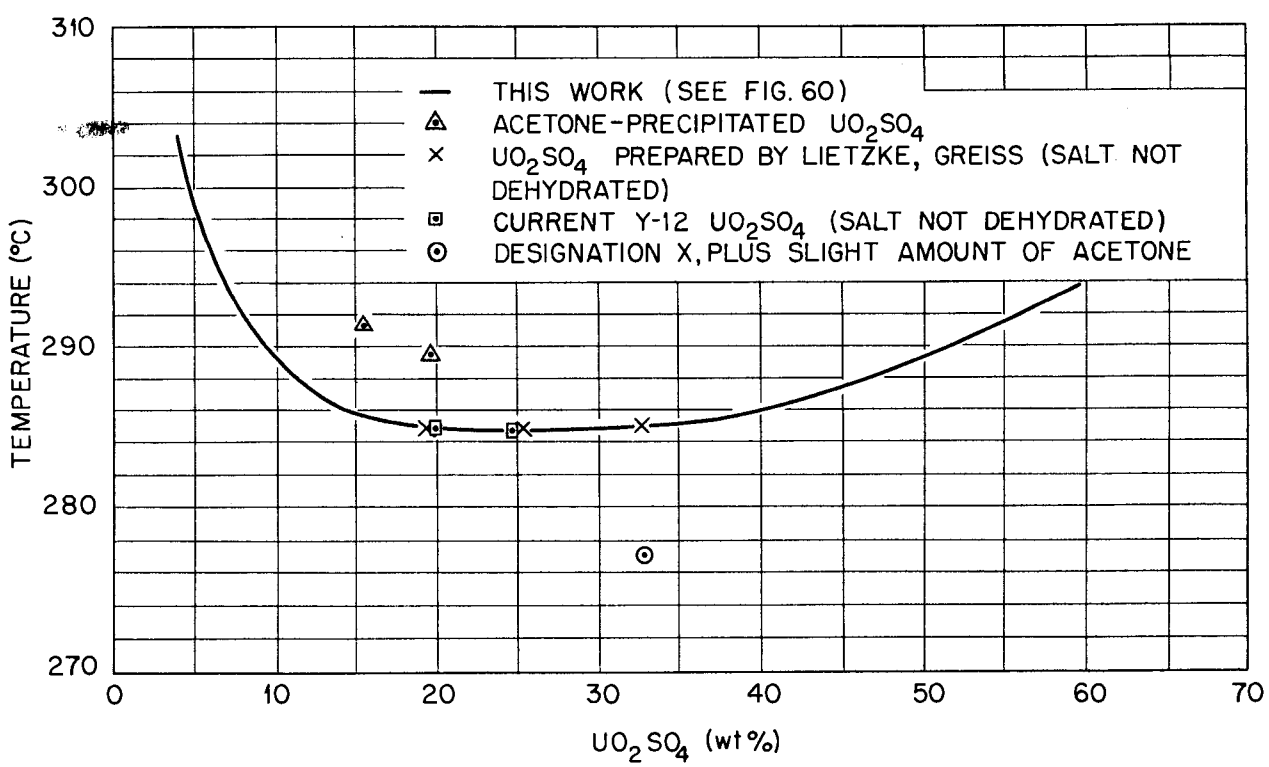

Fig. 61. Effects of Different UO_2SO_4 Solutions on the Two-Liquid-Phase Region of UO_2SO_4 in H_2O.

sulfuric acid; however, the acetone-precipitated material did give a 5-deg elevation in temperature. Free acetone added to the Lietzke-Griess solution lowered the two-liquid-phase temperature. Degassing some solutions (not one containing free acetone) appeared to have very little effect on the transition temperatures.

The data for uranyl fluoride are given in Table 49 and are shown in Fig. 62. There is the same significant 10-deg lowering of the liquid-phase transition temperature for the D_2O system as compared with water. Values for the UO_2F_2-H_2O system alone are about 2 deg higher than previously reported.[9] No satisfactory values for the fluoride system were obtained for concentrations below about 15 to 20% because of the previously observed reaction with the silica tube.[9]

Conclusions. The effect of impurities is apparently great for these two-liquid-phase transition temperatures. This conclusion is based upon consideration of the 10-deg lowering effect of 95 to 100% D_2O, the large difference in two-liquid-phase appearance temperature between the currently prepared uranyl sulfate and previously prepared acetone precipitated uranyl sulfate, the effect of excess acid, and fission-product effects (see previous reports in this series).

[9] W. L. Marshall, J. S. Gill, and C. H. Secoy, "The Uranyl Fluoride-Water System," *Chemistry Division Quarterly Progress Report for Period Ending June 30, 1950*, ORNL-795, p. 22.

CONDUCTIVITY OF URANYL SULFATE AND URANYL FLUORIDE SOLUTIONS

R. D. Brown

A description of the apparatus and experimental procedure used in the

TABLE 49

Two-Liquid-Phase Appearance Temperatures for Uranyl Fluoride in Water and in Deuterium Oxide

IN H_2O		IN D_2O	
TEMPERATURE (°C)	UO_2F_2 (wt %)	TEMPERATURE (°C)	UO_2F_2 (wt %)
None to 350	4.42	Crystals at 328	
326.2	14.73	No transition up to 340	5.24
315.8	24.77	Crystals at 309	
315.8	36.99	No transition up to 340	16.12
315.3	51.90	308.4	18.67
322.2	65.15	310.4	20.85
		307.4	26.01
		307.4	36.25
		308.7	52.43
		312.6	59.86
		313.1	62.80

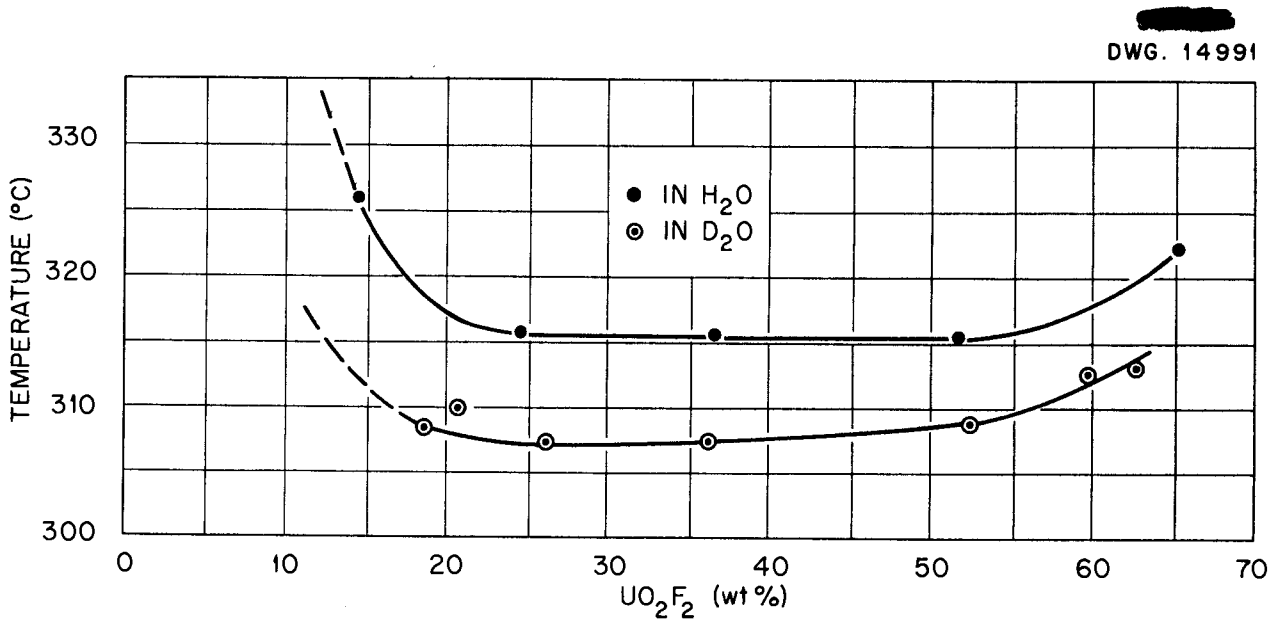

Fig. 62. Two-Liquid-Phase Region of UO_2F_2 in H_2O and D_2O.

study of the conductivity of uranyl sulfate was given in the last Homogeneous Reactor Project quarterly progress report. The data obtained included the equivalent conductivity of uranyl sulfate at 0 and 25°C in concentrations varying from 0.005 to 2.5 *N*. This work has been extended to measurements in concentrations from 0.0001 *N* to concentrations approaching saturation at room temperature and at 50 and 90°C.

In addition, the conductivity of uranyl fluoride has been measured in concentrations varying from 0.0001 to 6.0 *N* at 0, 25, 50, and 90°C. The data are summarized in Tables 50 and 51 and are shown in Figs. 63 and 64.

As pointed out in the last quarterly report, uranyl sulfate behaves as a weak electrolyte at ordinary temperatures, i.e., 0 and 25°C. The additional data obtained at 50 and 90°C show no change in the conductance characteristics of the solution except a normal increase in equivalent conductance over that at lower temperatures. A sharp increase in equivalent conductance usually occurs with weak electrolytes over some narrow concentration range. With uranyl sulfate this sharp increase is noted between 0.1 and 0.01 *N*.

Uranyl fluoride shows conductance characteristics similar to those of uranyl sulfate, but its equivalent conductance at a given temperature is considerably less than that of uranyl sulfate; at 90°C it is about equal to that of uranyl sulfate at 0°C. No explanation for this has been advanced except to assume that the degree of dissociation of uranyl fluoride is less than that of uranyl sulfate. A sharp increase in equivalent conductance occurs between concentrations of 0.05 and 0.005 *N* UO_2F_2.

A comparison of the conductance of the two electrolytes can be obtained from Figs. 63 and 64.

TABLE 50

Conductivity of Uranyl Sulfate

CONCENTRATION AT 25°C (equivalents/liter)	EQUIVALENT CONDUCTANCE ($ohms^{-1}$)			
	AT 0°C	AT 25°C	AT 50°C	AT 90°C
0.0001		175.65	288.0	505
0.0005	66.28	127.40	197.0	280
0.001	57.86	106.70	157.9	220.0
0.005	40.04	63.30	85.20	104.0
0.01	29.54	49.31	64.74	77.0
0.025	22.26	44.18		
0.05	17.71	27.70	35.66	43.80
0.1	14.24	22.22	29.01	37.30
0.5		14.45	20.34	28.64
1	9.37 (0.4 *N*)	11.61	16.88	24.43
2.52	2.51 (3 *N*)	6.16	9.59	14.49
4.66	0.465 (6 *N*)	2.78	4.69	7.77
7.28			1.02	

TABLE 51

Conductivity of Uranyl Fluoride

CONCENTRATION AT 25°C (equivalents/liter)	EQUIVALENT CONDUCTANCE ($ohms^{-1}$)			
	AT 0°C	AT 25°C	AT 50°C	AT 90°C
0.0001	34.45	73.45		
0.0005	18.39	35.70	62.48	104.2
0.001	12.47	26.10	44.22	71.30
0.005	6.16	12.31	19.51	30.40
0.01	4.62	9.17	14.41	22.70
0.05	2.73	5.43	8.60	13.52
0.1	2.37	4.74	7.50	11.88
0.5	1.87	3.75 (3.80)*	5.96	9.50
1.0	1.61	3.22 (3.22)*	5.10	8.15
3.0			3.12	4.91
6.0			1.40	2.27

*G. R. Dean, *Properties of Uranyl Fluoride*, Metallurgy Project Report CC-2092-G (Sept. 11, 1944).

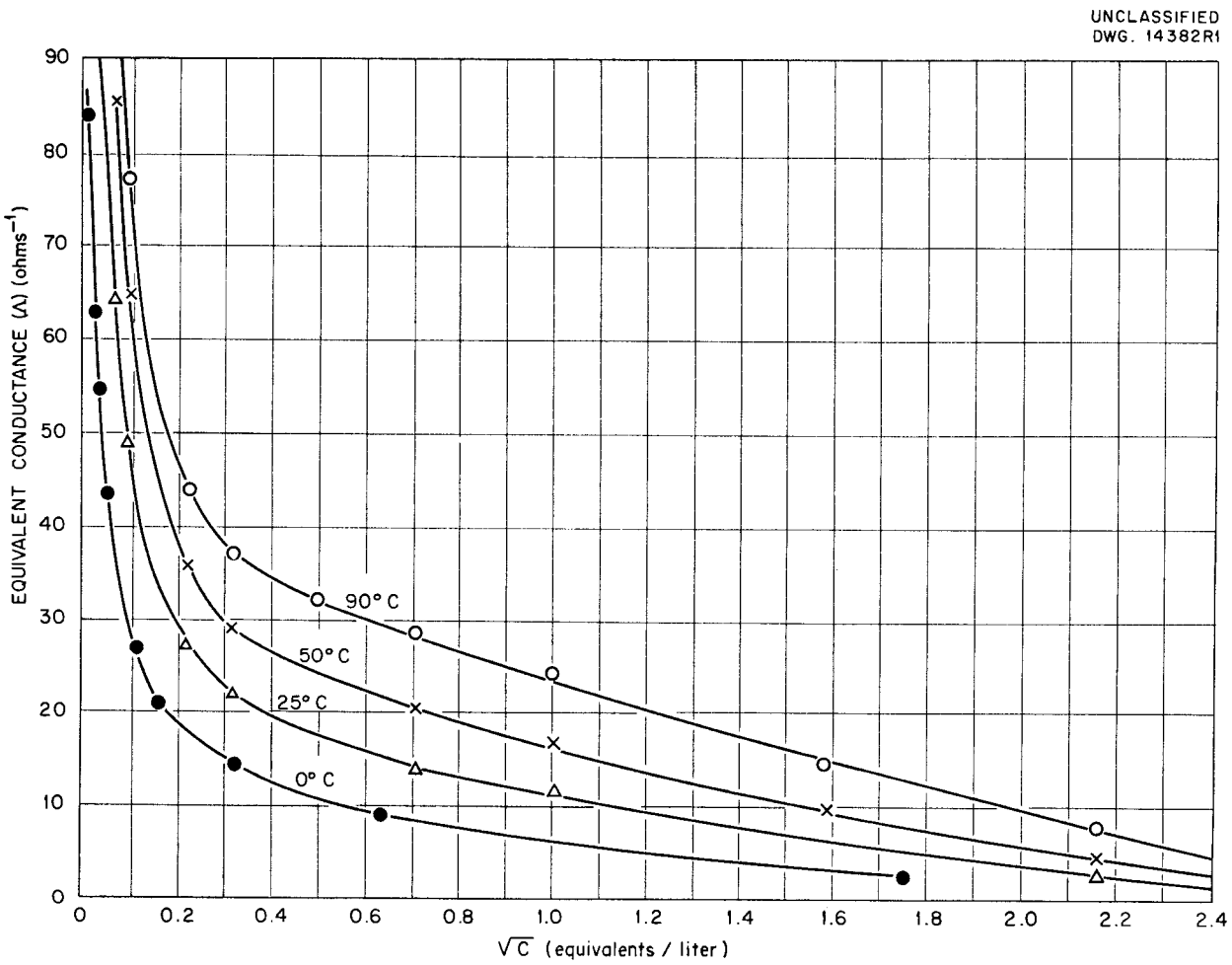

Fig. 63. Conductivity of Uranyl Sulfate.

VAPOR PRESSURES OF AQUEOUS URANYL SULFATE SOLUTIONS

H. O. Day

In the previous Homogeneous Reactor Project quarterly progress report[10] vapor pressure data of various uranyl salt solutions were given. The solutions contained dissolved air, and there was free air space above the solution in the bombs. Calculations were made to estimate the effect of the air on the pressure measurements. Since the volume of solution was known, as well as the geometry of the bomb, the original quantity of air present could be estimated. Experimental data were lacking, so assumptions were made as to the values of the densities of the uranyl sulfate solutions at the elevated temperatures and of the solubility of air in the solutions at these temperatures.

It was assumed that the density of a solution of particular concentration at some elevated temperature would be as much greater than that of pure water at this same temperature as the density of uranyl sulfate solution of the same concentration at 25°C is larger than that of pure water at 25°C.

[10] Marshall, Brown, Day, Gill, Jones, Warren, and Wright, *op. cit.*, ORNL-1221, p. 105.

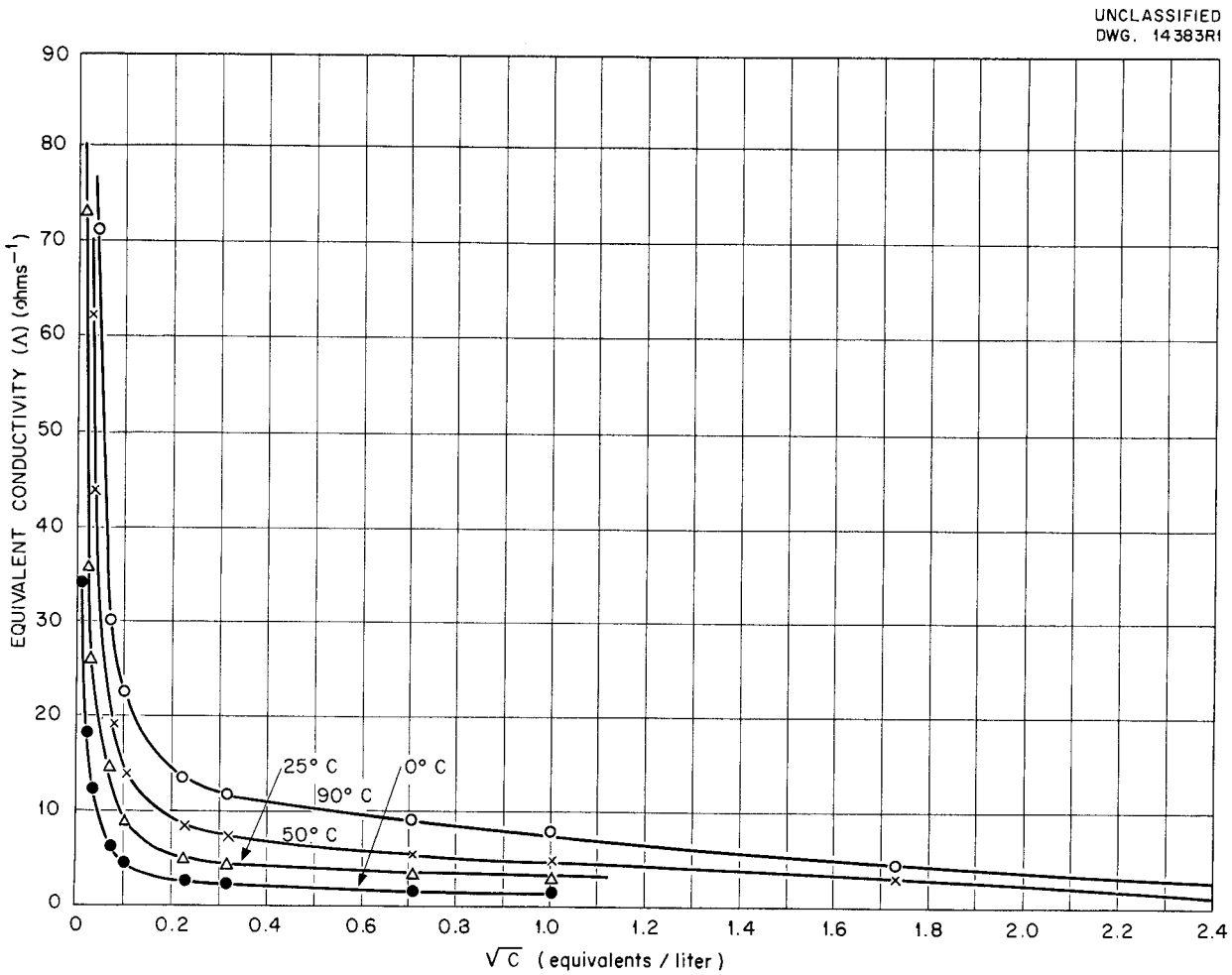

Fig. 64. Conductivity of Uranyl Fluoride.

The solubilities of O_2 and N_2 in pure water at elevated temperatures have been measured at Batelle Memorial Institute.[11] The literature gives the solubilities of these gases in potassium sulfate and sulfuric acid solutions of varying concentrations at room temperature. It was assumed that the fractional lowering of solubility of O_2 and N_2 by these solutions was the same at all higher temperatures, up to 350°C. It was next assumed that the solubility of O_2 and N_2 in UO_2SO_4 solutions of any particular concentration, thermodynamic activity, and temperature would be equal to the average of the solubilities in potassium sulfate and sulfuric acid solutions of equal activity and temperature. Activity data for uranyl sulfate solution at 0 and 25°C have been given by Secoy.[12] It is tacitly assumed that the activity coefficients of the uranyl sulfate, potassium sulfate, and sulfuric acid solutions are constant over the entire range of temperatures. This is undoubtedly in error, but the activity coefficient ratios of the solutions would probably be about constant, and

[11] H. A. Pray, C. E. Schweickert, and B. H. Minnich, *The Solubility of Hydrogen, Oxygen, Nitrogen, and Helium in Water at Elevated Temperatures*, BMI-T-25, May 15, 1950.

[12] C. H. Secoy, "The System UO_2SO_4 – H_2O," *Report of the Chemistry Division for the Months December, 1947, January and February, 1948*, CNL-37, p. 33.

since the basic assumption of a constant fractional solubility lowering is the most important factor, the error introduced would probably not be too great.

With the data obtained, the partial pressures of O_2 and N_2 were calculated and subtracted from the experimental pressures. The corrected values are given in Table 52.

As preliminary measurements prior to making very accurate vapor-pressure measurements on uranyl salt solutions from 50 to 150°C, the vapor pressures of pure water were checked. The water used was degassed by freezing and melting several times under vacuum and subliming the ice from one container to another a number of times. The pressure at the triple point was measured and checked with high accuracy (within 0.02 mm). Unfortunately, the vapor pressures at 100 and 110°C were lower than that of pure water by an amount larger than the experimental accuracy that the apparatus is capable of attaining (±0.05 to 0.10 mm). This error may have occurred because the pressure vessel was cleaned with a solution of sodium dichromate and sulfuric acid. There is a good possibility that the glass walls adsorbed enough impurities to cause error in the vapor-pressure measurements.

During these preliminary runs two pressure vessels were cracked owing to errors in technique of loading with water. Better stirring is assured with the new vessels.

Measurements have been started with saturated solutions of uranyl sulfate, but difficulty has been encountered in the attainment of true saturation. Work on these solutions and on dilute solutions is being continued.

DENSITY-WEIGHT PER CENT-MOLARITY CONVERSION EQUATIONS FOR URANYL SULFATE-WATER SOLUTIONS AT 25.0°C AND BETWEEN 100 AND 300°C

W. L. Marshall

Equations Applicable at 25°C. The equations given were evaluated from density-molarity data for uranyl sulfate-water solutions at 25.0 ± 0.2°C as determined by Lietzke, Wright, and

TABLE 52

Vapor Pressures of Uranyl Sulfate Solutions

TEMPERATURE (°C)	VAPOR PRESSURES (psia)		
	LITERATURE VALUES FOR WATER	6.84 wt % UO_2SO_4	32.82 wt % UO_2SO_4
200	225.54	$223._3$	$216._2$
225	369.90	$366._2$	$361._6$
250	576.91	$576._4$	$559._7$
275	862.80	$860._3$	$850._1$
300	1246.12	$1243._1$	$1234._2$
325	1748.39	$1742._9$	$1698._2$
350	2398.39	$2388._2$	

Marshall.[13] The initial equation was derived from the linear relationship of density to molarity. The experimental average deviation of the slope constant is 0.57%, and the probable error of ± 0.45% for this constant is used to determine the accuracy of the specific equations for the dependent variable if the independent variable is not in error.

Density-Volume Concentrations.

$$d = 0.9970 + 0.316_5 M \quad (1)$$

$$d = 0.9970 + 0.001329 g_u \quad (2)$$

$$d = 0.9970 + 0.000864_5 g_s \quad (3)$$

where

d = density (g/cm^3)

M = molarity of UO_2SO_4

g_u = grams of uranium per liter

g_s = grams of UO_2SO_4 per liter

Accuracy: d to ± 0.45(1 - 1/d)%
M, g_u, g_s to ± 0.45%

Density-Weight Concentrations.

$$d = \frac{0.9970}{1 - 0.01329U} \quad (4)$$

$$d = \frac{0.9970}{1 - 0.00864_5 S} \quad (5)$$

$$U = 75.2_2 - \frac{75.0_0}{d} \quad (6)$$

$$S = 115.7 - \frac{115.3}{d} \quad (7)$$

where

U = weight per cent of uranium

S = weight per cent of UO_2SO_4

Accuracy: d to ± 0.45(d - 1)%
U, S to ± 0.45%

Molarity-Weight Concentrations.

$$\frac{1}{M} = \frac{23.88}{U} - 0.317_4 \quad (8)$$

$$\frac{1}{M} = \frac{36.7_2}{S} - 0.317_4 \quad (9)$$

$$\frac{1}{U} = \frac{0.0418_8}{M} + 0.01329 \quad (10)$$

$$\frac{1}{S} = \frac{0.02723}{M} + 0.00864_5 \quad (11)$$

Accuracy: M to $\pm\ 0.45\left(\frac{24M}{U} - 1\right)\%$
or to $\pm\ 0.45\left(\frac{37M}{S} - 1\right)\%$
U to $\pm\ 0.45\left(\frac{U}{24M} - 1\right)\%$
S to $\pm\ 0.45\left(\frac{S}{37M} - 1\right)\%$

Equations Applicable Between 100 and 300°C. Sources of data from which the final equations were derived are given in the following, together with some of the density values and brief explanations where necessary.

1. Density data at 25.0 ± 0.2°C were determined by Lietzke, Wright, and Stoughton.[13]

2. Density data from 30 to 100°C were obtained from work of I. Helmholz and G. Friedlander, *Physical Properties of Uranyl Sulfate Solutions*, LAMS-30 (Dec. 15, 1943).

(13) M. H. Lietzke, H. W. Wright, and W. L. Marshall, "Uranyl Sulfate Production - Acidities, Refractive Indices, and Densities of Uranyl Sulfate Solutions," *op. cit.*, ORNL-1121, p. 124.

3. The density data given in Table 53 were obtained from the work of W. H. Davenport and R. H. Powell (private communication). They used the method described by Lietzke, Wright, and Stoughton.[13]

TABLE 53

Density Data

TEMPERATURE (°C)	MOLARITY OF UO_2SO_4 AT 25°C	DENSITY AT TEMPERATURE INDICATED (g/cm³)
50	0.08732	1.0159
50	0.125	1.0278
50	0.1622	1.0397
184	0.1299	0.9248 ± 0.0005
203	0.1299	0.9015 ± 0.0005
232	0.1299	0.8630 ± 0.0005

4. The density data for an initial 34.9% uranyl sulfate solution obtained from the work of Secoy (C. H. Secoy, "The System Uranyl Sulfate – Water," *Chemistry Division Quarterly Report for the Months December, 1948, January, February, 1949*, ORNL-336, p. 24) were corrected for loss of water to the vapor phase by using the densities of saturated water vapor (see paragraph 6). The vapor pressures of this system are not more than 4% different from that of pure water, at least up to about 350°C (experimental data of H. O. Day of ORNL). Concentration changes were corrected to the original value, 34.9%, by subtracting the equivalent number of density units that would be required for correction at 25°C. Corrections were not necessary on densities or concentrations below 108.8°C. Density values above 274°C represent the average density of the associated two-liquid phases. The corrected values for Secoy's data are given in Table 54.

5. Density data between 25 and 100°C were obtained from the work of J. D. Roarty, ORNL (private communication).

TABLE 54

Density Data

TEMPERATURE (°C)	DENSITY
22.3	1.432*
48.8	1.410*
70.0	1.393*
88.0	1.380*
108.8	1.360
129.2	1.340
152.6	1.317
175.7	1.294
187.0	1.282
231.7	1.227
249.4	1.199
274.0	1.153
303.8	1.081
325.8	1.004
345.8	0.911
356.3	0.861
366.5	0.787
371.5	0.753

*No correction necessary.

6. Density data for water at saturated vapor pressures were obtained from the work of N. E. Dorsey, *Properties of Ordinary Water Substances in All Its Phases*, p. 577, Reinhold, New York, 1940.

Evaluation of Data. At the suggestion of Compere (ORNL), a linear density scale was placed on the ordinate of a graph, a straight line of appropirate slope was drawn, and densities of water (at saturated vapor pressure) at different temperatures were plotted on the line; the individual temperatures were marked at the parallel positions on the abscissa to produce an empirical temperature scale. All solution densities were

plotted using this scale. The density lines were found to be parallel to the water curve between 120 and 280°C for the 34.9% uranyl sulfate solution and from 25 to at least 232°C for the 4.58% solution. Below 120°C there was a definite upswing of the density lines that appeared proportional to the molarity. From these data and the density equations at 25°C, the following equations were derived to express the solution density of water-uranyl sulfate solutions between 120 and 280°C for concentrations up to 51% salt:

$$d^t_{soln} = \frac{1}{\frac{78.65}{S} - 1.046} + d^t_{H_2O} , \quad (12)$$

$$d^t_{soln} = \frac{1}{\frac{120.9}{S} - 1.046} + d^t_{H_2O} , \quad (13)$$

where

$d^t_{H_2O}$ = density of water at t(°C) (at saturated vapor pressure),

U = weight per cent of uranium,

S = weight per cent of UO_2SO_4.

These equations are believed to be accurate to ± 0.5% from 25 to approximately 300°C for uranyl sulfate solutions of not over about 10 wt %. For higher concentrations they appear accurate to better than ± 1.0% between 120 and 250°C, the limitation at the lower and higher temperatures being the result of deviations in the linearity relationships from which the empirical equations were derived. Therefore the equations are accurate only to ± 2% in the temperature ranges 25 to 120 and 250 to 280°C for concentrations above approximately 10 wt %.

These empirical equations for upper temperatures were derived and checked with the experimental data. Van Winkle (ORNL) has accomplished the same purpose with an equation, derived purely on a theoretical basis,[14] that is not quite so accurate as the above expressions.

Substitution of Deuterium Oxide for Water. The following equations for D_2O-UO_2SO_4 solutions were derived by substitution of D_2O density for H_2O density in the previous relationships. There are no experimental data available to justify the correctness of these equations.

1. At 25.0 ± 0.2°C

$$d_{soln} = 1.1044 + 0.316_5 M$$

$$d_{soln} = \frac{1.1044}{1 - 0.01329U}$$

$$\frac{1}{M} = \frac{21.55}{U} - 0.286_6$$

2. Between 120 and 280°C

$$d^t_{soln} = \frac{1}{\frac{71.0_0}{U} - 0.943_9} + d^t_{D_2O}$$

where

d = density of D_2O-UO_2SO_4 solution

U = weight per cent of uranium

M = molarity of UO_2SO_4

$d^t_{D_2O}$ = density of D_2O at t(°C).

---

(14) R. Van Winkle, *Some Physical Properties of UO_2SO_4-D_2O Solutions*, ORNL CF-52-1-124, Jan. 18, 1952.

The equations derived before final substitutions for densities are:

$$d^{25^\circ}_{soln} = d^{25^\circ}_{H_2O} + 0.31651M$$

$$d^{25^\circ}_{soln} = \frac{d^{25^\circ}_{H_2O}}{1 - 0.013295U}$$

$$\frac{1}{M^{25^\circ}} = \frac{23.806}{d^{25^\circ}_{H_2O}U} - \frac{0.31651}{d^{25^\circ}_{H_2O}}$$

$$d^{t}_{soln} = \frac{1}{\dfrac{78.410}{d^{25^\circ}_{H_2O}U} - \dfrac{1.0425}{d^{25^\circ}_{H_2O}}} + d^{t}_{H_2O}$$

where

$$d^{25^\circ}_{H_2O} = 0.99704$$

or

$$d^{25^\circ}_{D_2O} = 1.1044 .$$

STATIC CORROSION TESTS OF ALTERNATE SYSTEMS

E. G. Bohlmann, Section Chief
J. L. English S. H. Wheeler

CORROSION STUDIES WITH CONCENTRATED URANYL SULFATE

The search for corrosion-resistant materials that can be used successfully in uranyl sulfate solutions of high concentration was continued during the past quarter. The list of possible choices narrows rapidly; titanium and a 5% tin-zirconium alloy offer the most promise from purely a corrosion-resistance standpoint. The static corrosion testing of these two materials is being enlarged gradually. Exploratory results obtained thus far continue to support the excellent corrosion behavior reported previously.

Corrosion of Titanium. The titanium metal used for the tests was obtained from the Titanium Metals Corporation in the form of 1.375-in.-OD. hot-rolled bar and was designated as Type TI-100A, an oxygen-nitrogen alloy. The physical properties of the metal in an annealed condition, as listed in the fourth edition of *Handbook on Titanium Metal* issued by Titanium Metals Corporation, were:

Tensile strength (psi)	100,000
Yield strength (psi)	75,000
Elongation (%)	20 to 25
Area reduction (%)	45

The measured hardness on the as-received bar was 96 to 97 R_B. Disk-shaped specimens were machined from the bar and degreased just prior to testing.

The tests were run in type-347 stainless steel autoclaves containing 150 ml of uranyl sulfate solution, which was changed weekly. In order to avoid galvanic-couple effects, the titanium specimens were electrically insulated from the autoclave mass by means of quartz hangers.

Effect of Oxygen Content on Corrosion of Titanium in Uranyl Sulfate Containing 40 g of Uranium per Liter at 250°C. Three tests were operated with partial pressures of oxygen of 100, 350, and 650 psia. These values correspond approximately to concentrations of 575, 2075, and 3710 ppm, respectively, of soluble oxygen in water at 250°C. The tests were operated for a total of 2016 hr (12 weeks). All test solutions were analyzed for total uranium; no reduction of uranium in solution was found in any of the corrosion test solutions. The corrosion data appear in Table 55.

As shown by the data in Table 55, the specimen tested with 100 psia of oxygen exhibited steady gains in weight as a result of the formation of a semidull, brown, noncontinuous film on the surfaces. Breaks in the film disclosed the titanium surfaces to be lustrous and golden-yellow. It was suspected that the heavy film was caused by the migration and deposition of corrosion products from the stainless steel autoclave. The specimen has been submitted for optical examination and determination of the film constituents.

The corrosion behavior of the specimens tested with 350 and 650 psia of oxygen was nearly identical, except that the lower oxygen-pressure test coupon showed a slightly higher initial corrosion rate of 0.44 mpy, compared with 0.29 mpy for the 650-psia test specimen. The final overall rate for both specimens was 0.05 mpy after 2016 hours. With increased

TABLE 55

Effect of Oxygen on Corrosion of Hot-Rolled Titanium Uranyl Sulfate Containing 40 g of Uranium per Liter at 250°C

CUMULATIVE TIME OF TEST (hr)	CUMULATIVE WEIGHT CHANGE				
	100 psia OF O_2	350 psia OF O_2		650 psia OF O_2	
	mg/cm^2	mg/cm^2	mpy	mg/cm^2	mpy
168	+0.18	-0.10	0.44	-0.06	0.29
336	+0.33	-0.07	0.16	-0.07	0.15
504	+0.36	-0.12	0.18	-0.07	0.11
672	+0.39	-0.10	0.12	-0.07	0.08
840	+0.44	-0.12	0.11	-0.07	0.07
1008	+0.41	-0.13	0.12	-0.11	0.08
1176	+0.46	-0.13	0.10	-0.10	0.07
1344	+0.48	-0.12	0.08	-0.10	0.05
1512	+0.46	-0.12	0.07	-0.12	0.07
1680	+0.48	-0.12	0.05	-0.11	0.05
1848	+0.49	-0.11	0.05	-0.13	0.05
2016	+0.46	-0.13	0.05	-0.14	0.05

exposure time, the physical appearance of the samples changed from extremely lustrous, straw-colored surfaces to vivid blue, lustrous surfaces. The surface films appeared to be very thin and completely continuous when viewed at 200X. Signs of corrosion damage were essentially negligible.

Effect of Uranium Content at Constant Oxygen Partial Pressure on Corrosion of Titanium at 250°C. Three tests were run in which the uranyl sulfate contained 100, 200, and 300 g of uranium per liter. The oxygen partial pressure was made 350 psia in all tests by the use of concentrated hydrogen peroxide. The tests were operated in newly machined type-347 stainless steel autoclaves with a solution capacity of 150 milliliters. Uranium determinations were run on all solutions, and the analytical results showed no reduction of the uranyl ion in any of the test solutions, which were replaced weekly. The cumulative weight losses and corrosion rates are shown in Table 56.

Very little difference in the corrosion behavior of the titanium specimens was observed as the uranium concentration increased. Corrosion attack was very slight in all cases. The physical appearance of the specimens followed a trend generally characteristic of titanium in uranyl sulfate solutions. During the first two to three weeks of exposure, lustrous, straw-colored, thin films formed on the surfaces. With increased time, the color turned purple and finally developed very lustrous blue tints. The films were thin, tenacious, and continuous on the three test specimens.

In conclusion, increasing the uranium content from 100 to 300 g per liter of solution had little or no effect on the corrosion of titanium in uranyl sulfate solutions pressurized with 350 psia of oxygen at 250°C. Further studies will be made under similar conditions.

Corrosion of Zirconium. Results from a single static corrosion test

TABLE 56

Effect of Uranium Concentration on Corrosion of Hot-Rolled Titanium in Uranyl Sulfate Solution Pressurized with 350 psia of Oxygen at 250°C

CUMULATIVE TIME OF TEST (hr)	CUMULATIVE WEIGHT CHANGE					
	100 g OF U/l		200 g OF U/l		300 g OF U/l	
	mg/cm^2	mpy	mg/cm^2	mpy	mg/cm^2	mpy
168	-0.01	0.06	-0.01	0.06	-0.01	0.06
336	-0.04	0.09	0	0	-0.04	0.09
504	-0.06	0.09	-0.05	0.07	-0.04	0.06
672	-0.04	0.05	-0.06	0.07	-0.04	0.05
840	-0.04	0.04	-0.06	0.06	-0.03	0.03
1008	-0.07	0.05	+0.03		-0.02	0.01
1176	-0.06	0.04	-0.03	0.02	-0.06	0.04
1344	-0.06	0.04	-0.01	<0.01	-0.03	0.02
1512	-0.04	0.02	-0.09	0.04	-0.04	0.02
1680	-0.05	0.02	-0.01	<0.01	-0.04	0.02
1848	-0.05	0.02	-0.04	0.02	-0.04	0.02
2016	-0.06	0.02	-0.06	0.02	-0.07	0.03

with Bureau of Mines zirconium containing 5.37% tin have indicated very favorable corrosion behavior. The test specimen was exposed to uranyl sulfate solutions containing 530 to 540 g of uranium per liter at 250°C. A titanium autoclave with a solution capacity of 15 ml was used to contain the test specimen.

The zirconium-tin alloy, which was procured from the Bureau of Mines at Albany, Oregon, was induction melted, cast in a graphite mold, sheathed, hot-form forged, hot swaged to 1 1/2 in. in dia, unsheathed, and finally swaged semihot to a diameter of 1 inch. Chemical analysis of the alloy was:

Tin	5.37%
Nitrogen	0.011%
Copper	0.001%
Silicon	0.008%
Iron	1.10%
Aluminum	0.005%
Lead	0.005%
Titanium	<0.005%

No attempt was made to ensure the presence of an excess of oxygen in the system during operation of the test. The available oxygen was confined to the amount initially present in the 15-ml solution volume plus that in the 15-ml vapor space of the autoclave. The test solution was replaced at the end of each run.

After 1344 hr the condition of the zirconium specimen was excellent. The surfaces were highly lustrous, metallic gray in color, and free of visible, bulky, oxide films. Weight changes of the sample were extremely light at the end of the first 168 hr; a weight loss of 0.4 mg was the highest value measured during the six runs made thus far. This loss corresponded to a corrosion rate of 0.2 mpy in 168 hours. After 1344 hr the corrosion rate was 0.006 mpy, based on as-removed cumulative weight losses. This test is continuing.

A test program was started to determine the effects of oxygen and

uranium contents on the corrosion behavior of zirconium-tin alloys at 250°C. The uranyl sulfate solutions to be used will contain 40, 100, 200, 300, and 500 g of uranium per liter; the oxygen partial pressures to be investigated are 25, 75, 150, and 500 psia. Results of this series will be included in the next progress report.

CORROSION STUDIES WITH URANYL FLUORIDE

Work has continued on a study of the corrosive properties of aqueous uranyl fluoride solutions at 250°C. These studies are being conducted under static test conditions similar to those described previously for uranyl sulfate corrosion tests.

Effect of Oxygen and Uranium Content on Corrosion of Type-347 Stainless Steel at 250°C. A test series, analogous to one in progress with uranyl sulfate solutions, was started with uranyl fluoride solutions containing 100 and 300 g of uranium per liter. Thus far, the tests have operated four weeks at 250°C. Oxygen partial pressures included in the study were 25, 75, 150, and 500 psia obtained by the hydrogen peroxide addition technique. The tests are being run in duplicate, using the original test solutions. Although corrosion data are not complete, initial indications are that the uranyl fluoride system is more corrosive to type-347 stainless steel than the uranyl sulfate medium.

Corrosion of Tantalum in Uranyl Fluoride Containing 40 and 300 g of Uranium per Liter at 250°C. The corrosion behavior of rolled tantalum sheet was investigated in uranyl fluoride containing 40 and 300 g of uranium per liter at 250°C; an oxygen partial pressure of approximately 150 psia was used in both tests. The tests have run 5 weeks; corrosion data appear in Table 57.

The specimens tested in uranyl fluoride containing 40 g of uranium per liter showed interference patterns when removed from the solutions. Corrosion attack appeared slight,

TABLE 57

Corrosion of Tantalum in Uranyl Fluoride Solutions Pressurized with 150 psia of Oxygen at 250°C

CUMULATIVE TIME OF TEST (hr)	U CONTENT (g/l)	WEIGHT CHANGES* (mg/cm^2)	CORROSION RATE (mpy)
162	40	+0.24	
325	40	+0.09	
488	40	+0.09	
650	40	-0.16	0.05
813	40	-0.21	0.07
162	300	-1.19	1.53
325	300	-2.51	1.61
488	300	-3.70	1.57
650	300	-4.33	1.39
813	300	-5.68	1.45

*Weight changes measured on specimens as removed from solution.

although the sample started to show actual and increasing weight losses after the third week of exposure. There were no indications of localized corrosion attack.

After one week of exposure, the specimen tested in uranyl fluoride containing 300 g of uranium per liter was coated with a discontinuous, brown-colored film. Many small spots and one large area near the hanger hole were devoid of film. After two weeks of exposure, the film-free small areas had turned yellow; the large area near the hanger hole was coated with the brown film. With increased exposure time, the bulk of the surface area turned a golden color, except for the large area near the hanger support hole that remained black. The increase in corrosion with solutions containing 300 g of uranium per liter is quite evident from a comparison with the corrosion rates on tantalum in Table 57.

Corrosion Tests at 100°C in Uranyl Fluoride Solutions. A program was started to determine the corrosion resistance of various materials in uranyl fluoride solutions boiling around 100°C+. The tests have been in operation for 5 weeks. Aerated tests are planned for the future to study the effect of oxygen at 100°C. Materials for use in the construction of pump loops are now being investigated.

Tantalum, type-347 stainless steel (wrought and cast), Graphitar, and type-322W stainless steel have exhibited satisfactory corrosion resistance thus far in uranyl fluoride solutions containing 40 g of uranium per liter. Stellite 98M2, a bearing material, does not appear so good as the aforementioned materials, however. Complete corrosion data will be included in the next quarterly progress report.

Data on similar materials were obtained in solutions containing 300 g of uranium per liter at 100°C. Test results for 440 hr of exposure are included in Table 58. The weight losses are the as-removed-and-scrubbed losses measured on duplicate specimens. Of the four materials tested, tantalum appeared to be the only one not subject to marked corrosion attack by the concentrated uranyl fluoride solution.

During the first 24 hr of the tests all samples were characterized by the growth of silvery metallic crystals on the surfaces. A portion of the crystals was carefully removed for

TABLE 58

Corrosion of Various Materials in Uranyl Fluoride Containing 300 g of Uranium per Liter at 100°C

CUMULATIVE EXPOSURE (hr)	WEIGHT LOSS (mg/cm^2)							
	TYPE-347 STAINLESS STEEL		TANTALUM		STELLITE 98M2		INCONEL	
	No. 1	No. 2	No. 1	No. 2	No. 1	No. 2	No. 1	No. 2
23	0.15	0.20	0.05	0.04	0.90	0.72	1.81	1.75
112	0.96	1.15	0.04	0.04	3.18	2.77	12.46	13.40
275		2.29	0.08	0.08	7.80	7.35	Test stopped	
440		3.71	0.09	0.12	13.23	13.46		

analysis. Chemical, spectroscopic, and diffraction studies showed silver to be the major, if not the only, constituent. Further chemical analysis of the solution revealed a silver content of 0.1 g per liter. The presence of silver was traced to the use of silver-plated trays in the preparation of the uranyl fluoride salt. The importance of salt purity cannot be overemphasized, as is well illustrated by these test results.

Analysis of Precipitates Removed from Uranyl Fluoride Solutions. A test was run with type-347 stainless steel exposed to uranyl fluoride containing 40 g of uranium per liter pressurized with 25 psia of oxygen at 250°C. At the end of the twelfth run, 1416 hr, a considerable quantity of yellow, needle-shaped crystals was found on the wall of the autoclave at the solution-vapor interface and in the bottom of the autoclave. An analysis of a portion of the crystals showed:

U	84.00%
Fe	2.83%
Cr	1.21%
Ni	0.09%

The appearance and characteristics of the yellow crystals were such as to suggest UO_3. Calculations made by assuming the residue to consist of anhydrous oxides resulted in the following composition, in weight per cent:

UO_3	100.9
Fe_2O_3	4.1
Cr_2O_3	1.8
NiO	0.1
Total	106.9

A summary of chemical analyses on other residues removed from uranyl fluoride containing 300 g of uranium per liter used in tests at 150 and 250°C with various partial pressures of oxygen appears in Table 59. In each case, the test solution turned green and black scales precipitated.

The bulk of the corrosion product residues consisted of iron, probably in the form of oxides. Smaller quantities of uranium and chromium oxides were found. Nickel was present in the range 0.1 to 0.3%. These latter values were very low and may not be of any significance. One observation was made from the analytical data in Table 57 – the weight per cent of iron in the residues was affected very little by change in oxygen partial pressure at 150°C. At 250°C and 785 psia of oxygen pressure, however, the iron content was increased to 63.2%.

TABLE 59

Chemical Analyses of Residues Removed from Uranyl Fluoride Solutions Containing 300 g of Uranium per Liter

TEMPERATURE (°C)	PARTIAL PRESSURE OF OXYGEN (psia)	ANALYTICAL RESULTS (wt %)			
		U	Fe	Cr	Ni
150	115	3.30	52.5	1.98	0.15
150	225	4.28	52.0	6.82	0.14
150	225	2.80	50.4	4.79	0.09
250	785	1.00	63.2	5.90	0.32

FUNDAMENTAL CORROSION STUDIES

AN ATTEMPT TO DEVELOP A HIGH-TEMPERATURE REFERENCE ELECTRODE

M. H. Lietzke

A series of experiments is being performed in an attempt to develop a high-temperature reference electrode that may be useful in studying passive films on stainless steel. Also, it is of fundamental interest to measure the potentials of various half-cell combinations at high temperature (i.e., above 100°C) and to compare the values obtained with thermodynamic calculations. Apparently such a study has not been made previously.

The electrode compartments were sealed in a stainless steel bomb that was fitted with electrically insulated leads. The bomb wall was passivated so that measurements of the film potential could be made against the reference electrodes. The electrodes were mounted in quartz tubes, 2 in. in length, that were sealed at one end and fitted at the other end with Teflon plugs through which platinum wires were passed. The wires leading to the electrodes were coated with Teflon paint to insulate them from the solution in the bomb proper. The solution in the electrode compartment communicated with the solution in the bomb by means of a quartz capillary sealed to the side of the quartz compartment. The potential measurements were made with a vibrating-reed electrometer and recorded on a Brown recording potentiometer.

In the first experiment Pb(amalgam)-$PbSO_4$ and Ag-Ag_2SO_4 electrodes were tried. The lead electrode was 5 wt % lead amalgam with a platinum lead-in wire, and the quartz compartment was filled with a 0.1 *M* H_2SO_4 solution saturated with $PbSO_4$. The Ag-Ag_2SO_4 electrode had a silver wire dipping into 0.1 *M* H_2SO_4 solution saturated with Ag_2SO_4. Both the $PbSO_4$ and the Ag_2SO_4 were prepared by precipitation from solutions of the corresponding nitrates, and the precipitates were washed by decantation. The cells were evacuated before filling.

At equilibrium the cell combination 5% Pb-Hg-$PbSO_4$ | | Ag_2SO_4-Ag gave a potential reading of 997 mv at 23°C. This compares with a value of $E° = 1.012$ v estimated from the free energy values given in Latimer's tables.[1] Calculation of the entropy change for the reaction at 25°C, using Latimer's tables, indicates a value of −0.17 mv/deg. for $\partial E/\partial T$. At 100°C values of 1.00 v for the cell potential and −0.16 mv/deg. for $\partial E/\partial T$ are obtained by calculation; whereas at 250°C the corresponding values are 0.976 v and −0.16 mv/deg. Figure 65 shows values of the potentials obtained by measurement as a function of temperature. The curve gives a value of $\partial E/\partial T = -0.59$ mv/deg, which is about 3 1/2 times higher than the calculated value.

The discrepancy of 15 mv at 25°C may result partly from the lead having a lower activity than pure lead because of the solubility of the mercury in solid lead. The discrepancy in the values of $\partial E/\partial T$ may result from the change in the activity of the lead in the amalgam because of the large solubility change with temperature. (The solubility of lead in mercury is about 3.5% at 25°C and about 60% at 250°C.)

To check the low value of 997 mv for the cell potential at room temperature, another set of electrodes was prepared by using a 57.4 wt % lead

[1] W. M. Latimer kindly loaned K. A. Kraus a copy of the "Tables of Free Energies and Heats of Formation and Entropies" to be published in the forthcoming edition of *Oxidation Potentials*.

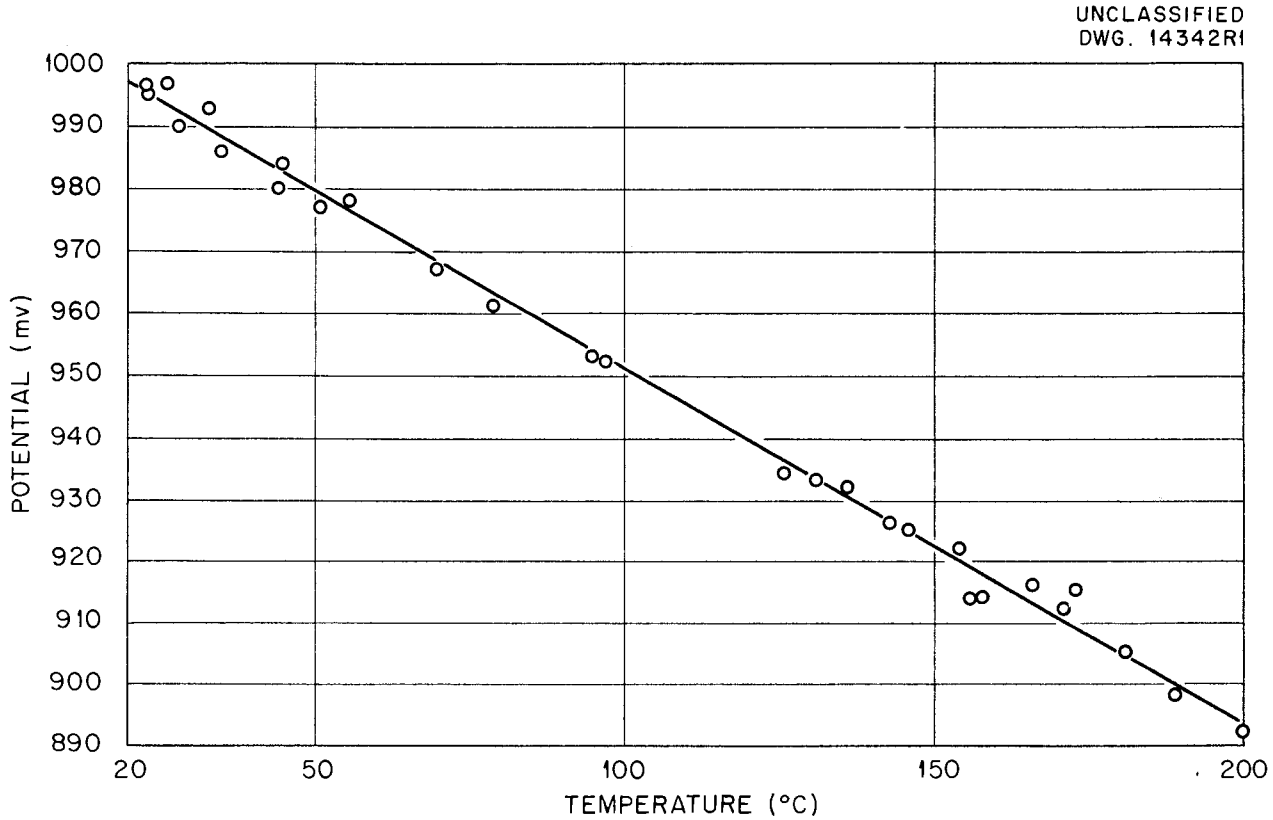

Fig. 65. Potential vs. Temperature Curve for the Pb-$PbSO_4$ and Ag-Ag_2SO_4 Electrodes in 0.1 *M* H_2SO_4.

amalgam and 0.05 *M* H_2SO_4. The new set of electrodes gave exactly the same value for the cell potential. A Pb-$PbSO_4$ electrode containing a lead wire and no amalgam was also tried, but even after one week the cell did not come to equilibrium; the potential for this cell vs. a Ag-Ag_2SO_4 electrode was only about 500 millivolts.

In order to determine how the electrodes would function in UO_2SO_4 solution, three electrodes were prepared as follows:

1. Ag-Ag_2SO_4 (electrode solution consisting of 0.13 *f* UO_2SO_4 solution saturated with Ag_2SO_4),

2. Pt-3.9% Pb-Hg-$PbSO_4$ (electrode solution consisting of 0.13 *f* UO_2SO_4 solution saturated with $PbSO_4$),

3. Pt-54.7% Pb-Hg-$PbSO_4$ (electrode solution consisting of 0.13 *f* UO_2SO_4 solution saturated with $PbSO_4$).

The electrodes were placed in the bomb (which had previously been passivated with 1% HNO_3 at 250°C for 24 hr) in 0.13 *f* UO_2SO_4 solution. Figure 66 shows the potentials obtained as a function of temperature. When the bomb containing the three electrodes was opened, it was found that reduction of the UO_2SO_4 had taken place in the electrodes containing the amalgams. However, the Ag-Ag_2SO_4 electrode was unchanged.

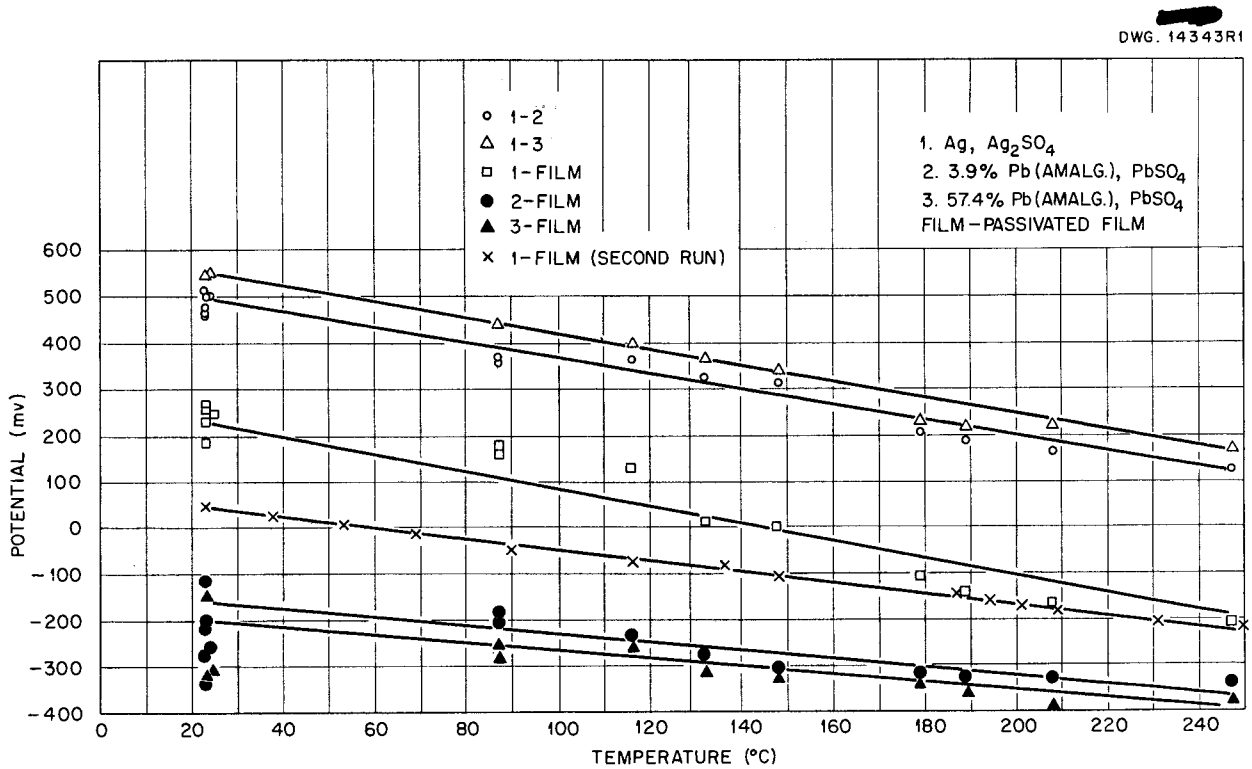

Fig. 66. Potential vs. Temperature for Various Electrode Combinations in 0.13 *f* UO_2SO_4 Solutions.

Since it appeared that the Ag-Ag_2SO_4 electrode might serve satisfactorily as a reference electrode in UO_2SO_4 solution, another run was made with just the Ag-Ag_2SO_4 electrode in the passivated bomb. The potentials obtained in this case as a function of temperature are also indicated on Fig. 66. The absolute values of the potentials of the Ag-Ag_2SO_4 electrode vs. the passive film obtained in this run differ from the corresponding values obtained in the first run, although the slopes of the curves are nearly parallel. This indicates that the absolute values of the potentials shown by films which have been made at different times cannot be directly compared and interpreted. Only the behavior of a given film toward the reference electrode may be meaningful.

Considerable difficulty has been experienced in setting up a Pb-$PbSO_4$ electrode that in combination with a Ag-Ag_2SO_4 or Hg-Hg_2SO_4 electrode will give a potential which agrees with the value calculated from thermodynamic data. This is being investigated further. Both the Ag-Ag_2SO_4 and Hg-Hg_2SO_4 electrodes, however, seem to function properly and can be used as high temperature reference electrodes in H_2SO_4. The Ag-Ag_2SO_4 electrode can also be used as a reference electrode in UO_2SO_4 solution.

Figure 67 shows how the Ag-Ag_2SO_4 and the Hg-Hg_2SO_4 electrodes can be used to show the failure of the passive film on type-347 stainless steel in 0.05 *M* H_2SO_4 at high temperatures. The passive film was produced by

heating with 1% HNO_3 for 24 hr at 250°C. As long as the film was intact the lower potential curves were obtained, but when the film broke, the potentials shifted sharply to the values indicated in the upper curves. The upper curves represent the potential of the reference electrodes against the bare steel in 0.05 *M* H_2SO_4. The shift in potential amounted to over half a volt.

At present the $Ag\text{-}Ag_2SO_4$ electrode is being tried to show the failure of the passive film in uranyl sulfate solution at high temperature. Curves have been obtained that show the break, but work on this phase of the problem is still incomplete. An attempt will be made to correlate the potential measurements with the durability of the passive film in various partial pressures of oxygen.

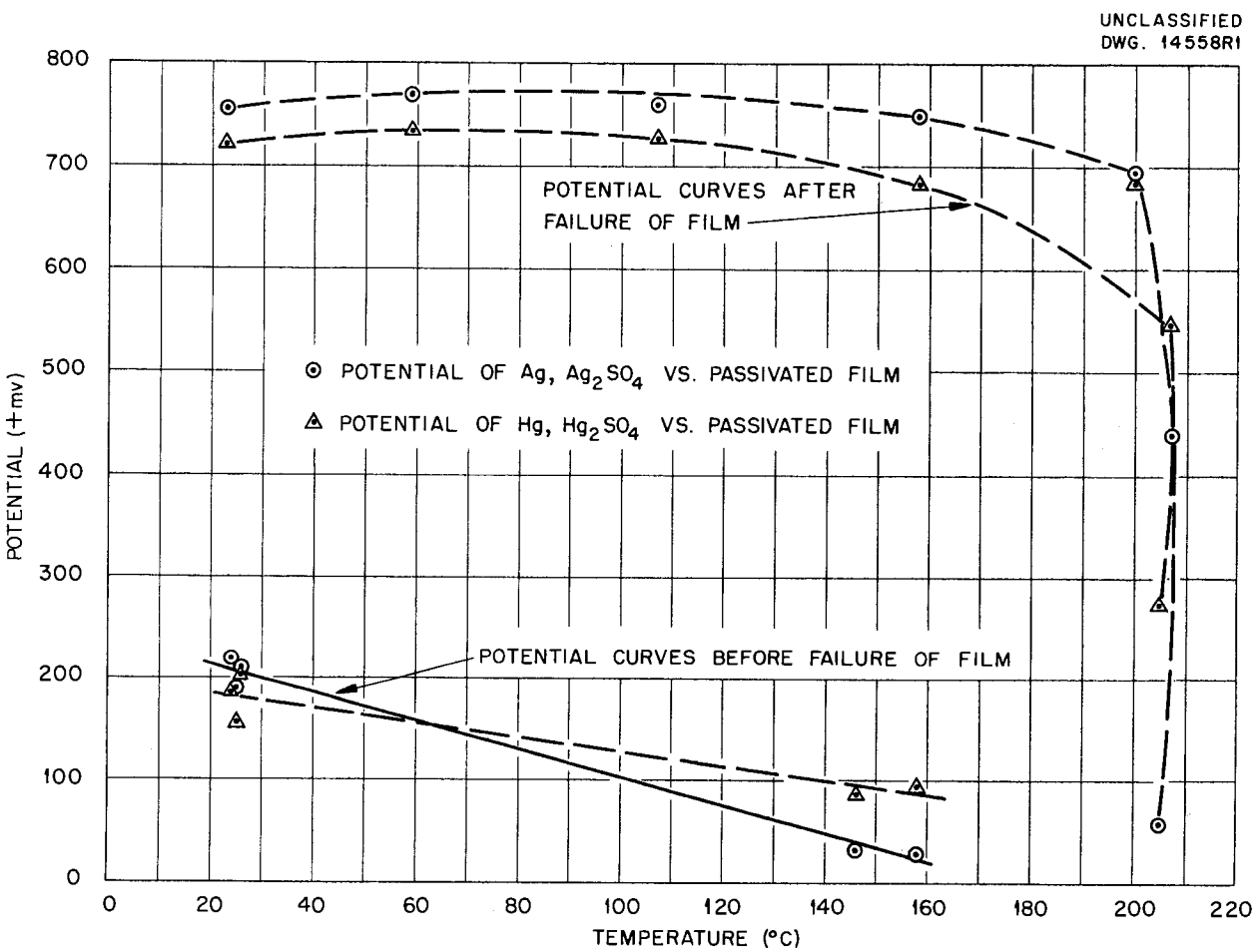

Fig. 67. Curves Showing Failure of Passive Film on Type-347 Stainless Steel in 0.05 M H_2SO_4.

METALLURGY

E. C. Miller A. R. Olsen

Since this is the first contribution of the metallurgy group to the HRP progress report, a general review of the materials problems and program plans are presented. The record of experimental progress will consequently be limited.

The general fields of investigation include:

1. metallurgical factors affecting corrosion,
2. development of specifications and procedures for procurement, acceptance, and fabrication of materials and components,
3. materials development, including properties evaluation,
4. application of nondestructive testing methods to homogeneous reactor problems,
5. radiation damage studies.

With the possible exception of radiation damage, a mass of information and experience has been accumulated in each of the above fields in related, but perhaps more conventional, applications. A necessary first and major step, then, is the collection and evaluation of existing pertinent data in terms of homogeneous reactor problems, and the development of contacts for obtaining information on current related work in the same fields at other locations. With this information as a background, many of the service responsibilities of the metallurgy group can be accomplished without the need for experimental work, and the remaining experimental work, although still substantial, can be planned with greater economy in personnel and facilities. Direct service work for other groups of the homogeneous reactor project is being performed, particularly in the examination of materials and components removed from the HRE and the corrosion loops, but this also provides invaluable experimental data toward accomplishing the longer range objectives of the HRP metallurgy group.

METALLURGICAL FACTORS IN CORROSION

The extensive program of investigating chemical and mechanical factors such as solution composition, temperature, pH, velocity, oxygen concentration, and passivation phenomena is described in detail in another section of this report. Only the metallurgical factors involved will be discussed here.

Examinations of corroded surfaces of type-347 stainless steel removed from pump test loops show many instances of seriously accelerated corrosion attack, which appear to be related to differences in the metallurgical structure of the corroded surfaces. However, in most of these instances the unusually severe conditions of solution velocity and turbulence prevailing have accelerated attack and complicated interpretation.

For a given set of conditions there apparently exists a threshold velocity above which passivation offers little protection to the stainless steel against attack. Examination of flow restrictors, pump impellers, sharp bends, welds, and fittings that produce such turbulence and velocities approximating threshold values produces evidence of selective corrosion attack related to the metallurgical structure

of the stainless steel surface. At velocities well in excess of threshold values the attack becomes severe, rapid, and relatively indiscriminate. Redesign to lessen velocity and turbulence is a first step in lowering the extreme attack resulting from these factors, but if design cannot achieve this completely, and it seldom can, the next remedy is the use of a more corrosion-resistant substitute material. In testing thus far, titanium, zirconium, and possibly tantalum appear more resistant to corrosion attack under extreme conditions than do the stainless steels; however, their use to any appreciable extent involves substantial problems of procurement, fabrication, mechanical properties, and the effects of hydrogen. Plans to study these factors are described under materials development.

There is much to be learned regarding the proper metallurgical preparation of the stainless steels to best resist selective attack under conditions of moderate solution velocity. The physical metallurgy of stainless steels is complex, and corrosion testing involving controlled variation of all the contributing metallurgical factors would be prohibitive. On the other hand, the observation of corrosion attack on components of operating and test equipment emphasizes the problems but is not a complete substitute for some controlled-variable testing.

From the metallurgical standpoint it is important to maintain control over the phases present in a stainless steel (or at least to know them) and to know the relative quantity, size, shape, orientation, distribution, and retained stresses. These are determined by chemical compositions of the base metal and welds, welding methods, severity of mechanical working, machining or polishing, and thermal history.

The metallurgy group is preparing specimens of type-347 stainless steel to be tested in the pump loops by the dynamic corrosion group. The sample holder and test methods to be employed are described in the dynamic corrosion section of this report (see chapter on "Corrosion," Part I). For the initial survey, samples are being prepared by welding.

In preparing the first series of samples the procedure listed was used. Weld; rough-machine weld flush with base metal and remove some base metal in the process; prepare different samples with the following treatment:

1. as machined,
2. light finish-machine cut,
3. dry abrasive polish,
4. wet abrasive polish,
5. shot-peen surface,
6. electrolytic polish,
7. 750°F partial stress-relief,
8. 1200°F sensitization,
9. 1500°F heat-stabilization,
10. 1950°F full anneal and water quench,
11. 1950°F full anneal and air cooling,
12. cold work by repeated bending and straightening.

The second series was welded and then, without machining, samples were prepared with the following treatment:

1. as welded,
2. 750°F partial stress-relief,
3. 1200°F sensitization,
4. 1500°F heat-stabilization,

5. full anneal, water quench, and sand blast,
6. full anneal, water quench, and pickling,
7. cold work by repeated bending and straightening.

For the third series the welded pieces will be tack-welded under stress and used (1) as welded, or (2) fully annealed after welding.

The first and second series of samples are now being tested under a variety of controlled temperatures, velocities, and solution compositions to establish the optimum test conditions for the metallurgical control samples.

SPECIFICATIONS AND FABRICATION PROCEDURES

The wide use of stainless steels in the chemical, steam power, and petroleum industries has resulted in the preparation of standard specifications for these materials and their fabrication by the American Iron and Steel Institute, the American Society for Testing Materials, and the ASME Boiler Code Committee. For many purposes these specifications are adequate. However, increasing demands are being placed on stainless steels for high pressure and elevated temperature applications by these industries and by military activities, which are in many respects similar to those of of the homogeneous reactor project.

In particular, procedures and specifications are by no means standardized for the fabrication, welding, and stress-relief of heavy walled (3/8 in. and thicker), large diameter, type-347 and other stainless steel piping, fittings, and pressure-containing equipment. The responsibilities of the HRP metallurgy group in this area involve keeping informed of the experience of interested industries and the work of professional groups and applying the information thus obtained to establish specifications for the HRP. Since the work thus far has been largely that of information-gathering, detailed reports of progress will be deferred until experimental results and actual HRP specifications are available.

ALTERNATE AND SUPPLEMENTARY MATERIALS

Type-347 stainless steel was selected as the principal material of construction for the HRE on the basis of its corrosion behavior in static tests, its availability (at that time) in the quantities and shapes required, and adequate experience in field welding techniques for making components. Although it may not be an ideal material, it still appears to have been the optimum choice for the experimental reactor.

However, columbium, which is an essential component of type-347 stainless steel, is now one of the most critical materials on the strategic list; experience in construction of the HRE and operation of dynamic test loops have contributed new information and emphasized limitations of this material; and the materials requirements for the proposed intermediate and large-scale, long-life operating reactors differ in many respects from those of a small-scale, primarily experimental reactor. It has thus become necessary to re-evaluate type-347 stainless steel and to investigate possible alternate and supplementary materials for use in subsequent phases of the program. This should take into account the critical shortage of columbium; severe corrosion-erosion effects observed in high-velocity and turbulent

sections of pump loops; metallurgical problems involved in fabricating, welding, and stress-relieving large pressure-containing structures; availability and suitability of (1) other series 18-8 and higher alloy stainless steels as substitute structural materials, (2) materials such as titanium, zirconium, and perhaps tantalum either as alternate structural materials or more probably as lining and reinforcing materials for points of severe corrosion-erosion attack, and (3) limited purpose materials for special applications, including neutron-absorbing control devices, valve trim, and wear-resistant pump bearings and journals.

Other stainless steels, with the possible exceptions of types 304 and 304 ELC (0.03% C), do not offer much promise from the standpoint of fabrication and availability, although dynamic corrosion survey tests now in progress may demand their consideration. Type 304 ELC should be seriously considered since it contains no columbium, is free of the coarse carbide inclusions that complicate the use of fittings and large parts machined from heavy sections of type 347, and, except for the absence of accumulated experience, should not be more difficult to weld than type 347. Type 304 ELC is now difficult to obtain in the quantities and forms and delivery dates required, but this situation may improve.

In the dynamic corrosion loops, titanium appears to be among the materials most resistant to corrosion-erosion and substantially better in this regard than the stainless steels. This superiority warrants intensive efforts to:

1. further confirm this corrosion-erosion resistance in more extensive dynamic tests,
2. determine the suitability of the material for specific requirements of the HRP – that is, fabrication into pressure-containing equipment and resistance to chemical action and embrittlement in aqueous environments at operating temperatures,
3. utilize the material as a lining or reinforcing material at critical locations in a stainless steel system.

In addition, the relative acceptability of zirconium under similar conditions should be determined.

With the foregoing in mind, a substantial part of the metallurgy group's effort will be placed on titanium and, if dynamic corrosion tests warrant, on zirconium. Close liaison must be maintained with other AEC and military groups that are now sponsoring intensive titanium and zirconium developmental work. Specific experimental effort will be directed toward determining the factors responsible for the lack of consistent notched-stress resistance of commercially available titanium and its alloys, and to the fabrication, welding, and testing of component parts of engineering test systems.

The metallurgy group is now assisting the dynamic corrosion group in the building of a test loop in which certain of the critical parts – in particular, a Model 100-A pump impeller and some of the piping – are made of titanium. The parts of the impeller will be joined by hot-pressed rivets, but there will be some welded joints in the system. Preliminary welding tests have been initiated to obtain experience and to learn the characteristics of the available material when welded. Sample welds have been made in an

inert atmosphere in a dry box using Ti-75A, RC-70, and titanium-to-zirconium. Bend and tensile tests on the Ti-75A welds showed greater strength and ductility than anticipated. The RC-70 tests were somewhat erratic, partly because of some unsatisfactory welds. The titanium-zirconium welds were brittle and unacceptable.

This work is continuing, and sample welds will be mechanically and corrosion tested in both the as-welded and the machined conditions.

HRE SAFETY PLATES

Operating difficulties in the HRE, described elsewhere in this report, were encountered because of the failure of the stainless steel-encased boral (35% B_4C-65% Al) safety plates. While the construction of the original plates was being modified, the powder metallurgy group of the Metallurgy Division undertook a parallel effort to develop a more suitable boron carbide-containing safety plate. Initial tests were made on samples of boral about 1 1/2 in. square produced by powder compaction. Attempts were made to obtain a metallurgical bond between these cores and two pieces of stainless steel cladding by rolling. The cladding was prepared in three ways: (1) type-302 stainless steel powder was sintered to the inside surface of the cladding at 1150°C; (2) copper powder was sintered to the cladding at 1120°C; and (3) the cladding was used in the bright-annealed condition. The sandwiches, made of cladding, powder compacts, and frames, were rolled together – one set at 600°C to obtain from 31 to 37% reduction and one set at 600°C for one pass, followed by two passes at 500°C, to accomplish the same reduction.

Metallographic examination of samples reduced entirely at 600°C showed a zone of interaction between the core and cladding, whereas no reaction zone was observed in the samples finished at 500°C. The sample plates were tested under conditions comparable with those in the HRE and found satisfactory.

When the size of plates being processed was scaled to about one half the actual size of the HRE control plates, difficulty was encountered in rolling owing to excessive reduction of the core material and accumulation of core material at the trailing ends of the frames and consequent rupture of the cladding. Lower rolling temperatures did not produce an acceptable bond between the core and cladding.

The efforts to clad boral were suspended because of the required HRE time schedule, and core matrix materials were selected with rolling characteristics more nearly approximating those of the cladding. Core materials were made of boron carbide powder mixed with powdered iron, chromium, type-302 stainless steel, and type-410 stainless steel, respectively. None of these mixtures proved acceptable when clad with type-347 stainless steel and rolled at 950, 1050, and 1100°C, owing to various combinations of poor bonding, blistering, core cracks, and metal-boron carbide interaction.

Copper powder, mixed with boron carbide, pressed, and rolled with stainless steel cladding at 1000°C, produced a much more satisfactory material, and a set of safety plates of the required dimensions was made and delivered to the HRE group. The acceptable plates were fabricated in the following manner:

1. press core material (82% copper, 16% boron carbide, and 2% stearic acid binder) in a 1- by 3-in. die at a pressure of 25 tons per square inch,

2. heat to 325°C to burn off binder,
3. sinter 1 hr at 950°C,
4. re-press at 50 tons per square inch,
5. re-sinter at 950°C for 15 min,
6. roll to thickness of frame (about 15% reduction),
7. load in frame, seal, evacuate,
8. roll at 1000°C to required dimensions (53% reduction),
9. shear excess cladding to leave 1/8-in. border around copper-boron carbide core,
10. seal edges by heliarc welding.

NONDESTRUCTIVE TESTING

The Y-12 Research Engineering Section is furnishing nondestructive testing assistance to the project. To date this has largely involved the use of radiography to inspect welding construction, pulsafeeder diaphragms, valves, and pressurizers. An ultrasonic reflectoscope has been obtained and will be used to extend this work, and the purchase of an Audigage thickness tester is contemplated. The application of nondestructive testing to determine the extent of corrosion attack is also contemplated.

RADIATION DAMAGE STUDIES

D. S. Billington R. G. Berggren
W. E. Taylor

The Solid State Division is working on radiation damage studies connected with the metallurgical problems of the HRP.

Some earlier work by Argonne National Laboratory, in cooperation with the Solid State Division of ORNL, on the inpact strength of carbon steels indicated a reduction of the impact strength in the range above the transition temperature, as well as a pronounced increase in the transition temperature after irradiation. Further study of this effect has been initiated by the Solid State Division. Impact specimens of AISI-1040 steel have been prepared for irradiation in the X-10 graphite pile for one- to two-month periods. Irradiation temperatures and metallurgical history will be controlled to determine possible effects on the HRE pressure vessel. Similar tests are planned to evaluate austenitic stainless steels and titanium.

CHEMICAL PROCESSING

F. R. Bruce, Section Chief

D. E. Ferguson R. G. Mansfield

W. E. Tomlin

The development of homogeneous reactor chemical processing has been based on a plutonium producing reactor in which the fuel is a uranyl sulfate-heavy water solution. The general approach has been to study application of tributyl phosphate solvent extraction to this separation problem and to use the process as a yardstick for evaluating attractive alternate methods of separation. The work has now progressed to the point at which a reliable chemical flowsheet has been obtained; however, this flowsheet does not necessarily represent the optimum method of chemical processing. For instance, the inherent advantage of starting with uranium in solution is lost because of the necessity of heavy water recovery, and the long cooling period for neptunium decay necessitates large storage facilities and large inventories of valuable materials.

PLUTONIUM CHEMISTRY

One of the most important questions that must be answered before an aqueous solution, homogeneous plutonium producing reactor and the associated chemical separations plant can be designed concerns the behavior of plutonium in the fuel solution under operating conditions. If plutonium precipitates in the reactor, the precipitation could be a convenient mechanism for continuously removing plutonium from the reactor to prevent the production of Pu^{240}. The plutonium could be filtered out of the fuel solution along with the insoluble fission and corrosion products. However, having plutonium in the reactor as a precipitate would complicate reactor design and operation.

It has been previously reported that the solubility of tetravalent plutonium in 1 *M* UO_2SO_4 is only 0.003 mg/ml at 250°C. When a solution of uranyl sulfate containing more than this concentration of plutonium is heated to 250°C, a precipitate forms. The precipitate was found to be plutonium dioxide by x-ray diffraction, which suggests hydrolysis of the plutonium sulfate under these conditions. The hydrolysis and subsequent precipitation are essentially complete in 12 hr at 250°C.

Behavior of Plutonium(VI) in Uranyl Sulfate Solution. It was found that in the absence of an oxygen pressure, hexavalent plutonium is reduced to tetravalent plutonium in 1 *M* UO_2SO_4 solution and that this reduction and the subsequent precipitation are complete in 12 to 24 hr at 250°C. Table 60 summarizes the study of plutonium behavior in the absence of oxygen. In these experiments, carried out in sealed glass tubes, a uranyl sulfate solution was used that was pretreated with a 200-psi partial pressure of oxygen at 250°C for 100 hr to eliminate organic impurities. In the first experiment reported in Table 60, the plutonium was introduced as plutonium(IV) to a concentration below the solubility of this valence state. After heating this solution for 206 hr at 250°C, analysis indicated that 95% or more of the plutonium remained in the tetravalent state. In the second experiment, the initial plutonium concentration was 0.20 mg/ml, of which 54% was plutonium(VI)

TABLE 60

Behavior of Plutonium(IV) and Plutonium(VI) in the Absence of Oxygen Pressure in a Plutonium Sulfate-Uranyl Sulfate System at 250°C

Starting solution: 1 *M* UO_2SO_4 preoxidized with 200 psi of oxygen at 250°C for 100 hours

CONDITIONS	SOLUBLE Pu (mg/ml)	Pu(VI) (mg/ml)	Pu(IV) (mg/ml)
Starting solution	0.0020	0	0.0020
Heated 206 hr	0.0023	0.00004	0.0023
Heated 206 hr	0.0023	0.0001	0.0022
Starting solution	0.201	0.108	0.093
Heated 206 hr	0.011	0.008	0.0030
Heated 206 hr	0.017	0.014	0.0026

and the remainder was plutonium(IV). After 206 hr at 250°C in the sealed glass tube, more than 90% of the plutonium had precipitated. The plutonium remaining in solution was plutonium(IV) at a concentration of 0.003 mg/ml (the solubility of this valence state) plus the residual hexavalent plutonium.

Effect of Oxygen Pressure on Plutonium Solubility. When a uranyl sulfate solution containing plutonium(IV) at a concentration below its solubility was heated under an oxygen pressure of 200 psi, the tetravalent plutonium was partly oxidized to the hexavalent state. In Table 61 plutonium valence state analyses are given for this plutonium solution after heating periods ranging from 27 to 206 hours. The experiments were carried out in pyrex glass tubes having a capillary hole near the top, and the autoclave was pressurized with oxygen. The exact equilibrium of plutonium(IV) and plutonium(VI) under these conditions cannot be predicted from these data, since plutonium(VI) reduces rapidly to plutonium(IV) at room temperature in uranyl sulfate solution and the valence state analyses were made several hours after the solutions were removed from the autoclave.

The data in Table 62 describe the reduction of plutonium(VI) to plutonium(IV) in 1 *M* UO_2SO_4 at room temperature. The percentage rate of reduction was much greater at a plutonium concentration of 0.003 mg/ml than at 0.15 mg/ml.

When a uranyl sulfate solution containing both plutonium(VI) and plutonium(IV) at a concentration of of 0.1 mg/ml was heated under a partial pressure of 200 psi of oxygen, the plutonium(VI) remained in the hexavalent state and in solution (Table 63). The plutonium(IV) was observed to precipitate, which indicated that hydrolysis and precipitation proceeded at a much faster rate than oxidation to the soluble plutonium(VI). The data given in Table 63 also indicate

TABLE 61

Oxidation of Plutonium(IV) by a Partial Pressure of Oxygen in a Plutonium Sulfate-Uranyl Sulfate-Oxygen System at 250°C

Starting solution: 1 *M* UO_2SO_4 preoxidized with 200 psi of oxygen at 250°C for 100 hours

Oxygen pressure: 200 psi

CONDITIONS	TOTAL Pu (mg/ml)	Pu(VI)* (%)	Pu(IV)* (%)
Starting solution	0.0020	0	100
Heated 27 hr	0.0023	4	96
Heated 80 hr	0.0026	4	96
Heated 130 hr	0.0027	87	13
Heated 206 hr	0.0033	50	50

*It has been observed that plutonium(VI) reduces to plutonium(IV) at room temperature in this uranyl sulfate solution. The valence state analyses were run as soon as practical after the samples were removed from the autoclave, but there was possibly some reduction of the plutonium. For this reason, the above percentages may not be accurate, but they do definitely show that plutonium(IV) is oxidized to plutonium(VI) by oxygen pressure.

TABLE 62

Effect of Time on Valence State of Plutonium in Uranyl Sulfate Solution at Room Temperature

Starting solution: 1 *M* UO_2SO_4

TOTAL Pu CONCENTRATION (mg/ml)	1st ANALYSIS Pu(VI) (%)	TIME ELAPSED	2nd ANALYSIS Pu(VI) (%)
0.0027	87	4 hr	3
0.0033	42	1 day	4
0.0033	50	1 day	3
0.015	96	4 hr	67
0.18	97	1 day	80
0.16	97	1 day	85

that no appreciable amount of the precipitate redissolved in 206 hr at 250°C under the oxygen pressure.

Effect of Type-347 Stainless Steel and Copper Sulfate on Plutonium Solubility. Table 64 summarizes the results of experiments in which 0.05 *M* $CuSO_4$ and specimens of type-347 stainless steel were added to the system. Under an oxygen pressure sufficient to stabilize hexavalent plutonium in the absence of these materials, untreated type-347 stainless steel, type-347 stainless steel pretreated with nitric acid, and 0.05 *M* $CuSO_4$

TABLE 63

Effect of Oxygen Pressure on the Behavior of Plutonium(IV) and Plutonium(VI) in a Plutonium Sulfate-Uranyl Sulfate-Oxygen System at 250°C

Starting solution: 1 *M* UO_2SO_4 preoxidized with 200 psi of oxygen at 250°C for 100 hours

Oxygen pressure: 200 psi (equivalent to 1000 ppm of O_2 in solution)

CONDITIONS	VOLUME AFTER HEATING (ml)	SOLUBLE Pu (mg/ml)	TOTAL WEIGHT OF Pu(VI) (mg)	TOTAL WEIGHT OF Pu(IV) (mg)
Starting solution		0.201	0.538	0.467
Heated 27 hr	4.6	0.126	0.548	0.032
Heated 80 hr	5.6	0.103	0.548	0.029
Heated 130 hr	3.6	0.147	0.509	0.020
Heated 206 hr	3.2	0.159	0.495	0.013

TABLE 64

Effect of Steel and Copper Sulfate on Plutonium Solubility in a Plutonium Sulfate-Uranyl Sulfate-Oxygen System at 250°C

Starting solution: 1 *M* UO_2SO_4 preoxidized with 200 psi of oxygen at 250°C for 100 hours

Oxygen pressure: 200 psi

CONDITIONS	CONCENTRATION OF Pu (mg/ml)	TOTAL WEIGHT OF Pu(VI) IN SOLUTION (mg)	TOTAL WEIGHT OF Pu(IV) IN SOLUTION (mg)	HEATING TIME (hr)
Starting solution	0.234	0.776	0.394	0
Control	0.189	0.668	0.201	72
Type-347 stainless steel[a]	0.039	0.118	0.050	72
$CuSO_4$, 0.05 *M*	0.038	0.134	0.033	72
$CuSO_4$, 0.05 *M*, and type-347 stainless steel[a]	0.013	0.045	0.012	72
Passive type-347 stainless steel[b]	0.054	0.179	0.064	72
Starting solution	0.252	1.163	0.087	0
Control	0.115	0.524	0.028	24
Pretreated type-347 stainless steel[c]	0.113	0.520	0.022	24

[a]Untreated.

[b]Pretreated with nitric acid.

[c]Pretreated by heating for 24 hr at 250°C in a 1 *M* UO_2SO_4 solution under a pressure of 200 psi of oxygen.

all caused reduction of plutonium(VI). However, type-347 stainless steel pretreated by heating to 250°C for 24 hr in a 1 *M* UO_2SO_4 solution under an oxygen pressure of 200 psi caused no reduction of hexavalent plutonium under the above conditions.

From these results it was concluded that plutonium(VI) was reduced during the formation of the protective film on stainless steel, and for this reason any corrosion of the reactor system would cause precipitation of plutonium.

Adsorption of Plutonium on Stainless Steel. A 5-ml volume of a 1 *M* UO_2SO_4 solution initially containing 0.057 mg/ml of tetravalent plutonium was sealed in two glass tubes; each tube contained four pieces of type-347 stainless steel having a total area of 0.38 in.^{2}. After heating for 72 hr at 250°C it was found that 0.021 mg of plutonium per square inch of surface was adsorbed on the stainless steel in one case and 0.026 mg in the duplicate experiment. This amount of plutonium adsorption would not be significant in the reactor system.

Filtration of PuO_2. In one experiment it was found that PuO_2 precipitated from 1 *M* UO_2SO_4 at 250°C could be satisfactorily filtered from the mother liquor with a fine filter medium.

Dissolution of PuO_2. It has been found that plutonium dioxide precipitated from uranyl sulfate solutions at 250°C can be easily dissolved in dilute nitric acid containing an oxidizing agent. Both ammonium hexanitratocerate and silver peroxide have been found to be satisfactory oxidizing agents for this purpose.

HEAVY WATER RECOVERY

Regardless of the method of removing plutonium from a homogeneous plutonium-producing reactor, some uranium must be removed for decontamination and re-enrichment. The first step in decontaminating the uranium would consist of heavy water recovery. It is now proposed that heavy water recovery be accomplished by evaporation of the uranyl sulfate solution to a slurry and that this slurry be dried for removal of residual water. Drying has been studied in the laboratory to determine the optimum drying temperature and time. Additional study of the method of heavy water recovery and of alternate procedures will be carried out by Vitro Chemical Co. under AEC contract.

Determination of the amount of moisture remaining in uranyl sulfate after heating for varying lengths of time at temperatures in the range 200 to 400°C indicated that 400°C is is the minimum temperature at which complete dehydration of the salt can be effected. At 400°C a 1-g sample of hydrated uranyl sulfate was completely dehydrated in 1 hour. Data (Table 65) were obtained by absorption and weighing of the water evolved.

The apparatus used consisted of a tube furnace and a quartz combustion tube in series with an absorption train. A dry-air sweep was used, and the moisture lost by a 1-g sample of uranyl sulfate was determined by direct weighing after absorption in an anhydrone-packed tube. A combustion tube served to absorb the oxides of sulfur resulting from decomposition of uranyl sulfate.

Later experiments, in which the water content of the residue after

TABLE 65

Dehydration of $UO_2SO_4 \cdot 3H_2O$ at Elevated Temperatures

DRYING* TEMPERATURE (°C)	MOISTURE REMAINING IN SAMPLE (wt %)					
	AFTER 1 hr	AFTER 2 hr	AFTER 3 hr	AFTER 4 hr	AFTER 5 hr	AFTER 6 hr
200	1.05	0.90	0.90	0.90	0.90	0.90
200	1.66	1.42	1.22	1.02	0.82	0.70
300	0.99	0.46	0.46	0.46	0.46	0.46
350	0.66	0.43	0.43	0.43	0.43	0.43
400	0	0	0	0	0	0

*Drying was carried out in a combustion tube by using dry-air sweep. Sample size: 1 g.

heating in a dry-air stream was determined indirectly by uranium and sulfate analyses, confirmed the results given in Table 65. Sulfate analyses indicated only 2% decomposition of sulfate after 6 hr at 400°C.

SOLVENT EXTRACTION

Extraction of Plutonium from Solutions Containing the Sulfate Ion and Uranium. It was found that adequate recovery of uranium and plutonium can be obtained from a Purex feed containing a mole ratio of sulfate to uranium of 1:2 without altering the present Purex flow sheet. However, since the mole ratio of sulfate to uranium will be 1:1 in processing a homogeneous reactor solution unless a special effort is made to destroy sulfate, an investigation was made of the extraction of plutonium(IV) from HNO_3-H_2SO_4 solutions by tributyl phosphate.

An empirical equation published in the last report[1] gives the distribution coefficient of plutonium(IV) at 25°C as a function of HNO_3, TBP, and H_2SO_4 molarity. This equation is

$$E_a^0[\mathrm{Pu(IV)}] = \frac{2.95\ (HNO_3)_{aq}^{3.8}\ (TBP)_{org}^{1.4}}{(HNO_3)_{aq}^{2.4} + 340\ (H_2SO_4)_{aq}},$$

where (HNO_3) and (H_2SO_4) are the molarities of HNO_3 and H_2SO_4 in the aqueous phase, and (TBP) is the molarity of TBP in the organic phase.

It was found that this same equation could be used to estimate the distribution of plutonium(IV) in the presence of uranium, if total TBP in the solvent phase is replaced by TBP uncomplexed by uranium in the solvent phase. This method is not entirely satisfactory, since the increase in the solvent phase volume must be considered in calculating the concentration of uncomplexed TBP. Table 66 gives a comparison of experimental values obtained for plutonium(IV) distribution with values calculated from the equation. Table 67 gives the distribution data obtained in the presence of uranium, nitric acid, and the sulfate ion used in Table 66.

(1) D. E. Ferguson, *Quarterly Report - Homogeneous Chemical Processing*, ORNL CF-51-8-152, Aug. 16, 1951.

The equation gives an estimate that is adequate for process calculations over the range 1 to 5 *N* HNO_3, 5 to 30% TBP in AMSCO, and 0 to 85% saturation of TBP with uranium. This equation is not adequate for predicting the distribution of plutonium(IV) in a system that contains appreciable nitrate other than nitric acid. In general, the plutonium distribution coefficient is directly proportional to the square of the nitrate concentration and inversely proportional to the 0.6 power of the hydrogen ion concentration. To incorporate this into the preceding equation makes it unwieldy, but in the absence of sulfate the corrected equation becomes

$$E_a^0[\text{Pu(IV) at } 25°\text{C}] = \frac{2.95\ (NO_3^-)^2\ (TBP)^{1.4}}{(H^+)^{0.6}}$$

TABLE 66

Comparison of Observed Plutonium(IV) Distribution Coefficients with Calculated Distribution Coefficient

TBP CONCENTRATION (*M*)	(NO_3^-) CONCENTRATION (*M*)	$SO_4^=$ CONCENTRATION (*M*)	SATURATION OF SOLVENT WITH U (%)	PLUTONIUM(IV) DISTRIBUTION COEFFICIENT	
				OBSERVED	CALCULATED*
0.185	1.1	0.1	0	0.009	0.012
1.11	0.9	0.1	0	0.06	0.066
0.185	3.0	0.1	0	0.56	0.39
1.11	2.6	0.375	0	4.15	2.95
0.185	2.0	0.375	0	0.04	0.03
0.74	1.8	0.375	0	0.16	0.14
0.185	5.0	0.375	0	0.62	0.72
0.74	4.6	1.0	0	3.90	3.90
0.555	2.8	1.0	0	0.22	0.18
1.11	2.5	1.0	0	0.33	0.32
0.555	4.7	1.0	0	0.94	1.26
1.11	4.3	1.0	0	1.85	2.44
1.0	3.6	1.0	43	0.52	0.48
1.0	3.9	0.5	72	0.51	0.45
1.0	3.9	0.25	75	0.80	0.58
1.0	4.4	1.0	85	0.25	0.19
1.0	4.3	0.5	90	0.33	0.15
1.0	4.4	1.0	83	0.23	0.19
1.0	4.3	0.0	93	0.87	0.82**
1.0	4.5	0.5	90	0.31	0.17

*Plutonium(IV) distribution coefficient calculated from equation $E_a^0[\text{Pu(IV)}] = \frac{2.95(NO_3^-)^{3.8}\ (TBP)^{1.4}}{(NO_3)^{2.4} + 340(SO_4^=)}$.

**Plutonium(IV) distribution coefficient calculated from equation $E_a^0[\text{Pu(IV)}] = \frac{2.95(NO_3)^2\ (TBP)^{1.4}}{(H^+)^{0.6}}$.

TABLE 67

Extraction of Plutonium(IV) from Solutions Containing Nitric Acid, Sulfate Ion, and Uranium

Aqueous phase: as indicated
Organic phase: 30% TBP in AMSCO
Temperature: 25°C

$SO_4^=$ CONCENTRATION (M)	HNO_3 CONCENTRATION (M)	U CONCENTRATION (aq. phase) (mg/ml)	$E_a^0(U)$	$E_a^0[Pu(IV)]$	$E_a^0(HNO_3)$
1.0	3.80	7.8	6.5	0.52	0.148
0.5	3.75	20	4.3	0.51	0.079
0.25	3.90	17	5.4	0.80	0.069
1.0	4.55	70	1.5	0.25	0.061
0.5	4.50	66	1.6	0.33	0.058
1.0	3.95	74	1.3	0.23	0.066
0.5	3.95	74	1.4	0.31	0.047
0	4.00	64	1.7	0.87	0.060

Unfortunately, these data do not give an adequate explanation for the mechanism of the extraction of plutonium by TBP. As has been pointed out, the distribution coefficient over the range 1 to 5 N HNO_3 varies as the square of nitrate concentration and as the TBP concentration to the 1.4 power. If it is considered that the dependence of plutonium extraction on nitrate and TBP over a much smaller range of concentration, where activity coefficients would not be expected to vary widely, a fourth power dependence on both nitrate and free TBP concentration can be obtained. In another small range a fourth power dependence on uncomplexed TBP holds, so this approach does not lead to a definite conclusion. It is reasonable to expect a fourth power dependence on the nitrate ion activity, if the assumption is made that it is the neutral $Pu(NO_3)_4$ molecule that enters into the complex formation with TBP.

It is difficult to obtain the concentration of uncomplexed tributyl phosphate, so a reasonable approach is to eliminate the activity of this solute in the solvent phase. This can be done in the following manner. It was suggested last quarter that in the concentration range 1 to 5 N HNO_3, the extraction of HNO_3 by tributyl phosphate can be considered to be

$$H^+_{aq} + NO^-_{3\,aq} + TBP_{org} \rightleftharpoons HNO_3 \cdot TBP_{org}$$

If the plutonium(IV) extraction is considered as

$$Pu^{+4}_{aq} + 4NO^-_{3\,aq} + nTBP_{org} \rightleftharpoons Pu(NO_3)_4 \cdot nTBP_{org} ,$$

the thermodynamic equilibrium constants for the two competing reactions can be written:

$$K_1 = \frac{[TBP \cdot HNO_3]_{org}}{[H^+]_{aq}\ [NO_3^-]_{aq}\ [TBP]_{org}} , \qquad (1)$$

$$K_2 = \frac{[Pu(NO_3)_4 \cdot nTBP]_{org}}{[Pu^{+4}]_{aq}\ [NO_3^-]^4_{aq}\ [TBP]^n_{org}} \qquad (2)$$

Following a similar analysis used by Savolainen,[2] Eq. 1 is solved for the activity of tributyl phosphate in the organic phase, $[TBP]_{org}$, which is substituted in Eq. 2 to obtain

$$K_2 \left[\frac{[TBP \cdot HNO_3]_{org}}{K_1 [H^+]_{aq}\ [NO_3^-]_{aq}}\right]^n$$

$$= \frac{[Pu(NO_3)_4 \cdot nTBP]_{org}}{[Pu^{+4}]_{aq}\ [NO_3^-]^4_{aq}} \qquad (3)$$

If the activities are replaced by concentrations and activity coefcients, and the logarithms are obtained,

$$\ln \frac{K_2}{K_1^n} + n \ln \frac{E_a^0(H^+)}{(NO_3^-)}$$

$$= \ln \frac{E_a^0(Pu^{+4})}{(NO_3)^4} - n \ln \frac{(\gamma HNO_3)_{org}}{(\gamma HNO_3)_{aq}}$$

$$+ \ln \frac{(\gamma Pu(NO_3)_4)_{org}}{(\gamma Pu(NO_3)_4)_{aq}} \qquad (4)$$

Figure 68 shows a plot of

$$\ln \frac{E_a^0(Pu^{+4})}{(NO_3^-)^4} \text{ vs. } \ln \frac{E_a^0(H^+)}{(NO_3^-)}$$

for all the plutonium and nitric acid data obtained in the HNO_3, TBP in AMSCO, and plutonium(IV) system. These data are given in Tables 68 and 69. It may be observed that all points obtained at a given total TBP concentration fall on a straight line and that for another concentration of TBP a parallel line is obtained.

In Fig. 69 all the data obtained in this system are plotted as

$$\ln \frac{E_a^0(Pu^{+4}) \cdot f}{(NO_3)^4} \text{ vs. } \ln \frac{E_a^0(H^+)}{(NO_3)^2}$$

where f is the total, complexed plus uncomplexed, TBP concentration in the solvent. It can be seen that with this modification, an excellent correlation is obtained between the distribution of nitric acid and plutonium(IV) over the range 1 to 5 *M* HNO_3 and 0.17 to 1.0 *M* TBP, since only about 3 out of 31 points deviate by more than 10% from a straight line with slope 2.4.

If this result is interpreted in terms of Eq. 5, it appears that $n = 2.4$; and since it has been shown that

$$\ln \frac{(\gamma HNO_3)_{org}}{(\gamma HNO_3)_{aq}}$$

is nearly constant over the range (Table 68)

$$\ln \frac{(\gamma Pu(NO_3)_4)_{org}}{(\gamma Pu(NO_3)_4)_{aq}} = \ln f ,$$

which is the total TBP concentration. It must be added that this type of analysis is not successful for the simultaneous extraction of uranium,

[2] J. E. Savolainen, *Quarterly Report – The Primary Extraction Mechanisms of Nitric Acid and Thorium Nitrate Extraction by TBP for Period 11/10/51 – 2/10/52*, ORNL CF-52-2-113, Feb. 13, 1952.

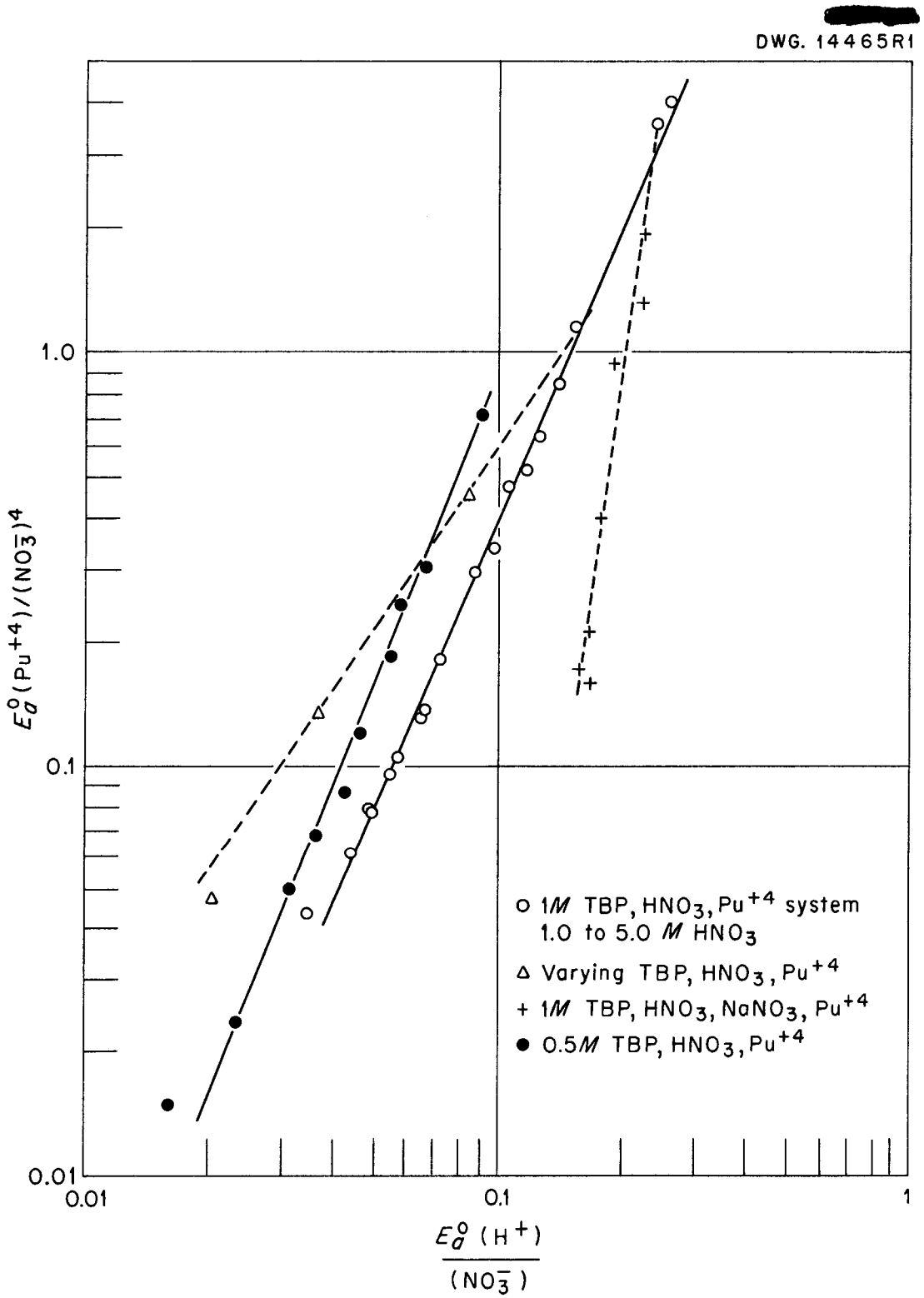

Fig. 68. Correlation of Pu(IV) and HNO_3 Distribution in TBP Extraction.

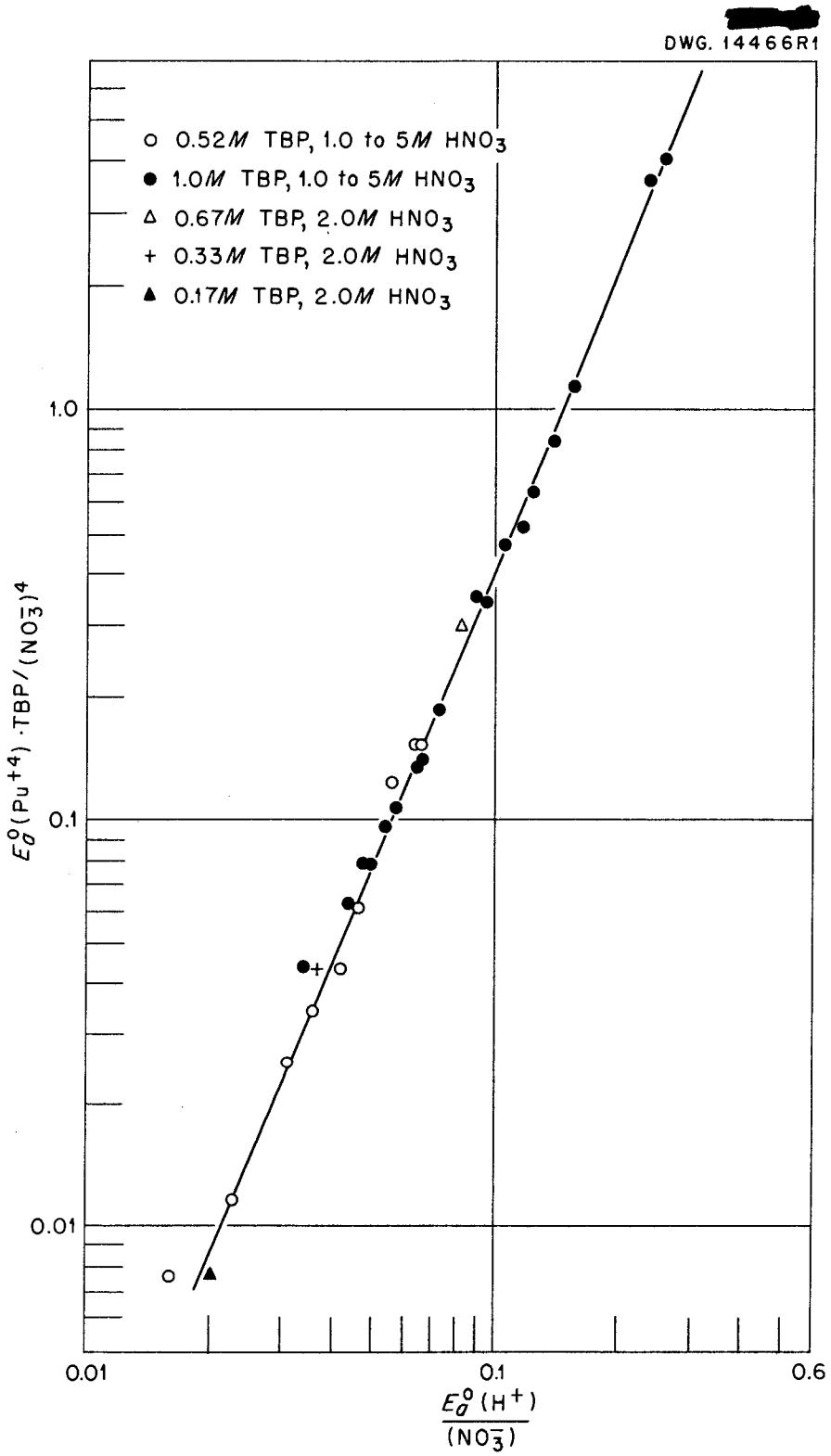

Fig. 69. Correlation of Pu(IV) and HNO_3 Distribution in TBP Extraction.

TABLE 68

Extraction of Nitric Acid and Plutonium(IV) from Nitric Acid Solutions by TBP

Aqueous phase: HNO_3, as indicated, and traces of plutonium(IV)
Solvent phase: TBP in AMSCO, as indicated
Temperature: 25°C

HNO_3 CONCENTRATION (M)	TBP CONCENTRATION (M)	E_a^0[Pu(IV)]	$E_a^0(HNO_3)$	K_1*
0.52	1.20	0.965	0.190	0.332
0.93	1.20	3.03	0.240	0.262
1.68	1.03	5.0	0.208	0.194
1.78	1.20	8.1	0.248	0.183
2.13	1.20	10.4	0.252	0.178
2.28	1.03	7.9	0.204	0.172
2.40	1.20	11.3	0.230	0.160
2.70	1.03	9.7	0.196	0.158
3.02	1.03	11.4	0.199	0.169
3.32	1.03	12.6	0.190	0.159
3.50	1.20	20.2	0.226	0.161
3.65	1.03	13.8	0.181	0.165
3.80	1.03	17.4	0.184	0.167
3.90	1.20	22.5	0.213	0.171
4.50	1.20	25.0	0.198	0.184
5.25	1.20	34.0	0.180	0.190

*$K_1 = \dfrac{E_a^0(HNO_3)}{(HNO_3)\ (TBP)}$, where (HNO_3) is the aqueous nitric acid concentration and (TBP) is the concentration of uncomplexed TBP in the solvent. The volume increase in the solvent phase was considered in calculating (TBP).

plutonium, and nitric acid. In Fig. 70

$$\ln \frac{E_a^0(UO_2^{++})}{(NO_3)^2} \text{ vs. } \ln \frac{E_a^0(H^+)}{(NO_3)}$$

is plotted for two series of equilibrations, one containing only trace quantities of uranium, the other with a uranium-to-TBP ratio of 1:7 on a molar basis. The data from which this plot was made are presented in Tables 69 and 70. Such correlation gives erratic results and yields a value of 1.4 for n, which is interpreted as the number of TBP molecules involved with each uranyl nitrate molecule in the organic soluble complex. It is also apparent from the data that the presence of only 0.08 M U in the solvent lowers the apparent K for nitric acid from 0.17 to 0.07. For these reasons it was concluded that the activity coefficients significantly affect the equilibrium distribution, and these as yet unknown activity coefficients must be considered in any analysis designed to

TABLE 69

Extraction of Nitric Acid, Plutonium(IV), and Uranium from Nitric Acid Solutions by TBP

Aqueous phase: HNO_3, as indicated, and traces of plutonium(IV) and U^{233}
Solvent phase: 0.52 *M* TBP in AMSCO
Temperature: 25°C

HNO_3 CONCENTRATION (*M*)	$E_a^0(HNO_3)$	E_a^0[Pu(IV)]	E_a^0(U)	K_1*
1.08	0.0975	0.965	3.60	0.218
1.48	0.0980	1.43	4.78	0.175
1.80	0.103	2.62	6.65	0.171
1.95	0.105	2.58	7.29	0.171
2.33	0.107	3.55	8.44	0.170
2.53	0.107	3.78	10.3	0.169
2.93	0.104	4.28	11.2	0.165
3.33	0.104	6.14	13.3	0.178
4.30	0.0975	8.04	9.22	0.227
5.30	0.0850	11.6	8.70	0.229

*$K_1 = \frac{E_a^0(HNO_3)}{(HNO_3)\ (TBP)}$, where (HNO_3) is the aqueous HNO_3 concentration and (TBP) is the concentration of uncomplexed TBP in solvent.

determine the mechanism of the extraction of nitric acid and plutonium(IV) by tributyl phosphate.

However, it is felt that the correlation obtained between the extraction of nitric acid and plutonium(IV) in Fig. 69 is significant, and that further study of the system may lead to a better understanding of both the extraction mechanism and the activities involved.

Application of TBP Extraction after Short Cooling Periods. Scouting experiments have shown that adequate decontamination of uranium and plutonium from neptunium cannot be obtained with the standard Purex process. The results of five batch countercurrent runs are given in Table 71. Apparently, no significant reduction in fission-product decontamination was caused by the presence of short-lived activities when the TBP extraction was made after only 15 days of cooling as compared with that obtained after a 60-day cooling period. However, owing to the break-through of neptunium, fission-product analyses on the product solutions were not entirely reliable.

The exact nature of the extraction of neptunium by TBP has not been established. There is a definite fractionation of neptunium under Purex 1A-column conditions. The neptunium distribution coefficient was found to be 0.1 at the feed plate, about 0.05 in the fifth extraction stage, and 0.3 in the fourth scrub stage. This seems to indicate the presence of more than one valence

TABLE 70

Extraction of Nitric Acid and Uranium from Nitric Acid Solutions by TBP

Aqueous phase: HNO_3, as indicated, and equilibrium concentration of uranium

Solvent phase: 0.52 *M* TBP in AMSCO and about 0.07 *M* $UO_2(NO_3)_2$

HNO_3 CONCENTRATION (*M*)	TOTAL NITRATE CONCENTRATION (*M*)	$E_a^0(HNO_3)$	$E_a^0(U)$	K_1*
1.27	1.32	0.0315	2.42	0.068
1.46	1.505	0.034	2.97	0.067
1.66	1.70	0.042	3.66	0.080
2.05	2.08	0.044	4.93	0.074
2.30	2.33	0.0435	5.52	0.070
2.60	2.62	0.046	6.38	0.070
2.90	2.92	0.048	6.92	0.072
3.38	3.40	0.0475	8.15	0.070
4.40	4.42	0.0455	9.45	0.065
5.20	5.22	0.0440	9.30	0.065
6.40	6.42	0.0375	8.70	0.045

$$^*K_1 = \frac{E_a^0(HNO_3)}{(HNO_3)\ (TBP)}.$$

TABLE 71

Decontamination of Uranium and Plutonium in the Purex 1A Column After 15 to 20 Days of Cooling

RUN NO.	DECONTAMINATION FACTORS (1A column)					
	GROSS β	Ru β	Zr β*	Mo β	TRE β*	Np β
2	30	300		700	10^4	8
3	30	1000		1500	10^4	4
4	20	1500	5000	3000	10^4	3
5	20	300		700	10^4	4
6	40	2000		1000	10^4	25

*The beta activity of the 1AP was 98+% neptunium beta, which makes the Zr and TRE analyses unreliable.

[redacted]

DWG. 14467R1

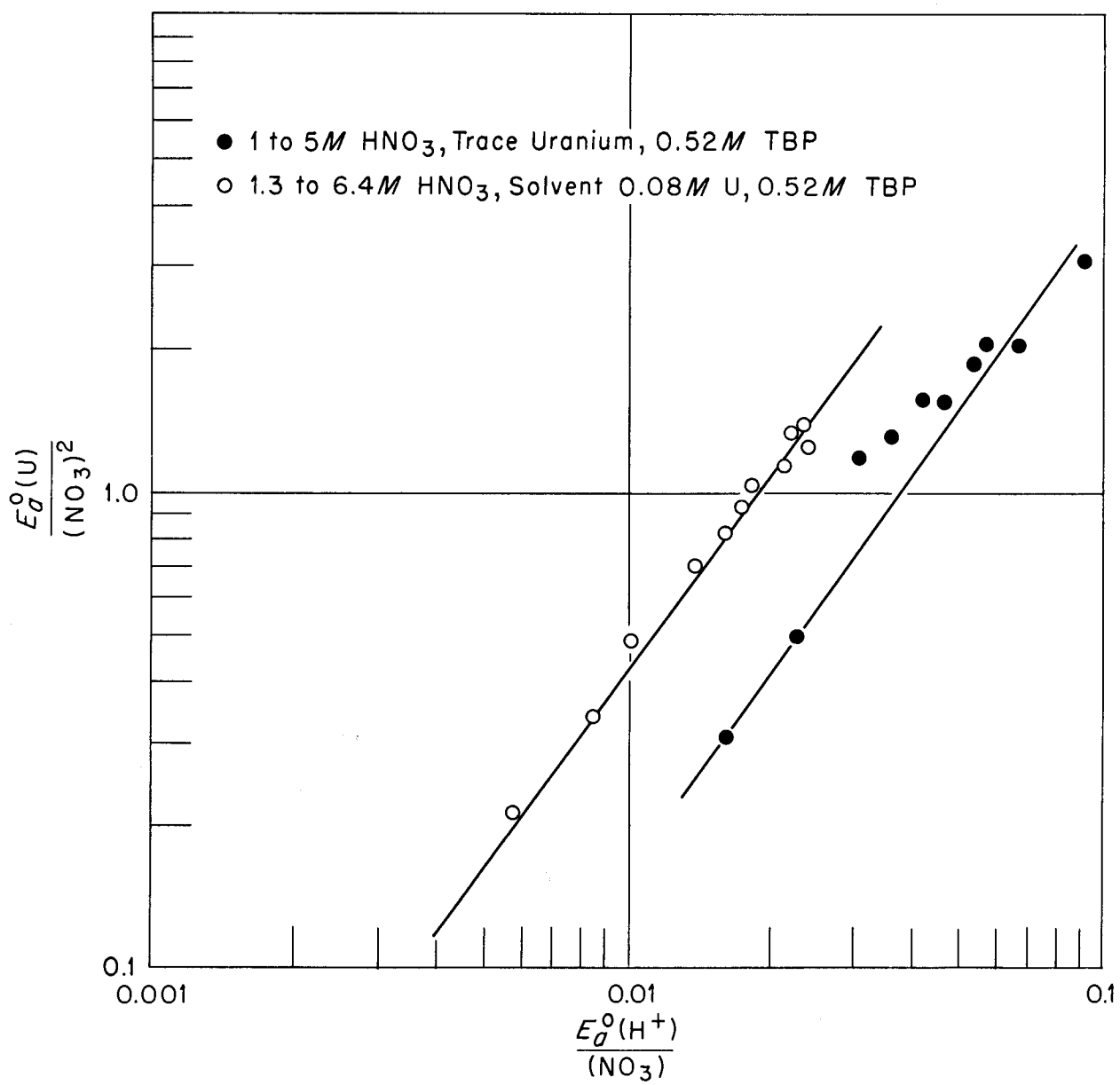

Fig. 70. Correlation of Uranyl and HNO_3 Distribution in TBP Extraction.

stage of this element. The behavior of neptunium in the 1B column was observed to be erratic. In one run it primarily followed the plutonium, in the other, the uranium (Table 72).

Hexavalent neptunium is extracted by tributyl phosphate and follows uranium and plutonium in the Purex 1A column. In two countercurrent batch tests greater than 99% of the neptunium was extracted from a Purex feed oxidized with 0.1 *M* $Na_2Cr_2O_7$. In the plutonium strip column, which is operated under reducing conditions, 97% of the neptunium was reduced and followed the

plutonium. If it is found that the lower valence states of neptunium do not extract with tributyl phosphate, it will be possible to adequately decontaminate uranium from neptunium activity by operating the second uranium cycle under reducing conditions, but it is doubtful that plutonium can be adequately separated from this element by tributyl phosphate extraction.

TABLE 72

Behavior of Neptunium in the Purex 1B Column

Batch countercurrent runs with standard Purex flow sheet

PRODUCT	DECONTAMINATION FACTORS			
	RUN 5		RUN 6	
	GROSS β	Np β	GROSS β	Np β
Uranium	30	6	450	170
Plutonium	45	10	50	30

Flow Sheets. Two flow sheets are given in Figs. 71 and 72. The flow sheet given in Fig. 71 assumes that the plutonium remains in the reactor, in solution or as a precipitate, and is discharged with the uranium fuel solution. From present data it is necessary to cool this material for at least 45 days, since for shorter cooling periods adequate decontamination from neptunium cannot be obtained.

The flow sheet given in Fig. 72 assumes that the plutonium precipitates in the reactor and is removed by filtration. The flow sheet also makes use of tributyl phosphate extraction to obtain separation of uranium and plutonium from fission products. It is possible to isolate the plutonium that has been filtered out of the reactor solution independently of the uranium; however, the uranium removed from the reactor for re-enrichment would contain a significant amount of neptunium, which after decay to plutonium must be recovered. If Purex is used for the uranium decontamination, a complete first cycle must be operated and the inclusion of the plutonium from the reactor filters would not greatly increase the cost of this solvent extraction.

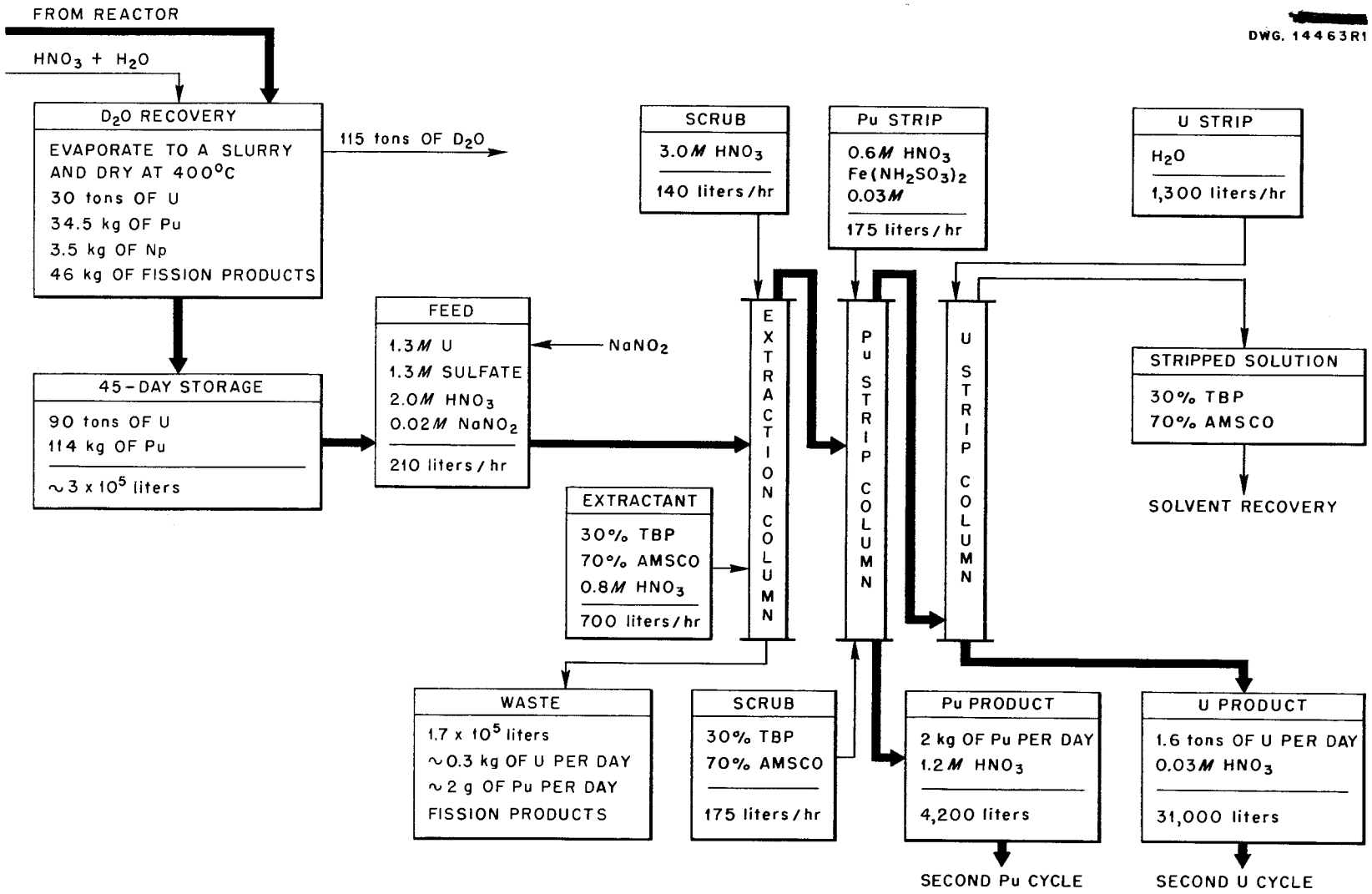

Fig. 71. Chemical Processing of Aqueous Homogeneous Plutonium Producer on the Basis of 30 Tons of Uranium and 38 kg of Plutonium Discharged Every 19 Days.

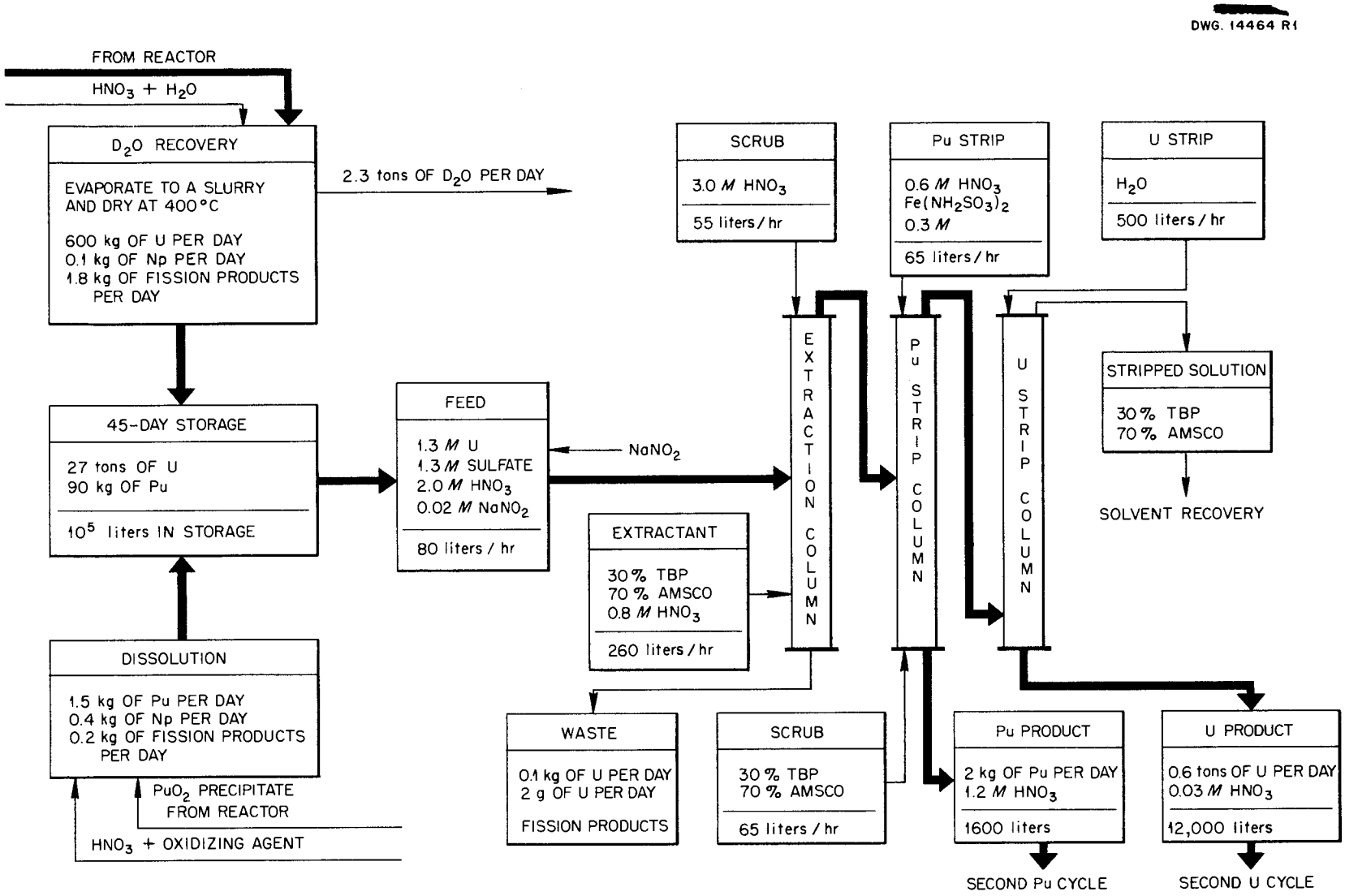

Fig. 72. Chemical Processing of Aqueous Homogeneous Plutonium Producer on the Basis of PUO_2 Precipitate Filtered from Reactor and 600 kg of Uranium Discharged each Day.